

https://dspace.org/

Performance evaluation of a desiccant-evaporative cooling air-conditioning system

Thom, Martin Gunther

1998

https://hdl.handle.net/10539/26842

Downloaded from a DSpace repository. https://dspace.org/

PERFORMANCE EVALUATION OF A DESICCANT-EVAPORATIVE COOLING AIR-CONDITIONING SYSTEM

Martin Gunther Thom

A project report submitted to the Faculty of Engineering, University of the Witwatersrand, Johannesburg, in partial fulfillment of the requirements for the degree of Master of Science in Engineering.

Johannesburg, 1998

Degree awarded with distinction on 30 June 1998

DECLARATION

I declare that this project report is my own, unaided work. It is being submitted for the Degree of Master of Science in Engineering in the University of the Witwatersrand, Johannesburg. It has not been submitted before for any degree or examination in any other University.



23 day of FEBRUARY 1998

ABSTRACT

The main objective of this project was to evaluate the performance of a desiccant-evaporative cooling (DEC) system operating in the ventilation (once-through) mode. An accurate data acquisition system was installed on a small DEC test installation located in the School of Mechanical Engineering, University of the Witwatersrand, Johannesburg. The DEC system was extensively tested to fully evaluate the overall system and each of its components. A mathematical model of the DEC system was developed and computer simulations were done for each of the experimental tests. Most of the experimental results followed the theoretical predictions but there were some deviations between the measured and simulated values that revealed points of interest including:

- The effect of air leakage that reduced performance by approximately 46 per cent.
- Water carryover from the return air spray chamber into the sensible heat exchanger reduced performance by up to 45 per cent.
- The moisture removal capacity of the experimental DEC system was 26 to 39 per cent lower than that of a new system because of desiccant (lithium chloride) degradation and air leakage.

Other experimental findings included:

- The DEC system typically operated at a COP of 0.23 and supplied 0.16 kg/s of air with a cooling capacity of 1.2 kW, when the ambient air conditions were the same as the room air conditions. These performance parameters decreased with increasing dry-bulb temperature and humidity ratio of the ambient air. The DEC system provided no cooling at ambient conditions typical of South African coastal summer conditions.
- Performance was found to be relatively insensitive to changes in desiccant wheel speed.
- Unbalanced flow between supply and return air improved performance by 15 to 38 per cent.
- A method of using single blow tests to maximise the energy efficiency of the desiccant wheel was developed.

The feasibility, operability and practical limitations of using DEC systems throughout South Africa were investigated. Johannesburg was found to be the region in which DEC systems would perform the best.

An alternative DEC arrangement was recommended based on the experimental findings that balanced flow DEC systems have low regenerating efficiencies. The recommendation involves the use of an additional heat exchanger that would significantly improve performance and simplify the control of the DEC system.

ACKNOWLEDGEMENTS

I would like to express my sincere gratitude to Klingenburg GmbH, Gladbeck, Germany, for supplying the necessary components of the system through their local representative Aero Duct (Pty) Ltd of Benoni. I would also like to express my gratitude to Mr Rudi Van Schaik of Aero Duct (Pty) Ltd for providing additional technical information and equipment.

I would like to thank my supervisor, Prof T J Sheer, for his advice during the course of this project. This project was supported financially by the Eskom Tertiary Education Support Programme (TESP), for which I am most grateful.

CONTENTS PAGE

DECLARATION ii
ABSTRACT iii
ACKNOWLEDGEMENTS v
CONTENTS vi
LIST OF FIGURES xii
LIST OF TABLES xv
LIST OF SYMBOLS AND NOMENCLATURE xviii

1 INTRODUCTION 1

1.1 Emergence of Desiccant Cooling 1
1.2 Desiccant-Evaporative Cooling Systems 3
1.3 Objectives of the Study 4

2 REVIEW OF DESICCANT-EVAPORATIVE COOLING (DEC) SYSTEMS 5

2.1 Components of DEC Systems 5
2.1.1 Rotary desiccant wheel 5
2.1.2 Sensible heat exchanger 6
2.1.3 Evaporative spray chambers 7
2.1.4 Auxiliary heating device 7

2.2 DEC Operating Modes 8
2.2.1 Ventilation mode 8
2.2.2 Ventilation credit mode 8
2.2.3 Recirculation mode 9
2.2.4 Make-up air mode 10
2.2.5 More complex cycles 11
2.2.6 Two stage evaporative cooling 13

2.2.7	Winter mode	14
3	LITERATURE REVIEW	15
3.1	**Mathematical Models of Desiccant Wheels**	15
3.2	**Factors Affecting DEC Performance**	17
3.3	**Desiccant Degradation**	24
3.4	**Feasibility Studies**	26
4	MATHEMATICAL MODEL OF A DEC SYSTEM	28
4.1	**Mathematical Model**	28
4.1.1	Desiccant wheel	28
4.1.2	Rotary heat exchanger	31
4.1.3	Air carryover in heat exchanger	31
4.1.4	Spray chambers	32
4.1.5	Regeneration heaters	33
4.2	**Sensitivity Analysis of Mathematical Model**	34
4.2.1	Results of sensitivity analysis	34
4.2.2	Discussion of sensitivity analysis	40
5	EXPERIMENTAL ARRANGEMENT OF DEC TEST SYSTEM	43
5.1	**Main Components of the Test System**	44
5.1.1	Rotary desiccant wheel	44
5.1.2	Rotary heat exchanger	44
5.1.3	Spray chambers	44
5.1.4	Fans	45
5.1.5	Regeneration heaters	45
5.1.6	Inlet air pre-conditioning system	45

5.2	**Data Acquisition and Reduction system**	46
5.2.1	Overview	46
5.2.2	Temperature measurement	47
5.2.3	Hygrotransmitters	47
5.2.4	Computer hardware	48
5.2.5	Air flow measurement	48
5.2.6	Electrical power measurement	49
5.3	**Computer Programs**	50
5.3.1	Data acquisition and processing program	50
5.3.2	Program to calculate air flow rate	51
5.3.3	DEC simulation program	51
6	**EXPERIMENTAL PROCEDURE AND RESULTS**	52
6.1	**Air Leakage and Flow rate Measurement**	53
6.1.1	Experimental procedure and results	53
6.1.2	Main findings	60
6.2	**Single Blow Tests**	63
6.2.1	Experimental procedure and results	63
6.2.2	Main findings	68
6.3	**Efficiency of Return Air Spray Chamber (EV_R) with Unbalanced Air Flow**	70
6.3.1	Experimental procedure and results	70
6.3.2	Main findings	76
6.4	**Efficiency of Return Air Spray Chamber (EV_R) with Balanced Air Flow**	78
6.4.1	Experimental procedure and results	78

6.4.2	Main findings	82
6.5	**Efficiency of Supply Air Spray Chamber (EV_S)**	84
6.5.1	Experimental procedure and results	84
6.5.2	Main findings	88
6.6	**Inlet Air Conditions and Regeneration Temperatures**	89
6.6.1	Experimental procedure and results	89
6.6.2	Main findings	106
6.7	**Desiccant Wheel Speed and Unbalanced Air Flow**	111
6.7.1	Experimental procedure and results	111
6.7.2	Main findings	114
6.8	**Test Results versus Catalogue Data**	115
7	**DISCUSSION OF TEST RESULTS**	116
7.1	**Air Leakage**	116
7.2	**Single Blow Tests**	118
7.2.1	Regeneration single blow tests	118
7.2.2	Dehumidification single blow tests	121
7.3	**Efficiency of Return Air Spray Chamber (EV_R) with Unbalanced Air Flow**	123
7.4	**Efficiency of Return Air Spray Chamber (EV_R) with Balanced Air Flow**	127
7.5	**Efficiency of Supply Air Spray Chamber (EV_S)**	128

7.6	**Inlet Air Conditions and Regeneration Temperatures**	129
7.6.1	Similar regeneration temperatures at different inlet air conditions	129
7.6.2	Similar inlet air conditions at different regeneration temperatures	131
7.6.3	Changing humidity ratio of inlet air with constant dry-bulb temperature	132
7.6.4	Changing dry-bulb temperature of inlet air with constant humidity ratio	133
7.7	**Desiccant Wheel Speed and Unbalanced Air Flow**	134
7.7.1	Balanced flow	134
7.7.2	Unbalanced flow	135
7.8	**Test Results versus Catalogue Data**	137
7.9	**General Observations**	139
7.9.1	Efficiency of sensible heat exchanger	139
7.9.2	Performance of the DEC test unit	139
7.9.3	Sources of experimental error	140
7.10	**Feasibility and Operability of DEC Systems in South Africa**	141
8	**CONCLUSIONS AND RECOMMENDATIONS**	142
8.1	**Conclusions**	142
8.2	**Recommendations**	146
8.2.1	Improvements to DEC systems	146
8.2.2	Recommendations for future work	149

APPENDICES	150
APPENDIX A Calibration results	150
APPENDIX B Data acquisition and processing computer program	155
APPENDIX C Computer program to calculate air flow rate	175
APPENDIX D DEC simulation computer program	177
APPENDIX E Specifications for instrumentation	186
APPENDIX F Equipment performance data	194
APPENDIX G Operability of DEC systems in South Africa	197
APPENDIX H Experimental results	225
H1. Air leakage results	225
H2: Regeneration and dehumidification single blow tests	229
H3: Efficiency of return air spray chamber	234
H4: Efficiency of supply air spray chamber	275
H5: Regeneration temperatures and inlet air conditions	290
H6: Rotational speed of desiccant wheel	343
REFERENCES	376

LIST OF FIGURES

FIGURE		PAGE
1.1	Schematic diagram of a DEC system operating in ventilation mode.	3
2.1	Schematic diagram of a rotary desiccant wheel.	5
2.2	Schematic diagram of a DEC system operating in recirculation mode.	9
2.3	Schematic diagram of a DEC system operating in make-up air mode.	10
2.4	Schematic diagram of the Dunkle cycle.	11
2.5	Schematic diagram of the refrigeration assisted DEC cycle.	12
2.6	Schematic diagram of a two stage evaporative cooling cycle.	13
2.7	Schematic diagram of a DEC system operating in winter mode.	14
3.1	Adsorption isotherm for the "ideal" desiccant material.	17
3.2	Adsorption isotherm for lithium chloride solutions.	18
3.3	Effect of supply air velocity on humidity ratio of dehumidified air.	21
3.4	Effect of humidity ratio of supply air on humidity ratio of dehumidified air.	22
3.5	Effect of regeneration temperature on humidity ratio of dehumidified air.	22
3.6	Effect of humidity ratio of supply air on dry-bulb temperature of dehumidified air.	23
3.7	Effect of regeneration temperature on dry-bulb temperature of dehumidified air.	23
3.8	Ageing characteristics and projections for a typical desiccant.	24
3.9	Capacity loss of silica gel exposed to cigarette smoke.	25
3.10	COP for ideal systems as a function of regenerating temperature, for July 1955 in Miami.	26
4.1	Method of determining the ideal humidity ratio W_{2I} and ideal dry-bulb temperature TDB_{2I}.	29
5.1	DEC test unit.	43
5.2	Air sampling device including aspirated psychrometer and radiation shield.	46
5.3	The "Log-Tchebycheff" method of air flow rate measurement.	49

6.1.1	Diagram of sealing arrangement for the desiccant wheel.	55
6.1.2	Static pressures measured at various air flow rate combinations.	56
6.1.3	Differential pressure at various air flow rate combinations.	57
6.1.4	Leakage air flow rate at various air flow rate combinations.	58
6.2.1	Regeneration single blow test (T_{reg}=57 °C) (test no. H2/1).	65
6.2.2	Regeneration single blow test (T_{reg}=87 °C) (test no. H2/2).	65
6.2.3	Dehumidification single blow test (test no. H2/3).	66
6.2.4	Dehumidification single blow test (test no. H2/4).	66
6.2.5	Temperature variation comparison from figures 6.2.3 and 6.2.4.	67
6.2.6	Humidity ratio variation comparison from figures 6.2.3 and 6.2.4.	67
6.3.1	Change in humidity ratio of supply air across sensible heat exchanger versus water flow rate.	73
6.3.2	Cooling capacity in ventilation credit mode versus water flow rate.	73
6.3.3	Heat exchanger efficiencies versus water flow rate.	74
6.3.4	Regeneration efficiency and change in humidity ratio of the supply air across the dehumidifier versus water flow rate.	74
6.3.5	Cooling capacity in ventilation mode versus water flow rate.	75
6.3.6	Dehumidifier inlet and outlet humidity ratios and outlet dry-bulb temperature TDB_2 versus water flow rate.	75
6.4.1	Cooling capacity in ventilation credit mode and return air spray chamber efficiency versus water flow rate.	81
6.4.2	Change in humidity ratios of supply air across dehumidifier and return air across spray chamber.	81
6.4.3	Change in humidity ratio and dry-bulb temperature in return air spray chamber.	82
6.5.1	Efficiency of the supply air spray chamber EV_S versus water flow rate to supply air spray chamber.	87
6.5.2	Changes in humidity ratio and dry-bulb temperature versus water flow rate to supply air spray chamber.	87
6.6.1	Inlet air conditions and regeneration temperatures for tests H5/1-H5/26 and H6/5-H6/10.	91

6.6.2	Dehumidification processes (1-2) of tests with regeneration temperature TDB_8 of 55 ± 5 °C.	96
6.6.3	Dehumidification processes (1-2) of tests with regeneration temperature TDB_8 of 65 ± 5 °C.	97
6.6.4	Dehumidification processes (1-2) of tests with regeneration temperature TDB_8 of 75 ± 5 °C.	98
6.6.5	Dehumidification processes (1-2) of tests with regeneration temperature TDB_8 of 85 ± 5 °C.	99
6.6.6	Dehumidification processes (1-2) of tests with regeneration temperature TDB_8 of 95 ± 5 °C.	100
6.6.7a	Dehumidification processes (1-2) for groups of two tests at similar inlet air conditions but different regeneration temperatures.	102
6.6.7b	Dehumidification processes (1-2) for groups of two tests at similar inlet air conditions but different regeneration temperatures.	103
7.1	Instantaneous and average sine values over a range of angles.	119
7.2	Example of a method to estimate the optimum regenerating period for a given desiccant wheel and regenerating air flow rate.	120
8.1	Recommendation for an additional heat exchanger.	147
8.2	Recommendation for the multiple use of regeneration air.	148
A1	Calibration results for the DELTA OHM, model 8908TC/150 hygrotransmitter (serial no. AMW 299) for different air humidity ratios.	154
A2	Calibration results for the DELTA OHM, model 8908TC/150 hygrotransmitter (serial no. AMU 739) for different air humidity ratios.	154
G2.1	Climatic zones of South Africa.	198
H1.1	Differential pressure at various air flow rate combinations.	226
H1.2	Leakage air flow rate at various air flow rate combinations.	227

LIST OF TABLES

TABLE		PAGE
4.2.1	Variation of efficiency of supply air spray chamber (EV_S).	35
4.2.2	Variation of efficiency of return air spray chamber (EV_R).	36
4.2.3	Variation of heat exchanger efficiency (EHX).	37
4.2.4	Variation of dry-bulb temperature of ambient air (TDB_1).	38
4.2.5	Variation of humidity ratio of ambient air (W_1).	39
6.1.1	Measured supply and return air flow rates for various flow combinations.	55
6.1.2	Estimated supply and return air flow rates at desiccant wheel (with both inspection doors closed).	59
6.1.3	Estimated supply and return air flow rates at heat exchanger (with both inspection doors closed).	59
6.3.1	Performance parameters for variation of efficiency of return air spray chamber EV_R (MA_R=98 g/s).	71
6.3.2	Property changes for variation of efficiency of return air spray chamber EV_R (MA_R=98 g/s).	72
6.4.1	Performance parameters for variation of efficiency of return air spray chamber EV_R (MA_R=147 g/s).	79
6.4.2	Property changes for variation of efficiency of return air spray chamber EV_R (MA_R=147 g/s).	80
6.5.1	Performance parameters for variation of efficiency of supply air spray chamber EV_S.	85
6.5.2	Property changes for variation of efficiency of supply air spray chamber EV_S.	86
6.6.1a	Performance parameters of tests listed in order of descending regeneration temperature (TDB_3)	92
6.6.1b	Performance parameters of tests listed in order of descending regeneration temperature (TDB_8)	93

6.6.2a	Process changes of tests listed in order of descending regeneration temperature (TDB_8).	94
6.6.2b	Process changes of tests listed in order of descending regeneration temperature (TDB_8).	95
6.6.3	Comparison of 8 groups of 2 tests at similar inlet air conditions but different regeneration temperatures (TDB_8).	101
6.6.4	Comparison of 4 groups of 2 tests at similar dry-bulb temperature TDB_1 but different humidity ratio W_1.	104
6.6.5	Comparison of 4 groups of 2 tests at similar humidity ratio W_1 but different dry-bulb temperature TDB_1.	105
6.7.1	Unbalanced flow at different regeneration temperatures and different desiccant wheel speeds.	112
6.7.2	Variation of regeneration temperature and inlet air conditions at different desiccant wheel speeds.	113
6.8.1	Comparison of test results with simulations based on catalogue data.	115
A1	Calibration measurements of LM 35 temperature sensors in microvolts over a temperature range.	151
A2	Calibration equations obtained from results in table A1.	152
A3	Calibration of Fluke multimeter to read TWB_2.	152
A4	Results of experiments to check accuracy of the calibration equations.	153
G2.1	Climatic zones of South Africa and representative cities.	198
G2.2a	Months when average dry-bulb temperature or humidity ratio exceeds room conditions.	199
G2.2b	Months when average dry-bulb temperature or humidity ratio exceeds room conditions.	200
G3.1	UPINGTON average monthly weather conditions.	201
G3.2	DEC simulated performance parameters for UPINGTON.	202
G4.1	CAPE TOWN average monthly weather conditions.	203
G4.2	DEC simulated performance parameters for CAPE TOWN.	204
G5.1	PORT ELIZABETH average monthly weather conditions.	205
G5.2	DEC simulated performance parameters for PORT ELIZABETH.	206
G6.1	EAST LONDON average monthly weather conditions.	207

G6.2	DEC simulated performance parameters for EAST LONDON.	208
G7.1	DURBAN average monthly weather conditions.	209
G7.2	DEC simulated performance parameters for DURBAN.	210
G8.1	LADYSMITH average monthly weather conditions.	211
G8.2	DEC simulated performance parameters for LADYSMITH.	212
G9.1	PHALABORWA average monthly weather conditions.	213
G9.2	DEC simulated performance parameters for P.	214
G10.1	PIETERSBURG average monthly weather con.	215
G10.2	DEC simulated performance parameters for PIETE	216
G11.1	JOHANNESBURG average monthly weather cond.	217
G11.2	DEC simulated performance parameters for JOHANNESBURG.	218
G12.1	BLOEMFONTEIN average monthly weather conditions.	219
G12.2	DEC simulated performance parameters for BLOEMFONTEIN.	220
G13.1	QUEENSTOWN average monthly weather conditions.	221
G13.2	DEC simulated performance parameters for QUEENSTOWN.	222
G14.1	BEAUFORT WEST average monthly weather conditions.	223
G14.2	DEC simulated performance parameters for BEAUFORT WEST.	224
H1.1	Estimated supply and return air flow rates at desiccant wheel (with inspection doors open).	228
H1.2	Estimated supply and return air flow rates at heat exchanger (with inspection doors open).	228

LIST OF SYMBOLS AND NOMENCLATURE

A	Seal gap area through which leakage occurs (m^2)
CC	Cooling capacity in ventilation mode (kW).
C_d	Coefficient of discharge (fraction).
COP	Coefficient of performance in ventilation mode (fraction).
EDH1	Efficiency of moisture removal in desiccant wheel (%).
EDH2	Efficiency of heat exchang esiccant wheel (%).
EER	Electricity efficiency ratio in ventilation mode (fraction).
EHX	Heat exchanger efficiency (%).
EHX_R	Efficiency of heat transfer to return air stream (%).
EHX_S	Efficiency of heat transfer to supply air stream (%).
ERG	Regeneration efficiency (%).
EV_R	Efficiency of the spray chamber in the return air stream (%).
EV_S	Efficiency of the spray chamber in the supply air stream (%).
FR_R	Water flow rate draining from return air spray chamber (g/s).
FR_S	Water flow rate draining from supply air spray chamber (g/s).
H	Enthalpy of the air (kJ/kg dry air).
LiCl	Symbol for lithium chloride.
MA_R	Mass flow rate of return air stream (kg/s).
MA_S	Mass flow rate of supply air stream (kg/s).
MC_R	Mass flow rate of air carryover to return air stream (kg/s).
MC_S	Mass flow rate of air carryover to supply air stream (kg/s).
MW	Rate of water absorption/regeneration from desiccant (g/s).
P_d	Pressure difference (Pa).
PP_R	Pump pressure of water to return air spray chamber (bar).
PP_S	Pump pressure of water to supply air spray chamber (bar).
RH	Relative humidity (%).
SV	Specific volume (m^3/kg).
t	Time (seconds).
TCC	Cooling capacity in ventilation credit mode (kW).
TCOP	Coefficient of performance in ventilation credit mode (fraction).

T_{cr}	Critical temperature (minimum regeneration temperature) (°C).
TDB	Dry-bulb temperature (°C).
TDB_{2I}, TDB_{9I}	Ideal dry-bulb temperatures (see fig. 4.1) (°C).
TDP	Dew point temperature (°C).
TEER	Electricity efficiency ratio in ventilation credit mode (fraction).
TFR_R	Total water flow rate supplied to return air spray chamber (g/s).
TFR_S	Total water flow rate supplied to supply air spray chamber (g/s).
T_{reg}	Regeneration temperature (=TDB_8) (°C).
TWB	Wet-bulb temperature (°C).
Q	Regeneration heat input (kW).
VA_R	Volumetric flow rate of return air stream (m^3/s).
VA_S	Volumetric flow rate of supply air stream (m^3/s).
W	Humidity ratio (g water/kg dry air).
W_{2I}	Ideal humidity ratio (see fig. 4.1) (g/kg).
%EV	Percentage of spray water that was evaporated in spray chamber (%).

Note:

1. Numbers attached to the symbols (e.g. TDB_1, TDB_2) refer to the moist air properties at that point in the process. These numbers refer to points in the ventilation mode process described in figure 1.1 unless specified otherwise.

2. M = measured variables.
   Sim = simulated variables.
   R = return air
   S = supply air

3. ARI (American Refrigeration Institute) outdoor conditions:
   35°C dry-bulb temperature and 14.2 g water/kg dry air.

CHAPTER 1
INTRODUCTION

1.1 Emergence of Desiccant Cooling

The purpose of air conditioning is to provide a physiologically comfortable environment for people, or to provide a specific air quality for an industrial process. This is done primarily by adding or removing heat from the conditioned air to control the temperature and by adding or removing water vapour to control the humidity of the air. In conventional air conditioning units, vapour compression refrigeration is used to cool the air below its dew point to remove sensible heat as well as to condense and remove moisture. Desiccant-Evaporative Cooling (DEC) systems are an alternative to vapour compression systems and use desiccants to remove moisture and use evaporative cooling to remove sensible heat.

The vapour compression systems are very reliable and have been used almost exclusively for air conditioning systems, since the 1930's, when Chlorofluorocarbons (CFC's) and Hydrochlorofluorocarbons (HCFC's) were developed for use in the refrigeration industry. However, in recent years, the use of vapour compression systems has become less favourable, because of the environmentally harmful effects of the refrigerants used. In June 1974, Professor Sherwood Rowlands and Dr Mario Molina of the University of California at Irvine proposed a theory that CFC's would ultimately cause the depletion of the ozone layer, which protects the earth against harmful levels of ultraviolet radiation from the sun (Anderson, 1987). CFC's also contribute to the greenhouse effect, which could result in global warming and climatic change. Extensive studies and research, confirming these factors, resulted in the European Economic Community and 24 other nations signing the Montreal Protocol, on 16 September 1987, in Canada. The aim was to cease the production and importation of CFC's after 1 January 1996 and eventually phase out the use of CFC's (Anderson, 1987). The production of HCFC's is also being phased out and production will cease in developed countries after 2030 in accordance with the Vienna Protocol

of 1996 (Edwards, 1996). This date could be brought forward depending on future international agreements.

Desiccant-Evaporative Cooling (DEC) air conditioning systems have consequently received more attention in recent years, since they are environmentally friendly and only use water and air as working fluids. DEC systems also have the advantages of being able to use low-grade heat as the main energy source to drive the process, as opposed to the large amounts of electrical energy used by vapour compression systems, to drive the mechanical compressors. Another advantage is that one of the possible modes of operation uses only ventilation air, which could solve the 'sick building' problem, commonly found in tightly sealed buildings. At present, DEC systems generally have a higher initial capital cost, lower performance and are less reliable than vapour compression systems. However, increased research and development over the last 20 years has resulted in significant improvements in DEC systems and they could be a viable alternative, or supplement, to vapour compression systems in the future.

1.2 Desiccant-Evaporative Cooling Systems

A schematic diagram of a basic DEC system, operating in the ventilation mode, is shown in figure 1.1 below.

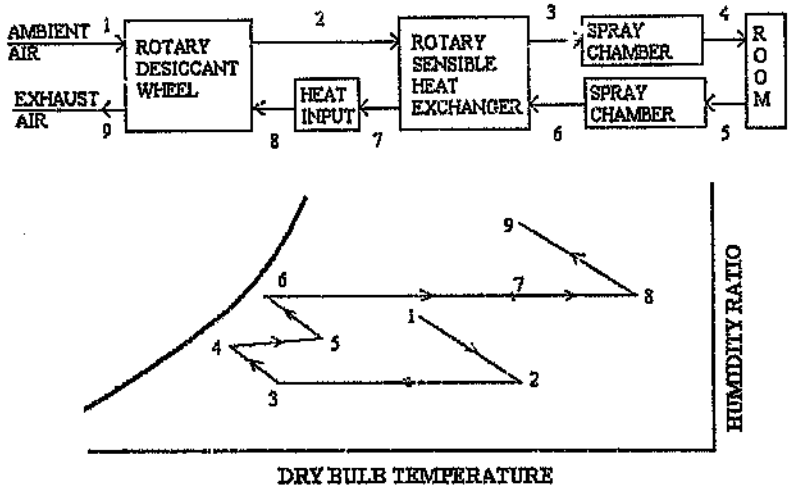

FIGURE 1.1: Schematic diagram of a DEC system operating in ventilation mode.

The possible DEC operating modes are described in detail in Chapter 2. The ventilation mode will be described here as an introduction to the basic principles of a DEC system: The process air (ambient air) is passed through one half of a rotating desiccant wheel (1-2) where water vapour is absorbed by the desiccant. The dry air is then sensibly cooled in a heat exchanger (2-3) and evaporatively cooled in a spray chamber (3-4). This cool, dry air is then supplied to the room to offset any sensible and latent heat loads (4-5). A second air stream (room air), is evaporatively cooled in a spray chamber (5-6) to provide a cold sink for the heat exchanger, where the air is heated (6-7). An auxiliary heating device (7-8) further heats it and this very hot air is then used to regenerate the desiccant in the other half of the rotating desiccant wheel (8-9). This moist and hot regeneration air is then discharged outside.

1.3 Objectives of the Study

The main objectives of the study were as follows:

(1) To carry out tests on a DEC experimental installation to evaluate the following:
   (a) Performance of the complete system under varying operating conditions.
   (b) Performance of individual components of the system.
   (c) Effect of different operating conditions on performance.

(2) To develop a simple mathematical computer model to simulate the DEC process.

(3) To run simulations using the mathematical model and compare these theoretical results with actual test results, to identify deviations.

(4) To do a study on climatic conditions in South Africa and together with the test results, determine the feasibility and practical implications of using DEC systems in South Africa.

CHAPTER 2
REVIEW OF DESICCANT-EVAPORATIVE COOLING (DEC) SYSTEMS

The basic components of a DEC system are described in section 2.1 and the different operating modes are described in section 2.2. The theory concerning DEC systems is described in the literature review (chapter 3) and is also illustrated in the sensitivity analysis (chapter 4.5).

2.1 Components of DEC Systems

The various components of the DEC system are described in the following sections.

2.1.1 Rotary desiccant wheel

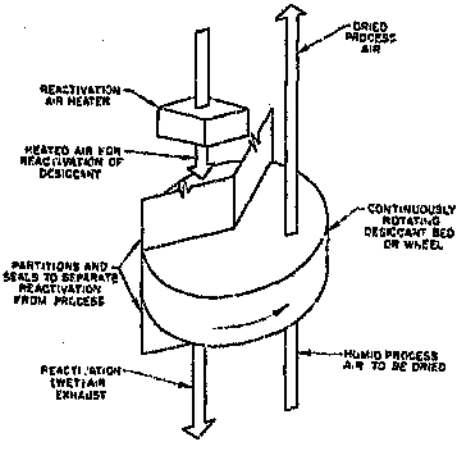

FIGURE 2.1: Schematic diagram of a rotary desiccant wheel (ASHRAE, 1996)

Desiccants are materials that have a very strong affinity for water. This project is concerned only with rotating wheels containing solid desiccants (see figure 2.1), but other options available are stationary beds of solid desiccant subjected alternately to process air and regenerating air streams, by switching valves. Another process

involves spraying liquid desiccant into the process air stream and then regenerating the liquid in a separate unit.

In practice solid desiccant wheels are made of an inert matrix such as cellulose, in which is embedded a desiccant such as silica gel, zeolite or lithium chloride. The wheel is divided in two halves by seals, to enable the process air to pass through one half, while the regeneration air passes through the other half. The matrix is constantly rotating between the air streams so that both processes occur on a continual basis. When the process air passes through the narrow parallel passages of the matrix, the water vapour in the air is adsorbed or absorbed by the desiccant. This is approximately a constant wet-bulb temperature process. Adsorption is a process, usually in solid desiccants, where water vapour is drawn into pores in the desiccant and held onto the surface by weak intermolecular forces. Absorption is a similar process, usually in liquid desiccants, but involves the formation of a chemical bond between the desiccant and water. Both processes only occur if the vapour pressure of the air exceeds that of the desiccant. In the regeneration process, the air is heated to a temperature sufficiently high to cause the vapour pressure in the desiccant to exceed that in the air and the water is released. When the water vapour is adsorbed or absorbed, it condenses onto the desiccant surface and releases energy to the air, called the heat of sorption, which is equal to the latent heat of vaporisation of the water, plus a much smaller heat of wetting. This results in an increase of air temperature and decrease in moisture content. The opposite occurs during the regeneration, where energy equal to the heat of sorption is removed from the air to release the water vapour. Some heat, stored in the matrix during regeneration, is transferred to the supply air stream during dehumidification. This can cause both processes to deviate from a constant wet-bulb temperature process.

2.1.2 Sensible heat exchanger

The desiccant wheel removes moisture from the process air and the heat exchanger removes sensible heat, to complete the process of air conditioning. Most systems use rotary heat exchangers (regenerators), because of their compactness and low cost

relative to the heat transfer capability. The heat exchanger is important not only to remove sensible heat from the process air but also to heat up the regeneration air and thereby reduce the amount of regeneration energy required. The heat exchanger efficiency should therefore be high to increase the cooling capacity and reduce the energy consumption of the system.

2.1.3 Evaporative spray chambers

The purpose of the evaporative spray chamber on the process air side is to adjust the sensible heat ratio of the process air. The spray chamber cools the air by direct evaporative cooling, which is approximately a constant wet-bulb temperature process provided that the evaporation rate is high and the water temperature is close to that of the air wet-bulb temperature. If the efficiency is zero, then very dry and moderately cool air is supplied. If the efficiency is 100 per cent, then colder (but less dry) air is supplied.

The purpose of the spray chamber on the regeneration air stream is to cool the air by direct evaporative cooling to provide a cold sink for the heat exchanger. The efficiency of this spray chamber should therefore be as high as possible to maximise the cooling capacity of the system.

2.1.4 Auxiliary heating device

The heating device supplies energy to heat the return air to regenerate the desiccant wheel. The heating device can consist of electrical heaters, gas burners, solar collectors, or any other source of waste or primary heat energy. The regenerating temperature required is mainly dependent on the inlet conditions of the process air and can be as low as 45 °C. The maximum temperature limit usually depends on the bonding material used in the desiccant wheel to bond the desiccant to the matrix and is usually less than 200 °C.

2.2 DEC Operating Modes

There are two main modes of DEC operation: The ventilation and the recirculation modes. There are two variations of each of these two modes, called the ventilation credit and make-up air modes. Then there are an almost unlimited number of combinations and more complex improvements of these modes, of which only the Dunkle cycle and refrigeration assisted cycles will be described. Finally, the DEC system can also be operated using only the two stage cooling feature, or by changing the operating parameters to allow heating and humidification in winter mode.

2.2.1 Ventilation mode

The ventilation mode is described in the introduction and a schematic diagram of a DEC system, operating in the ventilation mode, is shown in figure 1.1. Ambient air is dehumidified, sensibly cooled, evaporatively cooled and supplied to the room. The room exhaust air is used to cool the process air and to regenerate the desiccant wheel (Collier et al, 1982). The following equations describe the main performance parameters of this mode, where the numbers are defined by figure 1.1:

$$CC = MA_S \cdot (H_5 - H_4) \quad (2.1)$$

$$Q = MA_R \cdot (H_8 - H_7) \quad (2.2)$$

$$COP = CC/Q \quad (2.3)$$

2.2.2 Ventilation credit mode

This mode is the same as the ventilation mode, but the amount of ventilation air supplied is equal to the fresh air requirement due to the building code or user requirements. The heat load of the ventilation air is taken into account in the ventilation credit mode (Collier et al, 1982). The performance parameters are the same as for the ventilation mode, except for the cooling capacity, which is given by:

$$CC = MA_S \cdot (H_1 - H_4) \quad (2.4)$$

2.2.3 Recirculation mode

This mode is shown in figure 2.2. Room air is circulated in a closed loop. It is dehumidified, sensibly cooled, evaporatively cooled and then supplied back to the room. Ambient air is used to cool the process air, to regenerate the desiccant and is then exhausted back outside. This mode usually has the advantage of a smaller moisture load on the desiccant wheel, but has the disadvantage of a higher cold sink temperature and no fresh air supply (Collier et al, 1982). The performance parameters are given by:

$$CC = MA_S \cdot (H_1 - H_4) \quad (2.5)$$

$$Q = MA_R \cdot (H_8 - H_7) \quad (2.6)$$

$$COP = CC/Q \quad (2.7)$$

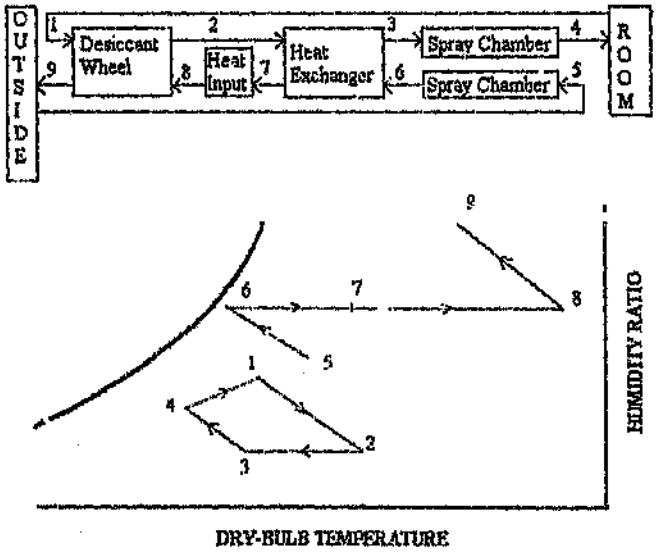

FIGURE 2.2: Schematic diagram of a DEC system operating in the recirculation mode.

2.2.4 Make-up air mode

This mode is shown in figure 2.3. Ambient air is dehumidified, sensibly cooled, evaporatively cooled and supplied to the room, as with the ventilation mode. Ambient air is also used to cool the process air and to regenerate the desiccant, as with the recirculation mode. This creates a positive pressure inside the room and room air is exhausted by leaking outside through openings in the building. An advantage of this mode is that it prevents dust ingress from outside, but the cooling potential of the exhaust air is wasted (Collier et al, 1982). The performance parameters are given by:

$$CC = MA_S \cdot (H_{room} - H_1) \quad (2.8)$$

$$Q = MA_R \cdot (H_8 - H_7) \quad (2.9)$$

$$COP = CC/Q \quad (2.10)$$

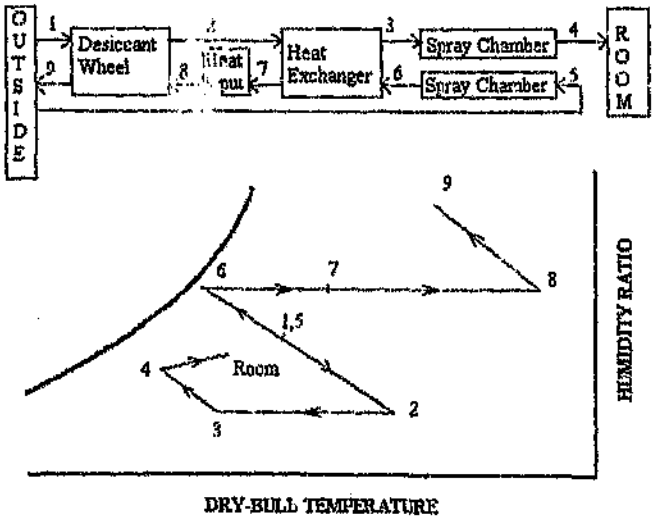

FIGURE 2.3: Schematic diagram of a DEC system operating in the make-up air mode.

2.2.5 More complex cycles

The ventilation, ventilation credit, recirculation and make-up air modes use only the basic components of a DEC system. By adding more components, one can improve the performance of the system at the expense of complexity and cost. An almost unlimited number of variations can be designed, but only the Dunkle cycle and the refrigeration-assisted modes are described here.

2.2.5.1 Dunkle cycle

The Dunkle cycle is shown in figure 2.4. It is similar to the recirculation mode, but uses the room air to provide a lower cold sink temperature, as in the ventilation mode. This additional cooling capacity is at the expense of higher moisture loading on the desiccant, which therefore requires more regeneration energy. Generally, the Dunkle cycle performs better than the basic DEC modes, but requires an additional heat exchanger (Collier et al, 1982).

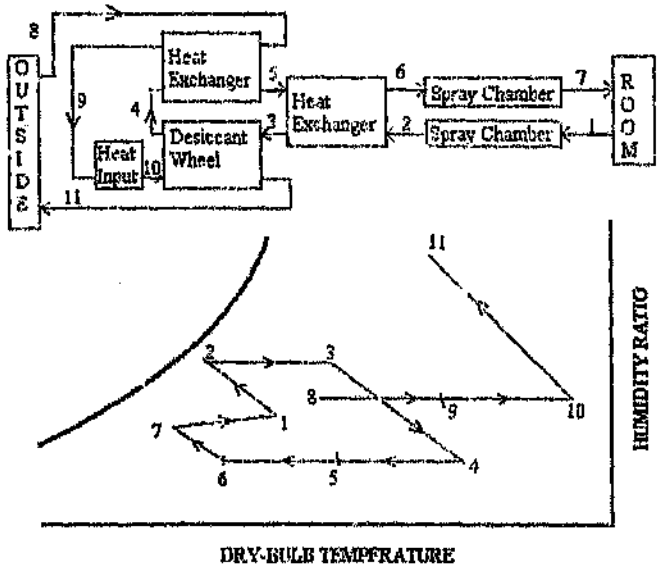

FIGURE 2.4: Schematic diagram of the Dunkle cycle.

2.2.5.2 Refrigeration assisted DEC cycle

The refrigeration-assisted cycle is shown in figure 2.5. The combination of DEC systems with conventional vapour compression refrigeration, has many advantages:

(1) The refrigeration condenser heat can be used to regenerate the desiccant.

(2) The process air can have a dew point below 0 °C after dehumidification. The refrigeration unit can therefore cool the air to low temperatures without the risk of ice buildup on the cooling coils.

(3) The humidity ratio and dry-bulb temperature, of the process air, can be made lower than for any other DEC or conventional air conditioning system. This means that smaller equipment and ducting are required, which means lower initial capital cost of the system.

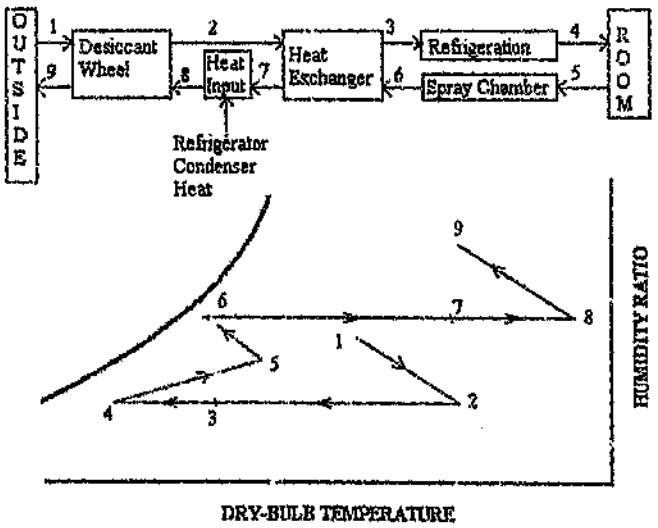

FIGURE 2.5: Schematic diagram of the refrigeration assisted DEC cycle.

2.2.6 Two stage evaporative cooling

The two stage evaporative cooling mode is shown in figure 2.6. When the humidity ratio of the outside air is less than that in the room, then evaporative cooling alone could provide sufficient cooling, depending on the latent and sensible heat loads. The room exhaust air is directly evaporatively cooled in a spray chamber (4-5) and is used to cool the supply air in a heat exchanger (1-2 and 5-6). The supply air is further cooled in a spray chamber (2-3), by evaporative cooling, to adjust the sensible heat ratio of the supply air. The DEC system shown in figure 1.1 could be operated as a two stage evaporative cooling system by providing bypass ducts around the desiccant wheel. Alternatively, the desiccant wheel could be kept stationary without being regenerated, in the case of desiccants in which deliquescence does not occur (such as silica gel). The performance equations are:

$$CC = MA_S \cdot (H_4 - H_3) \quad (2.11)$$

$$Q = 0 \quad (2.12)$$

$$COP(\text{thermal}) = CC/Q = \text{infinite} \quad (2.13)$$

$$EER = CC/(\text{electrical energy used}) \quad (2.14)$$

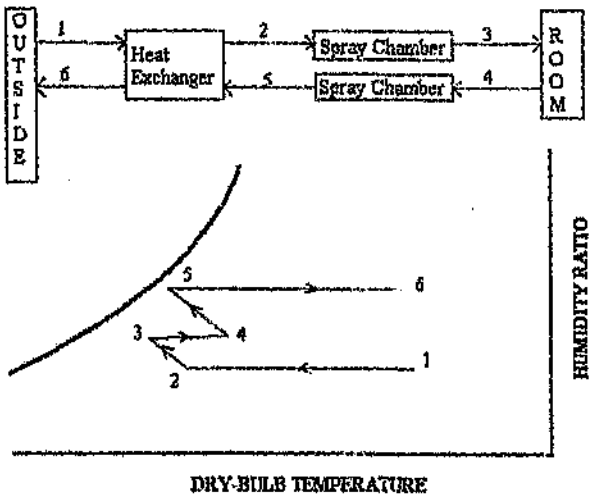

FIGURE 2.6: Schematic diagram of a two stage evaporative cooling cycle

2.2.7 Winter mode

One of the possible configurations of the winter mode is shown in figure 2.7. When the room requires heating and humidification (such as in winter), then the winter mode can be used. The speed of rotation of the desiccant wheel is increased from typically 0.25 revolutions per minute, to approximately 10 revolutions per minute. The return air is passed through the desiccant wheel, which acts as an enthalpy exchanger and transfers heat and moisture from the return air to the supply air stream. The supply air is further heated and humidified (in the spray chamber). The DEC system shown in figure 1.1 could be operated in the winter mode by keeping the heat exchanger stationary, adding an auxiliary heating device, and by not supplying water to the return air spray chamber. Other possible configurations of the winter mode include using a sensible heat exchanger (if the heat capacity of the desiccant wheel is insufficient) between the heater (in figure 2.7) and the desiccant wheel.

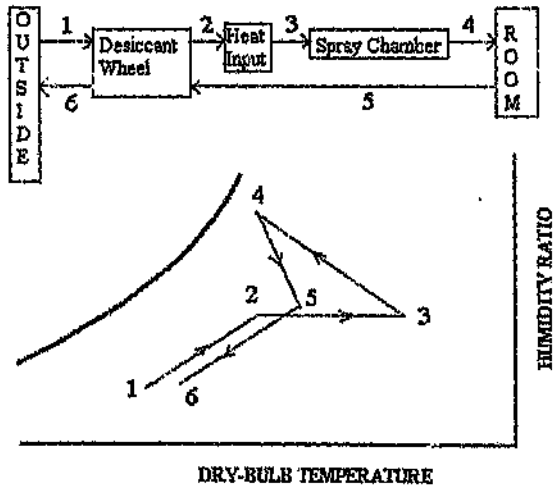

FIGURE 2.7: Schematic diagram of a DEC system operating in winter mode.

CHAPTER 3
LITERATURE REVIEW

3.1 Mathematical Models of Desiccant Wheels

The heat and mass transfer in the desiccant wheel (sometimes referred to as an enthalpy exchanger) is a complex process that is described by four non-linear coupled hyperbolic simultaneous partial differential equations. Several methods have been developed to solve or simplify these equations, to predict the performance of the desiccant wheel.

Bullock and Threlkeld (1966) developed one of the first mathematical models based on numerical solutions. The theoretical performance predictions compared well with the experimental results.

Banks (1971) described the process of heat and mass transfer in a desiccant wheel, in terms of characteristic potentials and specific capacity ratios in heat transfer alone. This method was used by **Close and Banks (1971)** to develop a model for the silica gel-water-air system. The characteristic potentials and specific capacity ratios were presented as plots on a psychrometric chart. The chart was used for predicting the behaviour of the system. The predictions were compared to measurements taken from a real system and were found to provide a guide to the behaviour of the system.

Maclaine-Cross and Banks (1972) solved the non-linear coupled hyperbolic simultaneous partial differential equations by replacing the former dependent variables of enthalpy and humidity ratio, by characteristic potentials and specific capacity ratios. Assumptions were made to simplify the model and theoretical predictions compared well with results from more accurate finite difference solutions.

Holmberg (1979) applied numerical methods of the finite-difference type to predict

the steady-state performance of a silica gel desiccant wheel.

Mathipraksam and Lavan (1980) linearized the governing equations for the desiccant wheel, by making certain approximations. These linearized equations were solved for a silica gel desiccant wheel.

Jurinak and Mitchell (1984) used a finite difference model to investigate the effect of various matrix properties on the dehumidifier performance.

Banks (1985) predicted the performance of the desiccant wheel by an analogy between heat and mass transfer and heat transfer alone. Approximate non-linear expressions for the combined potentials, used in the analogy, were derived for silica gel.

Van den Bulck et al (1985) modelled the desiccant wheel with infinite transfer coefficients using the method of characteristic potentials and the shock wave method. This was used in an Effectiveness-NTU (Number of Transfer Units) model that calculated the performance of the desiccant wheel more rapidly than other models.

Rau et al (1991) developed a finite difference model to predict the heat and mass transfer in rotary heat and mass exchangers using lithium chloride as the desiccant. The isotherms of lithium chloride exhibit discontinuities and therefore conventional numerical methods could not be used to solve the system.

3.2 Factors Affecting DEC Performance

Collier et al (1982) gave an overview of DEC systems, including the following items:

(1) For most desiccants, the heat of adsorption/absorption is only 5 to 10 per cent greater than the heat of condensation/vaporisation of water. This means that the sorption process is approximately a constant enthalpy process.

(2) The ideal desiccant has an isotherm where the critical temperature (T_c) is equal to the temperature of the dehumidified air leaving the desiccant wheel (point 2, figure 1.1). The critical temperature is the minimum temperature required to regenerate the desiccant (point 8, figure 1.1). The large deviation of the lithium chloride solution isotherms from the ideal behaviour means that the regeneration temperature must be raised much higher than the dehumidifier outlet temperature. This is illustrated by the isotherms given in figures 3.1 and 3.2.

(3) The desiccant isotherm depends on factors such as desiccant particle size. This means that a specific wheel can be designed to yield a variety of adsorption isotherm shapes using the same desiccant material.

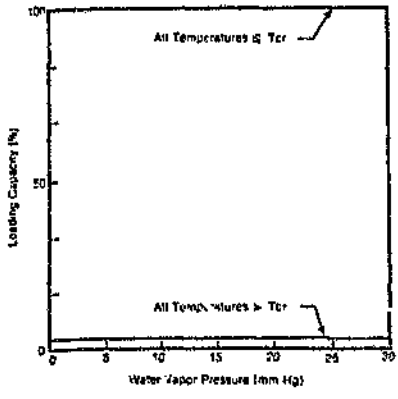

T_{cr} = minimum regeneration temperature

FIGURE 3.1: Adsorption isotherm for the "ideal" desiccant material (Collier et al, 1982).

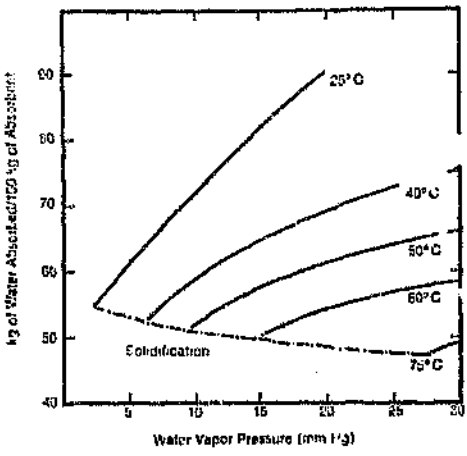

FIGURE 3.2: Adsorption isotherm for lithium chloride solutions (Collier et al, 1982).

Jurinak (1983) found that unbalanced flow (larger ratio of supply air to exhaust air) could increase the COP by 10 to 15 per cent in the ventilation mode and by up to 50 per cent in the recirculation mode.

Jurinak (1984) used a finite difference model to determine the effect of six matrix properties on performance:

(1) The desiccant sorption isotherm shape was found to have the greatest effect on performance.

(2) The maximum water content of the desiccant was found to have the second greatest effect.

(3) Desiccants with the smallest heat of sorption performed the best.

(4) A high thermal capacitance had a detrimental impact on dehumidification.

(5) The matrix moisture diffusivity was investigated but had little effect on performance.

(6) Sorption isotherm hysteresis was found to impair dehumidifier performance.

Epstein et al (1985) found that the addition of inert material to the desiccant wheel

matrix improved performance, provided that the heat exchanger performance was greater than about 85 per cent (to recover the heat carryover in the desiccant wheel). The optimum mass fraction of silica gel in the matrix was found to be 0.2.

Charoensupaya and Worek (1988) investigated the effect on performance of the following matrix characteristics:

(1) A longer channel length improved performance.

(2) The optimum mass fraction of lithium chloride to the total matrix mass was found to be 0.1. Different optimum fractions were found for other desiccants.

Van den Bulck et al (1988) found, from experimentation, that the maximum COP could be achieved with a regeneration temperature of 65 to 85 °C. The following optimal control strategy was proposed:

(1) Vary the exhaust air flow in direct proportion to the supply air flow rate. The exhaust air flow rate should be maintained at 60 to 80 per cent of that of the supply air for optimum performance.

(2) The wheel speed of rotation should be kept constant, since it has little effect on performance.

(3) Keep the regeneration temperature between 85 and 100 °C, since the COP is not affected much by operating variations in this range and the COP is near its maximum.

Collier and Cohen (1988) examined methods of improving the performance of DEC systems and described the following:

(1) The addition of inert heat capacity to the desiccant matrix can optimise the COP. However, this requires a larger desiccant wheel because of the additional material and requires a larger heat exchanger to recover the additional heat transferred to the supply air stream.

(2) Staging the regeneration process yields the best improvement of COP.

(3) The flow in the heat exchanger should be balanced but should be unbalanced in the desiccant wheel.

The overall conclusion was that staged regeneration with no inert material gave the

optimum COP, which increased from 0.80 to 1.10.

Holmberg (1989) predicted the minimum temperatures at which condensation and frosting would occur in rotating desiccant wheels. The temperatures are lower than in sensible heat exchangers, because moisture is removed and the dew point lowered. Condensation must be avoided with hygroscopic desiccants such as lithium chloride, since the desiccant will run out with the water.

Collier (1989) investigated the effect of matrix properties on the performance of a DEC system. The following was found:
(1) An increase in matrix heat capacity always decreases the cooling capacity. However, no general statement can be made concerning the COP.
(2) The heat and mass resistance is not influenced appreciably by the desiccant type.

Collier et al (1990) investigated various factors that influence DEC performance by means of computer simulations based on a desiccant with a type 1M isotherm shape (similar to that of lithium chloride) with the following findings:
(1) A reduction of the desiccant mass fraction in the desiccant wheel from 1 to 0.5 only reduced the COP slightly.
(2) The quantity of desiccant moisture uptake at saturation (100 % relative humidity) had no effect on COP but a smaller moisture uptake decreased the cooling capacity.
(3) An increase in dry-bulb temperature or humidity ratio decreased the COP in the ventilation mode.
(4) At ARI conditions (see nomenclature for definition), a COP of 0.91 to 1.07 was obtained in the ventilation mode and a COP of 0.75 to 0.90 was obtained in the recirculation mode. The ventilation mode performed better in dry climates and the recirculation mode performed better in humid climates.
(5) An increase in regenerating temperature increased the cooling capacity, but the COP remained relatively constant.
(6) The degree of staged regeneration was the second most influential parameter affecting performance, after the isotherm shape.

Worek et al (1991) investigated various factors affecting DEC performance (for desiccants in general), with the following findings:

(1) The COP was insensitive to changes in regenerating fraction, for a desiccant moisture loading greater than 0.2.

(2) The sorption time (inversely proportional to wheel rotational speed) is strongly dependent on the moisture loading and the desiccant isotherm shape.

(3) The type 1M isotherm (similar to that of lithium chloride) gives the best COP.

(4) The heat exchanger has a significant effect on performance. A reduction in efficiency from 93 to 87 per cent reduced the COP from 1.09 to 0.81.

ASHRAE (1996) describes many of the relationships between the operating parameters in solid desiccant systems. These relationships are illustrated graphically for a silica gel system in figures 3.3 to 3.7:

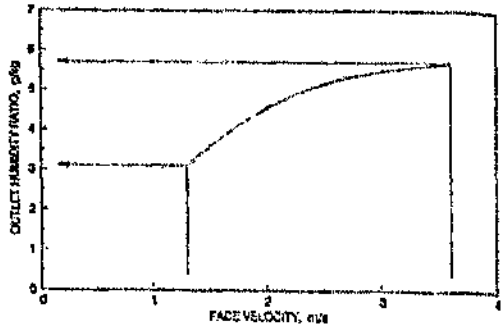

FIGURE 3.3: Effect of supply air velocity on humidity ratio of dehumidified air (ASHRAE, 1996).

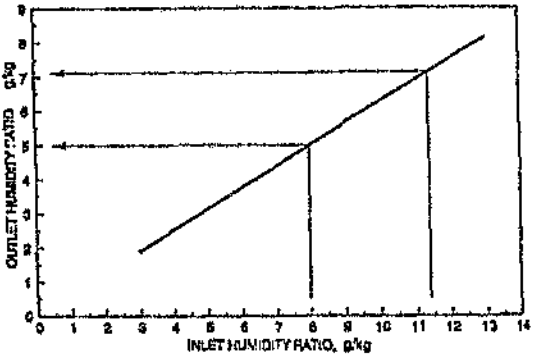

FIGURE 3.4: Effect of humidity ratio of supply air on humidity ratio of dehumidified air (ASHRAE, 1996).

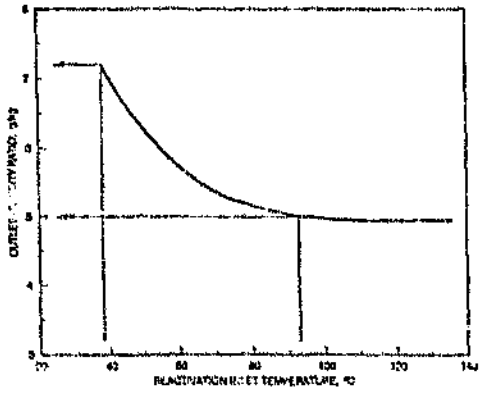

FIGURE 3.5: Effect of regeneration temperature on humidity ratio of dehumidified air (ASHRAE, 1996).

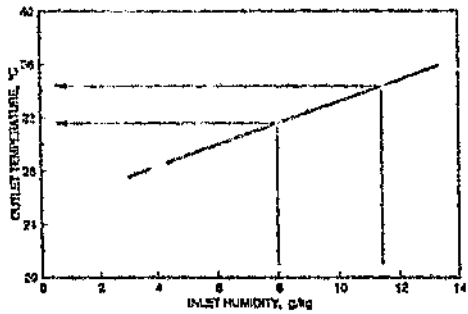

FIGURE 3.6: Effect of humidity ratio of supply air on dry-bulb temperature of dehumidified air (ASHRAE, 1996).

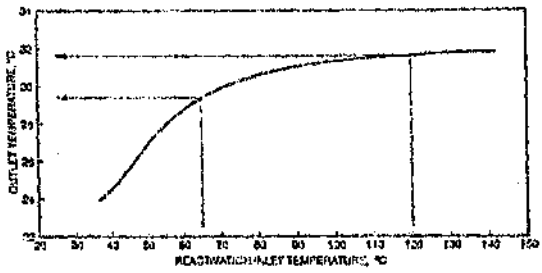

FIGURE 3.7: Effect of regeneration temperature on dry-bulb temperature of dehumidified air (ASHRAE, 1996).

Pesaran and Helden (1994) investigated the effect of ambient pressure on DEC performance using computer simulations. As ambient pressure decreases from 1.0 to 0.8 atm the thermal COP increases by 8 per cent for both fixed-mass and fixed-volume flow rates. The cooling capacity deceased by 14 per cent for the fixed-volume flow rate but increased by 7 per cent for the fixed-mass flow rate.

Menon (1996) did random tests on a DEC system (the same system used in this project). Although the results were inconclusive, they indicated that DEC and two stage evaporative cooling systems could be viable for air conditioning.

3.3 Desiccant Degradation

Pesaran and Penny (1991) simulated the effect of airborne contaminants and thermal cycling, on desiccants. The results showed a decrease in cooling capacity and COP of 10 to 35 per cent. This degradation can be compensated for, to some degree, by increasing the rotational speed of the desiccant wheel.

Belding et al (1991) investigated several factors affecting performance of desiccant wheels. One of these factors was desiccant cyclic ageing. The results showed that most degradation occurred early in the life of the desiccant and could be described by an expenential decay function (see figure 3.8). The experiments also showed that lithium chloride deliquescence occurred as low as 15 per cent relative humidity. This only occurred above 80 per cent relative humidity for all other desiccants.

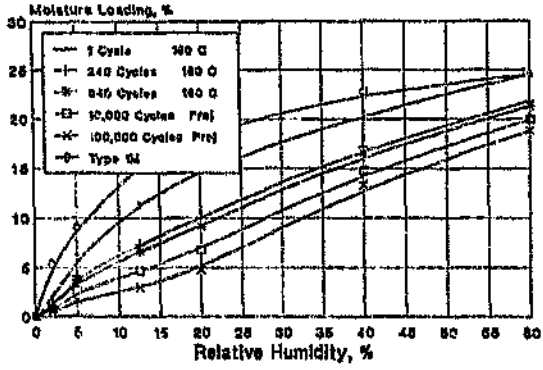

FIGURE 3.8: Ageing characteristics and projections for a typical desiccant (Belding et al, 1991).

Pesaran (1993) experimented with five desiccants, including lithium chloride to determine the extent of the degradation due to exposure to cigarette smoke and thermal cycling. The moisture absorption capacity decreased by 30 to 70 per cent over an equivalent period of 4 to 8 years of field operation (see figure 3.9).

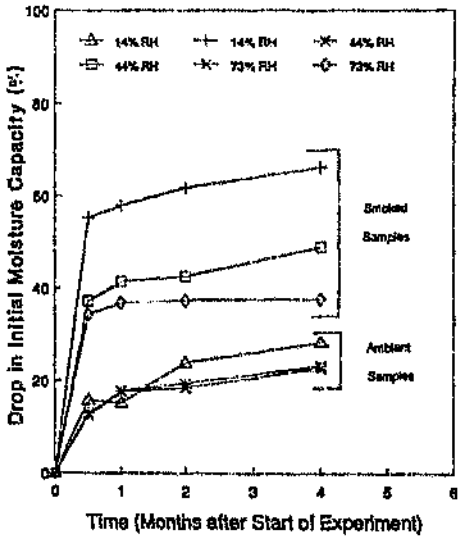

FIGURE 3.9: Capacity loss of silica gel exposed to cigarette smoke (Pesaran, 1993).

3.4 Feasibility Studies

Cohen and Slosberg (1988) did performance simulations to evaluate the potential of DEC systems for economical space conditioning. The results showed that the ventilation mode had the best overall COP.

Nelson et al (1978) did a feasibility study of a DEC system using solar energy. The computer simulations showed that energy requirements for the ventilation mode, were approximately half that required for the recirculation mode. The results of COP versus regeneration temperature are shown in figure 3.10 below. A control strategy was proposed that involved varying regeneration temperature and both spray chamber efficiencies.

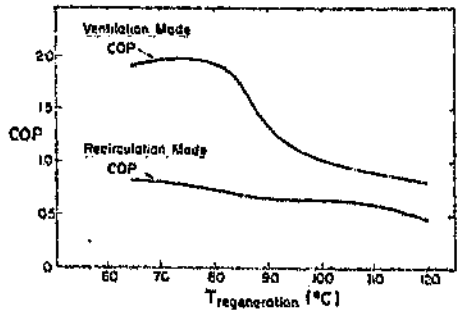

FIGURE 3.10: COP for ideal systems as a function of regenerating temperature, for July 1955 in Miami (Nelson et al, 1978).

Marciniak et al (1991) tested a DEC system in a quick service restaurant in Houston, Texas. Off-the-shelf equipment was used and the system generally operated satisfactorily and maintained the room design conditions. However, the system frequently failed due to problems associated with the controls and gas burners. The system was found to be more unreliable and expensive than conventional air conditioning units commercially available and of the same capacity.

Claasen (1995) presented a model for evaluating the feasibility of evaporative

cooling in South Africa. He found that evaporative cooling could reduce the cooling requirements of existing conventional plants by up to 30 per cent.

Stiesch et al (1995) investigated the feasibility of enthalpy exchangers for use in the USA. The results showed that significant cost saving could be achieved with both enthalpy exchangers and sensible heat exchangers.

CHAPTER 4
MATHEMATICAL MODEL OF A DEC SYSTEM

4.1 Mathematical Model

The purpose of developing this simple mathematical model of a DEC system was to provide a means of predicting the performance of the system with reasonable accuracy based on easily obtainable information. The model uses manufacturer's catalogue information and the accuracy depends on the accuracy of this information. This model calculates two moist air properties, at each point in the process, from which the remaining properties and performance parameters can be calculated. The equations to calculate these moist air properties were taken from ASHRAE (1994) and Jones (1973). The ambient air conditions, room air conditions and regeneration temperature or heat input are usually known and the other information can be calculated from the processes that occur in each component of the system.

4.1.1 Desiccant wheel

The manufacturer's information usually gives the dehumidifier outlet conditions (see appendix F), from which the regeneration outlet conditions can be calculated. This information can then be used to calculate operating efficiencies, or alternatively the air conditions can be calculated if the efficiencies are supplied by the manufacturer. The definition of the desiccant wheel efficiencies depends on the text consulted. For the purposes of this project, the performance of the desiccant wheel can be described by three efficiencies:

EDH1 = efficiency of moisture removal
EDH2 = efficiency of heat transfer
ERG = efficiency of regeneration

4.1.1.1 Efficiency of moisture removal (EDH1)

$$EDH1 = (W_1-W_2)/(W_1-W_{21}) \quad (4.1)$$

where W_{21} (see figure 4.1) is the humidity ratio at a point at which the wet-bulb temperature of the inlet air (TWB_1) intersects the relative humidity of the regeneration air (RH_8). This is approximately the lowest humidity ratio that can be obtained by the supply air leaving the desiccant wheel, for the given operating conditions (if the air is allowed sufficient time to reach equilibrium with the desiccant, and if no heat carryover occurs). The exact value of W_{21} varies depending on the characteristics of the desiccant used, but the definition given here is a good normalising parameter (Jurinak, 1983). The efficiency of moisture removal EDH1 can be calculated from the humidity ratio W_1 (ambient conditions' humidity ratio W_2 (from catalogue data) and humidity ratio W_{21} (by the method shown in figure 4.1).

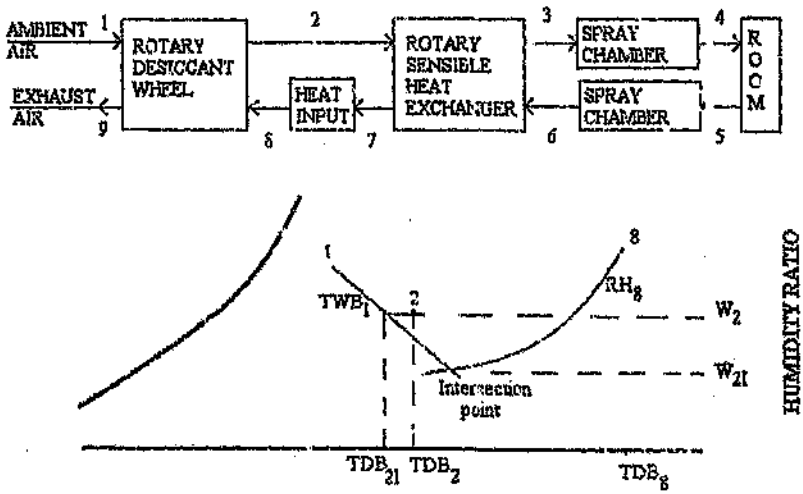

FIGURE 4.1: Method of determining the ideal humidity ratio W_{21} and ideal dry-bulb temperature TDB_{21}. (Note: This figure is based on the ventilation mode described in figure 1.1).

4.1.1.2 Efficiency of heat transfer (EDH2)

$$EDH2 = (TDB_2-TDB_{21})/(TDB_8-TDB_{21}) \quad (4.2)$$

where TDB_{21} (see figure 4.1) is the dry-bulb temperature if no heat is transferred to the supply air from the matrix of the desiccant wheel, i.e. the dry-bulb temperature at the intersection of the wet-bulb temperature TWB_1 and humidity ratio W_2. The efficiency of heat transfer EDH2 can be calculated from TDB_{21} (see figure 4.1), TDB_2 (from catalogue data) and TDB_8 (regeneration temperature).

4.1.1.3 Regeneration efficiency (ERG)

This is a measure of the amount of regeneration heat (Q) used to evaporate the water vapour during regeneration i.e. the ratio of latent heat increase to regeneration heat supplied (see figure 4.1 for numbering).

$$ERG = 2501\cdot(W_9-W_8)\cdot MA_R/Q \quad (4.3)$$

The humidity ratio $W_8 = W_7$ which can be calculated (equations 4.11 and 4.27).
The regeneration heat input Q can be measured or calculated (see section 4.1.5).
The humidity ratio W_9 can be calculated (from equation 4.4).

4.1.1.4 Linking dehumidification and regeneration processes

The following equations represent the heat and mass conservation between the two processes in the desiccant wheel (see figure 4.1 for numbering):

Moisture transfer: $(W_1-W_2)\cdot MA_S = (W_9-W_8)\cdot MA_R$ (4.4)

Heat transfer: $(TDB_2-TDB_{21})\cdot MA_S = (TDB_{91}-TDB_9)\cdot MA_R$ (4.5)

Where TDB_{91} is the dry-bulb temperature if no heat is transferred from the return air

to the desiccant wheel, i.e. the dry-bulb temperature at the intersection of the wet-bulb temperature TWB_8 and humi ratio W_9. This method is similar to that for determining the dry-bulb temperature TDB_{3I} (see figure 4.1).

4.1.2 Rotary heat exchanger

The heat exchanger efficiency (EHX) is the bigger of the following (see figure 4.1 for numbering):

Efficiency of heat transfer to the supply air:

$$EHX_S = (TDB_2-TDB_3)/(TDB_2-TDB_6) \quad (4.6)$$

Efficiency of heat transfer to the return air:

$$EHX_R = (TDB_7-TDB_6)/(TDB_2-TDB_6) \quad (4.7)$$

EHX_S and EHX_R can be obtained from catalogue information for given mass flow-rates of the supply air and return air. The moist air properties at points 3 and 7 (see figure 4.1) can then be calculated by rearranging equations 4.6 and 4.7:

$$TDB_3 = TDB_2 - EHX_S\cdot(TDB_2-TDB_6) \quad (4.8)$$

$$TDB_7 = TDB_6 + EHX_R\cdot(TDB_2-TDB_6) \quad (4.9)$$

$$W_3 = W_2 \quad \text{(see 4.1.1.1 for } W_2 \text{ and } TDB_2) \quad (4.10)$$

$$W_7 = W_6 \quad \text{(see 4.1.4 for } W_6 \text{ and } TDB_6) \quad (4.11)$$

4.1.3 Air carryover in heat exchanger

As the heat exchanger rotates, air in the matrix is carried over from one air stream to the next in both directions. This air mixing was significant only with the heat exchanger because its rotational speed was 40 times fa than that of the desiccant wheel. The volume of air carryover in the heat exchanger was calculated to be 0.0138 m³ from the wheel volume and rotational sp d, therefore (see figure 4.1 for numbering):

Mass flow-rate of carryover to supply air stream: $MC_S = 0.01384/SV_6$ (4.12)

Mass flow-rate of carryover to return air stream: $MC_R = 0.01384/SV_2$ (4.13)

Where SV = specific volume of the air.

The air properties, calculated in section 4.1.2 therefore had to be recalculated to allow for the air mixing (superscript RC denotes recalculated value):

$W_3^{RC} = [W_3 \cdot (MA_S - MC_S) + W_6 \cdot MC_S]/MA_S$ (4.14)

$W_7^{RC} = [W_7 \cdot (MA_R - MC_R) + W_2 \cdot MC_R]/MA_R$ (4.15)

$H_3^{RC} = [H_3 \cdot (MA_S - MC_S) + ((H_6 + H_7)/2) \cdot MC_S]/MA_S$ (4.16)

$H_7^{RC} = [H_7 \cdot (MA_R - MC_R) + ((H_2 + H_3)/2) \cdot MC_R]/MA_R$ (4.17)

$TDB_3^{RC} = (H_3^{RC} - 2501 \cdot W_3^{RC})/(1.005 + 1.84 \cdot W_3^{RC})$ (4.18)

$TDB_7^{RC} = (H_7^{RC} - 2501 \cdot W_7^{RC})/(1.005 + 1.84 \cdot W_7^{RC})$ (4.19)

The remaining moist air properties were then calculated from these values.

4.1.4 Spray chambers

The user can set the efficiency of both spray chambers, by increasing the water flow rate and nozzle discharge pressure. The efficiency can be as high as 100 per cent. See figure 4.1 for numbering.

$EV_S = (TDB_3 - TDB_4)/(TDB_3 - TWB_3)$ (4.20)

Therefore: $TDB_4 = TDB_3 - EV_S \cdot (TDB_3 - TWB_3)$ (4.21)

$TWB_4 = TWB_3$ (see note below) (4.22)

$EV_R = (TDB_5 - TDB_6)/(TDB_5 - TWB_5)$ (4.23)

Therefore: $TDB_6 = TDB_5 - EV_R \cdot (TDB_5 - TWB_5)$ (4.24)

$TWB_6 = TWB_5$ (see note below) (4.25)

Note: if the temperature of the spray water is close to the wet-bulb temperature of

the air and the evaporation rate is high, then the evaporative cooling is virtually a constant wet-bulb process (Jones, 1973).

4.1.5 Regeneration heaters

$$Q = MA_R \cdot (1.805) \cdot (TDB_8 - TDB_7) \quad (4.26)$$

$$W_8 = W_7 \quad \text{(no moisture gain in heaters)} \quad (4.27)$$

If the regeneration temperature TDB_8 (see figure 4.1 for numbering) is given, then the regeneration heat input Q can be calculated, or vice versa.

4.2 Sensitivity Analysis of Mathematical Model

4.2.1 Results of sensitivity analysis

A DEC simulation program was written based on the mathematical model (sections 4.1.1 to 4.1.5). This computer program is described in section 5.3.3 and is given in appendix D. This section (4.2.1) gives the results of simulations to test the performance sensitivities of the DEC system to variations in the following operating parameters:

- Efficiency of supply air spray chamber (EV_S).
- Efficiency of return air spray chamber (EV_R).
- Heat exchanger efficiency (EHX).
- Dry-bulb temperature of ambient air (TDB_1).
- Humidity ratio of ambient air (W_1).

The simulation results are given in tabular form and a brief summary of the main observations (from the results) is given below each table. The findings and general trends from the sensitivity analysis are discussed in section 4.2.2.

TABLE 4.2.1: Variation of efficiency of supply air spray chamber (EVs)

EVs (%)	0	20	40	60	80	100
TDB_4 (°C)	19.9	18.3	16.7	15.1	13.5	11.9
W_4 (g/kg)	7.37	8.03	8.68	9.34	9.99	10.65
EDH1 (%)	56	56	56	56	56	56
EDH2 (%)	19	19	19	19	19	19
ERG (%)	28	28	28	28	28	28
Q (kW)	4.60	4.60	4.60	4.60	4.60	4.60
CC (kW)	2.03	2.03	2.02	2.02	2.01	2.01
COP	0.44	0.44	0.44	0.44	0.44	0.44
TCC (kW)	3.05	3.05	3.04	3.04	3.03	3.03
TCOP	0.66	0.66	0.66	0.66	0.66	0.66

Note: See figure below for numbering (from figure 1.1).



The following trends were observed with increasing EVs :

(1) The dry-bulb temperature TDB_4 decreases and humidity ratio W_4 increases.

(2) All other parameters remain constant, except for a very small decrease in CC (cooling capacity in ventilation mode) and TCC (cooling capacity in ventilation credit mode), due to water enthalpy gain.

TABLE 4.2.2: Variation of efficiency of return air spray chamber (EV_R).

EV_R (%)	0	20	40	60	80	100
W_2 (g/kg)	6.6	6.6	6.7	6.7	6.8	6.8
TDB_6 (°C)	23.0	21.6	20.2	18.8	17.4	16.0
W_6 (g/kg)	11.11	11.69	12.27	12.85	13.43	14.01
EDH1 (%)	54	55	55	56	56	56
EDH2 (%)	18	18	19	19	19	19
ERG (%)	31	30	29	28	28	28
Q (kW)	4.43	4.47	4.50	4.53	4.56	4.60
CC (kW)	1.20	1.39	1.54	1.68	1.83	2.01
COP	0.27	0.31	0.34	0.37	0.40	0.44
TCC (kW)	2.22	2.41	2.56	2.70	2.85	3.03
TCOP	0.50	0.54	0.57	0.60	0.62	0.66

Note: See figure below for numbering (from figure 1.1).



The following trends were observed with increasing EV_R:

(1) A small decrease in moisture removal capability (since humidity ratio W_2 is higher), due to reduced regeneration efficiency (ERG), because of the higher vapour pressure in the regeneration air (higher humidity ratio W_6).

(2) The dry-bulb temperature TDB_6 decreases and humidity ratio W_6 increases.

(3) The regeneration heat input Q required increases slightly (to achieve the same relative humidity of the regenerating air) but cooling capacities CC and TCC increase more (lower cold sink) which results in increased COP and TCOP.

TABLE 4.2.3: Variation of heat exchanger efficiency (EHX).

EHX (%)	0	20	40	60	80	100
EDH1 (%)	56	56	56	56	56	56
EDH2 (%)	19	19	19	19	19	19
ERG (%)	15	17	19	22	25	31
Q (kW)	8.53	7.65	6.78	5.91	5.03	4.16
CC (kW)	-1.90	-1.01	-0.11	0.72	1.60	2.45
COP	-0.22	-0.13	-0.02	0.12	0.32	0.59
TCC (kW)	-0.88	0.02	0.91	1.74	2.62	3.48
TCOP	-0.10	0.00	0.13	0.30	0.52	0.84

Note: See figure below for numbering (from figure 1.1).



The following trends were observed with increasing EHX:

(1) The regeneration heat input Q required decreases, since more energy is recovered by the heat exchanger.

(2) The cooling capacities CC and TCC increase, since more heat is removed from the supply air.

(3) The COP and TCOP increase, because of (1) and (2) above.

TABLE 4.2.4: Variation of dry-bulb temperature of ambient air (TDB_1).

W_1 (g/kg)	10					15				
TDB_1 (°C)	20	24	28	32	36	20	24	28	32	36
W_2 (g/kg)	5.6	6.0	6.3	6.8	7.2	8.5	9.0	9.4	9.8	10.4
TDB_2 (°C)	37.5	40.3	43.0	45.8	48.4	42.1	44.8	47.5	50.0	52.5
W_1-W_2 (g/kg)	4.4	4.0	3.7	3.2	2.8	6.5	6.0	5.6	5.2	4.6
EDH1 (%)	61	59	59	56	55	61	60	59	59	58
EDH2 (%)	17	17	17	19	20	18	19	20	20	22
ERG (%)	30	30	30	28	27	51	51	51	52	51
Q (kW)	5.79	5.39	5.00	4.60	4.22	5.13	4.74	4.35	3.99	3.63
CC (kW)	2.63	2.45	2.29	2.01	1.83	1.47	1.21	1.04	0.82	0.52
COP	0.46	0.46	0.46	0.44	0.43	0.29	0.26	0.24	0.20	0.14
TCC (kW)	1.68	2.16	2.65	3.03	3.51	2.56	2.96	3.44	3.89	4.25
TCOP	0.29	0.40	0.53	0.66	0.83	0.50	0.62	0.79	0.97	1.17

Note: See figure below for numbering (from figure 1.1).



The following trends were observed with increasing TDB_1:

(1) The moisture removal capability (W_1-W_2) and efficiency of moisture removal EDH1 decrease since the relative humidity RH_1 is lower.

(2) More moisture is removed for a higher humidity ratio W_1 for the same dry-bulb temperature TDB_1.

(3) The efficiency of heat transfer in the desiccant wheel EDH2 increases, since the difference between the dry-bulb temperatures TDB_8 and TDB_2 decreases for the same amount of heat transferred.

(4) The regeneration heat Q decreases, since the dry-bulb temperature TDB_2 increases and more heat is regained by the return air.

(5) The cooling capacity CC decreases, because the humidity ratio W_2 increases and

the 10 per cent of the heat not recovered by the heat exchanger increases (higher dry-bulb temperature TDB_2).

(6)The cooling capacity TCC increases, since the increase in the heat recovered by the heat exchanger, is included in the cooling calculation.

(7) COP decreases only slightly, because of (4) and (5) above.

(8) TCOP increases, because of (4) and (6) above.

(9) A lower humidity ratio W_1 results in higher CC and COP, but lower TCC and TCOP.

TABLE 4.2.5: Variation of humidity ratio of ambient air (W_1).

TDB_1 (°C)	24					36				
W_1 (g/kg)	8	10	12	14	16	8	10	12	14	16
TDB_2 (°C)	38.2	40.3	42.2	44	45.7	46.4	48.5	50.3	51.9	53.2
W_2 (g/kg)	5.0	6.0	7.2	8.3	9.5	5.9	7.2	8.4	9.7	11.1
W_1-W_2 (g/kg)	3.0	4.0	4.8	5.7	6.5	2.1	2.8	3.6	4.3	4.9
EDH1 (%)	56	59	59	60	61	55	55	57	58	57
EDH2 (%)	17	17	18	18	19	18	20	21	22	23
ERG (%)	21	30	38	47	56	19	27	36	46	55
Q (kW)	5.69	5.39	5.12	4.86	4.61	4.51	4.21	3.95	3.72	3.53
CC (kW)	2.83	2.45	1.97	1.52	1.02	2.36	1.83	1.35	0.83	0.28
COP	0.50	0.46	0.38	0.31	0.22	0.52	0.44	0.34	0.22	0.08
TCC (kW)	1.73	2.16	2.49	2.86	3.17	3.22	3.51	3.85	4.15	4.42
TCOP	0.30	0.40	0.49	0.59	0.69	0.71	0.83	0.97	1.12	1.25

Note: See figure below for numbering (from figure 1.1).



The following trends were observed with increasing humidity ratio W_1 (reasons are the same as for table 4.2.4):

(1) The moisture removal capability (W_1-W_2) and efficiency of moisture removal EDH1 increase.

(2) The efficiency of regeneration ERG increases.

(3) The regeneration heat input Q decreases and the dry-bulb temperature TDB_2 increases.

(4) CC and COP decrease and are lower for higher humidity ratio W_1.

(5) TCC and TCOP increase and are higher for higher humidity ratio W_1.

4.2.2 Discussion of sensitivity analysis

4.2.2.1 Spray chambers

The efficiency of the supply air spray chamber did not affect the performance of the DEC system, but only changed the sensible heat ratio of the supply air to the room.

The efficiency of the return air spray chamber had a significant effect on cooling capacity and COP. An increase in spray chamber efficiency decreased the cold sink temperature of the heat exchanger, which resulted in more heat being removed from the supply air.

4.2.2.2 Heat exchanger

The efficiency of the heat exchanger had a very large effect on performance (more significant than the efficiency of the supply air spray chamber). An increase in heat exchanger efficiency resulted in more heat being recovered from the supply air, which increased the cooling capacity and COP. The recovered heat also reduced the amount of regeneration energy required, which further increased the COP.

4.2.2.3 Ambient air conditions

An increase in the dry-bulb temperature of the ambient air (TDB_1) reduced the cooling capacity and COP in the ventilation mode, but increased the cooling capacity and COP in the ventilation credit mode. The same trends were observed for an increase in the humidity ratio of the ambient air (W_1).

The reason for these trends is that the dry-bulb temperature and humidity ratio of the supply air leaving the desiccant wheel is higher in both cases. This means that the energy of the supply air leaving the heat exchanger is higher, since the efficiency of the heat exchanger does not change significantly. These factors reduce the cooling capacity and COP in the ventilation mode. However, a greater quantity of heat is removed in the heat exchanger, which increases the cooling capacity and COP in the ventilation credit mode.

An increase in the dry-bulb temperature of the ambient air reduces the absorption capability of the desiccant wheel (less cooling of the wheel) which results in a higher humidity ratio of the supply air leaving the desiccant wheel. The supply air temperature leaving the desiccant wheel is also higher as a result of the inlet air temperature being higher.

An increase in the humidity ratio of the ambient air results in more moisture being absorbed from the air. However, despite the increase in moisture removal efficiency, the humidity ratio of the air leaving the desiccant wheel is also higher. The dry-bulb temperature of the supply air leaving the desiccant wheel is also higher (more latent heat converted to sensible heat).

4.2.2.4 Desiccant wheel

The three performance parameters of the desiccant wheel: efficiency of moisture absorption (EDH1), efficiency of heat exchange in the desiccant wheel (EDH2), and efficiency of regeneration (ERG), are strongly dependent on the regeneration

temperature. However, the manufacturer's information (see appendix F) was only available for a regeneration temperature of 70 °C and simulations were therefore not possible for the performance parameters of the desiccant wheel.

The following performance trends would be expected:

- An increase in efficiency of regeneration (ERG) should increase COP since less regeneration energy would be required.
- An increase in the efficiency of heat transfer in the desiccant wheel (EDH2) should reduce cooling capacity since more heat is being carried over to the supply air.
- An increase in the efficiency of moisture absorption (EDH1) should increase the cooling capacity.

CHAPTER 5
EXPERIMENTAL ARRANGEMENT OF DEC TEST SYSTEM

A basic desiccant-evaporative cooling test system was installed at the School of Mechanical Engineering, University of the Witwatersrand, Johannesburg, in 1995, and some random tests were done (Menon, 1996). A German company, Klingenburg, manufactured the main components of the system and a local South African company, Aero Duct, installed the overall system. An instrumentation and data acquisition and reduction system was installed as part of this project. The complete test system is shown in figure 5.1.



FIGURE 5.1: DEC test unit

5.1 Main Components of the Test System

5.1.1 Rotary desiccant wheel

The Klingenburg SECO 800 desiccant wheel is a cylindrical structure with small corrugated parallel passages. It is made of cellulose impregnated with lithium chloride. The wheel is 200 mm long and has a diameter of 705 mm. It is belt driven, by a 3-phase, 34 W, 50 Hz motor running at 1300 rpm. The desiccant wheel was supplied with a 174 mm diameter pulley, which rotates the wheel at 0.24 rpm. A second pulley, with a diameter of 87 mm, was made up to reduce this speed to 0.12 rpm.

5.1.2 Rotary heat exchanger

The Klingenburg RRT 800 rotary compact heat exchanger has the same dimensions as the desiccant wheel, but is made of thin corrugated aluminium sheets. It rotates at 11 rpm and is belt driven by a 3-phase, 90 W, 50 Hz, 1350 rpm motor.

5.1.3 Spray Chambers

The supply and return air spray chambers (manufactured by Klingenburg) were identical. Each had a reciprocating pump, driven by a 550 W motor, to supply tap water to the spray nozzles. The pump pressure was set by means of a frequency control box, which controlled the motor rotational speed. The maximum allowable pressure was 90 bar. Each spray chamber had two 0.17 mm nozzles that sprayed a fine aerosol mist. The internals of the spray chamber were designed to provide turbulence and to provide acoustic resonance, which improves the evaporation efficiency. Mist eliminators were situated at the exit to remove any remaining water droplets from the air stream.

5.1.4 Fans

The supply air and return air centrifugal fans were identical. Each fan had a 220 V, 50 Hz, 8 A variable resistance controller with which to set the rotational speed and hence air flow rate.

5.1.5 Regeneration heaters

There were four 1.8 kW electrical heaters to heat up the return air for regeneration.

5.1.6 Inlet air pre-conditioning system

In order to test the DEC system at different ambient conditions, it was necessary to control the inlet air conditions. This was done with two 1.8 kW electrical heaters and a humidifier. The Electro-Vap EL-9 humidifier was capable of supplying a maximum of 6 kilograms of steam per hour, despite being rated at 10 kg/hr. A problem with the humidifier was that the steam output was not constant, but dropped slightly as cold water was added to the boiler and then slowly increased until more water was added.

The humidifier and heaters alone were not sufficient during the winter months and a further modification was done to increase the inlet air temperature and humidity: The exhaust air ducting was changed to discharge the hot humid air at the inlet of the supply air duct. This modification, together with the heater and humidifier, was sufficient to simulate any ambient conditions.

5.2 Data Acquisition and Reduction system

5.2.1 Overview

Aspirated psychrometers were used to measure the air properties at various points in the process (see figure 5.2). Sample points were installed that used small computer fans to draw an average air sample from 16 to 24 points (depending on the size of the duct) across the cross-section of the duct. This air sample was passed over two temperature sensors, one to measure the dry-bulb temperature and the other, covered with a wetted cotton wick, to measure the wet-bulb temperature. The analogue signal from these temperature sensors was converted to a digital signal using a PC 30 A/D card. A software program read the digital voltages and convert them to temperature values, which could be used to calculate the air properties and performance parameters. Hyg transmitters, that measure relative humidity, were used to check the accuracy of aspirated psychrometer readings at low relative humidities. A MedM-500 micromanometer and pitot tube were used to measure air flow rate and a Fluke multimeter was used to measure electrical power consumption of the components of the DEC system.



FIGURE 5.2: Air sampling device including aspirated psychrometer and radiation shield.

5.2.2 Temperature measurement

A third year student installed an instrumentation system in 1996, as a laboratory project. This system used thermocouples but was useless because of false readings, due to excessive electrical noise and various other problems such as static electricity grounding through the thermocouples. All these problems were solved at the start of this project but the best accuracy that could be obtained with the thermocouples was within 0.5 °C. This was insufficient to satisfy the minimum requirements of 0.3 °C accuracy specified by ASHRAE 41.1-1986. Precision integrated circuit (IC) temperature sensors (LM 35's) were then used and after calibration, resulted in a precision of 0.1 °C and accuracy of 0.2 °C for the 18 sensors (see appendix A). This accuracy was only achieved by installing a low pass filter on each LM 35, to filter out electrical noise and to offset the capacitive load of the wiring. The electrical noise was further filtered in the data reduction software program, where a sample of 100 measurements was statistically analysed to get the mean value and confidence limits. The calculated error was incorporated in the error analysis software program. The sampling devices from the third year project (figure 5.2) were slightly modified, to comply with ASHRAE 41.1-1986 and were reused for this project. Radiation shields were installed on the 5 sample points near the regeneration air heaters and the desiccant wheel to avoid incorrect readings due to radiation from hot surfaces. The relative humidity of the hot regeneration air (point 8, figure 1.1) was too low for accurate measurement by the aspirated psychrometers or the hygrotransmitters. The calculated humidity ratio value upstream of the heaters (point 7, figure 1.1) was therefore used together with the measured dry-bulb temperature of point 8 to calculate the properties at point 8. This is acceptable since no air leakage occurs between these points and the humidity ratio remains constant.

5.2.3 Hygrotransmitters

Aspirated psychrometers can only be used accurately from 20 to 100 per cent relative humidity. Insufficient wet-bulb depression occurs below 20 per cent relative humidity and the error increases as the relative humidity decreases below 20 per

cent. Two Delta Ohm HD 8907TC/150 hygrotransmitters (see appendix E) were used to measure the relative humidity in such cases and the necessary correction was then applied to the wet-bulb measurement.

The hygrotransmitters have a capacitor made of a polymer desiccant that gives a certain capacitance reading depending on the moisture content of the desiccant, which is in turn dependant on the relative humidity. While using the hygrotransmitters, it was found that the relative humidity reading was only accurate at a humidity ratio of 14 g/kg. This was probably due to different desiccant characteristics at different air humidity ratios. The hygrotransmitters were therefore calibrated at different humidity ratios and actual values were interpolated from these curves to give an accuracy of approximately one per cent relative humidity. The calibration curves are given in appendix A.

5.2.4 Computer hardware

An Eagle Technology PC30 analog to digital card (see appendix E) was used in a 486 computer to convert the analog signals from the temperature sensors into digital signals. The PC30 card also had support software that could be used with the Turbo Pascal programming language. A software program was written and developed for data acquisition and analysis (see section 5.3.1).

5.2.5 Air flow measurement

The "Log-Tchebycheff" method was used to measure the air flow rate as shown in figure 5.3 (ASHRAE 41.2-1987 and BS 1042: Section 2.1-1983). Differential pressure traverses were carried out at one cross-section in the supply air duct and one cross-section in the return air duct. The pressure differentials were measured with a pitot tube and micromanometer. The micromanometer used was a MedM-500, which has a resolution of 0.1 Pascal and range of 0 to 500 Pa. The flow rate in the return duct could also be calculated from the measured electrical power of the regeneration heaters and the air temperature increase after heating.

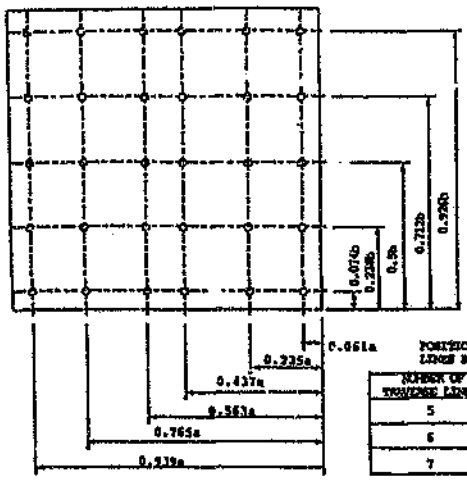

POSITION OF ALTERNATIVE MEASURING POINTS AND TRAVERSE LINES RELATIVE TO SIDE LENGTHS FOR RECTANGULAR DUCTS

NUMBER OF TRAVERSE LINES	POSITION RELATIVE TO INNER WALL
5	0.074, 0.238, 0.5, 0.712, 0.926
6	0.061, 0.235, 0.437, 0.563, 0.765, 0.939
7	0.053, 0.203, 0.366, 0.5, 0.634, 0.797, 0.947

FIGURE 5.3: The "Log-Tchebycheff" method of air flow rate measurement (ASHRAE 41.2-1987).

5.2.6 Electrical power measurement

The electrical current and voltage for each of the two-phase fan motors, pump motors and heaters (regeneration heat input) were measured using a Fluke multimeter. The electrical power consumption for each case was calculated by multiplying the measured voltage and current.

5.3 Computer Programs

The following three computer programs were written in Turbo Pascal for the purposes of this project:

5.3.1 Data acquisition and processing program

This program is given in appendix B. The PC30 analog to digital card had support software that could interface with the Turbo Pascal programming language. A software program was written and developed for data acquisition purposes to do the following:

(a) The temperature measurements in the form of binary output from the PC30 card were read.

(b) The binary readings were converted to voltage values.

(c) The actual temperature values were calculated from the voltages using calibration data. A statistical sample of 100 measurements was collected for each temperature sensor. The average was used as the measured value and the standard deviation was used in the error analysis in the process calculations. This improved the accuracy by a factor of five.

(d) All of the moist air properties were calculated for each step in the process using these measured dry-bulb and wet-bulb temperature measurements. The calculation method and formulae were in accordance with ASHRAE 41.6-1994.

(e) The process changes and performance parameters were calculated.

(f) An error analysis was done on all measurements and calculations. This was done in accordance with ASHRAE GDL2-1986 RA. The important error values were printed together with the nominal values of the results and can be seen in any of the results in appendix H.

(g) The mathematical model described in section 4.1 was included in this program. The process was simulated with the input variables being the measured ambient and room conditions, air conditions at point 2 (fig. 1.1),

measured heat input and calculated efficiencies of the heat exchanger and both spray chambers. This was done to identify deviations that were not included in the mathematical model.

(h) All results were displayed immediately on the computer screen in the form of tables and a psychrometric chart. This enabled one to detect any problems or inaccuracies with the system immediately.

(i) The results were then printed if requested.

5.3.2 Program to calculate air flow rate

This program is given in appendix C. Dynamic pressures were measured using a pitot tube and micromanometer. The measured values were recorded and entered into this computer program that calculated the volumetric air flow rate and error of measurement using the methods described in section 5.2.5. The resultant values were then used as input to the data acquisition and analysis program described in section 5.3.1.

5.3.3 DEC simulation program

This program is given in appendix D. This program used the mathematical model described in chapter 4 to simulate the DEC process. The model was used in the sensitivity analysis in section 4.2, was used to simulate the operation of DEC systems in appendix G and was also incorporated in the data acquisition program described in section 5.3.1. The dry-bulb temperature and humidity ratio of the air at points 1 and 5 (fig. 1.1) were entered as input. The DEC process can therefore be simulated in both ventilation and recirculation modes by entering the appropriate air conditions. The air conditions at point 2 (fig. 1.1) and the heat exchanger efficiency were read from charts supplied by the manufacturer (see appendix F). The spray chamber efficiencies were also entered as input and could be specified by the user to be anywhere between 0 and 100 per cent.

CHAPTER 6
EXPERIMENTAL PROCEDURE AND TEST RESULTS

All of the experimental results are given in appendix H. The analysis of these results is given in this chapter together with a description of the experimental methods used to get the results, and a description of the main findings. The values given here are nominal values since the inclusion of the error analysis would unnecessarily complicate the analysis. However, a good understanding of the error and accuracy of the results can be obtained by looking at a few of the test results given in appendix H. The main purpose of the error analysis was to provide the experimental range of measurement that could be compared with simulated values to determine deviations.

This chapter contains an analysis of the following experimental results:

- The supply and return air flow rates were varied to investigate the effect of air leakage (section 6.1).
- Single blow tests were done to investigate the heat and mass transfer processes within the desiccant wheel (section 6.2).

The following variables were varied to investigate their effect on overall system performance:

- The efficiency of the return air spray chamber with unbalanced air flow (section 6.3).
- The efficiency of the return air spray chamber with balanced air flow (section 6.4).
- The efficiency of the supply air spray chamber (section 6.5).
- Inlet air conditions and regeneration temperatures (section 6.6).
- Desiccant wheel speed and unbalanced supply and return air flows (section 6.7).

Some of these results were compared to the catalogue data to identify deviations (section 6.8).

6.1 Air Leakage and Flow rate Measurement

6.1.1 Experimental Procedure and results

The numbering referred to in this section (6.1.1) is defined in the figure below (extracted from figure 1.1).



It was obvious from the beginning that air leakage past the desiccant wheel and heat exchanger seals could be significant, compared to the total flow rate. This could be determined simply by placing one's hand near the seals and feeling the large quantity of air escaping through the seals. All that was required for the purposes of this project was an order of magnitude estimate (20 to 30 per cent accuracy) of the leakage, so that any deviations in experimental results, due to leakage, could be identified.

A series of tests was carried out with combinations of the maximum and minimum supply and return air flow rates. The air flow rates were measured for the supply side at point 2 and for the return side at point 9 (see figure above) for each test. The static pressure was measured at every point in the process, as well as in the desiccant wheel and heat exchanger casings. All of these measurements were done both with the inspection doors of both wheels open and closed. This was done to provide more information, since the leakage magnitude and direction changed in each case.

Most of the results given in this section are for the inspection doors closed, since this case is relevant to the remaining experimental results. The results for the inspection doors open were used only for additional information in determining leakage and are therefore given in appendix H1. The following results were obtained:

(1) All of the air flow rate measurements are shown in table 6.1.1.
(2) All of the static pressure measurements are shown in figure 6.1.2.

(3) The differential static pressures, across the air leakage paths, are shown in figure 6.1.3 for the inspection doors closed and figure H1.1 for the doors open (both calculated from the information in figure 6.1.2). Figure 6.1.1 shows the sealing arrangement and air leakage paths for the desiccant wheel, with the inspection doors closed. The sealing arrangement is identical for the heat exchanger, but the air leakage path directions are different.

(4) These differential pressures were used to estimate the magnitude of the air leakage flow rate, through each leakage path. This information is shown in figure 6.1.4. These results are also summarised in table 6.1.2 and table 6.1.3. The same information for the doors open is given in figure H1.2 and tables H1.1 and H1.2.

The following method was used to estimate the leakage flow:

$$\text{Air leakage} = A \cdot C_d \cdot \sqrt{(2 \cdot P_d \cdot SV)} \qquad (6.1)$$

Where:

A= seal gap area through which leakage occurs (based on average gap of 3 mm and wheel diameter of 705 mm)

$A = 2.115 \cdot 10^{-3}$ m^2 for direct leakage across air streams

$A = 3.322 \cdot 10^{-3}$ m^2 for perimeter leakage into/out of wheel casing

C_d= coefficient of discharge = 0.7 (from the shape of the seal gap, it was estimated to be between that for a venturi (± 0.9) and that of an orifice (± 0.5))

P_d= pressure differential in Pascal (figures 6.1.3 and H1.1)

SV= specific volume =1.05 m^3/kg (measured on day of test)

TABLE 6.1.1: Measured supply and return air flow rates for various flow combinations.

FLOW COMBINATION		Supply flow at point 2 (fig. 1.1) (litres/s)		Return flow at point 9 (fig. 1.1) (litres/s)	
		CLOSED	OPEN	CLOSED	OPEN
1	MAX SF & MAX RF	207	300	268	164
2	MAX SF & MIN RF	210	327	177	86
3	MIN SF & MAX RF	159	295	246	146
4	MIN SF & MIN RF	216	308	162	61

SF = supply air flow rate
RF = return air flow rate
OPEN = Both inspection doors open
CLOSED = Both inspection doors closed.

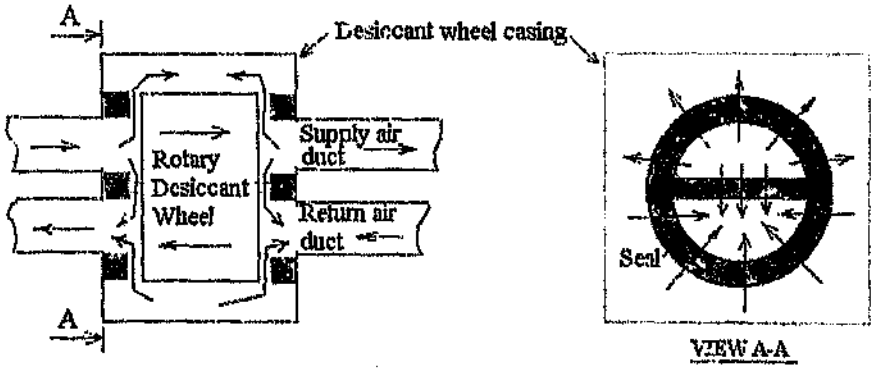

Note: (1) Arrows show leakage path, when inspection doors were closed.
(2) Shaded portion represents the seals.

FIGURE 6.1.1: Diagram of sealing arrangement for the desiccant wheel.

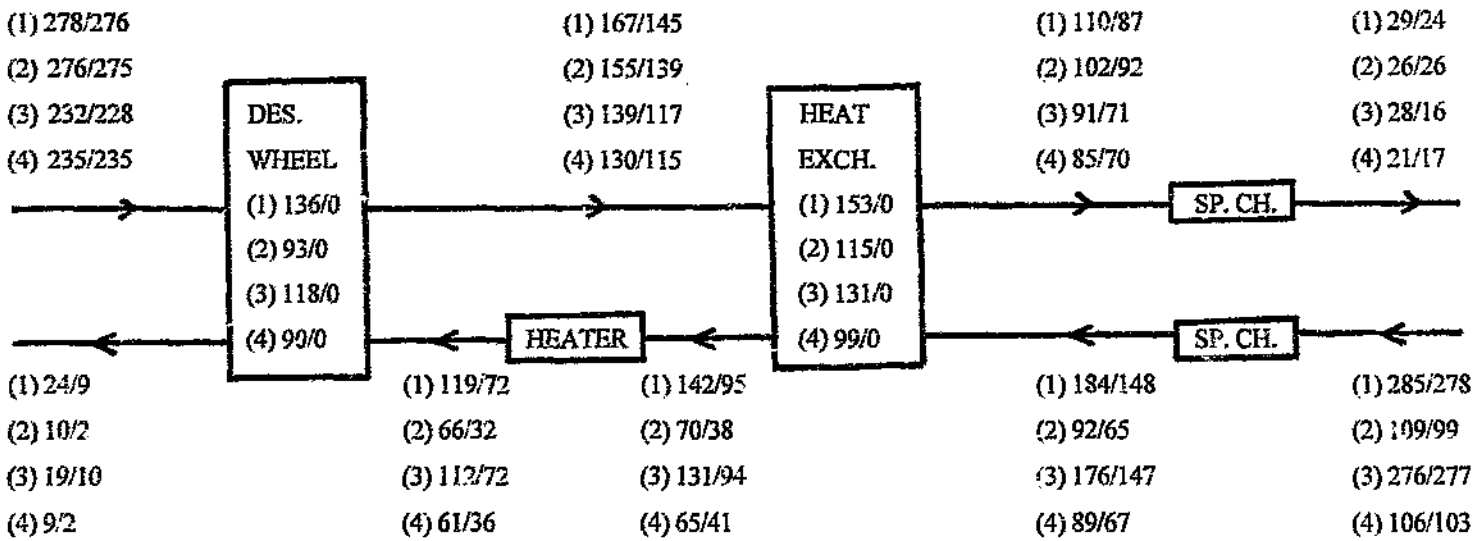

(1) = MAX SF & MAX RF
(2) = MAX SF & MIN RF
(3) = MIN SF & MAX RF
(4) = MIN SF & MIN RF

SF = supply air flow rate
RF = return air flow rate

Note: values are shown for both inspection doors closed and for both inspection doors open (i.e. CLOSED/OPEN)

FIGURE 6.1.2: Static pressures measured at various air flow rate combinations (Pascal).

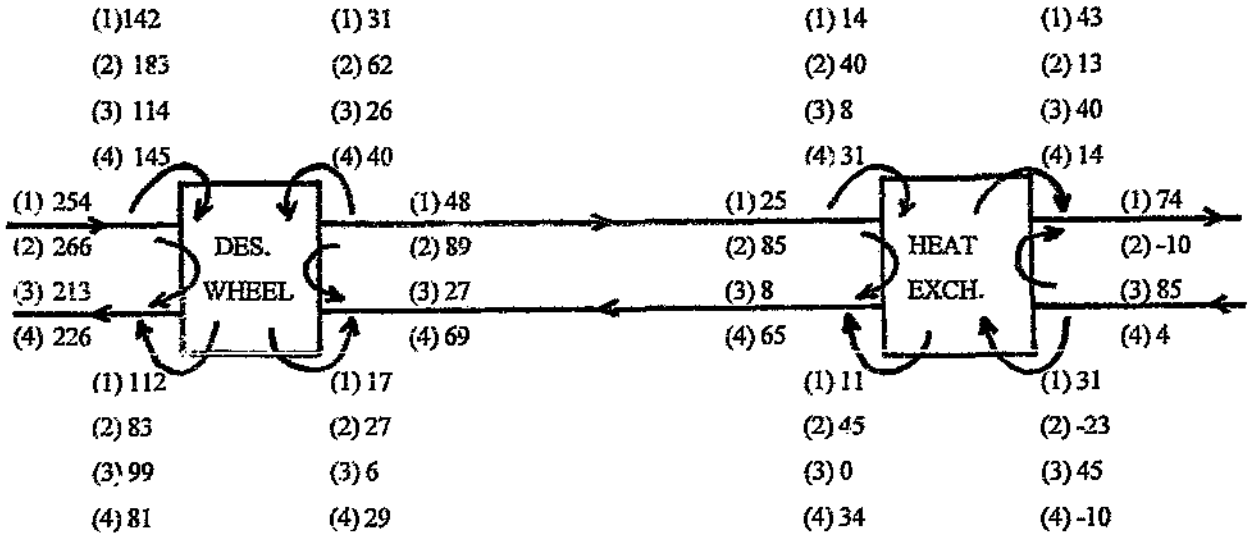

(1)= MAX SF & MAX RF
(2)= MAX SF & MIN RF
(3)= MIN SF & MAX RF
(4)= MIN SF & MIN RF

SF = supply air flow rate
RF = return air flow rate

Note: 1) values are shown for both inspection doors closed. See figure H1.1 for values with both doors open.

2) Positive differential pressure is in direction of arrows shown (see figure 6.1.1 for details on air leakage paths).

FIGURE 6.1.3: Differential pressure at various air flow rate combinations, in Pascal (calculated from figure 6.1.2).

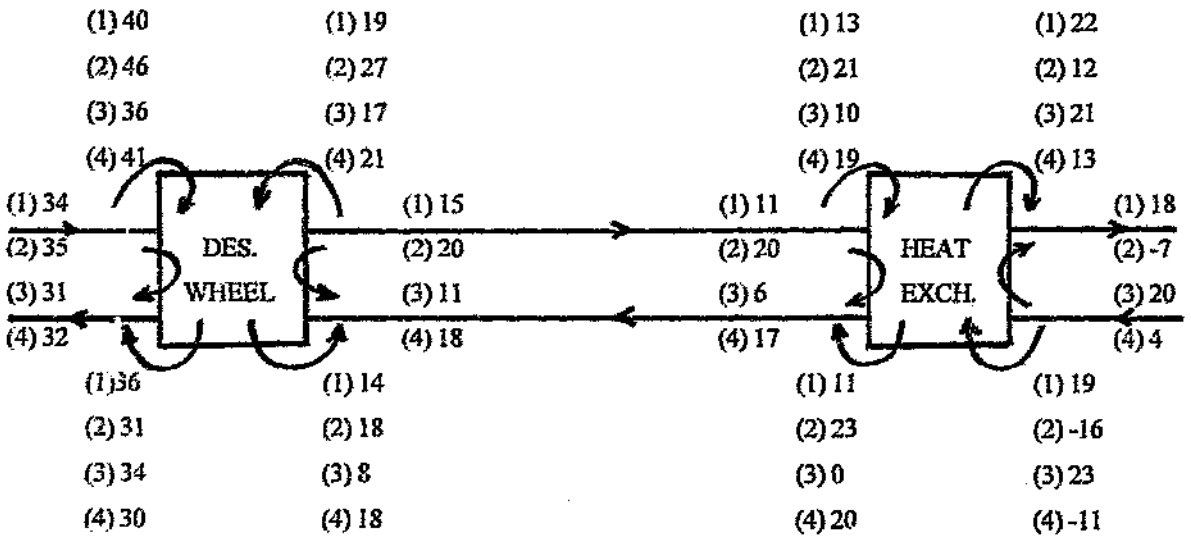

(1)= MAX SF & MAX RF
(2)= MAX SF & MIN RF
(3)= MIN SF & MAX RF
(4)= MIN SF & MIN RF

SF = supply air flow rate
RF = return air flow rate

Note: 1) values are shown for both inspection doors closed. See figure H1.2 for values with both doors open.

2) Positive leakage air flow is in direction of arrows (see figure 6.1.1 for details on air leakage).

FIGURE 6.1.4: Leakage air flow rate at various air flow rate combinations in litres/sec and (calculated from fig. 6.1.3).

TABLE 6.1.2: Estimated supply and return air flow rates at desiccant wheel (with both inspection doors closed).

FLOW COMBINATION		Supply air flow (litres/s)				Return air flow (litres/s)			
		in-let	leak out	leak in	out-let	in-let	leak out	leak in	out-let
1	MAX SF & MAX RF	315	108	0	207	169	0	99	268
2	MAX SF & MIN RF	338	128	0	210	73	0	104	177
3	MIN SF & MAX RF	254	95		159	162	0	84	246
4	MIN SF & MIN RF	328	112	0	216	64	0	98	162

SF = supply air flow rate
RF = return air flow rate

TABLE 6.1.3: Estimated supply and return air flow rates at heat exchanger (with both inspection doors closed).

FLOW COMBINATION		Supply air flow (litres/s)				Return air flow (litres/s)			
		in-let	leak out	leak in	out-let	in-let	leak out	leak in	out-let
1	MAX SF & MAX RF	207	24	40	223	184	37	22	169
2	MAX SF & MIN RF	210	41	5	174	7	0	66	73
3	MIN SF & MAX RF	159	16	41	184	199	43	6	162
4	MIN SF & MIN RF	216	36	17	197	20	0	44	64

SF = supply air flow rate
RF = return air flow rate

6.1.2 Main findings

The more significant findings described below are discussed in section 7.1. The numbering referred to in this section (6.1.2) is defined in the figure below (extracted from figure 1.1).



The total amount of air that leaked out of the supply air duct was 42 to 50 per cent of the original inlet air, compared with 2 to 13 per cent leaking into the supply duct. The following is a description of the leakage quantities and directions (see figure 6.1.4 for details).

POINT 1: The leakage path directions were:

(a) Directly into point 9.

(b) Into the desiccant wheel casing and from there into points 8 and 9.

Between 22 and 26 per cent of the initial supply air leaked into the exhaust air stream from point 1. This leakage had no effect on the process at point 1 but had significant effects at points 8 and 9.

POINT 2: The leakage path directions were:

(a) Directly into point 8.

(b) Into the desiccant wheel casing and from there into points 8 and 9.

(c) Directly into point 7.

(d) Into the heat exchanger casing and from there into points 3 and 7.

Between 24 and 33 per cent of the dehumidified supply air leaked into the exhaust air stream from point 2. This leakage resulted in a significant loss of dehumidified air, that had increased the moisture loading and regeneration requirements of the desiccant. The cooling capacity and COP were decreased by 24 to 33 per cent, by the leakage at point 2 alone.

POINT 3: The leakage path directions were:
(a) Generally from point 6 directly into point 3, although with the case of maximum supply air flow and minimum return air flow, the leakage was in the opposite direction.
(b) From the heat exchanger casing (mixture of air from points 2 and 6) into point 3.

The magnitude of the leakage into point 3 was between 3 and 29 per cent of the supply air flow through the heat exchanger. Most of the leakage air came from point 6 and therefore had an enthalpy close to that of the room air. The reduction in cooling capacity and COP of the final mixture at point 3 was therefore between 3 and 29 per cent. A small portion of the air that leaked in at point 3 came from point 2. This air bypassed the heat exchanger and was not sensibly cooled and thereby decreased the efficiency of the heat exchanger and contributed to the decreased cooling capacity.

POINT 4: No leakage.

POINT 5: No leakage.

POINT 6: The leakage path directions were:
(a) Directly into point 3, except in the case of minimum return air flow and maximum supply air flow, when the leakage was in the opposite direction.
(b) Into the heat exchanger casing, when the return air flow rate was high, but from the casing into point 6, when the air flow rate was low.

The leakage out of point 6 (0 to 20 per cent of initial return air flow) was a loss of cooling potential, which reduced the effectiveness of the heat exchanger and cooling capacity. In the case when leakage into point 6 occurred, the dry-bulb temperature was increased which also decreased the cooling potential of the air at point 6.

POINT 7: The leakage air path directions were:
(a) Directly from point 2 into point 7.

(b) From the heat exchanger casing (mixture of air from points 2 and 6) into point 7.

Most of the leakage into point 7 came from point 2. This was probably beneficial to the process, since hot dry air was mixed with the return air steam before being heated for regeneration purposes. However, a small portion of the leakage came from point 6 and had not been heated in the heat exchanger. This reduced the benefit of the leakage from point 2.

POINT 8: The leakage path directions were:
(a) From point 2 directly into point 8.
(b) From the desiccant wheel casing (mixture of air from points 1 and 2) into point 8.

The leakage air (12 to 56 per cent of the heated regeneration air) cooled down the regeneration air temperature and thereby had a significant influence on the regeneration process. The experimental tests (in appendices H3 to H6) were based on a flow combination that would have resulted in a leakage flow of 17 per cent. The decreases in regeneration temperature would have depended on the temperatures at points 1 and 2. With TDB_1=30 °C and TDB_2=46 °C, a regeneration temperature of 70 °C would have decreased to 65 °C. This did not reduce the regeneration energy input and only influenced the regeneration process.

POINT 9: The leakage path directions were:
(a) From point 1 directly into point 9.
(b) From the desiccant wheel casing (mixture of air from points 1 and 2) into point 9.

The magnitude of leakage air was 52 to 153 per cent of the regenerating air flow through the desiccant wheel. This leakage had no effect on performance, but had a great effect on the measured properties at point 9. This can be seen in all of the experimental results in appendices H3 to H6 where the more accurate simulated values of point 9 can be compared with the measured values.

6.2 Single Blow Tests

The numbering referred to in this section (6.2) is defined in the figure below (extracted from figure 1.1).



6.2.1 Experimental procedure and results

The purpose of the single step tests was to determine the air outlet conditions, from a specific part of the desiccant wheel after rotated through the dehumidification and regeneration cycles.

6.2.1.1 Regeneration single blow tests

The procedure for executing the regeneration single step test was to stop the return air fan and run the supply air fan, with the desiccant wheel rotating. Sufficient time (30 minutes) was allowed for the desiccant to reach equilibrium with the supply air. The regeneration heaters were then allowed 10 minutes to warm up before starting each test and the supply air fan and desiccant wheel were stopped (after the 10 minutes). The return air fan was started (with the electrical heaters on), together with a computer program, modified from the one shown in appendix B. The desiccant wheel inlet and outlet return air conditions were measured and the properties calculated at regular intervals, using the program. Two regeneration single step tests, at different regeneration temperatures, are shown in figures 6.2.1 and 6.2.2.

6.2.1.2 Dehumidification single blow tests

The procedure for executing the dehumidification single step tests was to stop the supply air fan and run the return air fan, with the desiccant wheel rotating. The regeneration heaters were switched on and sufficient time (30 minutes) was allowed

for the desiccant to reach equilibrium with the regenerating air. The ambient air conditions were measured by placing the sampling device for point 2 outside the building. These inlet conditions were entered into a computer program similar to that used for the regeneration single step tests and the sampling device was then returned to its correct position. This same sampling device was then used to measure the air conditions at point 2 and accurate air property differences were therefore obtained. The return air fan, regeneration air heaters and desiccant wheel were stopped and the supply air fan was started, together with the computer program. The outlet air conditions (point 2) were measured and the properties calculated at regular time intervals. Two tests were done for different ambient air conditions, with approximately the same regeneration temperatures (figures 6.2.3 and 6.2.4). These results are also given in figures 6.2.5 and 6.2.6, for comparison between the two tests.

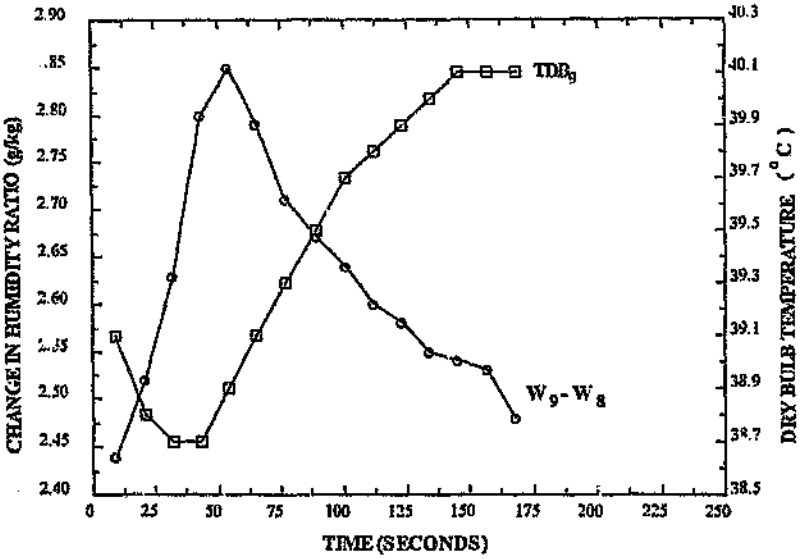

FIGURE 6.2.1: Regeneration single blow test (T_{reg}=57 °C) (test no. H2/1)

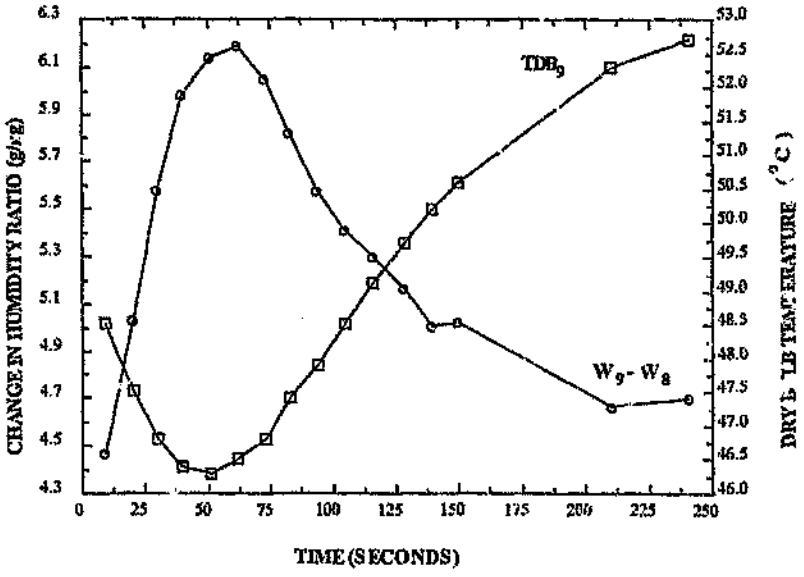

FIGURE 6.2.2: Regeneration single blow test (T_{reg}=87 °C) (test no. H2/2)

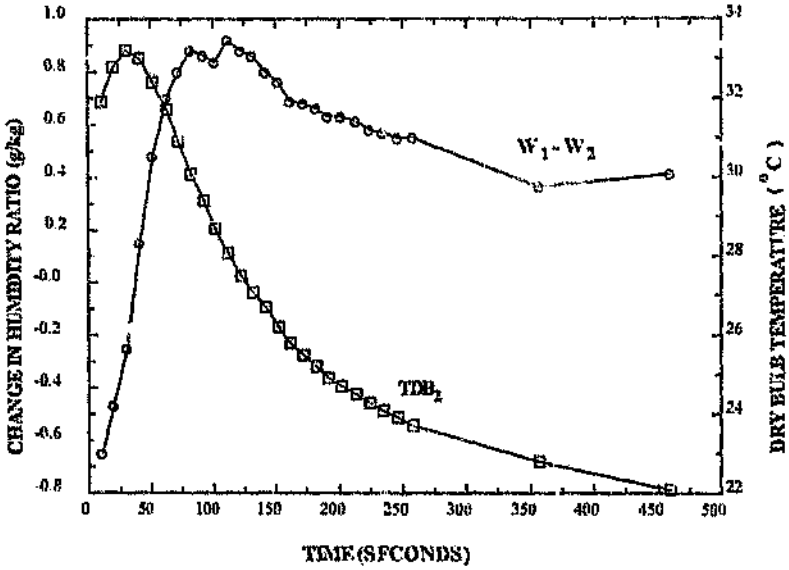

TDB_1=19.1 °C W_1=5.15 g/kg RH_1=31 % T_{REG}=75.4 °C

FIGURE 6.2.3: Dehumidification single blow test (test no. H2/3)

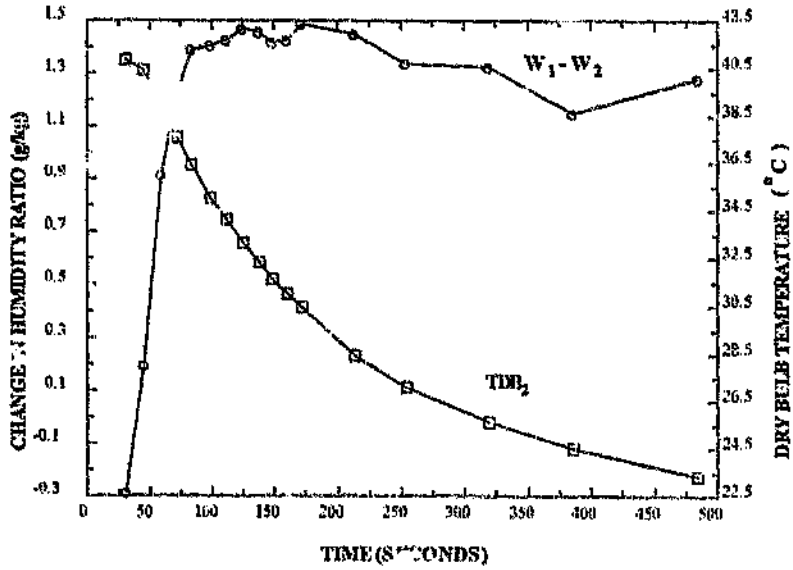

TDB_1=17.0 °C W_1=8.00 g/kg RH_1=53 % T_{REG}=73.6 °C

FIGURE 6.2.4: Dehumidification single blow test (test no. H2/4)

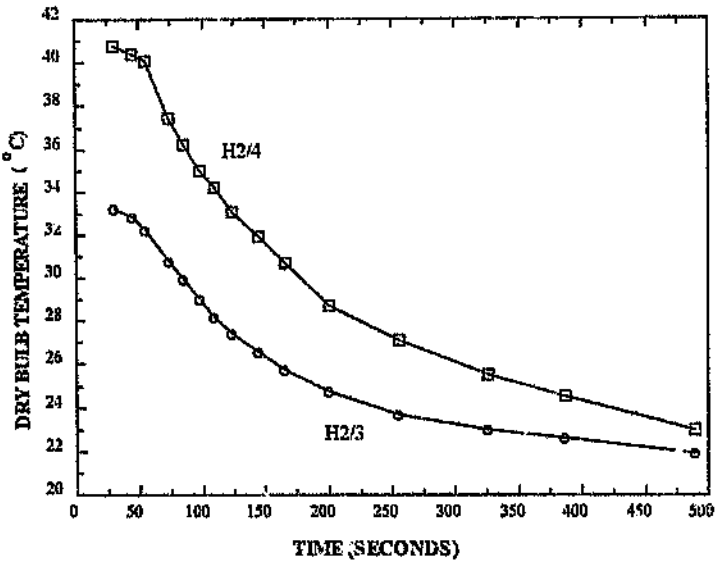

FIGURE 6.2.5: Temperature variation comparison from figures 6.2.3 and 6.2.4

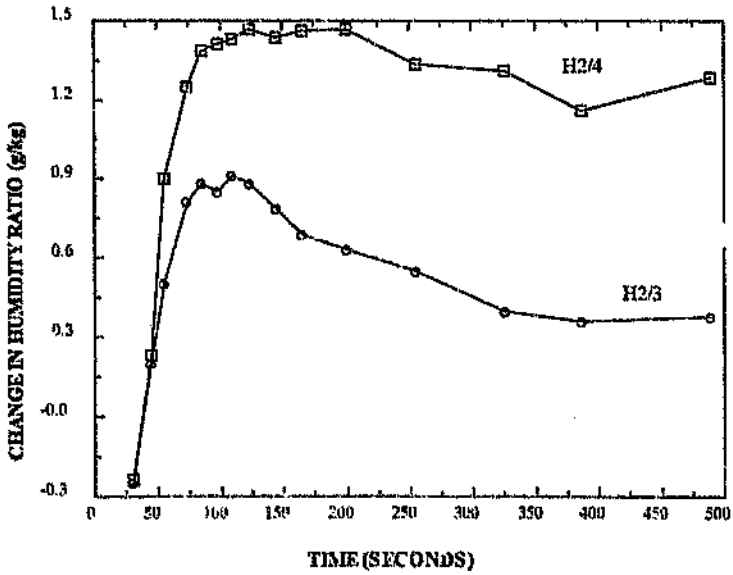

FIGURE 6.2.6: Humidity ratio variation comparison from figures 6.2.3 and 6.2.4.

6.2.2 Main findings

The more significant findings described below are discussed in detail in section 7.2.

6.2.2.1 Regeneration single blow tests

The results for two regeneration single step tests are given in graphical form in figures 6.2.1 and 6.2.2. The regeneration temperatures were different in each case, but the inlet air conditions were similar. The following observations were made, from these graphs:

(a) The increase in humidity ratio (W_9-W_8) in the regeneration air reached a maximum value after approximately the same time period, in both cases (see sections 7.2.1 (a), (b) and (c)).

(b) The magnitude of the maximum W_9-W_8 value was lower with the test with the lower regeneration temperature. This was expected since the vapour pressure in the desiccant was lower and less moisture was evaporated.

(c) The dry-bulb temperature (TDB_9) curve, in both cases, was almost a mirror image of the W_9-W_8 curve and reached a minimum value at the same time as W_9-W_8 reached the maximum value. This was a result of the sensible heat in the regeneration air being converted to latent heat.

(d) The outlet temperature (TDB_9) was higher for the test with the higher regeneration temperature (TDB_8).

(e) The graphs for both tests were similar. This showed that the regeneration process was similar for different regenerating temperatures (see section 7.2.1 (d)).

6.2.2.2 Dehumidification single blow tests

The results for two dehumidification single step tests are given in graphical form in figures 6.2.3 to 6.2.6. The regeneration temperature was approximately the same in both cases, but the inlet air conditions were different. The following observations were made, from these graphs:

(a) The maximum W_1-W_2 value was higher with a higher humidity ratio (W_1) of the inlet air. This was expected, since the vapour pressure of the ambient air was higher and the absorption potential at the desiccant was greater.

(b) The maximum W_1-W_2 values were reached at approximately the same time for both tests (see section 7.2.2 (a)).

(c) The graphs both have curves of similar shape (see section 7.2.2 (b)).

(d) The dry-bulb temperature (TDB_2) decreased almost from the start of the process (see section 7.2.2 (c)).

(e) The position of the breakthrough point (when the desiccant becomes saturated and turns to liquid) in the W_1-W_2 curves was not sharply defined (see section 7.2.2(d)).

(f) The W_1-W_2 curve was negative during the first 30 seconds of the process (see section 7.2.2 (e)).

6.3 Efficiency of Return Air Spray Chamber (EV_R) with Unbalanced Air Flow

The numbering referred to in this section (6.3) is defined in the figure below (extracted from figure 1.1).



6.3.1 Experimental procedure and results

Two sets of tests were done to evaluate the performance characteristics of the return air spray chamber. The first was at a return air flow rate (MA_R) of 98 g/s (unbalanced flow with supply air) and the second at 146 g/s (balanced flow). The results given in this section are for the unbalanced flow tests (see section 6.4 for balanced flow test results).

In the tests only the water flow rate to the spray chamber was varied and the other operating parameters were kept constant at the following values:
MA_S = 146 g/s (supply air flow rate)
EV_S = 100 % (efficiency of supply air spray chamber)

The room air condition was kept constant, but the ambient air conditions varied slightly during the period of testing. The range of these operating conditions are given below:

TDB_1 = 20.3-23.4 °C W_1 = 8.59-10.59 g/kg (ambient conditions)
TDB_5 = 23.1-24.0 °C W_5 = 9.80-10.33 g/kg (room conditions)
EV_R = 0-100 %

The test results for unbalanced flow are given in tables 6.3.1 and 6.3.2. Significant variations are shown graphically in figures 6.3.1 to 6.3.6.

TABLE 6.3.1: Performance parameters for variation of efficiency of retur. air spray chamber (EV_R) (MA_R=98 g/s)

TEST NO.	TFR_R (g/s)	EDH1 (%)	EDH2 (%)	ERG (%)		EHX_S (%)	EHX_R (%)	EV_R (%)	CC (kW)		COP		TCC (kW)		TCOP	
				M	Sim				M	Sim	M	Sim	M	Sim	M	Sim
H3/1	0.09	38	12	13	30	66	88	35	0.69	0.67	0.19	0.18	0.37	0.35	0.10	0.10
H3/2	0.77	39	10	10	29	67	88	50	0.83	0.87	0.23	0.24	0.49	0.53	0.13	0.14
H3/3	1.09	40	10	8	27	67	88	67	0.94	0.95	0.26	0.26	0.74	0.75	0.20	0.20
H3/4	1.43	41	12	11	28	70	83	90	0.90	1.14	0.24	0.31	0.75	0.99	0.20	0.27
H3/5	1.61	37	11	4	26	70	86	98	0.94	1.11	0.26	0.30	0.85	1.01	0.23	0.28
H3/6	1.89	40	10	6	28	73	83	99	1.00	1.21	0.27	0.33	1.02	1.23	0.28	0.34
H3/7	2.06	41	12	7	28	76	81	101	0.93	1.28	0.25	0.35	0.93	1.28	0.25	0.35
H3/8	2.42	38	10	3	26	76	85	100	1.02	1.32	0.28	0.36	0.94	1.24	0.26	0.34
H3/9	2.65	37	10	3	25	76	86	101	1.07	1.36	0.29	0.37	0.90	1.20	0.25	0.33
H3/10	2.84	41	10	-4	24	74	89	100	1.36	1.82	0.37	0.50	0.56	1.02	0.15	0.28

TABLE 6.3.2: Property changes for variation of efficiency of return air spray chamber (EV_R) (MA_R=98g/s)

TEST NO.	EV_R (%)	TDB_1 (°C)	W_1 (g/kg)	TDB_2 (°C)	W_2 (g/kg)	H_2-H_1 (kJ/kg)	W_1-W_2 (g/kg)	W_6-W_5 (g/kg)	FR_R (g/s)	TFR_R (g/s)	PP_R (bar)	W_3-W_2 (g/kg)		%EV (%)	TDB_6 (°C)
												M	Sim		
H3/1	35	20.3	10.59	32.6	7.58	4.8	3.01	0.86	0	0.09	0	0.33	0.34	---	20.5
H3/2	50	21.3	10.10	32.7	7.18	4.2	2.92	1.46	0.62	0.77	2	0.65	0.42	19	19.2
H3/3	67	22.4	9.57	32.7	6.88	3.7	2.68	2.21	0.87	1.09	10	0.89	0.47	20	17.6
H3/4	90	22.7	9.85	34.3	7.06	4.7	2.79	2.84	1.15	1.43	20	1.28	0.55	20	16.0
H3/5	98	22.5	10.15	33.4	7.54	4.5	2.62	3.12	1.30	1.61	30	1.11	0.53	19	15.4
H3/6	99	22.9	10.37	33.5	7.54	3.6	2.83	3.14	1.58	1.89	40	1.39	0.54	16	15.4
H3/7	101	23.4	10.26	34.7	7.43	4.4	2.83	3.18	1.74	2.06	50	1.71	0.56	16	15.4
H3/8	100	23.4	10.01	33.6	7.43	3.8	2.58	3.19	2.10	2.42	60	1.60	0.56	13	15.4
H3/9	101	23.1	9.86	33.2	7.36	3.9	2.50	3.48	2.30	2.65	70	1.66	0.57	13	15.5
H3/10	100	23.1	8.50	33.2	6.10	4.1	2.40	3.65	2.47	2.84	80	2.39	0.70	13	15.9

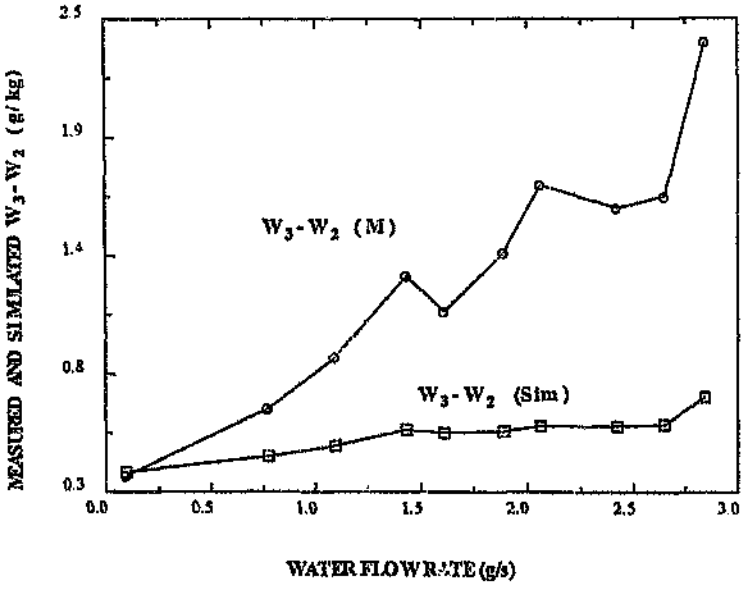

FIGURE 6.3.1: Change in humidity ratio of supply air across sensible heat exchanger versus water flow rate.

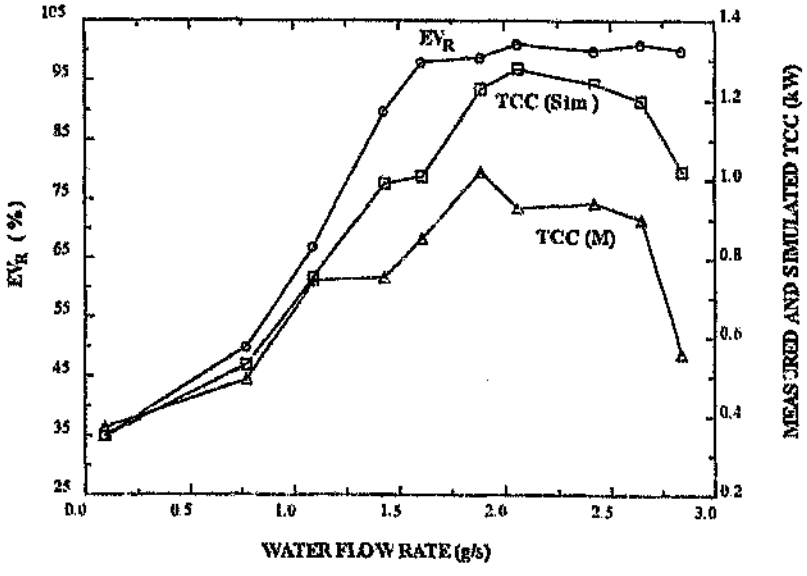

FIGURE 6.3.2: Cooling capacity in ventilation credit mode versus water flow rate.

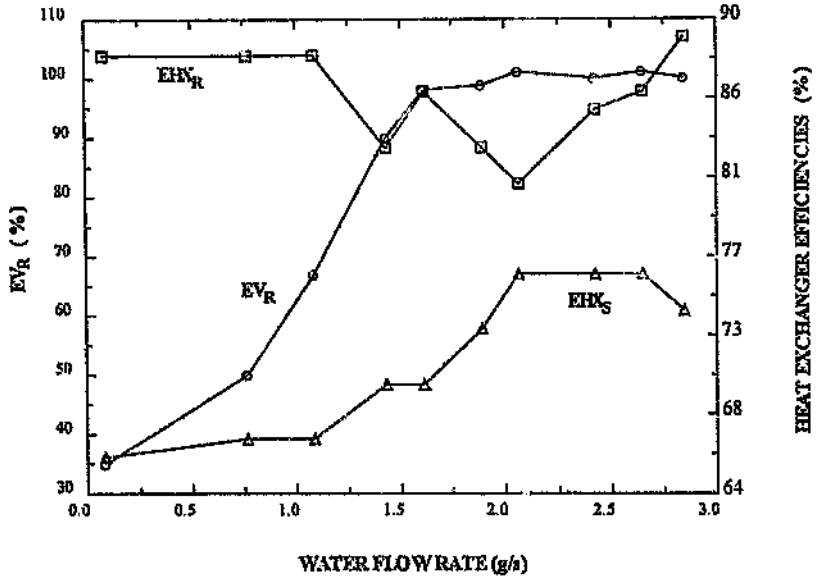

FIGURE 6.3.3: Heat Exchanger efficiencies versus water flow rate.

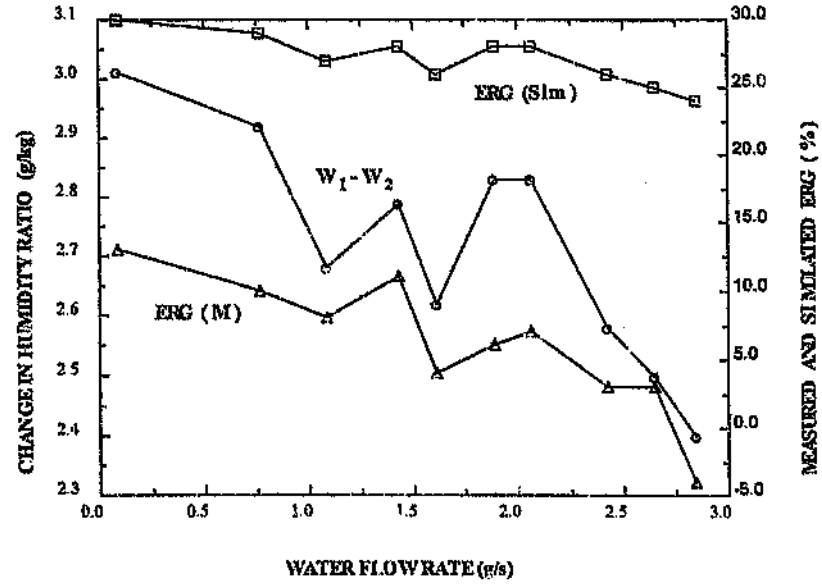

FIGURE 6.3.4: Regeneration efficiency and change in humidity ratio of the supply air across the dehumidifier versus water flow rate.

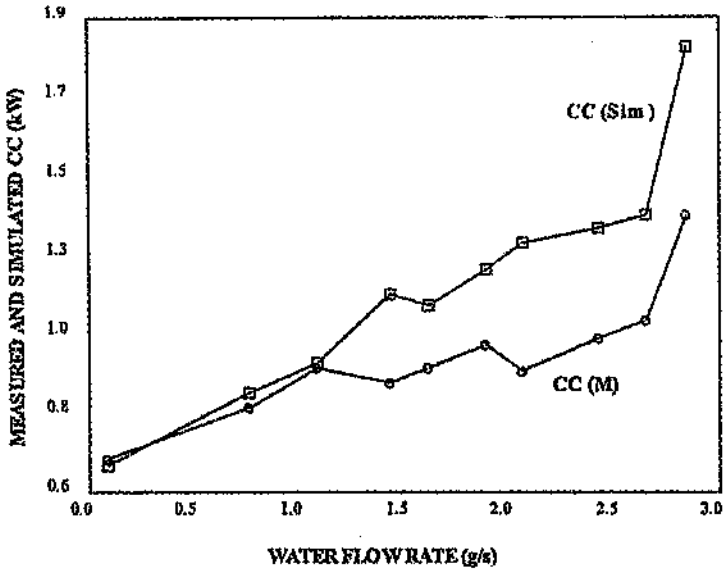

FIGURE 6.3.5: Cooling capacity in ventilation mode versus water flow rate

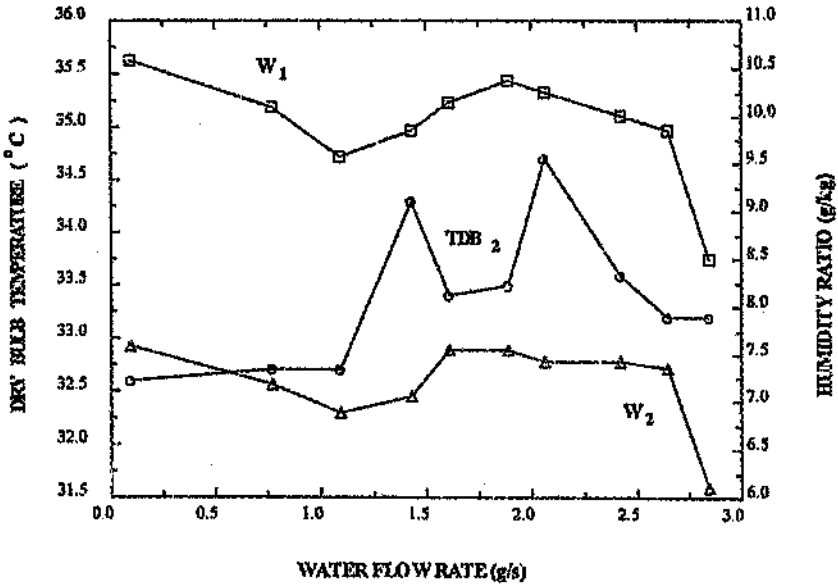

FIGURE 6.3.6: Dehumidifier inlet and outlet humidity ratios and outlet dry-bulb temperature TDB_2 versus water flow rate.

6.3.2 Main findings

The more significant findings described below are discussed in detail in section 7.3.

The test results are given in tables 6.3.1 and 6.3.2 and figures 6.3.1 to 6.3.6. The following observations were made:

(a) The results of the tests on air leakage (see sections 6.1 and 8.1) showed that there was little or no air leakage into the supply air duct for the given flow combination (MA_R=98 g/s and MA_S=146 g/s). However, there was significant leakage into the return air duct.

(b) Figure 6.3.6 showed that there was some fluctuation in the inlet air conditions. This had a significant effect on the results and complicated the analysis.

(c) During the tests, water was visually observed to be dripping from the joints in the return air ducting, between the spray chamber and the heat exchanger. The demister at the exit of the spray chamber therefore did not remove all the water droplets from the return air stream (see section 7.3 (b)).

(d) The change in evaporator efficiency (EV_R) is shown in figure 6.3.2. The efficiency increased with increasing spray water flow rate until a flow rate of approximately 2 g/s, when the efficiency EV_R was 99 per cent (effectively 100 per cent). A further increase in flow rate maintained EV_R at 100 per cent.

(e) The cooling capacity for the ventilation credit mode (TCC) was less sensitive to changes in inlet conditions and provided more reliable information concerning the trends in performance parameters (see section 7.3 (a) and (c)).

(f) The cooling capacity in the ventilation mode CC generally followed the same trends (see figure 6.3.5) as the cooling capacity in the ventilation credit mode TCC (see section 7.3 (d)).

(g) Figure 6.3.3 shows the heat exchanger performance trends. The supply and return air mass flow rates were constant for this set of tests and the heat exchanger efficiency should also have remained constant. The efficiency of heat transfer to the supply air (EHX_S) and to the return air (EHX_R) was constant until spray chamber efficiency EV_R was 67 per cent. At this point EHX_S increased and EHX_R decreased (see section 7.3 (e)).

(h) The regeneration efficiency ERG also changed significantly in these tests (see figure 6.3.4). The measured values were lower than the simulated values, because of air leakage from points 1 and 2 into point 9. This gave a false measurement of the true condition of the regeneration exit air at point 9 and resulted in a false calculation of the measured regeneration efficiency. The simulated values are more accurate in this case. The reduction in desiccant loading (represented by W_1-W_2) because of changes in inlet air conditions caused a general reduction in regeneration efficiency in both measured and simulated values.

(i) When water carryover occurred, only the spray chamber end of the heat exchanger was visually seen to be wet (see section 7.3 (f)).

6.4 Efficiency of Return Air Spray Chamber (EV_R) with Balanced Air Flow

The numbering referred to in this section (6.4) is defined in the figure below (extracted from figure 1.1).



6.4.1 Experimental procedure and results

Two sets of tests were done to evaluate the performance characteristics of the return air spray chamber. The first was at a return air flow rate (MA_R) of 98 g/s (unbalanced flow with supply air) and the second at 146 g/s (balanced flow). The results given in this section are for the balanced flow tests (see section 6.3 for unbalanced flow test results).

In the tests only the water flow rate to the spray chamber was varied and the other operating parameters were kept constant at the following values:

MA_S = 146 g/s (supply air flow rate)

EV_S = 100 % (efficiency of supply air spray chamber)

The room air conditions were kept relatively constant, but the ambient air conditions varied slightly during the period of testing. The range of these operating conditions are given below:

TDB_1 = 22.4-24.4 °C W_1 = 7.96-10.80 g/kg (ambient conditions)

TDB_5 = 21.4-22.1 °C W_5 = 8.86-10.04 g/kg (room conditions)

EV_R = 0-98 %

The test results for unbalanced flow are given in tables 6.4.1 and 6.4.2. Significant variations are shown graphically in figures 6.4.1 to 6.4.3.

TABLE 6.4.1: Performance parameters for variation of efficiency of return air spray chamber (EV_R) (MA_R=147 g/s)

TEST No	TFR_R (g/s)	EDH1 (%)	EDH2 (%)	ERG (%)		EHX_S (%)	EHX_R (%)	EV_R (%)	CC (kW)		COP		TCC (kW)		TCOP	
				M	Sim				M	Sim	M	Sim	M	Sim	M	Sim
H3/11	0.02	46	11	16	23	85	82	7	0.71	0.90	0.13	0.17	0.17	0.91	0.13	0.17
H3/12	0.76	43	11	18	23	86	80	27	0.63	0.80	0.12	0.15	0.92	1.09	0.17	0.21
H3/13	1.07	36	12	18	19	86	81	42	0.68	0.68	0.13	0.13	1.23	1.22	0.23	0.23
H3/14	1.43	44	10	15	22	85	82	60	0.89	1.13	0.17	0.21	1.19	1.44	0.22	0.27
H3/15	1.59	41	11	15	21	85	83	73	0.77	0.99	0.15	0.19	1.35	1.57	0.25	0.29
H3/16	1.95	51	11	10	19	85	83	83	1.24	1.88	0.23	0.35	0.83	1.47	0.16	0.28
H3/17	2.16	47	10	16	23	85	80	89	0.83	1.26	0.16	0.24	1.35	1.78	0.25	0.34
H3/18	2.57	44	9	13	21	84	83	94	0.88	1.28	0.16	0.24	1.30	1.70	0.24	0.32
H3/19	2.77	47	9	13	21	85	81	97	1.10	1.50	0.21	0.28	1.42	1.83	0.27	0.34
H3/20	3.02	39	9	10	17	85	79	98	1.08	1.20	0.20	0.23	1.59	1.71	0.3	0.32

TABLE 6.4.2: Property changes for variation of efficiency of return air spray chamber (EV_R) (MA_R=147 g/s)

TEST NO.	EV_R (%)	TDB_1 (°C)	W_1 (g/kg)	H_2-H_1 (kJ/kg)	W_1-W_2 (g/kg)	W_6-W_5 (g/kg)	FR_R (g/s)	TFR_R (g/s)	PP_R (bar)	W_3-W_2 (g/kg)		%EV (%)	TDB_6 (°C)	W_6-W_2 (g/kg)
										M	Sim			
H3/11	7	22.4	9.92	4.3	3.38	0.15	0	0.02	0	1.18	0.34	---	21.6	3.64
H3/12	27	22.5	10.42	4.5	3.30	0.78	0.64	0.76	2	1.00	0.32	16	20.0	3.30
H3/13	43	23.4	10.80	5.0	2.81	1.18	0.89	1.07	10	0.48	0.30	17	18.8	3.16
H3/14	60	23.3	9.92	3.7	3.15	1.75	1.17	1.43	20	1.38	0.44	18	17.4	4.68
H3/15	73	23.7	10.43	4.2	3.02	2.18	1.26	1.59	30	1.19	0.41	21	16.4	4.37
H3/16	83	23.9	7.96	4.4	2.78	2.38	1.59	1.95	40	2.57	0.66	18	15.8	7.04
H3/17	89	23.7	10.39	3.9	3.43	2.69	1.76	2.16	50	1.94	0.50	19	15.3	5.36
H3/18	94	23.9	9.95	3.5	3.00	2.90	2.13	2.57	60	1.82	0.51	17	15.0	5.53
H3/19	97	24.4	9.61	3.2	3.11	2.94	2.33	2.77	70	2.05	0.57	16	14.8	6.15
H3/20	98	23.3	9.46	3.4	2.50	3.09	2.56	3.02	80	1.32	0.46	15	13.8	4.98

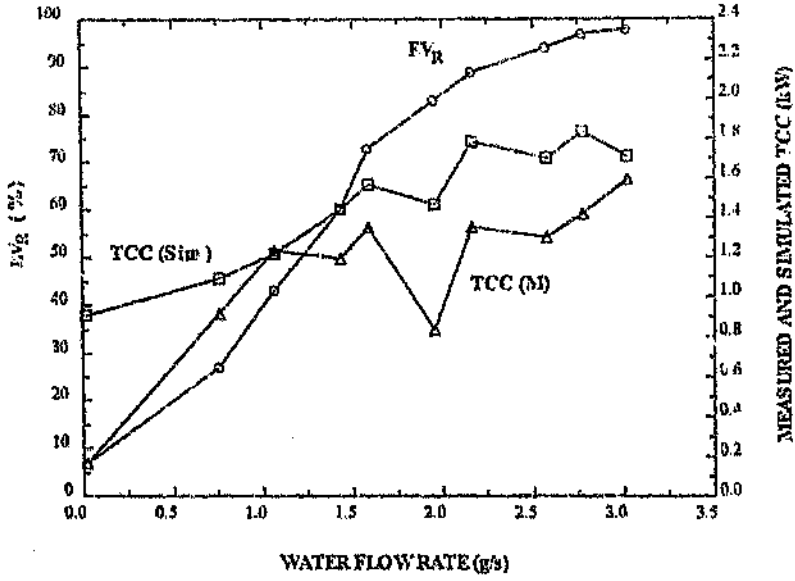

FIGURE 6.4.1: Cooling capacity in ventilation credit mode and return air spray chamber efficiency versus water flow rate.

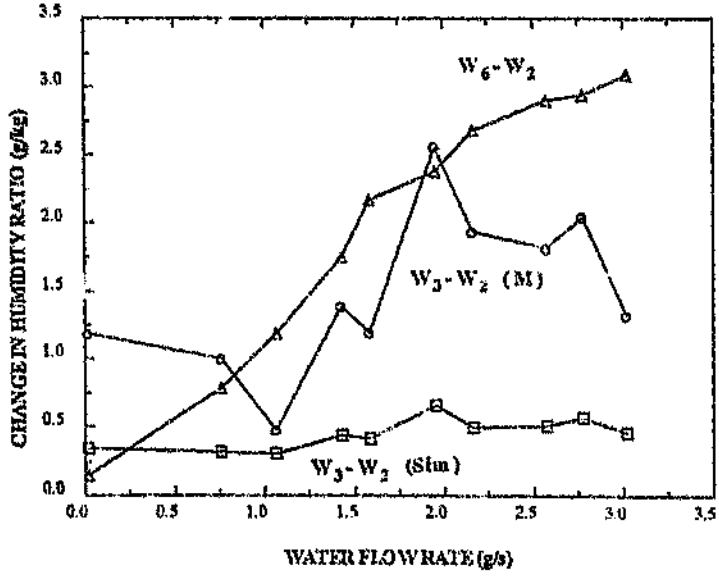

FIGURE 6.4.2: Change in humidity ratios of supply air across dehumidifier and return air across spray chamber.

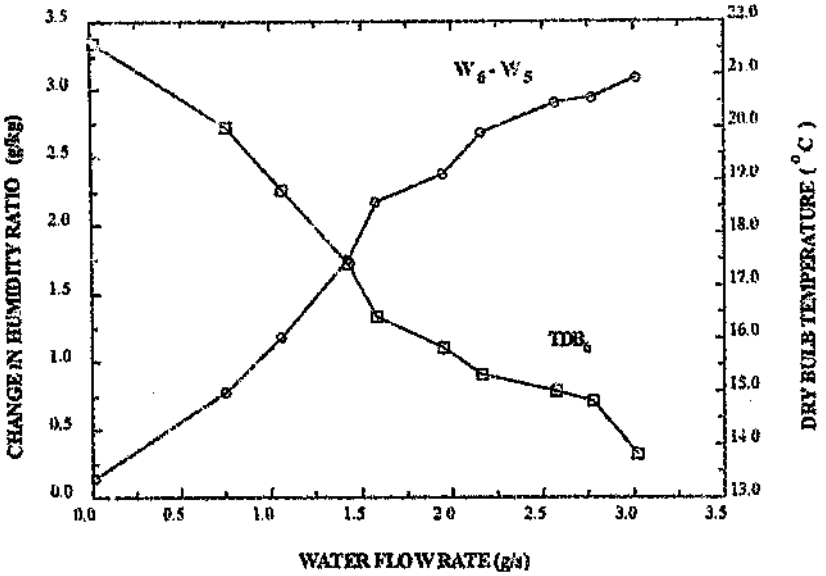

FIGURE 6.4.3: Change in humidity ratio and dry-bulb temperature in return air spray chamber.

6.4.2 Main findings

The more significant findings described below are discussed in detail in section 7.4.

The test results are given in tables 6.4.1 and 6.4.2 and figures 6.4.1 to 6.4.3. The following observations were made:

(a) The results of the tests on air leakage (see sections 6.1 and 7.1) showed that there was leakage into the supply air duct at point 3, mainly from point 6, for the given flow combination (MA_R=147 g/s and MA_S=146 g/s). There was also leakage into the return air duct at point 7 mainly from point 2.

(b) Table 6.4.1 showed that there was fluctuation in the inlet air conditions. This had a significant effect on the results and complicated the analysis. The large fluctuation

in inlet conditions was a result of unsteady flow from the humidifier that was used to increase the moisture content of the dry winter

(c) No evidence of water carryover from the spray chamber could be visually observed for this set of tests.

(d) Figure 6.4.1 shows the spray chamber efficiency as a function of the water flow rate. The maximum efficiency of 98 per cent was only achieved with the maximum flow rate of 3.09 g/s, compared with 1.61 g/s required for the unbalanced flow tests to also achieve 98 per cent. However, the room conditions were drier and the return air flow rate was approximately 50 per cent higher for these balanced flow tests. The shape of the efficiency EV_R curve was the same as for the unbalanced flow tests, as expected.

(e) Figure 6.4.1 also includes the trends of the cooling capacity for the ventilation mode (TCC). The cooling capacity TCC generally increased with increasing spray chamber efficiency EV_R (see section 7.4 (a) and (b)).

(f) The ventilation mode cooling capacity (CC) also generally increased with increased efficiency EV_R but large fluctuations in these values were observed (see section 7.4 (c)).

(g) Dry-bulb temperature TDB_6 decreased as the change in humidity ratio W_6-W_5 increased. This was expected since sensible heat in the air was converted to latent heat.

6.5 Efficiency of Supply Air Spray Chamber (EV_S)

The numbering referred to in this section (6.5) is defined in the figure below (extracted from figure 1.1).

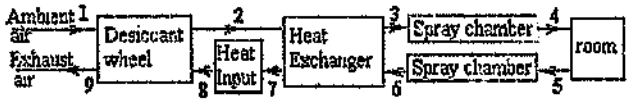

6.5.1 Experimental procedure and results

A set of tests was done to evaluate the effect on performance of the efficiency of the supply air spray chamber. The air flow was balanced and was approximately 150 g/s for both the supply and return air and all operating parameters were kept constant. Only the flow rate of the water to the nozzles of the spray chamber was varied to change the efficiency of the spray chamber. The results are given in tables 6.5.1 and 6.5.2 and figures 6.5.1 and 6.5.2.

TABLE 6.5.1: Performance parameters for variation of the efficiency of the supply air spray chamber (EV_S)

TEST NO.	EDH1 (%)	EDH2 (%)	ERG (%)		EHX_S (%)	EHX_R (%)	EV_S (%)	EV_R (%)	CC (kW)		COP		TCC (kW)		TCOP	
			M	Sim					M	Sim	M	Sim	M	Sim	M	Sim
H4/1	35	9	13	16	80	89	17	87	1.01	1.05	0.18	0.19	1.40	1.44	0.25	0.26
H4/2	35	9	15	15	80	90	30	87	0.96	1.02	0.17	0.18	1.35	1.42	0.24	0.25
H4/3	35	8	16	16	79	91	56	89	1.15	1.13	0.21	0.20	1.48	1.46	0.26	0.26
H4/4	33	8	19	15	79	92	73	88	1.06	0.98	0.19	0.17	1.50	1.42	0.27	0.25
H4/5	33	7	20	16	80	89	89	89	0.72	0.70	0.13	0.12	1.68	1.66	0.30	0.30
H4/6	33	9	18	15	80	90	93	89	0.86	0.87	0.15	0.16	1.50	1.52	0.27	0.27
H4/7	35	9	16	16	80	90	97	90	0.87	1.02	0.16	0.18	1.36	1.51	0.24	0.27

TABLE 6.5.2: Property changes for variation of the efficiency of the supply air spray chamber (EV_S)

TEST NO.	EV_S (%)	TDB_1 (°C)	W_1 (g/kg)	H_2-H_1 (kJ/kg)	W_1-W_2 (g/kg)	W_4-W_3 (g/kg)		FR_S (g/s)	TFR_S (g/s)	PP_S (bar)	TDB_3-TDB_4 (°C)		%EV (%)
						M	Sim				M	Sim	
H4/1	17	24.7	9.57	3.8	2.41	0.49	0.56	0.49	0.56	2	1.3	1.4	13
H4/2	30	24.8	9.69	3.6	2.37	0.88	0.71	0.58	0.71	10	2.1	2.3	18
H4/3	56	24.8	9.50	3.1	2.40	1.42	1.03	0.82	1.03	20	4.1	4.4	20
H4/4	73	24.2	9.65	3.2	2.34	1.96	1.31	1.02	1.31	30	5.1	5.4	22
H4/5	89	25.3	10.21	3.0	2.39	2.44	1.63	1.26	1.63	44	5.8	6.2	23
H4/6	93	24.7	9.86	3.6	2.37	2.55	1.76	1.38	1.76	51	6.3	6.8	22
H4/7	97	24.6	9.66	3.5	2.41	2.75	1.91	1.50	1.91	60	6.3	7.2	21

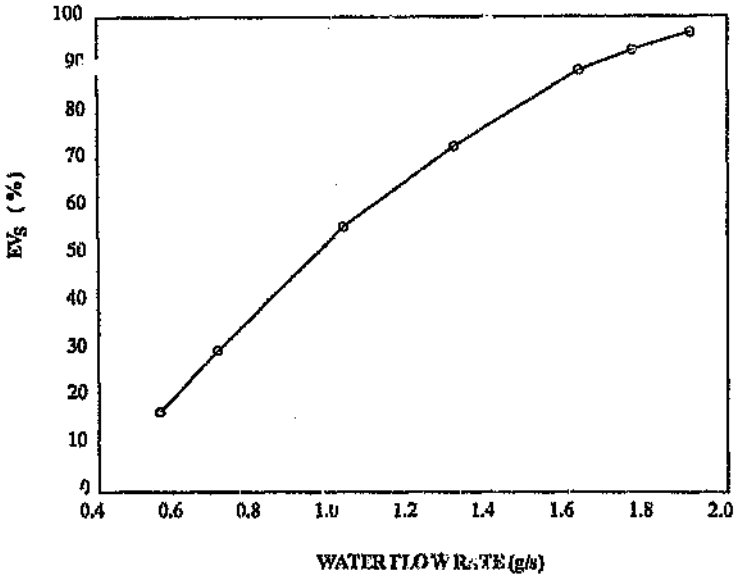

FIGURE 6.5.1: Efficiency of the supply air spray chamber EV_S versus water flow rate.

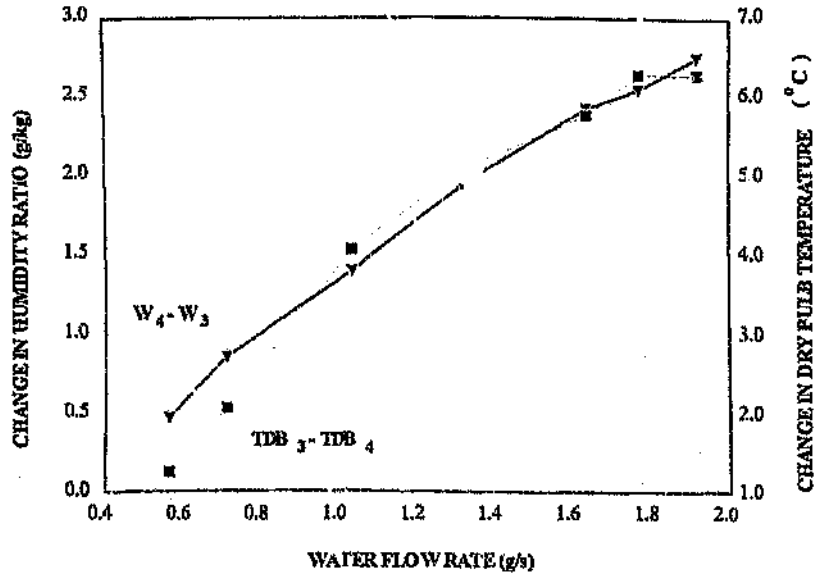

FIGURE 6.5.2: Changes in humidity ratio and dry-bulb temperature versus water flow rate to supply air spray chamber.

6.5.2 Main findings

The findings described below are discussed in detail in section 7.5.

The results are given in tables 6.5.1 and 6.5.2 and figures 6.5.1 and 6.5.2. The following observations were made:

(a) The spray chamber efficiency on the supply air side (EV_S) increased with increasing spray water flow rate (figure 6.5.1).

(b) The cooling capacity in the ventilation mode (CC) and in the ventilation credit mode (TCC) remained almost unchanged for changes in efficiency EV_S (i.e. no change in performance of the DEC system). The fluctuations were due to fluctuations of inlet air conditions.

(c) Dry-bulb temperature TDB_6 decreased and humidity ratio W_6 increased with increasing efficiency EV_S, as expected.

(d) The ratio of water evaporated to spray water supplied (%EV) was between 13 and 23 per cent. The percentage increased with increasing spray pressure, probably because the droplets were smaller and more total surface area was available for evaporation.

6.6 Inlet Air Conditions and Regeneration Temperatures

The numbering referred to in this section (6.6) is defined in the figure below (extracted from figure 1.1).



6.6.1 Experimental procedure and results

The inlet air conditions and regeneration temperatures were some of the most important operating parameters that determined the DEC performance characteristics. It was therefore important to test the system for a wide range of ambient conditions and regenerating temperatures.

Most of the tests were done during the winter months of June and July 1997 when the ambient air was cold and dry. The heaters and humidifier at the inlet to the supply air duct were insufficient to simulate summer conditions. A modification was therefore done to change the exhaust air ducting so that it discharged near the inlet of the supply air duct. The hot moist air from the regeneration process was therefore added to the supply air. A spray nozzle was also inserted into the discharge end of the exhaust air duct to further increase the humidity ratio and decrease the dry-bulb temperature, when required. This modification together with the two heaters and humidifier at the supply air inlet enabled one to simulate a wide range of ambient air conditions. The only limitation was that the condition of the supply air was determined to some extent by the outlet condition of the exhaust air. The sensitivity of the heater and humidifier controls was also very limited.

A series of tests was carried out where as many combinations as possible of the inlet air conditions and regeneration temperatures were tested. The limitations of the equipment (described above) limited the possible combinations. The test numbers,

inlet air conditions and regeneration temperatures for each test are shown on a psychrometric chart in figure 6.6.1.

The test results have been shown in this section in the following categories to illustrate different trends:

(a) The following shows the effect on performance of similar regeneration temperatures with different inlet air conditions: Tables 6.6.1a and 6.6.1b show all the results in appendix H5 in order of descending regeneration temperature. Tables 6.6.2a and 6.6.2b show the corresponding process changes for the same results. The dehumidification process for tests at different ranges of regeneration temperature are shown in figures 6.6.2 to 6.6.6.

(b) Table 6.6.3 and figures 6.6.7a and 6.6.7b show the effect on performance of different regeneration temperatures with similar inlet air conditions.

(c) Table 6.6.4 shows the effect on performance of keeping the dry-bulb temperature of the inlet air TDB_1 constant while varying the humidity ratio W_1.

(d) Table 6.6.5 shows the effect on performance of keeping the humidity ratio of the inlet air W_1 constant while varying the dry-bulb temperature TDB_1.

FIGURE 6.6.1 Inlet air conditions and regeneration temperatures (°C) for tests H5/1-H5/26 and H6/5-H6/10

TABLE 6.6.1a Performance parameters of tests listed in order of descending regeneration temperature (TDB_8)

(see table 6.6.2a for corresponding process changes for these tests)

TEST NO.	TDB_8 (°C)	EDH1 (%)	EDH2 (%)	ERG (%)		EHX_S (%)	EHX_R (%)	Q (kW)	CC (kW)		COP		TCC (kW)		TCOP	
				M	Sim				M	Sim	M	Sim	M	Sim	M	Sim
H5/22	93.8	32	21	47	26	85	77	7.683	-1.90	-2.38	-0.25	-0.31	3.68	3.20	0.48	0.42
H5/23	91.6	32	18	31	21	84	81	7.683	-0.91	-1.14	-0.12	-0.15	3.09	2.86	0.40	0.37
H5/7	90.9	31	22	67	24	84	79	7.683	-2.51	-2.84	-0.33	-0.37	4.20	3.88	0.55	0.51
H5/24	90.6	38	3	16	19	84	79	7.683	-0.17	-0.18	-0.02	-0.02	3.88	3.87	0.51	0.50
H5/21	87.7	26	30	61	28	84	74	5.763	-2.20	-3.06	-0.38	-0.53	3.58	2.72	0.62	0.47
H5/20	83.9	21	35	62	21	84	74	5.763	-2.04	-3.25	-0.35	-0.56	3.28	2.08	0.57	0.36
H5/8	82.4	28	14	59	21	84	71	1.382	-1.76	-2.03	-0.31	-0.36	4.18	3.91	0.73	0.69
H5/9	81.8	26	25	73	23	84	70	5.711	-2.22	-2.82	-0.39	-0.49	4.31	3.71	0.76	0.65
H5/19	81.2	18	32	44	15	82	79	5.763	-0.50	-1.36	-0.09	-0.24	2.24	1.38	0.39	0.24
H5/10	77.7	26	20	58	20	84	73	5.711	-1.36	-1.76	-0.24	-0.31	3.45	3.05	0.60	0.53
H5/4	77.2	37	18	25	16	82	83	7.566	0.40	0.30	0.05	0.04	0.98	0.89	0.13	0.12
H5/25	76.7	31	8	23	18	84	75	5.763	-0.07	-0.22	-0.01	-0.04	3.15	3.01	0.55	0.52
H5/11	71.2	40	20	55	32	84	72	5.711	-0.57	-0.74	-0.10	-0.13	2.38	2.22	0.42	0.39

TABLE 6.6.1b Performance parameters of tests listed in order of descending regeneration temperature (TDB_S)

(see table 6.6.2b for corresponding process changes for these tests)

TEST NO.	TDB_S (°C)	EDH1 (%)	EDH2 (%)	ERG (%)		EHX_S (%)	EHX_R (%)	Q (kW)	CC (kW)		COP		TCC (kW)		TCOP	
				M	Sim				M	Sim	M	Sim	M	Sim	M	Sim
H5/16	67.8	18	25	45	15	84	71	3.842	-0.88	-1.68	-0.23	-0.44	3.58	2.77	0.93	0.72
H5/17	67.6	20	28	68	20	85	68	3.842	-1.85	-2.89	-0.48	-0.75	4.00	2.96	1.04	0.77
H5/18	67.2	29	36	84	36	84	70	3.842	-1.78	-2.71	-0.46	-0.71	3.13	2.19	0.81	0.57
H5/12	64.3	39	24	78	42	84	68	3.842	-1.17	-1.59	-0.30	-0.41	3.18	2.76	0.83	0.72
H5/5	64.0	24	7	34	15	83	77	3.842	-0.89	-1.30	-0.23	-0.34	3.71	3.30	0.97	0.86
H5/3	63.6	44	20	31	26	81	79	5.676	0.49	0.49	0.09	0.08	0.86	0.83	0.15	0.15
H5/15	63.2	40	19	64	44	84	69	3.842	-1.59	-2.34	-0.41	-0.61	3.76	3.02	0.98	0.78
H5/14	60.7	36	-5	38	18	84	70	3.842	-0.03	-0.10	-0.01	-0.03	3.32	3.24	0.86	0.84
H5/26	59.5	36	10	32	24	83	76	3.807	0.04	-0.01	0.01	-0.00	2.29	2.25	0.60	0.59
H5/6	57.8	43	17	48	39	82	76	3.842	-0.58	-0.73	-0.15	-0.19	2.15	2.01	0.56	0.52
H5/2	54.7	41	20	36	31	82	75	3.786	-0.18	-0.32	-0.05	-0.08	1.83	1.69	0.48	0.45
H5/13	53.3	38	-7	147	54	83	69	1.905	-2.29	-3.34	-1.20	-1.75	4.79	3.73	2.51	1.96
H3/1	49.7	52	20	38	39	82	74	3.786	0.24	0.27	0.06	0.07	1.06	1.09	0.28	0.29

TABLE 6.6.2a Process changes of tests listed in order of descending regeneration temperature (TDB_8)

(see table 6.6.1a for corresponding performance parameters for these tests)

TEST NO.	TDB_8 (°C)	RH_8 (%)	TDB_1 (°C)	W_1 (g/kg)	TDB_2 (°C)	W_2 (g/kg)	H_2-H_1 (kJ/kg)	W_1-W_2 (g/kg)	TDP_2 (°C)	TDB_6 (°C)	TDB_7 (°C)	TDB_{9Sim} - TDB_7 (°C)	$TDB_{7'}$ - TDB_7 (°C)	W_3-W_2 (g/kg)	
														M	Sim
H5/22	93.8	3	32.3	27.21	56.6	21.26	10.2	5.95	22.5	18.7	48.1	73.1	8.5	-1.87	-0.49
H5/23	91.6	3	32.1	20.99	52.4	16.18	8.6	4.81	18.2	17.8	45.6	74.4	6.8	-0.59	-0.08
H5/7	90.9	2	38.5	26.66	60.4	21.18	8.8	5.47	22.5	17.6	47.8	76.1	12.6	-1.37	-0.61
H5/24	90.6	3	40.8	16.68	52.5	12.42	1.3	4.25	14.2	17.3	45.2	83.3	7.6	0.58	0.21
H5/21	87.7	4	32.1	29.40	57.0	24.57	13.7	4.83	24.8	19.7	47.4	59.7	9.6	-3.24	-0.71
H5/20	83.9	4	29.9	28.78	54.6	25.07	16.5	3.71	25.1	19.6	45.6	57.4	9.0	-4.24	-0.76
H5/8	82.4	3	42.3	21.31	55.7	17.77	4.7	3.54	19.7	16.9	44.4	67.8	11.3	-0.82	-0.35
H5/9	81.8	3	39.0	24.85	56.2	20.84	7.7	4.00	22.2	16.9	44.5	64.3	11.7	-2.17	-0.63
H5/19	81.2	4	28.1	20.83	49.4	18.29	15.6	2.54	20.1	19.2	42.9	58.0	6.5	-2.18	-0.15
H5/10	77.7	4	34.9	19.69	49.9	16.44	7.9	3.26	18.5	16.2	40.7	62.3	9.2	-1.41	-0.29
H5/4	77.2	3	15.8	10.78	33.9	7.41	9.9	3.37	6.6	13.2	30.4	59.8	3.5	0.42	0.23
H5/25	76.7	4	36.1	15.65	46.2	12.71	2.8	2.94	14.5	17.1	39.0	65.4	7.2	0.01	0.10
H5/11	71.2	4	22.6	18.29	42.5	15.02	7.4	3.27	14.9	15.3	35.0	51.3	7.8	-0.29	-0.01

TABLE 6.6.2b Process changes of tests listed in order of descending regeneration temperature (TDB_8)

(see table 6.6.1b for corresponding performance parameters for these tests)

TEST NO.	TDB_8 (°C)	RH_8 (%)	TDB_1 (°C)	W_1 (g/kg)	TDB_2 (°C)	W_2 (g/kg)	H_2-H_1 (kJ/kg)	W_1-W_2 (g/kg)	TDP_2 (°C)	TDB_6 (°C)	TDB_7 (°C)	TDB_{9Sim} -TDB_7 (°C)	TDB_2 -TDB_7 (°C)	W_3-W_2 (g/kg)	
														M	Sim
H5/16	67.8	8	38.9	21.85	49.2	20.18	6.5	1.67	21.7	19.4	40.7	54.2	8.5	-2.65	-0.30
H5/17	67.6	8	38.4	26.71	50.5	24.47	6.9	2.24	24.8	19.7	40.7	52.3	9.8	-3.85	-0.62
H5/18	67.2	8	28.4	27.48	48.8	23.42	10.9	4.06	24.1	19.3	40.0	44.3	8.8	-3.39	-0.62
H5/12	64.3	7	30.3	22.61	47.0	17.97	5.5	4.64	19.9	17.7	37.5	45.7	9.5	-1.45	-0.26
H5/5	64.0	7	39.8	16.44	45.4	14.74	1.4	1.70	16.8	15.9	38.5	56.4	6.9	-1.16	-0.15
H5/3	63.6	6	13.9	11.68	31.6	7.71	7.9	3.97	7.1	13.8	27.9	45.6	3.7	0.61	0.28
H5/15	63.2	8	29.8	24.62	45.8	19.70	4.1	4.93	21.3	17.1	37.0	45.1	8.8	-2.56	-0.49
H5/14	60.7	7	38.6	13.17	42.5	11.22	-1.0	1.96	12.7	16.2	34.7	54.5	7.8	0.40	0.17
H5/26	59.5	7	29.9	14.33	38.5	11.82	2.4	2.50	13.4	16.4	33.1	48.0	5.4	0.31	0.17
H5/6	57.8	9	23.0	17.36	37.5	13.16	4.2	4.20	15.1	15.9	32.3	41.7	5.2	-0.29	-0.03
H5/2	54.7	10	21.5	13.55	34.6	10.03	5.3	3.19	11.0	14.0	29.3	39.6	5.3	-0.11	0.08
H5/13	53.3	13	39.9	27.30	46.8	24.31	-0.5	2.99	24.6	18.3	38.1	[illegible].8	8.7	-3.98	-0.82
H5/1	49.7	11	14.0	11.91	28.9	7.96	[illegible]	3.96	7.6	13.1	24.7	33.0	4.2	0.55	0.20

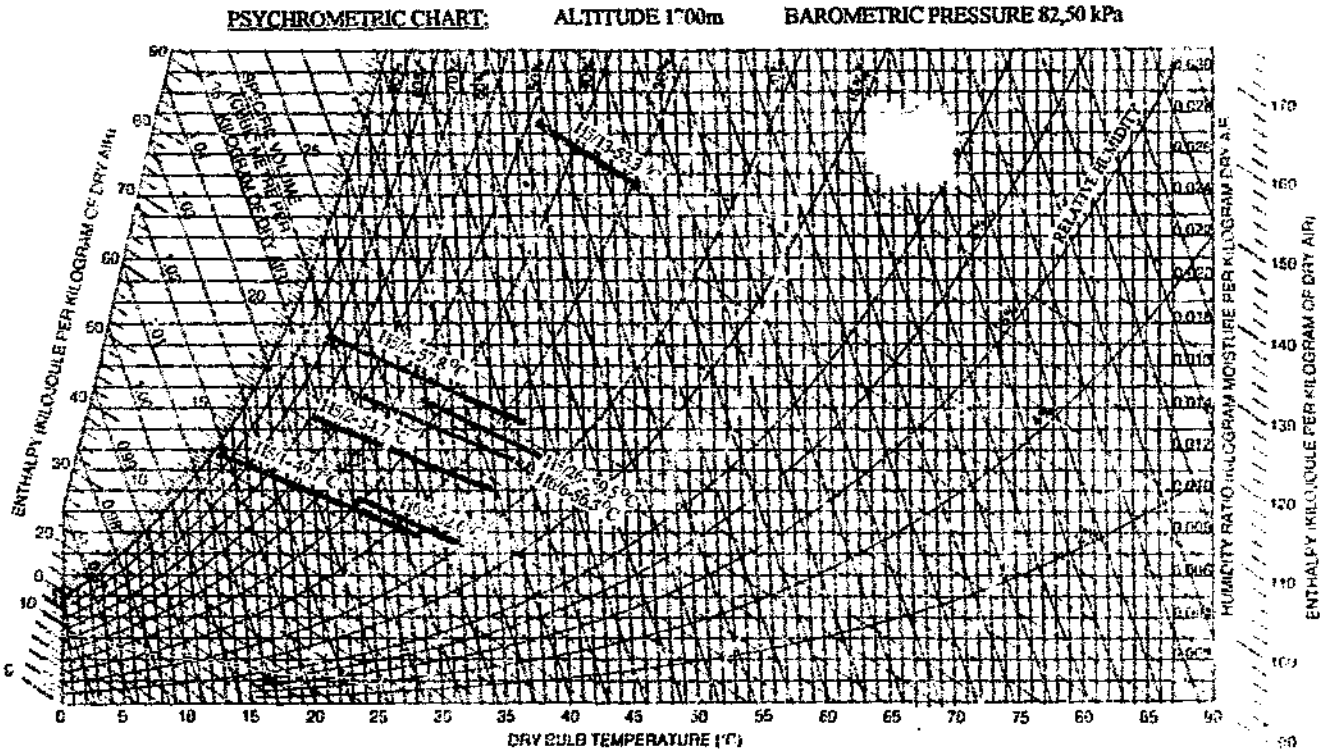

FIGURE 6.6.2 Dehumidification processes (1-2) of tests with regeneration temperature TDB_8 of 55 ± 5 °C

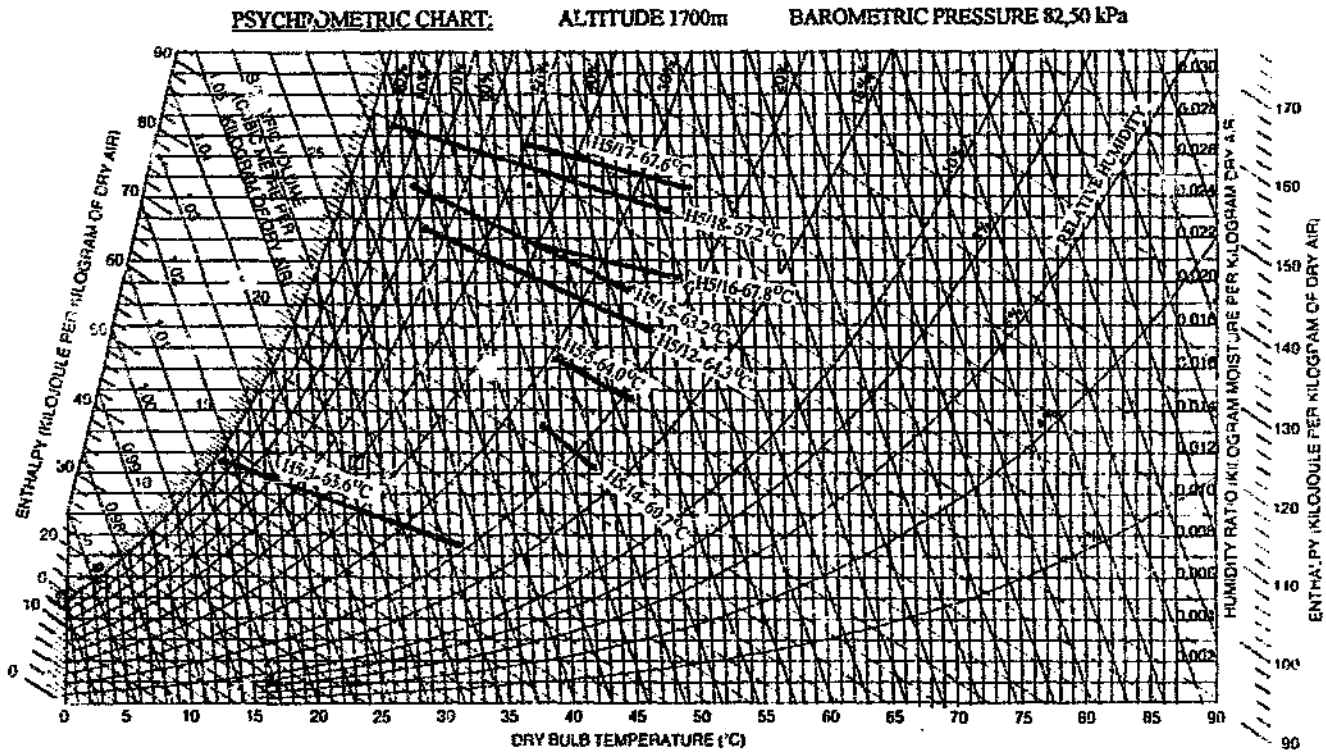

FIGURE 5.6.3 Dehumidification processes (1-2) of tests with regeneration temperature TDB_3 of 65 ± 5 °C

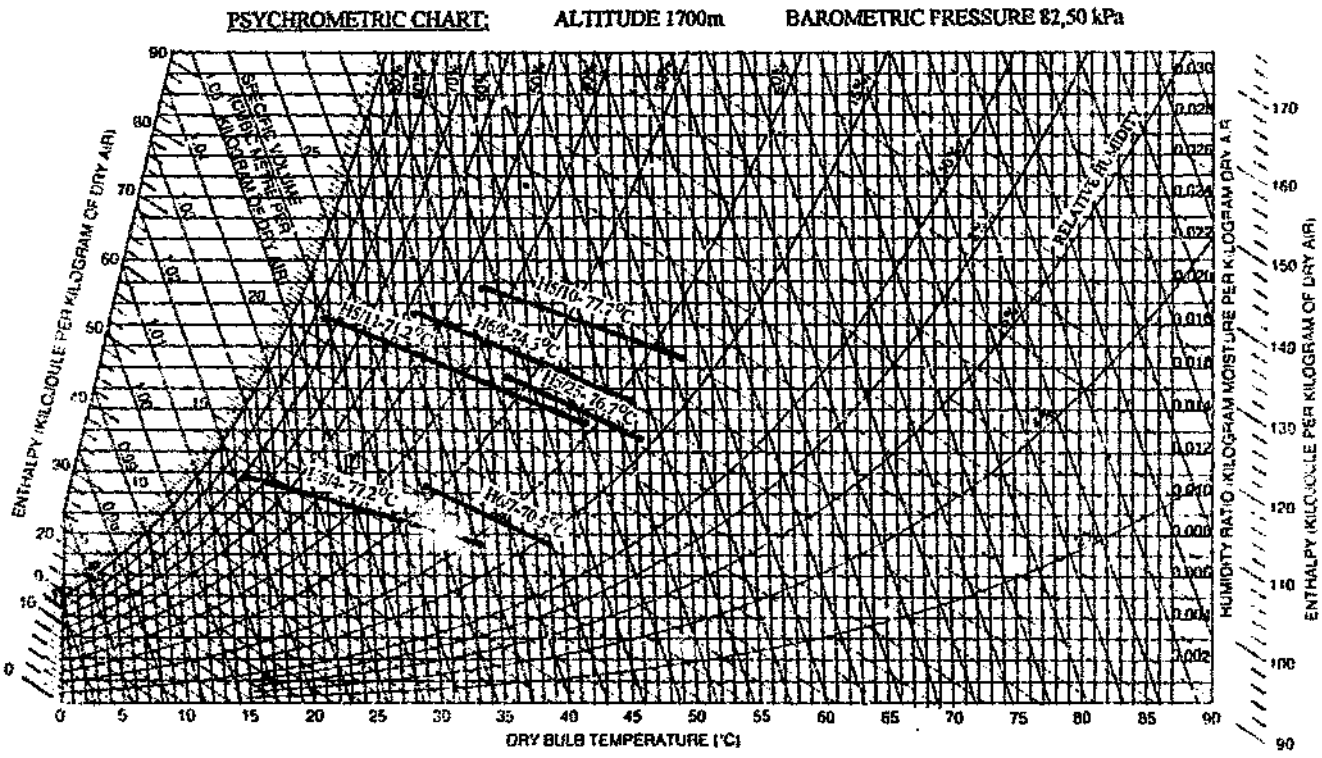

FIGURE 6.6.4 Dehumidification processes (1-2) of tests with regeneration temperature TDB_8 of 75 ± 5 °C

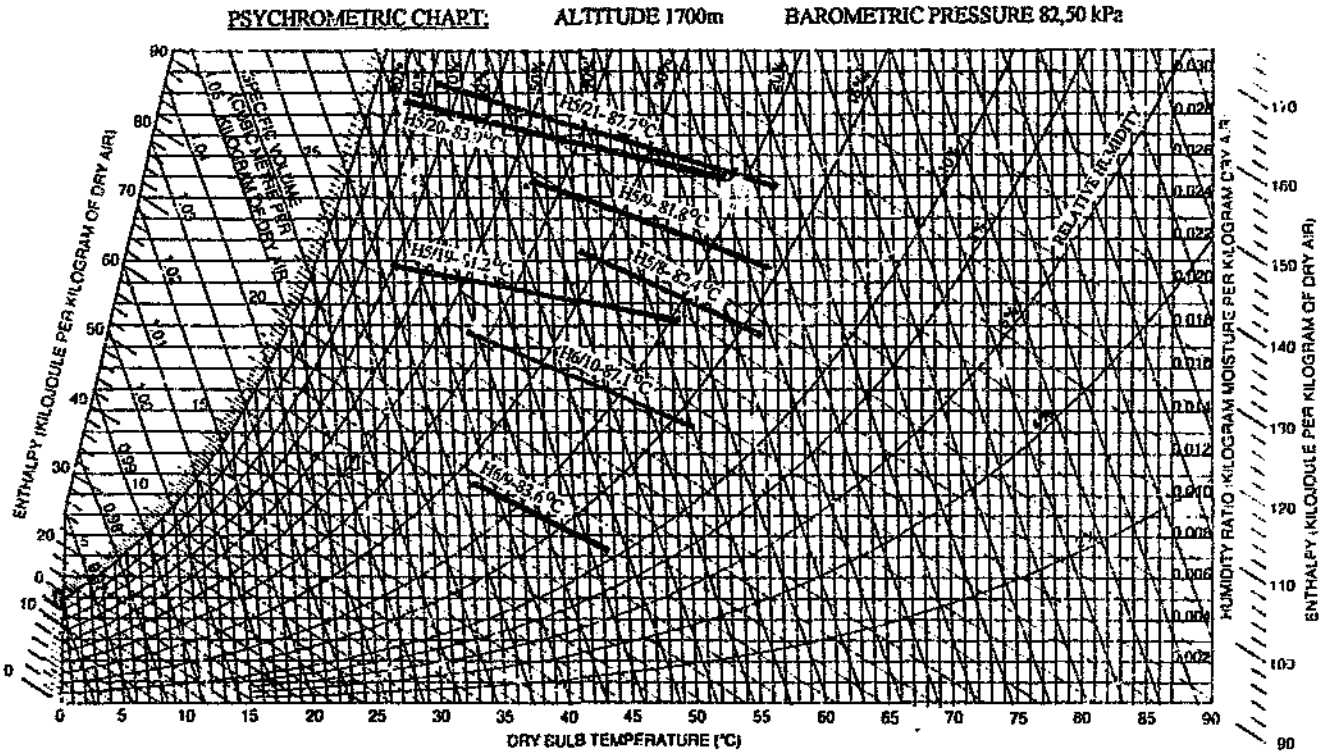

FIGURE 6.6.5 Dehumidification processes (1-2) of tests with regeneration temperature TDB_8 of 85 ± 5 °C

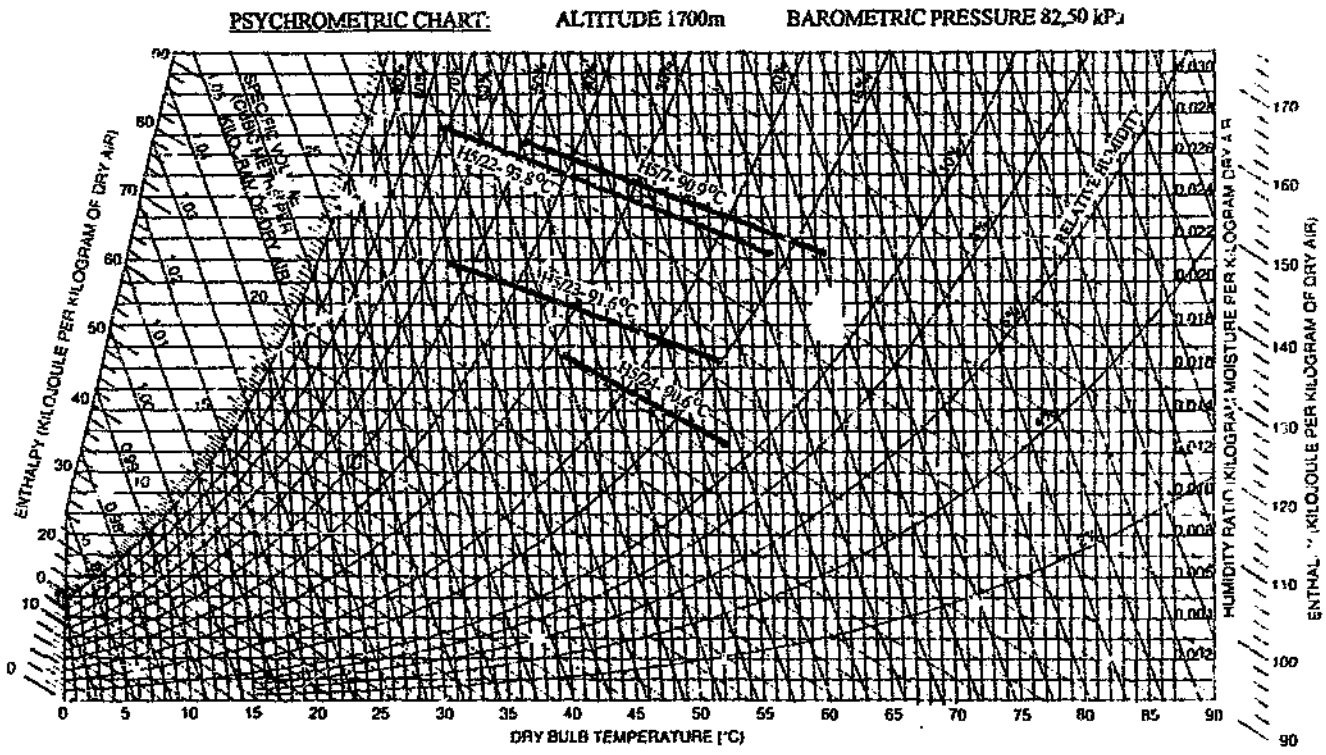

FIGURE 6.6.6 Dehumidification processes (1-2) of tests with regeneration temperature TDB_g of 95 ± 5 °C

TABLE 6.6.3 Comparison of 8 groups of 2 tests at similar inlet air condition but different regeneration temperatures (TDB_8)

GR	TEST NO.	TDB_8 (°C)	TDB_1 (°C)	W_1 (g/kg)	EDH1 (%)	EDH2 (%)	ERG (%)	EHX_S (%)	EHX_R (%)	Q (kW)	CC (kW)	COP	TCC (kW)	TCOP	H_2-H_1 (kJ/kg)	W_1-W_2 (g/kg)	TDB_2-TDB_7 (°C)
A	H5/22	93.8	32.3	27.21	32	21	26	85	77	7.683	-2.38	-0.31	3.20	0.42	10.2	5.95	8.5
A	H5/21	87.0	32.1	29.40	26	30	28	84	74	5.762	-3.06	-0.53	2.72	0.47	13.7	7.83	9.6
B	H5/7	90.9	38.5	26.66	31	22	24	84	70	7.683	-2.84	-0.37	3.88	0.51	8.8	5.4	12.6
B	H5/17	67.6	38.4	26.71	20	28	20	85	68	3.842	-2.89	-0.75	2.96	0.77	6.9	2.24	9.8
C	H5/9	81.8	39.0	24.85	26	22	23	84	70	5.711	-2.82	-0.49	3.71	0.65	7.7	4.00	11.7
C	H5/13	53.3	39.9	27.30	38	7	54	83	69	1.905	-3.34	-1.75	3.73	1.96	-0.5	2.99	8.7
D	H6/10	87.1	33.8	17.89	37	11	21	84	76	7.566	-1.07	-0.14	3.44	0.45	4.7	4.72	8.1
D	H5/10	77.7	34.9	19.69	26	20	20	84	73	5.711	-1.76	-0.31	3.05	0.53	7.2	3.26	9.2
[illegible]	H5/24	90.6	40.8	16.68	38	3	9	84	79	7.683	-0.18	-0.0[illegible]	[illegible].7	0.50	1.3	4.25	7.6
[illegible]	H5/5	64.0	39.8	16.44	24	7	15	83	77	3.842	-1.30	-0.34	3.30	0.86	1.4	1.70	6.0
F	H5/11	71.2	22.6	18.29	40	20	32	84	72	5.711	-0.74	-0.13	2.22	0.39	7.4	5.27	7.8
F	H5/6	57.8	23.0	17.36	43	17	39	82	76	3.842	-0.73	-0.19	2.01	0.52	4.2	4.20	5.2
G	H5/3	63.6	13.9	11.68	44	20	26	81	79	5.676	0.49	0.08	0.83	0.15	7.9	3.97	[illegible]
G	H5/1	49.7	14.0	11.91	52	20	39	82	74	3.786	0.27	0.07	1.19	0.29	5.2	3.96	[illegible].2
H	H6/9	83.6	33..	10.45	44	4	15	84	80	7.566	0.58	0.08	2.98	[illegible].39	1.9	3.30	5.7
H	H5/7	70.5	29.6	10.2[illegible]	42	8	17	83	78	5.676	0.63	0.11	2.34	[illegible].41	2.7	2.71	5.3

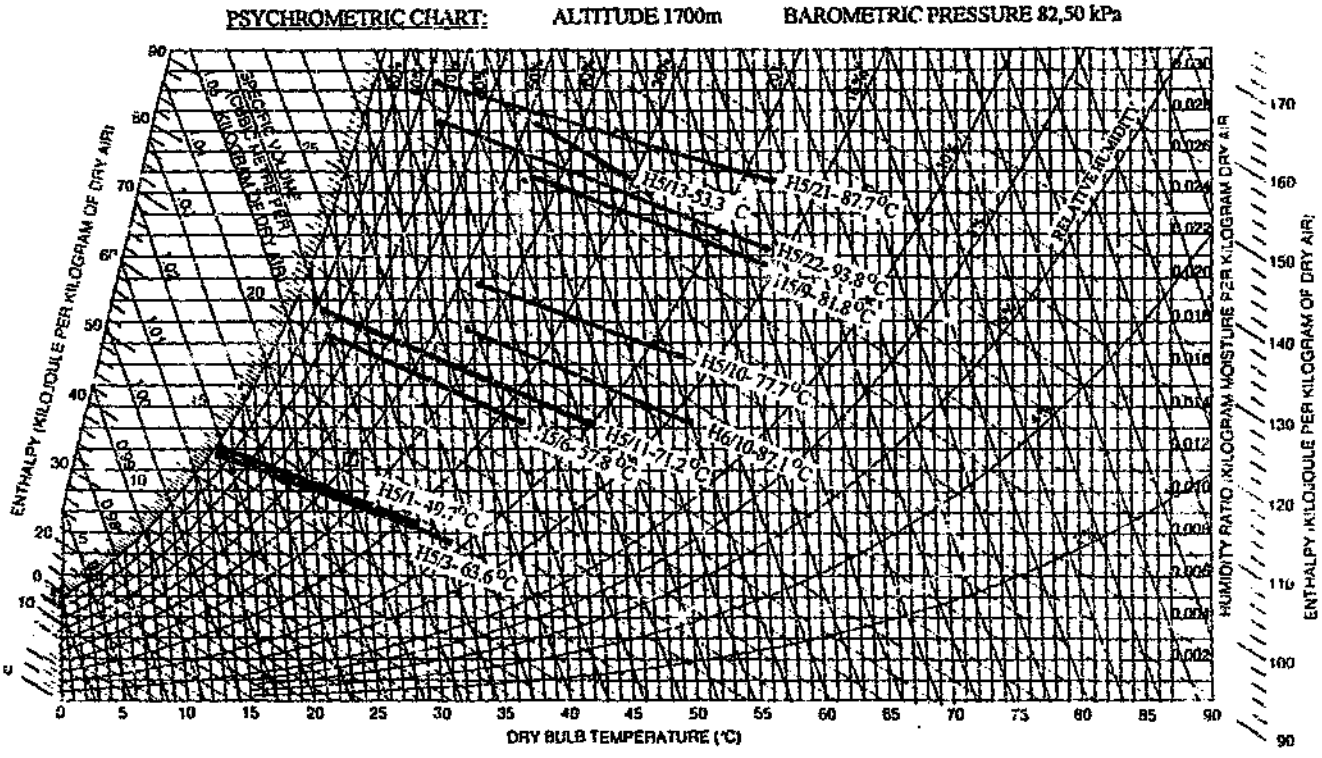

FIGURE 6.6.7a Dehumidification processes (1-2) for groups of two tests at similar inlet air conditions but different regenerating temperatures.

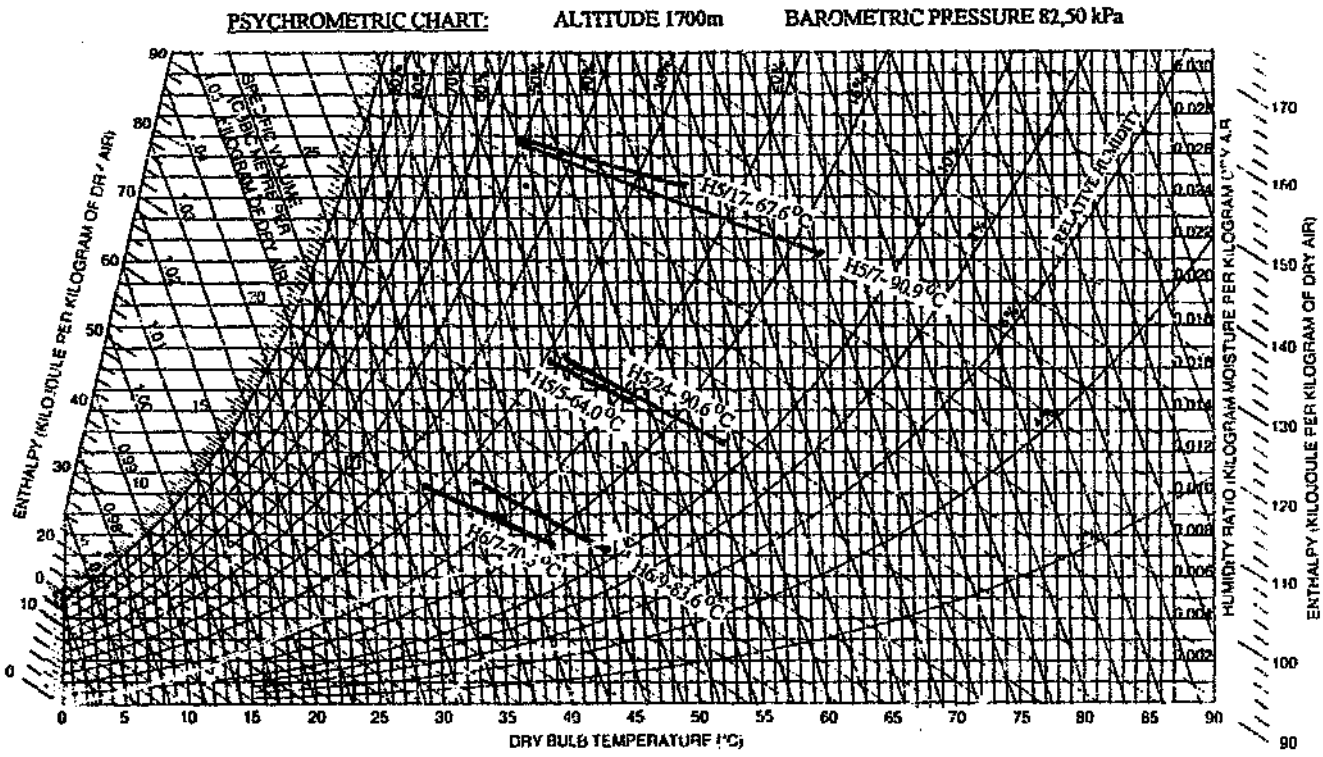

FIGURE 6.6.7b Dehumidification processes (1-2) for groups of two tests at similar inlet air conditions but different regenerating temperatures

TABLE 6.6.4 Comparison of 4 groups of 2 tests at similar dry-bulb temperature TDB_1 but different humidity ratio W_1

TEST NO.	TDB_3 (°C)	TDB_1 (°C)	W_1 (g/kg)	EDH1 (%)	EDH2 (%)	ERG (%)	Q (kW)	CC (kW)	COP	TCC (kW)	TCOP	H_2-H_1 (kJ/kg)	W_1-W_2 (g/kg)
H5/7	90.9	38.5	26.68	31	22	24	7.683	-2.84	-0.37	3.88	0.51	8.8	5.47
H5/24	90.6	40.8	16.68	38	31	19	7.683	-0.48	-0.06	3.87	0.51	3.13	4.25
H5/10	77.7	34.9	19.69	26	20	20	5.711	-1.76	-0.31	3.05	0.53	7.2	3.26
H5/25	76.7	36.1	15.65	31	8	23	5.763	-0.22	-0.01	3.01	0.52	2.8	2.94
H5/15	63.2	29.8	24.62	40	39	21	3.849	-2.24	-0.61	3.02	0.78	34	4.93
H5/26	59.5	29.9	19.69	36	10	24	3.807	-0.01	0.00	2.025	0.59	2.4	2.50
H5/6	57.8	23.0	17.36	43	17	39	3.842	-0.73	-0.19	2.01	0.52	4.2	4.20
H5/2	54.7	21.5	13.55	41	20	31	3.786	-0.32	-0.08	1.69	0.45	5.3	3.19

TABLE 6.6.5 Comparison of 4 groups of 2 tests at similar humidity ratio W_1 but different dry-bulb temperature TDB_1

TEST NO.	TDB_s (°C)	TDB_1 (°C)	W_1 (g/kg)	EDH1 (%)	EDH2 (%)	ERG (%)	Q (kW)	CC (kW)	COP	TCC (kW)	TCOP	H_2-H_1 (kJ/kg)	W_1-W_2 (g/kg)
H5/7	80.9	38.5	26.68	31	22	24	7.708	-2.[illegible]	-0.3[illegible]	3.88	0.5[illegible]	8.8[illegible]	5.47
H5/22	79.8	38.3	27.28	42	2[illegible]	26	7.683	-3.38	-0.5[illegible]	3.20	0.4[illegible]	10.2[illegible]	6.95
H5/10	77.7	34.9	19.69	26	20	20	5.711	-1.76	-0.31	3.05	0.53	7.2	3.26
H5/11	71.2	22.6	18.29	40	20	32	5.711	-0.74	-0.13	2.22	0.39	7.4	5.27
H5/17	67.6	38.4	26.91	20	28	20	3.842	-2.89	-0.75	2.96	0.77	6.9	2.24
H5/13	67.2	28.4	21.48	29	36	36	3.842	-2.71	-0.71	2.19	0.57	10.9	4.06
H5/5	64.0	39.4	16.44	24	7	15	3.842	-1.30	-0.34	3.30	0.86	1.4	1.70
H5/6	57.8	23.0	17.36	43	17	39	3.842	-0.73	-0.19	2.01	0.52	4.2	4.20

6.6.2 Main findings

The more significant findings described below are discussed in detail in section 7.6.

The numbering referred to in this section (6.6.2) is defined in the figure below (extracted from figure 1.1).



The results summarised in section 6.6.1 are described in this section in the following categories:

(a) Similar regeneration temperatures at different inlet air conditions.
(b) Similar inlet air conditions at different regeneration temperatures.
(c) Changing humidity ratio of inlet air with constant dry-bulb temperature.
(d) Changing dry-bulb temperature of inlet air with constant humidity ratio.

6.6.2.1 Similar regeneration temperatures at different inlet air conditions

Tables 6.6.1a and 6.6.1b show the tests in order of descending regeneration temperature. Tables 6.6.2a and 6.6.2b show the corresponding process changes. The dehumidifying processes for tests at various temperature ranges are shown in figures 6 6.2 to 6.6.6. The following observations were made from the tables:

(a) The efficiency of heat transfer to the supply air (EHX_S) was very stable at approximately 84 per cent. However, the efficiency of heat transfer to the return air (EHX_R) was unstable and varied from 68 to 83 per cent. The most probable cause was radiation from the regeneration heaters (see section 7.6.2 (e)).

(b) In most of the tests, the dew point temperature at point 2 was greater than the dry-bulb temperature at point 6 (see section 7.6.1 (a)).

(c) Air leakage into point 3 was observed by comparing the measured and simulated changes in humidity ratio W_3-W_2 (see section 7.6.1 (b)).

(d) The difference between the return air temperature at point 9 and at point 7 was between 30 and 60 °C for most tests within practical operating conditions (see section 7.6.1 (c) and (d)).

(e) The cooling capacity in the ventilation mode (CC) was negative (heating not cooling) for most tests (see section 7.6.1 (e)) .

(f) The cooling capacity in the ventilation mode (CC) and corresponding COP were generally higher for lower ambient dry-bulb temperature TDB_1 and lower ambient humidity ratio W_1 (see section 4.2.2.3, page 40 for reasons).

(g) The cooling capacity in the ventilation credit mode (TCC) and corresponding TCOP were generally higher for higher ambient dry-bulb temperature TDB_1 and higher ambient humidity ratio W_1 (see section 4.2.2.3, page 40 for reasons).

The following observations were made from figures 6.6.2 to 6.6.6:

(h) For a specific regeneration temperature, the dehumidification process ends at approximately the same relative humidity RH_2. Ambient conditions at lower relative humidities RH_1 were dehumidified to only a slightly lower relative humidity RH_2 (see section 4.1.1.1, page 29 for reasons).

(i) A higher regeneration temperature resulted in more dehumidification and a lower relative humidity RH_2 (see section 7.6.2 (a)).

(j) More moisture was removed from ambient air with a higher relative humidity RH_1 (see section 4.2.2.3, page 40 for reasons).

(k) The dehumidification process lines on the psychrometric charts in figures 6.6.2 to 6.6.6 were approximately parallel, for the same regeneration temperatures. This was applicable for all ambient conditions (see section 7.6.1 (f)). Lines that were not parallel were exceptions and probably represented faulty wet-bulb measurements at point 2 (usually a result of sudden dust contamination).

6.6.2.2 Similar inlet air conditions at different regeneration temperatures.

Eight groups of two tests at similar inlet air conditions but different regeneration temperatures are given in table 6.6.3. The dehumidification process for each of these tests is shown in figures 6.6.7a and 6.6.7b.

The following observations were made for increasing regeneration temperature:

(a) The moisture absorbed (W_1-W_2) during dehumidification increased (see section 7.6.2 (a)).

(b) The moisture absorption efficiency EDH1 increased in some cases and decreased in others (see section 7.6.2 (b)).

(c) The heat transfer efficiency of the desiccant wheel (EDH2) generally decreased, contrary to the expected increase (see section 7.6.2 (c)).

(d) The regeneration efficiency ERG increased in some cases and decreased in others (see section 7.6.2 (d)).

(e) The efficiency of heat exchange in the return air EHX_R increased (section 7.6.2(e)).

(f) The cooling capacity in the ventilation mode CC and corresponding COP generally increased with higher regeneration temperature (section 7.6.2(f)).

(g) The cooling capacity in the ventilation credit mode TCC and corresponding TCOP generally decreased with higher regeneration temperature (section 7.6.2(f)).

6.6.2.3 Changing humidity ratio of inlet air with constant dry-bulb temperature.

Four sets of two tests with similar dry-bulb temperatures TDB_1 and regeneration temperatures TDB_8 but different ambient humidity ratios W_1 are given in table 6.6.4.

The following observations were made for increasing ambient humidity ratios W_1:

(a) The amount of moisture removed (W_1-W_2) increased (see section 7.6.3 (a)).

(b) An increase in moisture absorption efficiency EDH1 was initially expected but this was not always the case (see section 7.6.3 (b)).

(c) The regeneration efficiency ERG increased (see section 7.6.3 (c)).

(d) The cooling capacity in the ventilation mode CC and corresponding COP decreased with increasing humidity ratio W_1 (see section 4.2.2.3, page 40).

(e) The cooling capacity in the ventilation credit mode TCC and corresponding TCOP increased with increasing, W_1 (see section 4.2.2.3, page 40).

6.6.2.4 Changing dry-bulb temperature of inlet air with constant humidity ratio.

Four sets of two tests with similar humidity ratios W_1 but different ambient dry-bulb temperatures TDB_1 are given in table 6.6.5.

The following observations were made for increasing dry-bulb temperature TDB_1:

(a) The moisture removed from the air W_1-W_2 decreased (see section 7.6.4 (a)).

(b) The heat transferred to the supply air H_2-H_1 decreased (see section 7.6.4 (b)).

(c) The regeneration efficiency ERG decreased (see section 7.6.4 (c)).

(d) The cooling capacity in the ventilation mode CC and corresponding COP decreased with increasing dry-bulb temperature TDB_1 (see section 4.2.2.3, page 40).

(e) The cooling capacity in the ventilation credit mode TCC and corresponding TCOP increased with increasing dry-bulb temperature TDB_1 (see section 4.2.2.3, page 40).

6.7 Desiccant Wheel Speed and Unbalanced Air Flow

The numbering referred to in this section (6.7) is defined in the figure below (extracted from figure 1.1).



6.7.1 Experimental procedure and results

The following two sets of tests were done to investigate the effects on performance, of unbalanced air flow, and of changing the rotational speed of the desiccant wheel:

(a) Balanced flow was maintained in the heat exchanger but some return air was vented downstream of the heat exchanger in the return air duct (point 7) which resulted in unbalanced flow in the desiccant wheel. Four tests were done at two different regeneration temperatures for two different wheel speeds (0.24 rpm and 0.12 rpm). The results are given in table 6.7.1.

(b) Balanced flow was maintained throughout the system and 12 tests were done at different regeneration temperatures and inlet air conditions, for two different wheel speeds (0.24 rpm and 0.12 rpm). The results are given in table 6.7.2.

TABLE 6.7.1: Unbalanced flow at different regeneration temperatures and different desiccant wheel speeds

TEST NO.	TDB_8 (°C)	TDB_1 (°C)	W_1 (g/kg)	EDH1 (%)	EDH2 (%)	ERG (%)	CC (kW)	COP	TCC (kW)	TCOP	Q (kW)	H_7-H_1 (kJ/kg)	W_1-W_2 (g/kg)	TDB_{8Sim} -TDB_7 (°C)
H6/1	[illegible]	22.5	17.03	36	[illegible]	31	-0.30	-0.08	1.97	0.62	5.786	6.[illegible]	3.82	13.8
H6/[illegible]	[illegible]	22.4	[illegible]	35	6[illegible]	30	-0.30	-0.08	1.99	0.65	5.786	6.22	4.08	18.9
H6/2	91.4	24.7	18.06	33	13	29	-0.45	-0.08	2.31	0.41	5.676	7.5	4.76	28.2
H6/3*	88.4	26.6	17.47	28	5	23	-0.47	-0.08	2.34	0.41	5.676	2.8	3.66	39.8

Notes:

(1) * = small pulley wheel (rotational speed of 0.12 rpm)

(2) TDB_{8Sim} = simulated TDB_8

TABLE 6.7.2: Variation of regeneration temperature and inlet air conditions at different desiccant wheel speeds

TEST NO.	TDB_8 (°C)	TDB_1 (°C)	W_1 (g/kg)	EDH1 (%)	EDH2 (%)	ERG (%)	CC (kW)	COP	TCC (kW)	TCOP	Q (kW)	H_2-H_1 (kJ/kg)	W_1-W_2 (g/kg)	TDB_{9Sim} -TDB_7 (°C)
H6/5*	52.6	24.5	9.51	42	10	20	-0.48	-0.18	1.81	0.48	3.786	2.4	2.02	15.8
H6/11*	52.7	25.8	9.99	30	0	14	-0.22	-0.06	1.68	0.49	3.786	0.1	1.44	19.2
H6/6	56.5	25.2	14.52	43	18	32	-0.45	-0.12	2.22	0.59	3.786	4.3	3.40	10.7
H6/12*	55.7	26.5	16.91	36	4	30	-1.22	-0.32	2.46	0.65	3.786	0.9	3.14	14.6
H6/7*	70.5	29.6	10.21	42	8	17	-0.63	-0.11	2.34	0.41	5.676	2.7	2.71	26.2
H6/13*	68.4	30.5	10.09	19	2	8	-0.20	-0.04	2.16	0.38	5.676	0.8	1.17	31.7
H6/8	74.6	29.4	18.02	38	16	27	-0.72	-0.13	2.64	0.47	5.676	5.7	4.39	19.6
H6/14*	69.8	29.1	17.31	30	5	21	-1.31	-0.23	2.73	0.48	5.676	1.7	3.29	25.6
H6/9*	83.6	33.3	10.45	44	4	15	-0.58	-0.08	2.98	0.39	7.566	1.9	3.30	38.6
H6/15*	80.9	33.3	10.01	24	2	8	-0.21	-0.03	2.77	0.37	7.566	0.8	1.70	44.7
H6/10	87.1	33.8	17.89	37	11	21	-1.07	-0.14	3.44	0.45	7.566	4.7	4.72	32.8
H6/16*	84.5	34.6	17.16	23	3	12	-1.41	-0.19	3.05	0.40	7.566	1.1	2.68	40.7

Notes:

(1) * = small pulley wheel (rotational speed of 0.12 rpm)

(2) TDB_{9Sim} = simulated TDB_9

6.7.2 Main findings

6.7.2.1 Balanced flow at different regeneration temperatures and different inlet air conditions

The test results are summarised in table 6.7.2.

(a) The amount of moisture removed (W_1-W_2) and moisture removal efficiency EDH1 were slightly lower for the slower wheel spee 1 (see section 7.7.1 (a)).

(b) The amount of heat transferred (H_2-H_1) and heat transfer efficiency EDH2 decreased for the slower wheel speed (see section 7.7.1 (b)).

(c) The regeneration efficiency (ERG) decreased with slower wheel speed (see section 7.7.1 (c)).

(d) The cooling capacity and COP were virtually the same for both wheel speeds, for both the ventilation and ventilation credit modes (see section 7.7.1 (d)).

6.7.2.2 Unbalanced flow at different regeneration temperatures

These results are summarised in table 6.7.1.

(a) The observations from section 6.7.2.1 were also applicable to these tests.

(b) The regeneration efficiencies ERG for these tests were significantly higher than those for balanced flow in table 6.7.2 (see section 7.7.2 (b)).

(c) Comparing tests H6/2 (unbalanced flow) with H6/8 (balanced flow) the performance of the unbalanced flow test was significantly better, in both ventilation and ventilation credit modes (see section 7.7.2 (c)).

6.8 Test Results versus Catalogue Data

Simulations were done based on the operating parameters of two experimental tests and information supplied by the manufacturer concerning the performance of the desiccant wheel. These simulation results and the results of the experimental tests are shown in table 6.8.1.

Table 6.8.1: Comparison of test results with simulations based on catalogue data.

Parameter	Test H5/25		Test H6/7	
	Measured	Simulated	Measured	Simulated
TDB_8 (°C)	76.7	76.7	70.5	70.5
TDB_1 (°C)	36.1	36.1	29.6	29.6
W_1 (g/kg)	15.65	15.65	10.21	10.21
TDB_2 (°C)	46.2	53.0	39.0	44.8
W_2 (g/kg)	12.71	10.86	7.50	6.53
W_1-W_2 (g/kg)	2.94	4.79	2.71	3.68
H_2-H_1 (kJ/kg)	2.8	5.02	2.7	6.05
EDH1 (%)	31	51	42	55
EDH2 (%)	8	17	8	19
ERG (%)	18	34	17	27
Q (kW)	5.763	4.85	5.676	4.87
CC (kW)	-0.22	0.20	0.63	0.84
COP (fraction)	-0.04	0.04	0.11	0.17
TCC (kW)	3.01	3.43	2.34	2.56
TCOP (fraction)	0.52	0.71	0.41	0.53

CHAPTER 7
DISCUSSION OF TEST RESULTS

Due to the large quantity of experimental results, the main findings and observations were briefly described together with the experimental results (chapter 6). This chapter discusses only the most important of these findings as well as those findings that require further clarification or discussion.

The numbering referred to in this chapter is defined in the figure below (extracted from figure 1.1).



7.1 Air Leakage

The effects of air leakage were investigated in detail because of the significant influence on the other experimental results.

The results of the air leakage tests assisted in the interpretation of the experimental results given in appendices H3 to H6. It also provided some interesting information concerning the hidden adverse consequences of air leakage (see section 6.1.2 for details).

These consequences included:

(a) Decrease in supply air flow rate and hence cooling capacity.

(b) Each individual process was degraded by the mixing of the processed air with the leakage air.

(c) The performance of each component in the system was affected by changes in flow rates.

(d) The parasitic power requirements were increased. This was especially applicable to the fans.

The air leakage that affected performance most was at points 2 and 3 (figure 1.1). The cooling capacity (CC) was reduced by 24 to 30 per cent, because of leakage of dehumidified air out of point 2. The cooling capacity of the supply air was then either reduced or increased, depending on the air enthalpy at point 3, by 3 to 29 per cent, by leakage of return air into the supply air. The overall influence on performance (increase and/or decrease of cooling capacity) for most test results in appendices H3 to H6 was approximately 46 per cent. The influence on COP and cooling capacity was probably even greater, because of effects such as the decrease in regenerating temperature, decrease in heat exchanger effectiveness and non-optimal air flow rates. It was not possible to quantify the influence on performance due to these effects.

The individual air leakage values given in figure 6.1.4 and tables 6.1.2 and 6.1.3, were only estimates, but were sufficiently accurate for determining the effect of the leakage on the process and performance of the system. The estimates of air leakage were found to be reasonably accurate, from the following observations:

(1) The return air flow rate at points 7 and 8 (figure 1.1) was calculated from the measured air temperature rise after heating and the measured electrical power consumption of the heaters. The calculated value for most of the tests was 0.165 m^3/s compared with the estimated value of 0.162 m^3/s.

(2) Several random air flow rate measurements were made at point 4. These measurements were within 10 per cent of the estimated flow rate for point 4.

(3) In all of the results in appendices H3 to H6, the measured point 9 (figure 1.1) fell between the simulated point 9 and a point between points 1 and 2 on a psychrometeric chart. The ratio of the distance between these points corresponds well with the air-mixing ratio of the leakage air with the return air at point 9. See tests H3/9 (balanced flow) and H6/2 (unbalanced flow) for typical examples.

7.2 Single Blow Tests

Only a few single blow tests are included in the results to illustrate the process that occurred in the desiccant wheel. The results are not accurate in regions where the air properties changed rapidly, because of the slow response of the aspirated psychrometers. However, despite not being accurate, the information provided by these tests was very useful.

7.2.1 Regeneration single blow tests

The results for two regeneration single blow tests are given in graphical form in figures 6.2.1 and 6.2.2. The regeneration temperatures were different in each case, but the inlet air conditions were similar. The following was observed from the results:

(a) The increase in humidity ratio (W_9-W_8) in the regeneration air reached a maximum value after approximately the same time period, in both cases (although the maximum value was greater with the higher regeneration temperature). This was because the heat capacity of the wheel and convection heat transfer coefficient were constant, and therefore the same amount of time was required to preheat the matrix. The time required for the increase in matrix temperature (matrix temperature minus TDB_1) to reach the same proportion of the original temperature difference (TDB_8-TDB_1) was a function of the convection heat transfer coefficient and heat capacity, but not of the original temperature difference. The reasons for this are described in references concerning transient heat conduction (Incropera and De Wit, 1985). The preheat time would therefore be a function of factors that influence the heat transfer rate such as the regeneration air flow rate. This was a very important observation, since the regeneration efficiency is determined by the total amount of moisture removed (see equation 4.3, page 30), which is influenced by the time taken for W_9-W_8 to reach the maximum value. Therefore the regeneration efficiency depends on the regeneration air flow rate (which mainly determines the convection heat transfer coefficient) and the heat capacity of the desiccant wheel.

(b) The W_9-W_8 curve values were proportional to the regeneration efficiency, since the regeneration heater power was constant during each test (see equation 4.3, page 30). Therefore the maximum regeneration efficiency can be achieved by fixing the rotational speed of the desiccant wheel to give a regeneration period that gives the maximum average value of W_9-W_8 over that ›d. A method of approximating this optimum period is described below:

Figure 7.1 shows that the maximum cumulative average value of a sine curve occurs at an angle of 133.6 degrees, which is 1.484 times the angle at which the maximum value occurs (i.e. 90 degrees). This maximum cumulative average value is equal to 0.7246 times the maximum amplitude of the sine wave. The W_9-W_8 curves in the regeneration tests could be approximated by sine curves and the optimum regenerating period was therefore 1.484 times the period at which the maximum value occurred.

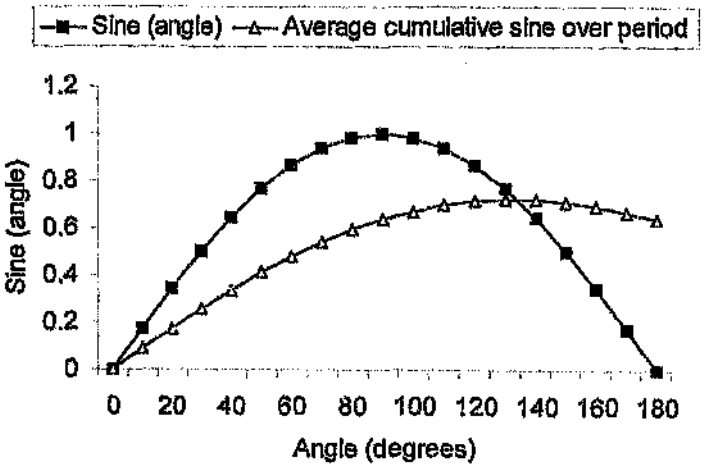

Figure 7.1: Instantaneous and average cumulative sine values over a range of angles.

An example of this method is illustrated in figure 7.2 for regeneration single blow

test number H2/2. The measured curve was approximated by the equation:

$$W_9-W_8 = 3.92+2.22\cdot\sin(90\cdot t/62) \qquad (7.1)$$

Where t = time period (seconds)

The method described here is only an approximation of the optimum regenerating period but should be sufficient for most practical purposes. One can determine this approximate optimum wheel speed by doing only one regeneration single blow test.

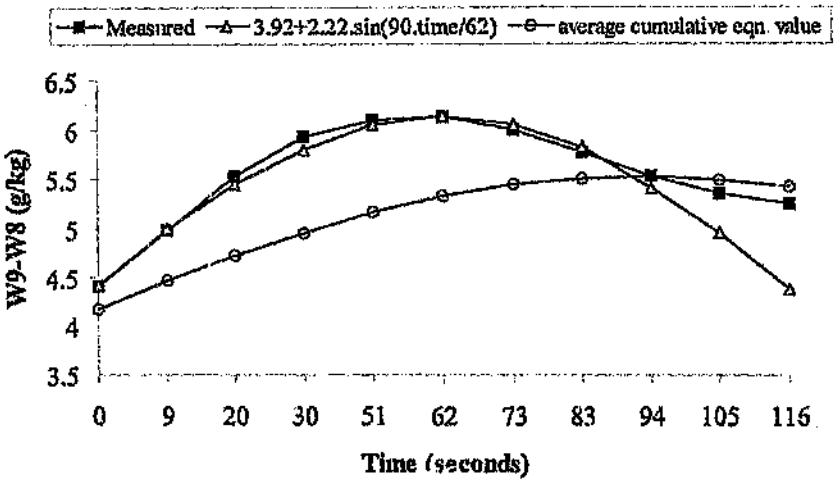

Test no.: H2/2 Optimum regenerating period=1.484×62=92 seconds.
Optimum wheel speed=60/(2×92)=0.32 rpm.

Figure 7.2: Example of the method to estimate the optimum regenerating period for a given desiccant wheel and regenerating air flow rate.

(c) The estimated optimum rotational speed of 0.32 rpm (in figure 7.2) compares well with the actual rotational speed of the wheel of 0.24 rpm. The upward deviation of the W_9-W_8 curve from the sine curve after 100 seconds and relatively flat nature of the cumulative average curve after the maximum point indicates that the experimental wheel was operating near the optimum rotational speed. Several experimental tests were also done with a smaller pulley wheel that reduced the rotational speed of the desiccant wheel to 0.12 rpm. This resulted in a lower energy

efficiency of the desiccant wheel (see sections 6.7 and 7.7) as was predicted by the above results.

(d) The graphs for both tests were similar. This showed that the regeneration process was similar for different regenerating temperatures (i.e. no significant deviations). It should be possible to do a series of more accurate single blow tests at different operating conditions and fit equations to the curves to describe the regenerating process under any operating conditions. This information would be more accurate than that calculated by finite difference models, since the isotherms for lithium chloride depend on the wheel manufacturing process and can only be determined accurately by experimentation (Collier et al, 1982). This would provide a simple and accurate method of predicting the regenerating process, which could be used in a control system to optimise performance.

7.2.2 Dehumidification single blow tests

The results for two dehumidification single blow tests are given in graphical form in figures 6.2.3 to 6.2.6. The regeneration temperatures were similar in each case, but the inlet air conditions were different. The following was observed from the results:

(a) The peak W_1-W_2 values were reached at approximately the same time for both tests. The reasons were the same as those given in section 7.2.1 (a) for the regeneration single blow tests: approximately the same amount of time was required to cool the matrix before the maximum dehumidification rate was achieved.

(b) The graphs both have similar curves, which indicates that several single blow tests could be done at different operating conditions and equations fitted to the curves. One could then get equations to describe the dehumidification process as functions of the operating parameters as described in section 7.2.1 (d).

(c) The dry-bulb temperature (TDB_2) decreased almost from the start of the process,

mainly as a result of the cooling of the desiccant wheel after regeneration but also because the rate of moisture removal decreased after an initial peak. The small increase at the beginning was probably a result of the slow response of the sensor to the step change in temperature. The TDB_2 curve values was higher in the test with the higher W_1-W_2 curve values. This was a result of more latent heat being converted to sensible heat as moisture was absorbed.

(d) The position of the breakthrough point (when desiccant becomes saturated and turns to liquid) in the W_1-W_2 curves was not sharply defined and it was not clear if that point occurred in the tests at all. However the flattening of the W_1-W_2 curve after 300 seconds in figure 6.2.3 and approximately 400 seconds in figure 6.2.4, indicated that these might have been the breakthrough points for the test operating conditions.

(e) The W_1-W_2 curve was negative during the first 30 seconds of the process. This was most likely a result of the slow response of the wet-bulb measurement in the aspirated psychrometer. However, the regeneration process is a non-equilibrium process and some moisture would still be given off at the start of the dehumidification process, while the wheel was still hot and the vapour pressure within the desiccant was higher than in the cooler inlet air.

7.3 Efficiency of Return Air Spray Chamber (EV_R) with Unbalanced Air Flow

The test results are given in tables 6.3.1 and 6.3.2 and figures 6.3.1 to 6.3.6. The following was observed from the results:

(a) The return air spray chamber efficiency (EV_R) increased with increasing spray water flow rate until a flow rate of 1.89 g/s, when the efficiency EV_R was 99 per cent (effectively 100 per cent). A further increase in flow rate maintained the efficiency EV_R at 100 per cent. The performance of the DEC system improved with increasing EV_R efficiency (CC, TCC, COP and TCOP all generally increased) as predicted by the simulations in section 4.2 (lower cold sink temperature). However, with an increase in spray water flow rate even before 100 per cent EV_R efficiency had been reached, the system performance began to decline. This was a result of water carry-over from the return air spray chamber into the sensible heat exchanger.

(b) During the tests, water was visually observed to be dripping from the joints in the return air ducting, between the spray chamber and the heat exchanger. The demister at the exit of the spray chamber therefore did not remove all the water droplets from the return air stream. Some of this water was carried over into the heat exchanger. This is well illustrated in figure 6.3.1 where the humidity ratio of the supply air increased (with increasing spray water flow rate) as it passed through the heat exchanger. There was no air leakage into the supply air duct and the only source of moisture was from the water carryover. The simulated values of the change in humidity ratio W_3-W_2 also increased slightly but this was due to the simulation of air carryover by the matrix as it rotated between the supply air and increasingly moist return air. The measured and simulated changes in humidity ratio (W_3-W_2) were initially (zero water flow rate) equal and this represented the effect of air carryover. However, as the spray water flow rate increased, the difference between the measured and simulated values increased as more water was carried over into the heat exchanger from the mist eliminator. The slight fluctuations in the measured W_3-W_2 curve corresponded to changes in dry-bulb temperature TDB_2 and humidity

ratio W_2 (see figure 6.3.6), which influenced the rate of water evaporation in the heat exchanger.

(c) The cooling capacity for the ventilation credit mode (TCC) was less sensitive to changes in inlet conditions and provided more reliable information concerning the trends in performance parameters. The TCOP varied in proportion to cooling capacity TCC since the regeneration heat input was constant in this set of tests.

The measured and simulated cooling capacity TCC followed the same increasing trend as EV_R, until EV_R was 67 per cent. A further increase in water flow rate caused the measured cooling capacity TCC to increase more slowly than the simulated value. The difference between the measured and simulated values followed the same trends as the measured change in humidity ratio W_3-W_2 values in figure 6.3.1. This implies that the decrease in measured cooling capacity TCC was a result of the water carryover. The heat exchanger is the component that reduces the enthalpy of the supply air to provide cooling. All other processes are approximately constant enthalpy processes. The inadvertent evaporative cooling in the rotary heat exchanger (approximately constant enthalpy process) resulted in less sensible heat reduction and hence less cooling. After the efficiency EV_R reached 100 per cent, the cooling capacity TCC decreased. This was partly because there was no more sensible cooling (minimum cold sink temperature had been reached) and more direct evaporative cooling. It was also a result of changing inlet air conditions, as was shown by the simulated values of cooling capacity TCC. A maximum reduction of 45 per cent in cooling capacity TCC was observed because of the water carry-over.

(d) The cooling capacity in the ventilation mode (CC) followed the same trends (see figure 6.3.5) as for the cooling capacity in the ventilation credit mode (TCC), with the same reasoning (see (c) above). However, the increase in cooling capacity CC over the last four data points was a result of changing inlet air conditions, as is shown by the simulated values of cooling capacity CC. The measured cooling capacity CC values were actually decreasing in relation to the simulated values.

(e) The supply and return air mass flow rates were constant for this set of tests and the heat exchanger efficiency should also have remained constant. The efficiency of heat transfer to the supply air (EHX_S) and to the return air (EHX_R) was constant until efficiency EV_R was 67 per cent. At this point efficiency EHX_S increased and efficiency EHX_R decreased. These changes occurred at the same point at which cooling capacities CC and TCC deviated from the simulated values. The efficiency EHX_S increase could have been explained by the evaporative cooling in the supply air stream, due to the water carryover. The efficiency EHX_R trends were more difficult to analyse and although efficiency EHX_R generally decreased, the effects of air leakage at points 6 and 7 could have contributed to the unstable trends of efficiency EHX_R. This was seen from the trends of the efficiency EHX_R which were similar to the trends of the air conditions at point 2 (figure 6.3.6) which was the source of air leakage into points 6 and 7. EHX_R would not necessarily be influenced much by water carryover in these tests: little evaporative cooling would have taken place in the return air side of the heat exchanger, since the air was already highly saturated. The supply air mass flow rate was also 50 per cent higher than the return air flow rate and even if some evaporative cooling took place in the supply air, there would still be sufficient energy available to heat up the return air. Only a small decrease in efficiency EHX_R would have been expected due to water carryover.

(f) When water carryover occurred, only the spray chamber end of the heat exchanger was visually seen to be wet. The other side was dry, which implied that the narrow channels of the matrix acted like a demister to remove the water droplets near the flow entrance. The high rotational speed of the heat exchanger would not have allowed sufficient time for the water to be blown all the way down the channels before being blown back in the opposite direction and evaporated by the supply air stream.

(g) The water carryover from the spray chamber only occurred outside a certain range of return air flow rates (this range was not determined in the tests). When the velocity was low, then fine droplets followed the air path and passed through the demister instead of contacting the plates. When the velocity was high, the water on

the demister plates was blown off in the form of big droplets. The effects due to high velocity could only be determined visually by bypassing the return air back into the room at point 7 to increase the flow rate, since the fan was not able to provide a high enough flow rate.

7.4 Efficiency of Return Air Spray Chamber (EV_R) with Balanced Air Flow

The test results are given in tables 6.4.1 and 6.4.2 and figures 6.4.1 to 6.4.3. The following was observed from the results:

(a) The cooling capacity TCC generally increased with increasing spray chamber efficiency EV_R. This was expected since the lower cold sink temperature removed more sensible heat from the supply air stream. The measured values of cooling capacity TCC were lower than the simulated values, because of air leakage (see (b) below).

(b) The evidence of moist air leakage into the dry supply air stream could be seen in figure 6.4.2 where the measured values of the change in humidity ratio W_3-W_2 were higher than the simulated values. This meant a moisture gain in the heat exchanger, even when no water was being supplied to the spray chamber. The only source of moisture gain was by air leakage from point 6 (compare figure 6.4.2 to the unbalanced flow results in figure 6.3.1 where no air leakage occurred). The fluctuations in the measured change in humidity ratio W_3-W_2 were a result of changing inlet air conditions (see table 6.4.2). The general shape of the measured change in humidity ratio W_3-W_2 curve was almost a mirror image of the measured cooling capacity TCC curve.

(c) The ventilation mode cooling capacity (CC) also generally increased with increased efficiency EV_R, but fluctuations in inlet air conditions and air leakage caused large fluctuations in these values (see table 6.4.1). The cooling capacity TCC values were more stable since they were less dependent on fluctuations in inlet conditions and were therefore a better indication of increase in performance due to a higher EV_R efficiency.

7.5 Efficiency of Supply Air Spray Chamber (EV_S)

The results are given in tables 6.5.1 and 6.5.2 and figures 6.5.1 and 6.5.2. The following was observed from the results:

The results followed the predictions of the simulations in section 4.2: The spray chamber efficiency on the supply air side (EV_S) increased with increasing spray water flow rate. The cooling capacity in the ventilation mode (CC) and in the ventilation credit mode (TCC) remained almost unchanged for changes in efficiency EV_S (i.e. no change to performance of system). The fluctuations were due to fluctuations of inlet air conditions. Dry-bulb temperature TDB_6 decreased and humidity ratio W_6 increased with increasing efficiency EV_S.

7.6 Inlet Air Conditions and regeneration Temperatures

The results in section 6.6 are discussed in this section in the following categories:

(a) Similar regeneration temperatures at different inlet air conditions.
(b) Similar inlet air conditions at different regeneration temperatures.
(c) Changing humidity ratio of inlet air with constant dry-bulb temperature.
(d) Changing dry-bulb temperature of inlet air with constant humidity ratio.

7.6.1 Similar regeneration temperatures at different inlet air conditions

(a) In most of the tests, the dew point temperature at point 2 was greater than the dry-bulb temperature at point 6. This meant that condensation probably occurred in the heat exchanger while cooling the supply air. This had an effect on the performance parameters. The magnitude of this effect could not be determined because of air leakage that complicated the analysis.

(b) The extent of air leakage (into point 3) was observed by comparing the measured and simulated changes in humidity ratio W_3-W_2 of the supply air as it passed through the heat exchanger. The significant effect of this air leakage on cooling capacity and other performance parameters can also be seen in the tables by comparing measured values with simulated values (i.e. calculated values without air leakage). The change of humidity ratio W_3-W_2 was significantly greater in cases where dew point condensation occurred (see point (a) above). The simulated value of the change in humidity ratio W_3-W_2 included the small effect of air carryover in the heat exchanger matrix.

(c) The difference between the return air temperatures at points 9 and 7 represented heat that could have been recovered to reduce the regeneration energy requirements. This temperature difference was between 30 °C and 60 °C for most tests within practical operating conditions. A temperature difference of 83 °C was calculated for one test, but those ambient conditions would not be expected in practice. The

simulated value of the dry-bulb temperature TDB_9 was used in the calculations to eliminate the significant effects of air leakage at that point. This energy wastage was a result of the fact that lithium chloride requires regeneration temperatures TDB_8 much higher than dry-bulb temperature TDB_2 because of the shape of the isotherms (see section 3.2, page 17, Collier et al, 1982). Recommendations have been made in chapter 8 concerning methods to recover this energy.

(d) The large amount of energy wasted in the exhaust air stream (see (c) above) was one of the reasons for the low regeneration efficiencies that were in the order of 20 per cent (based on simulated values). This meant that only 20 per cent of the regeneration energy was used to evaporate the moisture in the desiccant. This represents a significant opportunity to improve the energy efficiency and performance of the DEC test system.

(e) The cooling capacity in the ventilation mode CC was negative (heating not cooling) for most tests. Most of these tests were for ambient conditions that would not normally be expected in practice. However, the cooling capacity CC was still negative for many tests where the ambient conditions were typical of summer conditions in South Africa. The test system was therefore unable to provide sufficient cooling under these conditions.

(f) The dehumidification process lines on the psychrometric charts in figures 6.6.2 to 6.6.6 were approximately parallel for the same regeneration temperatures. This was applicable for all ambient conditions. The reason for this is that the dehumidification process deviates slightly from a constant wet-bulb temperature process because of the heat carryover in the matrix of the desiccant wheel. The quantity of heat that is carried over to the supply air stream is approximately proportional to the difference between the inlet dry-bulb temperature TDB_1 and the regeneration temperature TDB_8. This results in the dehumidification process lines on a psychrometric chart remaining approximately parallel for different ambient conditions (but similar regeneration temperatures).

7.6.2 Similar inlet air conditions at different regeneration temperatures

(a) The moisture absorbed (W_1-W_2) during dehumidification increased with higher regeneration temperature. Higher regeneration temperature meant deeper drying of the desiccant which increased the moisture absorption potential (also see section 4.1.1.1, page 29).

(b) The moisture absorption efficiency EDH1 increased with higher regeneration temperature in some cases and decreased in others. No general statement could be made since efficiency EDH1 depended on whether the regeneration temperature had been increased closer or away from the optimum regeneration temperature for the given set of operating conditions.

(c) The heat transfer efficiency of the desiccant wheel EDH2 generally decreased, with higher regeneration temperature contrary to the expected increase. This was a result of the small increase of heat transferred (H_2-H_1). In some cases the enthalpy difference H_2-H_1 decreased, but these cases were a result of differences in inlet air conditions (discussed in more detail in (d) and (e) below). The desiccant wheel was not a perfect sensible heat exchanger: the increase in regeneration temperature TDB_8 was partially balanced by an increase in dry-bulb temperature TDB_2 (latent heat converted to sensible heat) because of the increase in moisture absorbed (W_1-W_2). This resulted in a smaller increase in heat transferred than would have been the case in a sensible heat exchanger.

(d) The regeneration efficiency ERG increased with higher regeneration temperature in some cases and decreased in others. This depended on the increase in desiccant moisture loading in relation to the increase in regeneration energy.

(e) The efficiency of heat exchange to the return air EHX_R increased with higher regeneration temperature. This was most likely a result of radiative heat transfer from the regeneration heaters that were situated 300mm to 500 mm from the heat exchanger. The air leakage was not the cause, since a decrease in the dry-bulb

temperature difference TDB_2-TDB_7 corresponded with an increase in efficiency EHX_R. If air leakage was the cause of increased efficiency EHX_R the opposite should have happened. The decrease in dry-bulb temperature difference TDB_2-TDB_7 could only have happened as a result of an increase in dry-bulb temperature TDB_7. The ducting between the heaters and heat exchanger was also observed to get very hot which indicated that radiative heat transfer was significant. The increase in efficiency EHX_R also corresponded with an increase in regeneration energy input.

(f) An increase in regeneration temperature resulted in more heat carryover (from return air to supply air) in the matrix of the desiccant wheel. A portion of this heat was not regained by the sensible heat exchanger and represented a loss of sensible cooling. However, a higher regeneration temperature also resulted in more moisture removal, which reduced the latent heat of the supply air. Generally, a higher regeneration temperature reduced the enthalpy of the air relative to the room air conditions, but provided this additional cooling less efficiently. A higher regeneration temperature therefore generally resulted in a higher cooling capacity in the ventilation mode CC, but lower cooling capacity TCC and TCOP in the ventilation credit mode.

7.6.3 Changing humidity ratio of inlet air with constant dry-bulb temperature

(a) The amount of moisture removed (W_1-W_2) increased with increasing humidity ratio W_1. The increase in humidity ratio W_1 meant an increase in vapour pressure and hence an increase in desiccant potential to absorb moisture.

(b) An increase in moisture absorption efficiency EDH1 with increasing humidity ratio W_1 was initially expected but this was not always the case. At a higher humidity ratio value a higher desiccant loading W_1-W_2 is required for the same EDH1 value (see section 4.1.1.1, page 29). The efficiency EDH1 therefore decreased in some tests despite an increase in moisture absorbed (W_1-W_2).

(c) The regeneration efficiency ERG increased with increasing humidity ratio W_1 because more moisture was absorbed (W_1-W_2) and hence more moisture evaporated for the same amount of regeneration energy supplied.

7.6.4 Changing dry-bulb temperature of inlet air with constant humidity ratio

(a) The amount of moisture removed from the air (W_1-W_2) decreased with increasing dry-bulb temperature TDB_1. The efficiency of moisture removal EDH1 also decreased. The higher dry-bulb temperature TDB_1 meant that the desiccant was not cooled as much with resulting higher desiccant vapour pressure and lower potential to absorb moisture from the supply air (also see section 4.2.2.3, page 40).

(b) The amount of heat transferred to the supply air H_2-H_1 (heat carryover in matrix) decreased with increasing dry-bulb temperature TDB_1 because the temperature difference between the supply and return air streams was less. That also explained the generally lower heat transfer efficiency of the desiccant wheel EDH2.

(c) The regeneration efficiency ERG decreased with increasing dry-bulb temperature TDB_1 because less moisture was absorbed and therefore less was evaporated during the regeneration process for the same regeneration heat input.

7.7 Desiccant Wheel Speed and Unbalanced Air Flow

7.7.1 Balanced flow

(a) The amount of moisture removed (W_1-W_2) and moisture removal efficiency EDH1 were slightly lower for the slower wheel speed. The single blow tests in section 6.2 suggested that the slower wheel speed could improve these parameters, since the effect of the initial cooling period would have been smaller (see figures 6.2.3 to 6.2.6). However, the air in these tests was significantly more moist than the inlet air in the single blow tests and the amount of moisture removed was also more. This meant that the desiccant wheel would have been saturated faster and the moisture removal (W_1-W_2) potential would have decreased faster. This would have resulted in a reduction in the average amount of moisture removed (W_1-W_2) and decrease in moisture efficiency EDH1 for the slower wheel speed. However no general statement could be made concerning an optimum rotational speed since it depends on desiccant moisture loading and heat transfer characteristics of the desiccant wheel. The decrease in moisture absorption capacity was small in these tests since lithium chloride maintains a high absorption potential even after becoming saturated and turning to the liquid phase.

(b) The amount of heat transferred (H_2-H_1) and heat transfer efficiency EDH2 decreased for the slower wheel speed. This was expected since the rate at which heat was being carried over in the matrix was less.

(c) The regeneration efficiency ERG decreased with the slower wheel speed. This was expected from the analysis of the single blow tests (see section 7.2). The desiccant loading was greater since the average moisture removal (W_1-W_2) was only slightly less than for the faster wheel speed, but the dehumidification cycle was approximately twice as long. This increased the moisture removal peak in the regeneration cycle (see figures 6.2.1 and 6.2.2) but reduced the moisture removal rate at the end of the cycle. The average moisture evaporation rate was therefore less.

(d) The cooling capacity and COP were virtually the same for both wheel speeds, for either the ventilation or ventilation credit modes in table 6.7.1. The CC and COP values were slightly higher for the faster wheel speed in table 6.7.2 but this was a result of slightly more beneficial inlet air conditions as was indicated by the corresponding TCC and TCOP values that were lower. The reason for these similar performance characteristics was that although the faster wheel speed resulted in higher EDH1 and ERG, it also resulted in more heat transfer to the supply air (H_2-H_1). Approximately 16 per cent of this heat was not recovered by the sensible heat exchanger which represented a reduction in cooling capacity of approximately 0.14 kW for the faster wheel and only 0.05 kW for the slower wheel speed, at 90 °C regeneration temperature. This eliminated any benefit from improved moisture removal efficiency EDH1 and regeneration efficiency ERG for the faster wheel.

(e) These findings agreed well with Van den Bulck et al (1988) who found that the rotational speed of a desiccant wheel had little effect on performance. They proposed a control strategy in which the desiccant wheel was maintained at a constant rotational speed.

7.7.2 Unbalanced flow

The effect of unbalanced flow in the desiccant wheel was briefly investigated by four tests at different regeneration temperatures and two different desiccant wheel rotational speeds. These results are summarised in table 6.7.1. The following observations were made from these tests:

(a) The observations from section 7.7.1 were also applicable to these tests.

(b) The regeneration efficiencies ERG for these tests were significantly higher than those for balanced flow in table 6.7.2. This was because the regeneration process, when viewed on a psychrometric chart, moved higher up the wet-bulb temperature

line, for unbalanced flow ($MA_R \cdot (W_9 - W_8) = MA_S \cdot (W_1 - W_2)$). This resulted in better utilisation of regeneration heat and lower dry-bulb temperature TDB_9.

(c) Comparing tests H6/2 (unbalanced flow) with H6/8 (balanced flow) the performance of the unbalanced flow test was significantly better, in both ventilation and ventilation credit modes. Both tests had similar inlet air conditions and regeneration heat input and only the regeneration air flow rate in the desiccant wheel was different. The COP of the unbalanced flow test was 38 per cent higher than the balanced flow test and the TCOP was 15 per cent higher, with the same percentage increases in cooling capacity. The difference between the increase in TCOP and COP was a result of small differences in air inlet conditions that increased the difference in COP and decreased the difference in TCOP. The actual increase would have been at the same value, between 15 and 38 per cent for both COP and TCOP for identical inlet air conditions.

(d) Jurinak (1983) found that unbalanced flow improved COP by 10 to 15 per cent in the ventilation mode. These results were slightly lower than the results obtained in this project but his DEC system was probably better optimised and the benefits of unbalanced flow were therefore less.

7.8 Test Results versus Catalogue Data

Some information concerning the performance of the desiccant wheel was supplied by the manufacturer (see appendix F), but was for a limited range of inlet air conditions and specifically for a regeneration temperature of 70 °C. Only two of the experimental tests were within the limits of this information. The comparisons of these tests with simulations based on the manufacturer's information are shown in table 6.8 1. The moisture removal capacities (W_1-W_2) measured were 26 per cent and 39 per cent lower than predicted by the manufacturer's information. The extent of dehumidification was generally very low for all the tests compared with the manufacturer's information. The following are possible reasons for this lower than predicted performance:

(a) The manufacturer's information was based on slightly different operating conditions: the rotational speed of the desiccant wheel in the catalogue was 58 per cent greater than that of the test wheel and the supply air flow velocity was 2.5 m/s instead of 1.0 m/s in the tests. These factors would have affected the moisture removal characteristics of the catalogue wheel, but the test wheel should have performed better. The quantity of air that would pass through a specific part of the catalogue wheel during the dehumidification cycle was less for the test wheel. This would have resulted in a smaller desiccant loading and higher average moisture removal capability (W_1-W_2), which was not the case. It was therefore unlikely that the operating differences were the cause of reduced performance of the test system.

(b) The air leakage could have affected the performance since the leakage into point 8 reduced the regeneration temperature (70 °C) by approximately 5 °C (see section 7.1). One of the tests in table 6.8.1 was at a regeneration temperature of 76.7 °C, which should have compensated for the air leakage, however the moisture removal capacity of the test unit was still lower than the simulated values.

(c) The most likely causes of the reduced moisture removal capacity were airborne contaminants and thermal cycling as described by Pesaran (1993). He reported that

desiccant degradation of 30 to 70 per cent was common over a period of 4 to 8 years with much of the degradation occurring in the first year of operation. The test system had been in intermittent operation for almost two years and some desiccant degradation must have occurred.

(d) There were no filters at the inlets to either the supply or return air fans and it is possible that fine dust could have accumulated in the cellulose matrix to reduce the area for mass transfer. Some dust was observed in the ducting and some of this dust must have collected in the desiccant wheel matrix.

(e) Another very likely cause of reduced moisture removal capacity was over-saturation of the desiccant. During the summer months of February and March 1997, abnormally high rainfall was experienced in Johannesburg and the air was very humid. The details of the manufacturing process of the desiccant wheel were not known, but lithium chloride (LiCl) becomes saturated and liquefies at approximately 15 per cent relative humidity. The cellulose matrix probably acts as an emulsifying agent and keeps the LiCl in the solid matrix. However, LiCl can absorb several times its own weight in water and the desiccant wheel standing stationary and exposed to very humid air would have resulted in a significant increase in water content in the matrix. Much of the LiCl solution could have diffused to the bottom of the matrix and deprived much of the wheel of the original concentration. Tests showed that large LiCl crystals (5 to 10 mm diameter) liquefy completely within 10 hours and small crystals would liquefy and absorb large amounts of water even quicker. The over saturation and desiccant loss could therefore have occurred within a few hours. Holmberg (1989) recommended that dew point condensation should be avoided with lithium chloride systems because the lithium chloride dissolves into and runs out with the condensate. Belding et al (1991) also found that deliquescence of lithium chloride occurs at air relative humidities as low as 15 per cent.

(f) The most likely cause of reduced moisture adsorption capacity was probably a combination of points c, d and e above.

7.9 General Observations

7.9.1 Efficiency of sensible heat exchanger

The efficiency of the sensible heat exchanger was 84 per cent for most of the experimental tests. This was close to the value of 87 per cent read from the catalogue information in appendix F. However, the catalogue information shows that efficiencies above 90 per cent are possible with certain flow rate combinations. Choosing the correct flow rates could therefore significantly improve the performance of the entire system as is illustrated in table 4.2.3 where the COP almost doubled when the heat exchanger efficiency was increased from 80 to 100 per cent. The importance of the heat exchanger was also described by Worek et al (1991) where tests showed that the COP reduced from 1.09 to 0.81 as the efficiency reduced from 93 to 87 per cent.

Several researchers such as Van den Bulck et al (1991) have proposed control strategies that vary the supply and return air flow rates mainly to maximise the performance of the desiccant wheel. However, this could reduce the efficiency of the heat exchanger and thereby reduce overall performance. This can only be prevented by using a very sophisticated and expensive control system to take this factor into account. This type of control method is not recommended.

7.9.2 Performance of the DEC test unit

The DEC test unit performed poorly compared to the results published by other researchers. Collier et al (1990) measured COP values of 0.91 to 1.07 in the ventilation mode at ARI conditions. The test unit provided little to no cooling at these operating conditions. The reason for this is a combination of several factors including air leakage, possible desiccant degradation and non-optimal operating parameters. These factors have already been discussed in detail.

7.9.3 Sources of experimental error

Most of the sources of experimental error concerning the equipment used are described in chapter five but the following are further sources of error observed during the experimental tests:

(a) The aspirated psychrometers were generally very accurate and within 0.2 °C accuracy for the dry-bulb temperature and 0.3 °C for wet-bulb temperature measurements. The cotton wicks were replaced once a week and were washed 4 to 8 times a day with distilled water. Surgical gloves were used when handling the cotton wicks. The requirements of ASHRAE 41.1-1986 and ASHRAE 41.6-1994 were fully complied with. However, there were instances when sudden dust build-up occurred on the cotton wicks at sample points 1, 2 and 9 nearest the inlet of the supply air. This often occurred within a few minutes and was quickly noticeable by the shift of results displayed on the computer screen. These results were then discarded. Any slow build-up of dust was also noticeable by the difference between the simulated and measured values that were displayed on the computer screen.

(b) Unsteady operating conditions sometimes influenced the measurements and results. This occurred in the mornings or late afternoons when the outside ambient conditions changed rapidly. The humidifier in the inlet air duct also supplied a fluctuating steam load. These unsteady operating conditions were present to some degree in all of the tests and resulted in slightly non-equilibrium conditions being measured. This factor was taken into account in the analysis of the results and has been mentioned in the relevant sections of this report.

7.10 Feasibility and Operability of DEC systems in South Africa

DEC systems are generally not economically feasible at present. They require higher air flow rates than vapour compression systems to produce the same amount of cooling. This requires larger equipment that is generally more expensive than other systems commercially available. The energy efficiency is also low which means high running costs. However, research over the last 15 years has resulted in an improvement of thermal COP from below 0.5 to above 1.2. More complicated DEC cycles using additional components and improvements, such as staged regeneration and unbalanced flow have the potential to achieve even better performance in the future. Increased interest in DEC systems could also reduce the initial capital cost of such systems and they could become more competitive in the near future.

A study was done to determine the average monthly performance parameters of a DEC system operating in the ventilation, ventilation credit and recirculation modes in the 12 different climatic regions of South Africa (see appendix G). The purpose of the study was to determine the operational limitations, optimum modes of operation, practical considerations and possible future feasibility of such systems in these climatic regions.

The recirculation mode would perform best in the coastal regions and in Ladysmith and Phalaborwa. The ventilation mode would perform best in most inland regions. Two-stage evaporative cooling could generally provide sufficient cooling in the desert climatic regions including Upington and Beaufort West. Johannesburg was the region in which DEC systems perform the best with a minimum COP of 0.40 in the ventilation mode in summer. The COP approaches infinity during winter when the DEC system should be operated in winter mode. These results were based on the basic DEC system with balanced flow and significantly improved performance could be expected with better optimised systems.

CHAPTER 8
CONCLUSIONS AND RECOMMENDATIONS

8.1 Conclusions

All of the objectives of this project were met (see section 1.3). An accurate data acquisition system was installed on the DEC test unit. An extensive set of tests was then carried out to fully evaluate the DEC system and each of its components. A mathematical model of the DEC system was developed and computer simulations were done for each of the experimental tests. Most of the results followed the theoretical predictions but there were some deviations between the measured and simulated values that revealed several points of interest. The more important of these are summarised below:

- The air leakage between air streams at the desiccant wheel and the rotary heat exchanger was extensive. The total amount of air that leaked out of the supply air duct into the return air duct was 42 to 50 per cent (depending on the flow rate) of the original air supplied by the fan. Approximately 2 to 13 per cent of the return air leaked into the supply duct. The leakage reduced the cooling capacity and COP by approximately 46 per cent under normal operating conditions. This leakage was a characteristic of this specific prototype test unit and is not necessarily typical of other DEC systems.

- Increasing the spray chamber efficiency in the return air side increased the cooling capacity and COP. However, water carryover from the spray chamber into the heat exchanger occurred when the air velocity was outside a certain range. The cooling capacity and COP were significantly reduced by up to 45 per cent when this happened. When the return air velocity was low, small droplets were carried through the demister with the air. When the air velocity was high, water that had settled on the demister plates was blown off in the form of large droplets. This observation is important for DEC control systems that vary the return air flow rates to maximise performance.

- The moisture removal capacity of the DEC test system was 26 to 39 per cent lower than that specified for a new wheel by the manufacturer. This was most likely because of desiccant degradation because of pollution, dust, thermal ageing and occasional over-saturation. The air leakage also reduced the performance of the desiccant wheel since the temperature of the regeneration air was decreased.

Other findings included:

- The single blow tests well illustrated the process that occurs at a specific point in the desiccant wheel as it passes through the dehumidifying and regenerating processes. A significant observation from these test results was that the heat capacity of the desiccant wheel and velocity of the regeneration air determine the time required to reach the maximum rate of regeneration. The wheel rotational speed to give the maximum average regenerating rate can be determined from one regeneration single blow test for a given wheel and regeneration air velocity. The energy efficiency of the desiccant wheel is at a maximum at this rotational speed. Unfortunately the significance of this observation is minimised by the following findings:

- Changing the desiccant wheel speed of rotation had little effect on overall performance. This was because the improved dehumidifying and regenerating efficiencies with a faster rotational speed were offset by the increased rate of heat carryover of which 16 per cent was not recovered by the sensible heat exchanger. Performance is therefore relatively insensitive to rotational speed of the desiccant wheel.

- The time required to reach maximum dehumidifying potential can also be determined from one single blow test. However, this process is dependent on the inlet air conditions and the optimum rotational speed could not be determined only from one single blow test.

- Increasing the spray chamber efficiency in the supply air side had little effect on performance and only the sensible heat ratio of the air was changed. As with the spray chamber in the return air side up to 100 per cent efficiencies were measured. The evaporation rates were also high with 13 to 23 per cent of the spray water evaporating into the air.

- The tests in which the inlet air conditions and regeneration temperatures were varied provided a different perspective of the same results published by other researchers. However, the results illustrated the low regeneration efficiencies and energy wastage typical of balanced flow DEC systems. This lead to two recommendations for the performance improvement of DEC systems.

- The most important of the recommendations made in this report involved the use of an additional heat exchanger (see section 8.2.1.1, page 146). This DEC arrangement would automatically optimise performance and increases the cooling capacity of the system by a factor of at least four. The COP would be a minimum of 1 with expected COP approaching 2 for normal operating conditions in summer. The control strategy would also be significantly simplified.

- Unbalanced flow in the desiccant wheel with balanced flow in the heat exchanger increased both the cooling capacity and COP by 15 to 38 per cent.

The operability of DEC systems in the 12 climatic regions of South Africa was investigated by simulations using the mathematical model. The recirculation mode would perform best in the coastal regions and in Ladysmith and Phalaborwa. The ventilation mode would perform best in most inland regions. Two stage evaporative cooling alone could generally provide sufficient cooling in the desert climatic regions including Upington and Beaufort West. Johannesburg was the region in which DEC systems perform the best with a minimum COP of 0.40 in the ventilation mode in summer. The COP approaches infinity during winter when the DEC system should be operated in winter mode. These results were based on the basic DEC system with

balanced flow and significantly improved performance could be expected with better optimised systems.

The initial capital cost and running costs for DEC systems are higher than for other systems commercially available at present. DEC systems are generally not economical at present but this could change in future with ongoing improvements in performance.

8.2 Recommendations

8.2.1 Improvements to DEC systems

The main reason for the low performance of DEC systems is that much regeneration energy is wasted in the exhaust air. The recovery or optimum use of this energy is the area of greatest potential improvement in the performance and energy efficiency of DEC systems. The following are suggestions and recommendations for such improvements.

8.2.1.1 Additional heat exchanger

High regeneration temperatures are usually required to increase cooling capacity. However this usually results in a decrease in COP because more energy is lost in the exhaust air. It is also difficult to optimise the regeneration temperature for a given set of operating conditions and energy is then lost. This was illustrated in most of the tests where the difference between the temperature of the regeneration air leaving the desiccant wheel and the temperature of the air before being heated was 30 °C to 60 °C, which represents a significant waste of energy that could have been recovered. Figure 8.1 illustrates a recommendation of using a secondary heat exchanger to recover this energy. This system would also simplify the control system since the cooling capacity could then be controlled simply by changing the regenerating temperature. The heat input would be varied to keep the regeneration temperature at the required level. Most heat not used for regeneration would be recovered by the secondary (additional) heat exchanger and the regeneration efficiency would be maintained at a maximum at all times no matter what the regeneration temperature. The regeneration efficiency would equal the efficiency of the secondary heat exchanger (80 to 90 per cent). This represents a significant improvement in energy efficiency since the regeneration efficiency for most of the experimental tests was approximately 20 per cent. All other operating parameters would be constant including air flow rates and wheel rotational speeds.

Many researchers such as Collier and Cohen (1983) found that the addition of inert heat capacity to the desiccant wheel optimises COP. This inert heat capacity has the same function as the secondary heat exchanger described here since it recovers some of the heat that would otherwise have been lost in the discharged air. However, the use of additional heat capacity results in a larger desiccant wheel and a larger main heat exchanger to recover the heat carryover. The cooling capacity is also reduced because of the lower desiccant absorption potential. The recommendation described here eliminates the need for inert heat capacity in the desiccant wheel and would enable manufacturers to increase the desiccant mass fraction in a desiccant wheel to increase the capacity of a given wheel size. The size of the main sensible heat exchanger could be reduced since most of the heat recovery would occur in the secondary heat exchanger.

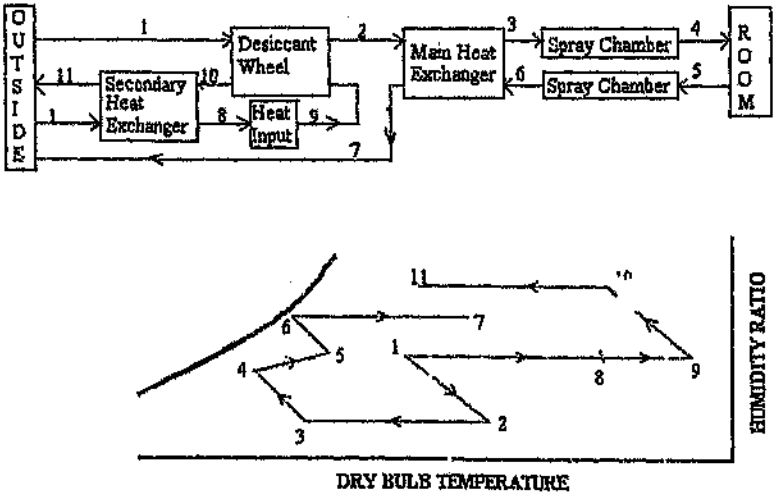

FIGURE 8.1: Recommendation for an additional heat exchanger.

8.2.1.2 Using the regeneration air twice

When two or more DEC systems are being used then the exhaust air from one regeneration process can be reused in the second wheel. This recommendation is illustrated in figure 8.2. The amount of additional heating required would be that used to evaporate the moisture in the previous regeneration process. The regeneration efficiency in the first process would therefore be 100 per cent compared to 20 per cent typically obtained in the experimental tests. Several wheels could be placed in series to decrease the humidity ratio of the process air with intercooling between each stage. This type of system would be most effective in humid climates and could provide process air at a very low enthalpy that would reduce the process air flow rate and the size of ducting and other equipment. This recommendation would only be feasible for special applications and the recommendation in section 8.2.1.1 would still be the first option.

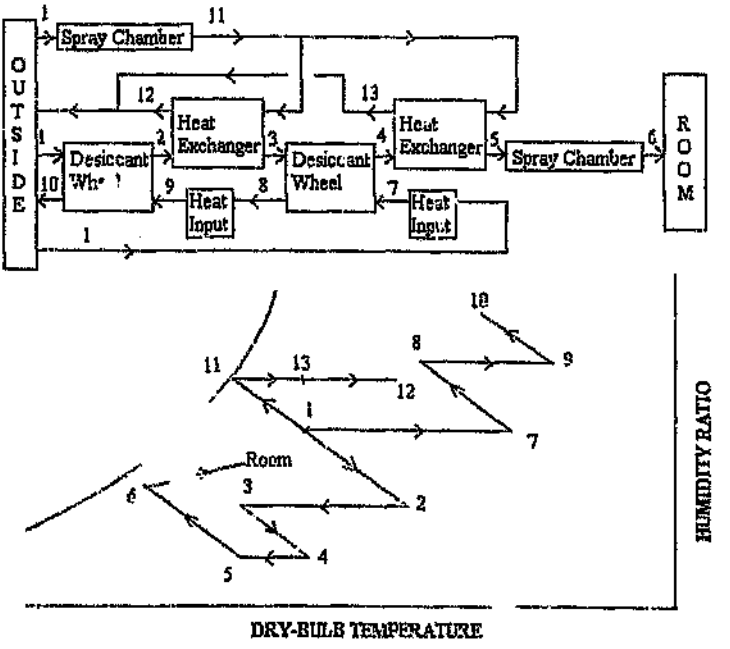

FIGURE 8.2: Recommendation for the multiple use of regeneration air.

8.2.2 Recommendations for future work

Any further research projects using the existing test unit should include the following modifications:

(a) Improving the sealing arrangement in the desiccant wheel to reduce air leakage.
(b) Installing dust filters at the inlets of both fans.
(c) Replacing the humidifier with a unit that supplies a more constant flow of steam.
(d) Consider replacing the desiccant wheel (if sufficient funding is available)
(e) Modify the ducting to include facilities for more accurate air flow rate measurement.

The following two projects are recommended for future research into DEC systems:

- Section 7.2 mentioned doing a series of single blow tests at different operating conditions to get empirical solutions to the governing equations for the performance of the desiccant wheel. These equations could be used in a mathematical model to simulate the actual performance of the experimental DEC test system.

- The recommendation in section 8.2.1.1 to install an additional heat exchanger could be tested and evaluated. The recommended DEC configuration is relatively insensitive to the condition of the desiccant wheel (see section 8.2.1.1) and the existing desiccant wheel could be reused for this project.

APPENDIX A

CALIBRATION RESULTS

The calibration results for the LM 35 temperature sensors and the hygrotransmitters are given in this appendix.

TABLE A1: Calibration measurements of LM35 temperature sensors in microvolts over a temperature range.

Sensor	PC30	Temperature measured with a calibrated thermometer (°C)													
	Channel	-0.08	2.69	6.73	9.63	13.8	16.7	20.23	23.85	28.58	31.34	35.36	39.68	45.49	50.43
TDB_1	0	8764	36230	75806	104760	146948	177026	212988	248876	296997	324780	365698	410131	468920	518506
TWB_1	1	3710	30639	70654	99292	141964	170678	206836	243017	291015	318359	358886	402670	461377	510522
TDB_2	2	7348	34301	74438	102734	145507	175463	210864	246996	294995	322632	363501	407690	466406	515844
TDB_3		8574	35766	75560	104052	146362	176025	211523	247533	295312	323340	363843	407592	466333	515307
TWB_2	4	10058	36572	76123	104980	147631	177636	213305	249657	296704	324829	365381	410204	468945	517724
TDB_4	5	8178	34814	75366	103979	146362	176293	212304	248388	295532	324414	364087	408544	467675	517285
TWB_3	6	4272	31615	70923	100342	142041	171752	207397	244067	291943	319726	359814	403320	462597	512206
TDB_5	7	8838	35742	75386	104159	146337	176049	211767	247680	295483	323876	363892	407959	466479	516162
TWB_4	8	1879	30781	66821	95849	138159	167602	202807	239355	286499	315111	354907	399121	458129	507935
TDB_6	9	8276	35382	75561	104320	146435	176513	211987	248510	295678	324316	363989	408544	466821	516674
TWB_5	10	8325	35693	75439	104467	146679	176342	212084	248559	295605	324365	364160	408496	467383	17089
TDB_7	11	9033	36157	75635	104809	146899	176635	212475	248949	295605	324707	364673	409301	468286	517504
TWB_6	12	4785	31911	71728	100390	142822	172802	207715	244092	292382	319653	359790	403369	462133	512206
TDB_8	13	8838	35913	75610	104594	146313	176171	212231	248412	295654	323999	364111	407983	467016	516552
TDB_9	14	2197	27196	68205	96850	139233	168530	205004	241552	288696	317041	357543	401464	460693	510424
TWB_7	15	2392	29248	69726	98168	140039	169726	205615	241796	290307	317749	358520	402197	461206	510254

TABLE A2: Calibration equations obtained from results in Table A1.

Sensor	PC30 Channel	Temperature(°C) = (measured microvolts - A0)/A1	
		A0	A1
TDB_1	0	6949	10226.99
TWB_1	1	1843	10178.87
TDB_2	2	5457	10206.61
TDB_3	3	6736	10177.00
TWB_3	4	7732	10203.59
TDB_4	5	6351	10211.31
TWB_4	6	2577	10185.98
TDB_5	7	6868	10180.03
TWB_5	8	-121	10155.73
TDB_6	9	-3573	10201.81
TWB_6	10	6756	10198.54
TDB_7	11	7120	10199.93
TWB_7	12	3183	10172.12
TDB_8	13	7000	10183.08
TDB_9	14	-691	10210.56
TWB_9	15	478	10201.15

TABLE A3: Calibration of Fluke multimeter to read TWB_2.

Measured Temperature (°C) using calibrated Thermometer	Voltage (mV) read from fluke multimeter
20.61	212.2
22.20	228.0
23.22	237.9
24.04	246.3
25.00	256.0
25.58	261.5
26.13	267.3
28.78	294.0

Calibration equation (from table A3): TWB_2 (°C) = (measured mV - 5.3)/10.023

TABLE A4: Results of experiments to check accuracy of the calibration equations.

Sensor	PC30 Channel	Temperatures (°C) measured using LM35 sensors and data acquisition system.			
TDB_1	0	21.99	26.70	35.65	43.04
TWB_1	1	22.10	26.68	35.63	43.04
TDB_2	2	21.95	26.66	35.71	43.00
TDB_3	3	21.98	26.67	35.74	43.01
TWB_3	4	22.12	26.67	35.75	43.10
TDB_4	5	22.00	26.67	35.73	43.03
TWB_4	6	22.05	26.62	35.66	43.07
TDB_5	7	21.98	26.71	35.61	42.99
TWB_5	8	22.06	26.60	35.60	43.01
TDB_6	9	21.94	26.65	35.72	43.04
TWB_6	10	21.97	26.57	35.53	42.89
TDB_7	11	21.98	26.66	35.70	43.06
TWB_7	12	22.10	26.66	35.66	43.09
TDB_8	13	22.01	26.73	35.79	43.09
TDB_9	14	22.03	26.67	35.51	42.86
TWB_9	15	22.00	26.66	35.63	43.05
TWB_2	Fluke mu	22.02	26.70	35.65	43.07
Temperature (°C) measured by calibrated thermometer		22.0	26.7	35.7	43.0
Max. positive deviation:		0.12	0.03	0.09	0.10
Max. negative deviation:		0.05	0.13	0.19	0.14

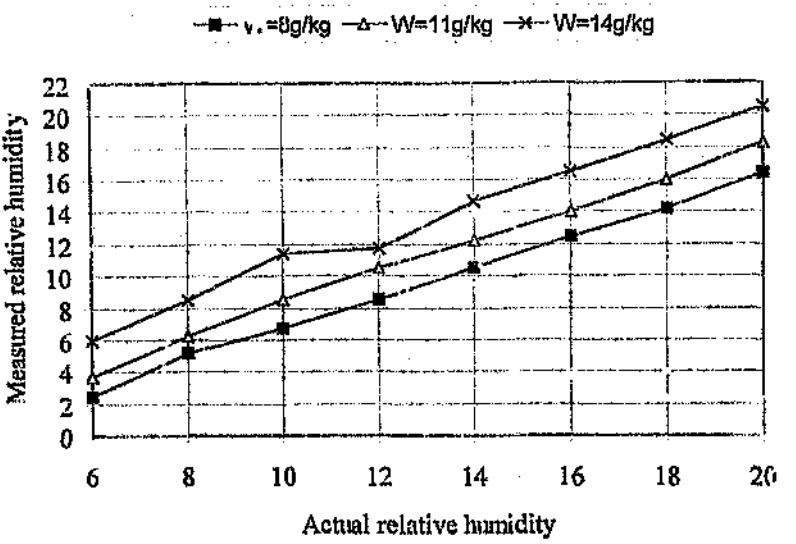

Figure A.1: Calibration results for the DELTA OHM, model HD 8908TC/150 hygrotransmitter (serial no. AMW 299) for different air humidity ratios.

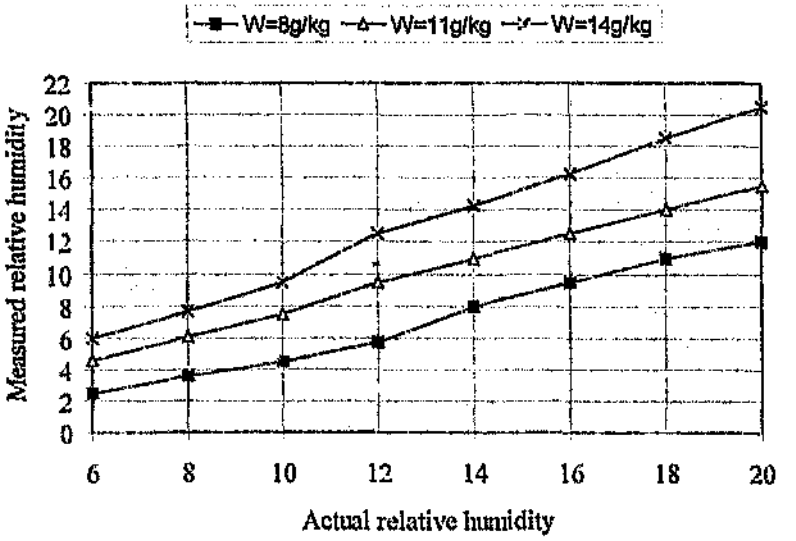

Figure A.2: Calibration results for the DELTA OHM, model HD 8908TC/150 hygrotransmitter (serial no. AMU 739) for different air humidity ratios.

APPENDIX B

DATA ACQUISITION AND PROCESSING COMPUTER PROGRAM

This appendix is a printout of the computer program that was used for data acquisition during the experimental tests (see section 5.3.1).

```
PROGRAM DEC;

(*This program does the following:
*(1) Reads binary output from PC30 A/D card and converts to voltage.
*(2) Converts voltage to temperature value, using calibration data.
*(3) Calculates all moist air properties at the measured points.
*(4) Calculates changes for each step in the process.
*(5) Calculates performance parameters.
*(6) Does a complete error analysis of all measured and calculated values.
*(7) Simulates the measured process using a mathematical model.
*(8) Displays all results in tables and on a psychrometric chart.
*(9) Prints results, if requested.*)

uses
 crt, graph, dos, printer;
var
bh : integer; (* board handle *)  t, I, J, zz, yy, xx : integer; (* dummy variables *)

(* variables for error anaysis: *) EMAS, EMAR, VAS, EVAS, VR, EVR, ECC, ETCC,
EQ, EEHXR, EEHXS, EEVS, EEVR, ECOP, ETCOP, EEER, ETEER, EEDH1, EEDH2,
EERG, EW2, ENOR, ENOE : real;
    EHT:ARRAY[1..9] OF REAL; EW:ARRAY[1..9] OF REAL;
  ETDB:ARRAY[1..9] OF REAL; ETWB:ARRAY[1..9] OF REAL;
ECHTOT:ARRAY[1..8] OF REAL; ECW:ARRAY[1..8] OF REAL;

DESCRIP : string[35];  y,m,mm,d,dow,h,s,s100 : integer; (* date, time *)

  VAS:ARRAY[1..4]  OF REAL; (* supply air flow rate in m3/s *)
   VR:ARRAY[1..4]  OF REAL; (* return air flow rate in m3/s *)
  MAS:ARRAY[1..4]  OF REAL; (* supply air flow rate in kg/s *)
  MAR:ARRAY[1..4]  OF REAL; (* return air flow rate in kg/s *)
  NOR:ARRAY[1..4]  OF REAL; (* heat input in kW*)
  NOE:ARRAY[1..4]  OF REAL; (* total electrical energy input in kW *)
```

```
TWSC:ARRAY[1..4]  OF REAL; (* temp of supply water to spray chambers*)
 FRS:ARRAY[1..4]  OF REAL;  (*water flow-rate to supply air spray chambers*)
 FRR:ARRAY[1..4]  OF REAL;(*water flow-rate to return air spray chambers*)
 PPS:ARRAY[1..4]  OF REAL; (*press. of water to supply air spray chambers*)
 PPR:ARRAY[1..4]  OF REAL; (*press. of water to return air spray chambers*)
  W2:ARRAY[1..4]  OF REAL; (* max. possible humidity ratio for pt 2 *)
  CC:ARRAY[1..4]  OF REAL; (* cooling capacity in kW (basic vent. mode)*)
  CC:ARRAY[1..4]  OF REAL; (* cooling capacity in kW (vent. credit mode)*)
   Q:ARRAY[1..4]  OF REAL; (* regen. heat supplied in kW *)
 COP:ARRAY[1..4]  OF REAL; (* COP for basic vent. mode *)
TCOP:ARRAY[1..4]  OF REAL; (* COP for vent. credit mode *)
 EER:ARRAY[1..4]  OF REAL; (* electrical eff. ratio for basic vent. mode *)
TEER:ARRAY[1..4]  OF REAL; (* electrical eff. ratio for vent. credit mode*)
EDH1:ARRAY[1..4]  OF REAL; (* eff. of dehumidifier (moisture removal*)
EDH2:ARRAY[1..4]  OF REAL; (* eff. of dehumidifier (heat transfer)*)
 ERG:ARRAY[1..4]  OF REAL; (* efficiency of regeneration *)
EHXS:ARRAY[1..4]  OF REAL; (* eff. of heat exchanger (supply air)*)
EHXR:ARRAY[1..4]  OF REAL; (* efficiency of heat exchanger (return air)*)
 EVS:ARRAY[1..4]  OF REAL; (* eff. of supply air spray chambers *)
 EVR:ARRAY[1..4]  OF REAL; (* eff. of return air spray chambers *)
A:ARRAY[0..15,1..3]  OF LONGINT;(* averaged voltages in microvolts *)
  CL:ARRAY[0..15]  OF LONGINT; (* confidence limits in microvolts *)
 TDB:ARRAY[1..9,1..4] OF REAL; (* dry bulb temp. °C *)
 TWB:ARRAY[1..9,1..4] OF REAL; (* wet bulb temp. °C *)
  RH:ARRAY[1..9,1..4] OF REAL; (* relative humidity (frac) *)
PSDB:ARRAY[1..9,1..4] OF REAL; (* sat. press. at TDB kPa *)
PSWB:ARRAY[1..9,1..4] OF REAL; (* sat. press. at TWB kPa *)
  PA:ARRAY[1..9,1..4] OF REAL; (* air pressure kPa *)
   W:ARRAY[1..9,1..4]OF REAL; (* humidity ratio kg/kg *)
  SV:ARRAY[1..9,1..4] OF REAL; (* specific volume m³/kg *)
   U:ARRAY[1..9,1..4] OF REAL; (* percentage saturation % *)
  HT:ARRAY[1..9,1..4] OF REAL; (* total specific enthalpy air kJ/kg *)
 TDP:ARRAY[1..9,1..4] OF REAL; (* dew point temperature °C *)
  PW:ARRAY[1..9,1..4] OF REAL; (* vapour pressure kPa *)
CHTOT:ARRAY[1..8,1..4] OF REAL; (* change of total sp. enthalpy kJ/kg *)
```

```
CW:ARRAY[1..8,1..4] OF REAL; (* change of humidity ratio kg/kg *)

FUNCTION psat(T:real):real;  (* calculates sat. pressure for given T *)
var  Z : real;
begin T:=T+273.16;   Z:=(28.59051+0.0024804*T-3142.31/T)*ln(10)-8.2*ln(T);
PSAT:=100*exp(Z);
end;

FUNCTION tsat(P:real):real;  (* calculates dew point temp. oC *)
var z:real;
begin
if P<0.001 THEN P:=0.001,   z:=ln(P);
if p>0.6112 then   (* ie. TDP>0 oC *)
tsat:= 6.54+(14.526*z)+(0.7389*z*z)+(0.09486*z*z*z)+(0.4569*(exp(0.1984*z)))
else   tsat:= 6.09+(12.608*z)+(0.4959*z*z);
end;

PROCEDURE tablep; (* prints results in tabular form *)
begin
writeln(LST,' '); writeln(LST,' ');
writeln(LST,' THE FOLLOWING INPUT WAS ENTERED:');
writeln(LST,' ************************************');
writeln(lst,' TWB[2]  (oC): ', TWB[2,1]:6:2);
writeln(LST,' SUPPLY AIR FLOWRATE (m3/s) nom : ',VAS[1]:5:3);
writeln(LST,'                                min : ',VAS[2]:5:3),
writeln(LST,'                                max : ',VAS[3]:5:3);
writeln(LST,' RETURN AIR FLOWRATE (m3/s) nom : ',VR[1]:5:3);
writeln(LST,'                                min : ',VR[2]:5:3);
writeln(LST,'                                max : ',VR[3]:5:3);
writeln(LST,' REGENERATION ENERGY INPUT (KW) : NOR[1]:5:3);
writeln(LST,' ELEC. ENERGY (EXL. REGEN)      (KW) : ',NOE[1]:5:3);
writeln(LST,' SPRAY WATER INLET TEMP.        (oC)  : ',TWSC[1]:3:1);
writeln(LST,' SUPP. AIR SP. CH.: WATERFLOW RATE (g/s) :',FRS[1]:4:2);
writeln(LST,'                  : PUMP PRESSURE (bar)  :',PPS[1]:3:0);
writeln(LST,' RET. AIR SP. CH. : WATER FLOW RATE (g/s) :',FRR[1]:4:2);
```

```
writeln(LST,'                    : PUMP PRESSURE (bar)  :',PPR[1]:3:0);
reaum; writeln(LST,' '); writeln(LST,' '); writeln(LST,' '); writeln(LST,' ');writeln(LST,' ');
write(LST,' RESULTS OF DEC TEST     (sheet 1 of 2) ');
writeln(LST,'  DATE: ',d,'-',m,'-',y);
writeln(LST,' ********************                    TIME: ',h,'H',mm);
writeln(LST,' '); writeln(LST,' TEST NUMBER: ',DESCRIP);  writeln(LST,' ');
writeln(LST,' OPERATING PARAMETERS (MEASURED AND ENTERED AS
INPUT)');
writeln(LST,' ------------------------------          NOM.   MIN.   MAX. ');
write(LST,' Supply air flow rate   (g/s)= 1000*MAS[1]:6:0,1000*MAS[2]:8:0);
writeln(LST,1000*MAS[3]:8:0);
write(LST,' Return air flow rate    (g/s)= ',1000*MAR[1]:6:0,1000*MAR[2]:8:0);
writeln(LST,1000*MAR[3]:8:0);
writeln(LST,' Regen. heat input    (kW)= NOR[1]:6:3,NOR[2]:8:3,NOR[3]:8:3);
writeln(LST,' Elec. energy (excl. reg.) (kW)= ',NOE[1]:6:3,NOE[2]:8:3,NOE[3]:8:3);
writeln(LST,' Spray chambers: water T   (oC)=
',TWSC[1]:6:1,TWSC[2]:8:1,TWSC[3]:8:1{,TWSC[4]:6:1});
writeln(LST,' Water flow rate (S S/CH) (g/s)=
,FRS[1]:6:2,FRS[2]:8:2,FRS[3]:8:2{,FRS[4]:6:1});
writeln(LST,'                  at pressure   (bar)= ',PPS[1]:6:0,PPS[2]:8:0,PPS[3]:8:0);
writeln(LST,' Water flow rate (R S/CH) (g/s)=
',FRR[1]:6:2,FRR[2]:8:2,FRR[3]:8:2{,FRR[4]:6:1});
writeln(LST,'                  at pressure   (bar)= ',PPR[1]:6:0,PPR[2]:8:0,PPR[3]:8:0);
writeln(LST,' ');
writeln(LST,' PROCESS CHANGES OF ENTHALPY AND HUMIDITY RATIO ');
writeln(LST,' ------------------------------------------------------------') ;
writeln(LST,' ST END H (kJ/KG)              W (g/kg)  ');
writeln(LST,' PT  PT  NOM.  MIN.  MAX.  SIM.   NOM.  MIN.  MAX.  SIM. ');
for  I:= 1 to 8 do    begin
write(LST,I:15,(I+1):3,CHTOT[I,1]:7:1,CHTOT[I,2]:6:1,CHTOT[I,3]:6:1,
CHTOT[I,4]:6:1);
writeln(LST,CW[I,1]*1000:8:2,CW[I,2]*1000:6:2,CW[I,3]*1000:6:2,
CW[I,4]*1000:6:2);
end;
writeln(LST,' '); writeln(LST,' PERFORMANCE PARAMETERS (CALCULATED) ') ;
```

```
writeln(LST,' ---------- ---          NOM. MIN. MAX  SIM. ');
writeln(LST,' Dehumidifier eff.(W)  (%) EDH1=',
100*EDH1[1]:5:0,100*EDH1[2]:6:0,100*EDH1[3]:6:0,100*EDH1[4]:6:0);
writeln(LST,' Dehumidifier eff.(Q)  (%) EDH2=',
100*EDH2[1]:5:0,100*EDH2[2]:6:0,100*EDH2[3]:6:0,100*EDH2[4]:6:0);
writeln(LST,' Regeneration eff.     (%)  ERG=',
100*ERG[1]:5:0,100*ERG[2]:6:0,100*ERG[3]:6:0,100*ERG[4]:6:0);
writeln(LST,' Regen. heat input    (kW)  Q =', Q[1]:5:2,Q[2]:6:2,Q[3]:6:2,Q[4]:6:2);
writeln(LST,' Heat Exch. eff. (SUP) (%) EHXS=',
100*EHXS[1]:5:0,100*EHXS[2]:6:0,100*EHXS[3]:6:0,100*EHXS[4]:6:0);
writeln(LST,' Heat Exch. eff. (RET) (%) EHXR=',
100*EHXR[1]:5:0,100*EHXR[2]:6:0,100*EHXR[3]:6:0,100*EHXR[4]:6:0);
writeln(LST,' Sup. air spr. ch. eff.(%)  EVS=',
100*EVS[1]:5:0,100*EVS[2]:6:0,100*EVS[3]:6:0,100*EVS[4]:6:0);
v      (LST,' Ret. air spr. ch. eff.(%)  EVR=',
100*EVR[1].5:0,100*EVR[2]:6:0,100*EVR[3]:6:0,100*EVR[4]:6:0);
writeln(LST,' FOR VENTILATION MODE: '); writeln(LST,' Cooling capacity    (kW)
CC =', CC[1]:5:2,CC[2]:6:2,CC[3]:6:2,CC[4]:6:2);
writeln(LST,' Coeff. of performance    COP=',
COP[1]:5:2,COP[2]:6:2,COP[3]:6:2,COP[4]:6:2);
writeln(LST,' Electricity eff. ratio    EER=',
EER[1]:5:2,EER[2]:6:2,EER[3]:6:2,EER[4]:6:2);
writeln(LST,' FOR VENTILATION CREDIT MODE: ');
writeln(LST,' Cooling capacity    (kW) TCC =',
TCC[1]:5:2,TCC[2]:6:2,TCC[3]:6:2,TCC[4]:6:2);
writeln(LST,' Total Coeff. of perf.    TCOP=',
TCOP[1]:5:2,TCOP[2]:6:2,TCOP[3]:6:2,TCOP[4]:6:2);
writeln(LST,' Electricity eff. ratio   TEER=',
TEER[1]:5:2,TEER[2]:6:2,TEER[3]:6:2,TEER[4]:6:2);
READLN; writeln(LST,' ');
writeln(LST,' '); writeln(LST,' '); writeln(LST,' '); writeln(LST,' ');
 write(LST,' RESULTS OF DEC TEST   (sheet 2 of 2) ');
 writeln(LST,'  DATE: ',d,'-',m,'-',y);
 writeln(LST,' ********************                TIME: ',h,'H',mm);
```

```
writeln(LST,' '); writeln(LST,' MOIST AIR PROPERTIES AT MEASURED POINTS
IN PROCESS');
writeln(LST,' ---------- ------ ----------') ; writeln(LST,' ');
writeln(LST,' NOMINAL MEASURED VALUES: ');
writeln(LST,' PT TDB TWB TDP PW W RH U SV H');
writeln(LST,' (oC) (oC) (oC) (kPa) (g/kg) (%) (%)(m3/kg)(kJ/kg)');
for I:= 1 to 9 do
writeln(LST,I:15,TDB[I,1]:6:1,TWB[I,1]:6:1,TDP[I,1]:6:1,PW[I,1]:6:2,
W[I,1]*1000:7:2,RH[I,1]*100:5:0,U[I,1]*100:4:0,SV[I,1]:7:3,HT[I,1]:7:2);
writeln(LST,' '); writeln(LST,' VALUES FOR TDB & W FROM ERROR ANALYSIS &
SIMULATION : ');
writeln(LST,' (UNITS As ABOVE)');
writeln(LST,' PT 1 2 3 4 5 6 7 8 9');
writeln(LST,' TDB(MIN) ',TDB[1,2]:5:1, TDB[2,2]:5:1,TDB[3,2]:5:1,
TDB[4,2]:5:1,TDB[5,2]:5:1,TDB[6,2]:5:1,TDB[7,2]:5:1, TDB[8,2]:5:1,TDB[9,2]:5:1);
writeln(LST,' TDB(MAX) ',TDB[1,3]:5:1,TDB[2,3]:5:1,TDB[3,3]:5:1,TDB[4,3]:5:1,
TDB[5,3]:5:1,TDB[6,3]:5:1,TDB[7,3]:5:1, TDB[8,3]:5:1,TDB[9,3]:5:1);
writeln(LST,' W (MIN) ',W[1,2]*1000:5:1,W[2,2]*1000:5:1,W[3,2]*1000:5:1,
W[4,2]*1000:5:1, W[5,2]*1000:5:1,W[6,2]*1000:5:1,W[7,2]*1000:5:1,
W[8,2]*1000:5:1, W[9,2]*1000:5:1);
writeln(LST,'W (MAX) ',W[1,3]*1000:5:1,W[2,3]*1000:5:1,
W[3,3]*1000:5:1,W[4,3]*1000:5:1,W[5,3]*1000:5:1,W[6,3]*1000:5:1,
W[7,3]*1000:5:1,W[8,3]*1000:5:1,W[9,3]*1000:5:1);
writeln(LST,' TDB(SIM) ',TDB[1,4]:5:1,TDB[2,4]:5:1,TDB[3,4]:5:1,TDB[4,4]:5:1,
TDB[5,4]:5:1,TDB[6,4]:5:1,TDB[7,4]:5:1,TDB[8,4]:5:1,TDB[9,4]:5:1);
writeln(LST,' W (SIM) ',W[1,4]*1000:5:1,W[2,4]*1000:5:1,W[3,4]*1000:5:1,
W[4,4]*1000:5:1,W[5,4]*1000:5:1,W[6,4]*1000:5:1,W[7,4]*1000:5:1,
W[8,4]*1000:5:1,W[9,4]*1000:5:1);
end;

PROCEDURE presult; (* choose to print results *)
var xx:integer;
begin clrscr; writeln('ENTER 1=PRINT RESULTS, 2=CONT.'); readln(xx);
   if xx=1 then tablep else xx:=2;
end;
```

```
PROCEDURE psychart;  (* displays psychromatric chart showing process *)
var  grdriver, grmode, grerror, x, y : integer;  P, GG, T : real;
begin
grdriver:=detect;  initgraph(grdriver,grmode,'');  grerror:=graphresult;  if grerror<>grok
then  writeln('graphics error:',grapherrormsg(grerror))  else
begin
setcolor(green);  moveto(0,380);  lineto(600,380);  (* draws axes *)
lineto(600,110);  moveto(250,420); setcolor(5); outtext('DBT (oC)');  moveto(595,40);
outtext('W'); moveto(592,60);  outtext('g/kg');
end;
setcolor(5);  for I:=0 to 8 do  (* displays TDB increments on horizontal axis *)
begin      T:=10*I;  putpixel(I*75,385,5);  moveto(I*75,390);
case I of  0:outtext('0'); 1:outtext('10'); 2:outtext('20'); 3:outtext('30');  4:outtext('40');
5:outtext('50'); 6:outtext('60'); 7:outtext('70');  8:outtext('80');  end;
end;
for I:=0 to 6 do  (* prints humidity ratio increments on vertical axis *)
begin GG:=5*I;  putpixel(602,380-I*45,5);  moveto(605,380-I*45);
case I of  0:outtext('0');  1:outtext('5');  2:outtext('10'); 3:outtext('15');  4:outtext('20');
5:outtext('25');  6:outtext('30');  end;
end;
setcolor(6);  moveto(0,340);
for I:=0 to 14 do  (* draws saturation curve *)
begin T:=2*I; P:=psat(T); GG:=0.622*P/(82.5-P); X:=I*15; Y:=round(380-G*9000);
lineto(X,Y);  end;
setcolor(7); line(0,100,30,100); outtextxy(33,100,'inlet'); setcolor(5); line(0,110,30,110);
outtextxy(33,110,'room');  setcolor(9); line(0,120,30,120); outtextxy(33,120,'outlet');
setcolor(12); line(0,130,30,130); outtextxy(33,130,'simulated');
setcolor(7); (* plots measured point on chart *)  X:=round(7.5*TDB[1,1]);
Y:=round(380-W[1,1]*9000);  moveto(X,Y);outtext('1');
for I:=2 to 9 do
begin case I of 2,3,4:setcolor(7); 5:setcolor(5); 6,7,8,9:setcolor(9); end;
 X:=round(TDB[I,1]*15/2); Y=round(380 -W[I,1]*9000); lineto(X,Y);
```

```
case I of   2:outtextxy(x,y,'2'); 3:outtextxy(x,y,'3'); 4:outtextxy(x,y,'4');
5:outtextxy(x,y,'5'); 6:outtextxy(x,y,'6'); 7:outtextxy(x,y,'7'); 8:outtextxy(x,y,'8');
9:outtextxy(x,y,'9'); end;    end;
setcolor(12); (* plots SIMULATED point on chart *)  X:=round(7.5*TDB[1,1]);
Y:=round(380-W[1,1]*9000); moveto(X,Y);outtext('1');
for I:=2 to 9 do  begin  X:=round(TDB[I,4]*15/2);  Y:=round(380 -W[I,4]*9000);
lineto(X,Y); case I of  2:outtextxy(x,y,'2'); 3:outtextxy(x,y,'3'); 4:outtextxy(x,y,'4');
6:outtextxy(x,y,'6'); 7:outtextxy(x,y,'7'); 8:outtextxy(x,y,'8'); 9:outtextxy(x,y,'9'); end;
end; readln;
closegraph
end;

PROCEDURE tableD; (* displays results in tabular form *)
begin   clrscr;
write('RESULTS OF DEC TEST      '); write('DATE: ',d,'-',m,'-',y);writeln('  TIME:
',h,'H',mm); writeln('*******************');
writeln('PURPOSE OF TEST:',DESCRIP); writeln('OPERATING PARAMETERS');
writeln('----------  -------'); writeln('Supply air flow rate  = ',MAS[1]:4:2,' kg/s');
writeln('Return air flow rate  = ',MAR[1]:4:2,' kg/s');
writeln('Regen. heat input   = ',NOR[1]:4:3,' kW'); writeln;
writeln('MOIST AIR PROPERTIES AT MEASURED POINTS IN PROCESS');
writeln('-------------------------------------------' );
writeln('PT TDB  TWB  TDP  PW   W   RH   U   SV   H');
writeln('  (oC) (oC) (oC) (kPa) (g/kg) (%)  (%) (m3/kg) (kJ/kg)');
for  I:= 1 to 9 do
writeln(I,TDB[I,1]:7:1,TWB[I,1]:6:1,TDP[I,1]:5:1,PW[I,1]:7:2,W[I,1]*1000:8:2,
RH[I,1]*100:5:0,U[I,1]*100:6:0,SV[I,1]:8:3,HT[I,1]:8:2);  readln;  clrscr;
writeln('PROCESS CHANGES OF ENTHALPY AND HUMIDITY RATIO ');
writeln('-------------------------------------------' );
writeln('ST END h (kJ/KG)              W (g/kg)  ');
writeln('PT PT NOM. MIN. MAX. SIM.   NOM. MIN. MAX. SIM. ');
for  I:= 1 to 8 do   begin
write(I:1,(I+1):3,CHTOT[I,1]:7:1,CHTOT[I,2]:6:1,CHTOT[I,3]:6:1,CHTOT[I,4]:6:1);
writeln(CW[I,1]*1000:8:2,CW[i,2]*1000:6:2,CW[I,3]*1000:6:2,CW[I,4]*1000:6:2);
end;  readln; clrscr;
```

```
writeln('PERFORMANCE PARAMETERS (CALCULATED) ') ;
writeln('----------------------        NOM.  MIN.  MAX.  SIM. ');
writeln('Dehumidifier eff.(W)  (%)
EDH1=',100*EDH1[1]:5:0,100*EDH1[2]:6:0,100*EDH1[3]:6:0,100*EDH1[4]:6:0);
writeln('Dehumidifier eff.(Q)  (%)
EDH2=',100*EDH2[1]:5:0,100*EDH2[2]:6:0,100*EDH2[3]:6:0,100*EDH2[4]:6:0);
writeln('Regeneration eff.     (%)
ERG=',100*ERG[1]:5:0,100*ERG[2]:6:0,100*ERG[3]:6:0,100*ERG[4]:6:0);
writeln('Regen. heat input   (kW)  Q =',Q[1]:5:2,Q[2]:6:2,Q[3]:6:2,Q[4]:6:2);
writeln('Heat Exch. eff. (SUP) (%)
EHXS=',100*EHXS[1]:5:0,100*EHXS[2]:6:0,100*EHXS[3]:6:0,100*EHXS[4]:6:0);
writeln('Heat Exch. eff. (RET) (%)
EHXR=',100*EHXR[1]:5:0,100*EHXR[2]:6:0,100*EHXR[3]:6:0,100*EHXR[4]:6:0);
writeln('Sup. air spr. ch. eff.(%)
EVS=',100*EVS[1]:5:0,100*EVS[2]:6:0,100*EVS[3]:6:0,100*EVS[4]:6:0);
writeln('Ret. air spr. ch. eff.(%)
EVR=',100*EVR[1]:5:0,100*EVR[2]:6:0,100*EVR[3]:6:0,100*EVR[4]:6:0);
writeln('FOR VENTILATION MODE: ');
writeln('Cooling capacity    (kW)  CC =',CC[1]:5:2,CC[2]:6:2,CC[3]:6:2,CC[4]:6:2);
writeln('Coeff. of performance
COP=',COP[1]:5:2,COP[2]:6:2,COP[3]:6:2,COP[4]:6:2);
writeln('Electricity eff. ratio    EER=',EER[1]:5:2,EER[2]:6:2,EER[3]:6:2,EER[4]:6:2);
writeln('FOR VENTILATION CREDIT MODE: ');
writeln('Cooling capacity    (kW) TCC =',TCC[1]:5:2,TCC[2]:6:2,TCC[3]:6:2,
TCC[4]:6:2);
 writeln('Total Coeff. of perf.    TCOP=',TCOP[1]:5:2,TCOP[2]:6:2,TCOP[3]:6:2,
TCOP[4]:6:2);
writeln('Electricity eff. ratio   TEER=',TEER[1]:5:2,TEER[2]:6:2,TEER[3]:6:2,
TEER[4]:6:2);   readln;
end;

PROCEDURE result;
var xx:integer;
begin   clrscr; repeat  psychart;  tableD;
writeln('ENTER 1=SEE PSYCH. CHART AGAIN, 2=CONT.');  readln(xx);
```

```
until ) x=2;
end;

PROCEDURE process; (* calculates changes in process conditions and
overall performance parameters *)
var  E11,E2?,31,E2:real;
begin     MAS[1]:=VAS/SV[2,1];
EMAS:=MAS[1]*(EVAS/VAS); (*error of SV small compared to VAS*)
MAS[2]:=MAS[1]-EMAS;  MAS[3]:=MAS[1]+EMAS;  MAR[1]:=VR/SV[9,1];
EMAR:=MAR[1]*(EVRE/VR); (*error of SV small compared to VR*)
MAR[2]:=MAR[1]-EMAR; MAR[3]:=MAR[1]+EMAR;
FOR I:=1 TO 9 DO  begin
EHT[I]:=(HT[I,3]-HT[I,2])/2; EW[I]:=(W[I,3]-W[I,2])/2;
ETDB[I]:=(TDB[I,3]-TDB[I,2])/2; ETWB[I]:=(TWB[I,3]-TWB[I,2])/2;
end;
FOR I:=1 TO 8 DO  begin
ECHTOT[I]:=sqrt(EHT[I+1]*EHT[I+1]+EHT[I]*EHT[I]);
CHTOT[I,1]:=HT[I+1,1]-HT[I,1]; CHTOT[I,2]:=CHTOT[I,1]-ECHTOT[I];
CHTOT[I,3]:=CHTOT[I,1]+ECHTOT[I];
ECW[I]:=sqrt(EW[I+1]*EW[I+1]+EW[I]*EW[I]);
CW[I,1]:=W[I+1,1]-W[I,1]; CW[I,2]:=CW[I,1]-ECW[I]  CW[I,3]:=CW[I,1]+ECW[I];
end;
E1:=ECHTOT[4]/CHTOT[4,1]; E2:=EMAS/MAS[1];
CC[1]:=(CHTOT[4,1])*MAS[1]; ECC:=CC[1]*sqrt(E1*E1+E2*E2);
CC[2]:=CC[1]-ECC;  CC[3]:=CC[1]+ECC;
E11:=sqrt(EHT[1]*EHT[1]+EHT[4]*EHT[4]);
E1:=E11/(HT[1,1]-HT[4,1]); E2:=EMAS/MAS[1];
TCC[1]:=(HT[1,1]-HT[4,1])*MAS[1];  ETCC:=TCC[1]*sqrt(E1*E1+E2*E2);
TCC[2]:=TCC[1]-ETCC;  TCC[3]:=TCC[1]+ETCC;
E1:=ECHTOT[7]/(CHTOT[7,1]); E2:=EMAR/MAR[1];
Q[1]:=CHTOT[7,1]*MAR[1]; EQ:=Q[1]*sqrt(E1*E1+E2*E2);
Q[2]:=Q[1]-EQ;  Q[3]:=Q[1]+EQ;
E11:=sqrt(ETDB[7]*ETDB[7]+ETDB[6]*ETDB[6]);
E1:=E11/(TDB[7,1]-TDB[6,1]); E22:=sqrt(ETDB[2]*ETDB[2]+ETDB[6]*ETDB[6]);
E2:=E22/(TDB[2,1]-TDB[6,1]);
```

```
EHXR[1]:=(TDB[7,1]-TDB[6,1])/(TDB[2,1]-TDB[6,1]);
EEHXR:=EHXR[1]*sqrt(E1*E1+E2*E2);
EHXR[2]:=EHXR[1]-EEHXR; EHXR[3]:=EHXR[1]+EEHXR;
E11:=sqrt(ETDB[2]*ETDB[2]+ETDB[3]*ETDB[3]); E1:=E11/(TDB[2,1]-TDB[3,1]);
E22:=sqrt(ETDB[2]*ETDB[2]+ETDB[6]*ETDB[6]); E2:=E22/(TDB[2,1]-TDB[6,1]);
EHXS[1]:=(TDB[2,1]-TDB[3,1])/(TDB[2,1]-TDB[6,1]);
EEHXS:=EHXS[1]*sqrt(E1*E1+E2*E2);
EHXS[2]:=EHXS[1]-EEHXS; EHXS[3]:=EHXS[1]+EEHXS;
E11:=sqrt(ETDB[3]*ETDB[3]+ETDB[4]*ETDB[4]); E1:=E11/(TDB[3,1]-TDB[4,1]);
E22:=sqrt(ETDB[3]*ETDB[3]+ETWB[4]*ETWB[4]); E2:=E22/(TDB[3,1]-TWB[4,1]);
EVS[1]:=(TDB[3,1]-TDB[4,1])/(TDB[3,1]-TWB[4,1]);
EEVS:=EVS[1]*sqrt(E1*E1+E2*E2);
EVS[2]:=EVS[1]-EEVS; EVS[3]:=EVS[1]+EEVS;
E11:=sqrt(ETDB[5]*ETDB[5]+ETDB[6]*ETDB[6]); E1:=E11/(TDB[5,1]-TDB[6,1]);
E22:=sqrt(ETDB[5]*ETDB[5]+ETWB[6]*ETWB[6]); E2:=E22/(TDB[5,1]-TWB[6,1]);
EVR[1]:=(TDB[5,1]-TDB[6,1])/(TDB[5,1]-TWB[6,1]);
EEVR:=EVR[1]*sqrt(E1*E1+E2*E2);
EVR[2]:=EVR[1]-EEVR; EVR[3]:=EVR[1]+EEVR;
E1:=ECC/CC[1]; ENOR:=(NOR[3]-NOR[2])/2;
E2:=ENOR/NOR[1]; COP[1]:=CC[1]/NOR[1];
ECOP:=COP[1]*sqrt(E1*E1+E2*E2);
COP[2]:=COP[1]-ECOP; COP[3]:=COP[1]+ECOP;
E1:=ETCC/TCC[1]; ENOR:=(NOR[3]-NOR[2])/2; E2:=ENOR/NOR[1];
TCOP[1]:=TCC[1]/NOR[1]; ETCOP:=TCOP[1]*sqrt(E1*E1+E2*E2);
TCOP[2]:=TCOP[1]-ETCOP; TCOP[3]:=TCOP[1]+ETCOP;
E1:=ECC/CC[1]; ENOE:=(NOE[3]-NOE[2])/2;
E2:=ENOE/NOE[1]; EER[1]:=CC[1]/NOE[1];
EEER:=EER[1]*sqrt(E1*E1+E2*E2);
EER[2]:=EER[1]-EEER; EER[3]:=EER[1]+EEER;
E1:=ETCC/TCC[1]; ENOE:=(NOE[3]-NOE[2])/2;
E2:=ENOE/NOE[1]; TEER[1]:=TCC[1]/NOE[1];
ETEER:=TEER[1]*sqrt(E1*E1+E2*E2);
TEER[2]:=TEER[1]-ETEER; TEER[3]:=TEER[1]+ETEER;
E1:=ECW[1]/CW[1,1]; EW2:=(W2[3]-W2[2])/2;
E22:=sqrt(EW[1]*EW[1]+EW2*EW2); E2:=E22/(W[1,1]-W2[1]);
```

```
EDH1[1]:=(-CW[1,1])/(W[1,1]-W2[1]); EEDH1:=EDH1[1]*sqrt(E1*E1+E2*E2);
EDH1[2]:=EDH1[1]-EEDH1; EDH1[3]:=EDH1[1]+EEDH1;

E11:=ECW[8]/CW[8,1]; E22:=EMAR/MAR[1];
E1:=2501*CW[8,1]*MAR[1]*(sqrt(E11*E11+E22*E22));
E11:=E1/(2501*CW[8,1]*MAR[1]); E22:=ENOR/NOR[1];
ERG[1]:=(2501*CW[8,1]*MAR[1])/NOR[1];
EERG:=ERG[1]*sqrt(E11*E11+E22*E22);
ERG[2]:=ERG[1]-EERG; ERG[3]:=ERG[1]+EERG;
EDH2[1]:=CHTOT[1,1]/(CHTOT[1,1]+(TDB[8,1]-TDB[2,1])*(1.005+W[2,1]*1.805));
EDH2[2]:=CHTOT[1,2]/(CHTOT[1,2]+(TDB[8,3]-TDB[2,2])*(1.005+W[2,3]*1.805));
EDH2[3]:=CHTOT[1,3]/(CHTOT[1,3]+(TDB[8,2]-TDB[2,3])*(1.005+W[2,2]*1.805));
end;

PROCEDURE map2;
var WS:REAL;
begin
PSDB[I,J]:= PSAT(TDB[I,J]);   PSWB[I,J]:=PSAT(TWB[I,J]);
WS:=0.622*PSWB[I,J]/(82.5-PSWB[I,J]);
W[I,J]:=((2501-2.381*TWB[I,J])*WS-(TDB[I,J]-TWB[I,J]))/(2501+1.805*TDB[I,J]-
4.186*TWB[I,J]);
end;

PROCEDURE map1;
var T,P,Z,WS,WT:real;
begin
PSDB[I,J]:= PSAT(TDB[I,J]); W[8,J]:=W[7,J]; PW[I,J]:=(W[I,J]*82.5)/(W[I,J]+0.622);
TDP[I,J]:=tsat(PW[I,J]); T:=TDP[I,J]-1;
 repeat  T:=T+2;  TWB[I,J]:=T;  PSWB[I,J]:=psat(T);
WS:=0.622*PSWB[I,J]/(82.5-PSWB[I,J]);  WT:=((2501-2.381*TWB[I,J])*WS-
(TDB[I,J]-TWB[I,J]))/(2501+1.805*TDB[I,J]-4.186*TWB[I,J]);
Z:=W[I,J]-WT;  until Z<0.0 ;
repeat  T:=T-0.1; TWB[I,J]:=T;  PSWB[I,J]:=psat(T);
 WS:=0.622*PSWB[I,J]/(82.5-PSWB[I,J]);  WT:=((2501-2.381*TWB[I,J])*WS-
(TDB[I,J]-TWB[I,J]))/(2501+1.805*TDB[I,J]-4.186*TWB[I,J]);
```

```
Z:=W[I,J]-WT;   until Z>0.0 ;
end;
PROCEDURE maxw; (* calculates max. possible humidity ratio of pt 2 *)
var T,P,Ps,WS,WT,RH2,PSDB2,PSWB2,Z:real;
begin   T:=TWB[1,J];  PSWB[1,J]:=psat(TWB[1,J]);
WS:=0.622*PSWB[1,J]/(82.5-PSWB[1,J]);
repeat  T:=T+2;
WT:=((2501-2.381*TWB[1,J])*WS-(T-TWB[1,J]))/(2501+1.805*T-4.186*TWB[1,J]);
P:=(WT*82.5)/(WT+0.622);  Ps:=PSAT(T);  RH2:=P/Ps;  Z:=RH[8,J]-RH2;
until Z>0.0 ;
repeat  T:=T-0.1;
WT:=((2501-2.381*TWB[1,J])*WS-(T-TWB[1,J]))/(2501+1.805*T-4.186*TWB[1,J]);
P:=(WT*82.5)/(WT+0.622);  Ps:=PSAT(T);  RH2:=P/Ps;  Z:=RH[8,J]-RH2;
until Z<0.0 ;
W2[J]:=WT;
end;

PROCEDURE moisteqns; (* equations for moist air properties *)
begin
PW[I,J]:=(W[I,J]*82.5)/(W[I,J]+0.622);
RH[I,J]:=PW[I,J]/PSDB[I,J];
SV[I,J]:=287*(TDB[I,J]+273.16)/((82.5-PW[I,J])*1000);
U[I,J]:=RH[I,J]*(82.5-PSDB[I,J])/(82.5-PW[I,J]);
TDP[I,J]:=tsat(PW[I,J]);
HT[I,J]:=(1.005*TDB[I,J])+W[I,J]*(2501+1.805*TDB[I,J]);
end;

PROCEDURE simulation;
var M3,M7,M9,H2:real;
begin    writeln;
{writeLN('EHXS[1]= ',EHXS[1]:4:3,'  enter EHXS[4] ');readln(EHXS[4]);
writeLN('EHXR[1]= ',EHXR[1]:4:3,'  enter EHXR[4] ');readln(EHXR[4]);
writeLN('EVS[1]= ',EVS[1]:4:3,'  enter EVS[4] ');readln(EVS[4]);
writeLN('EVR[1]= ',EVR[1]:4:3,'  enter EVR[4] ');readln(EVR[4]);  READLN; }
```

```
EHXS[4]:=EHXS[1];  HXR[4]:=EHXR[1];  EVS[4]:=0;  EVR[4]:=EVR[1];
MAS[4]:=MAS[1];  MAR[4]:=MAR[1];  Q[4]:=NOR[1];  NOR[4]:=NOR[1];
NOE[4]:=NOE[1]; TDB[1,4]:=TDB[1,1]; TWB[1,4]:=TWB[1,1];
I:=1; J:=4; map2;  moisteqns;
TDB[5,4]:=TDB[5,1]; TWB[5,4]:=TWB[5,1]; I:=5;J:=4; map2; moisteqns;
TDB[6,4]:=TDB[5,4]-EVR[4]*(TDB[5,4]-TWB[5,4]); TWB[6,4]:=TWB[5,4];
I:=6;J:=4; map2; moisteqns;
{TDB[8,4]:=TDB[8,1]; (*first estimate*) RH[8,4]:=RH[8,1]; }  ZZ:=0;
repeat
W[2,4]:=W[2,1];  (* calculates point 2 for constant wbt process*)
TWB[2,4]:=TWB[1,4]; PSWB[2,4]:=psat(TWB[2,4]);
PW[2,4]:=W[2,4]*82.5/(W[2,4]+0.622);
TDB[2,4]:=((PSWB[2,4]-PW[2,4])/(82.5*0.000666))+TWB[2,4];
I:=2; J:=4; map2; moisteqns; H2:=HT[2,4];
TDB[2,4]:=TDB[2,1]; (*actual point 2*) TWB[2,4]:=TWB[2,1];
I:=2; J:=4; map2; moisteqns;
TDB[7,4]:=TDB[6,4]+EHXR[4]*(TDB[2,4]-TDB[6,4]); W[7,4]:=W[6,4];
TDB[3,4]:=TDB[2,4]-EHXS[4]*(TDB[2,4]-TDB[6,4]); W[3,4]:=W[2,4];
J:=4; I:=3;map1;moisteqns;
I:=7;map1;moisteqns;
M3:=0.01384/SV[6,4];   (*air carryover*)  M7:=0.01384/SV[2,4];
W[3,4]:=(W[3,4]*(MAS[4]-M3)+W[6,4]*M3)/MAS[4];
W[7,4]:=(W[7,4]*(MAR[4]-M7)+W[2,4]*M7)/MAR[4];
HT[3,4]:=(HT[3,4]*(MAS[4]-M3)+((HT[6,4]+HT[7,4])/2)*M3)/MAS[4];
HT[7,4]:=(HT[7,4]*(MAR[4]-M7)+((HT[2,4]+HT[3,4])/2)*M7)/MAR[4];
TDB[3,4]:=(HT[3,4]-2501*W[3,4])/(1.005+1.84*W[3,4]);
TDB[7,4]:=(HT[7,4]-2501*W[7,4])/(1.005+1.84*W[7,4]);
J:=4; I:=3;map1;moisteqns;
I:=7;map1;moisteqns;
TDB[8,4]:=TDB[7,4]+(NOR[4]/(MAR[4]*(1.005+1.84*W[7,4])));
J:=4;I:=8; map1;moisteqns;  ZZ:=ZZ+1;
until ZZ=1;
W[9,4]:=W[8,4]+(W[1,4]-W[2,4])*(MAS[4]/MAR[4]); TWB[9,4]:=TWB[8,4];
PW[9,4]:=W[9,4]*82.5/(W[9,4]+0.622); PSWB[9,4]:=psat(TWB[9,4]);
TDB[9,4]:=((PSWB[9,4]-PW[9,4])/(82.5*0.000666))+TWB[9,4]
```

```
-((MAS[4]/MAR[4])*(HT[2,4]-H2)/(1.005+1.84*W[9,4])); J:=4;I:=9; map1; moisteqns;
TDB[ .   =TDB[3,4]-EVS[4]*(TDB[3,4]-TWB[3,4]); TWB[4,4]:=TWB[3.4];
I:=4;J:=4; map2; moiste  s;

maxw;   J:=4;
for I:=1 to 8 do begin CHTOT[I,4]:=HT[I+1,4]-HT[I,4]; CW[I,4]:=W[I+1,4]-W[I,4];end;
CC[4]:=(HT[5,4]-HT[4,4])*MAS[4];
TCC[4]:=(HT[1,4]-HT[4,4])*MAS[4];
Q[4]:=(HT[8,4]-HT[7,4])*MAR[4];
COP[J]:=CC[J]/(NOR[J]+0.0001);
TCOP[J]:=TCC[J]/(NOR[J]+0.0001);
EER[J]:=CC[J]/(NOE[4]);
TEER[J]:=TCC[ ]/(NOE[4]);
EDH1[J]:=(W[1,J]-W[2,J])/(W[1,J]-W2[J]+0.000001);
EDH2[J]:=CHTOT[1,J]/(CHTOT[1,J]+(TDB[8,J]-TDB[2,J])*(1.005+W[2,J]*1.84));
ERG[J]:=(2501*CW[8,J]*MAR[J])/(NOR[J]+0.0001);
end;

PROCEDURE moistairprop; (* calculates all moist air properties at
meas   points *)
begin
for J:=1 to 3 do   begin   for I:=1 to 9 do  begin  case I of   1..7,9:map2;
8:map1;  end;   moisteqns;   end;   maxw;   end;
end;

PROCEDURE addinfo;   (* input operating parameters*)
var TV2,rh8:real;
begin
repeat  writeln('ENTER THE FOLLOWING:  :'); writeln('*******************');
write('FLUKE MM. VOLTAGE FOR TWB[2] (mV) :'); readln(TV2);
TWB[2,1]:=(TV2-6.4)/10.05844;
writeln('SUPPLY AIR FLOWRATE (m3/s) nom,min,max   :');
readln(VAS[1]);readln(VAS[2]);readln(VAS[3]);
writeln('RETURN AIR FLOWRATE (m3/s) nom,min,max   :');
readln(VR[1]);readln(VR[2]);readln(VR[3]);
```

```
write('REGENERATION HEAT INPUT  (KW):'); readln(NOR[1]);
write('ELEC. ENERGY (EXCL. REG) (KW):'); readln(NOE[1]);
write('SPRAY WATER INLET TEMP. (oC) :');readln(TWSC[1]);
write('SUPPLY AIR SP. CH.: WATER FLOW RATE (g/s) :'); readln(FRS[1]);
write('              : PUMP PRESSURE (bar)   :');readln(PPS[1]);
write('RETURN AIR SP. CH.: WATER FLOW RATE (g/s) :');readln(FRR[1]);
write('              : PUMP PRESSURE (bar)   :');readln(PPR[1]);
TWB[2,2]:=TWB[2,1]-0.3; TWB[2,3]:=TWB[2,1]+0.3;
{VAS[2]:=VAS[1]*0.9; VAS[3]:=VAS[1]*1.1;
VR[2]:=VR[1]*0.9, VR[3]:=VR[1]*1.1;}
NOR[2]:=NOR[1]*0.96; NOR[3]:=NOR[1]*1.04;
NOE[2]:=NOE[1]*0.96; NOE[3]:=NOE[1]*1.04;
PPS[2]:=PPS[1]-2; PPS[3]:=PPS[1]+2;
PPR[2]:=PPR[1]-2; PPR[3]:=PPR[1]+2;
FRS[2]:=FRS[1]*0.95; FRS[3]:=FRS[1]*1.05;
FRR[2]:=FRR[1]*0.95; FRR[3]:=FRR[1]*1.05;
TWSC[2]:=TWSC[1]-0.2; TWSC[3]:=TWSC[1]+0.2; writeln;
writeln('ENTER 1=redo input, 2=cont.');readln(zz);
until zz=2
end;

PROCEDURE tempconv; (* (1) gets voltages from binary input (2) calculates and
displays the average, confidence limits and std. deviation of these voltages.
(3) converts voltages to temp. values *)
var       uvolts, vv : longint;  zz,I,J,r:integer;  s,ss:real;    bin:word;
begin
repeat (* reads voltages *) for J:=1 to 100 do  begin for I:=0 to 15 do
begin
r:=EDR_ADINBINONESAMPLE(bh,I,bin); if r<0 then printerror(r);
EDR_ADINBINTOVOLTAGE(bh,I,uvolts,bin); V[I,J]:=uvolts;
delay(3); end; end; clrscr;
writeln('MEASURED VOLTAGES (ALL VALUES IN MICROVOLTS)');
writeln('_____');
writeln('ch average confidence con.lim standard');
writeln('no. voltage limit(+/-)  (%)  deviation');
```

```
for I:=0 to 15 do   (* statistical analysis *)
begin  A[I,1]:=0;vv:=0;s:=0;ss:=0;SD[I]:=0;CL[I]:=0;ZCL[I]:=0;
for J:=1 to 50 do  vv:= vv + V[I,J];  A[I,1]:= vv div 50 ; (* average voltage *)
for J:=1 to 50 do  begin  s:=sqr(A[I,1]-V[I,J]);  ss:=(ss+s);  end;
SD[I]:=round(sqrt(ss/50));  (* standard deviation *)
CL[I]:= SD[I] div 5;   (* confidence limits *)  ZCL[I]:= 100*CL[I] / A[I,1];
writeln(I:2, A[I,1]:9, CL[I]:9, ZCL[I]:10:2, SD[I]:9);
A[I,2]:=A[I,1] - CL[I];  A[I,3]:=A[I,1] + CL[I];
readln;  end;
(* calibration equations*)
TDB[1,1]:= (A[0,1] - 6949)/10226.99;
TWB[1,1]:= (A[1,1] - 1843)/10178.87;
TDB[2,1]:= (A[2,1] - 5457)/10206.61;
TDB[3,1]:= (A[3,1] - 6736)/10177.00;
TWB[3,1]:= (A[4,1] - 7732)/10203.59;
TDB[4,1]:= (A[5,1] - 6351)/10211.31;
TWB[4,1]:= (A[6,1] - 2577)/10185.98;
TDB[5,1]:= (A[7,1] - 6868)/10180.03;
TWB[5,1]:= (A[8,1] + 121)/10155.73;
TDB[6,1]:= (A[9,1] + 6628)/10201.81;
TWB[6,1]:= (A[10,1] - 6756)/10198.54;
TDB[7,1]:= (A[11,1] - 7120)/10199.93;
TWB[7,1]:= (A[12,1] - 3183)/10172.12;
TDB[8,1]:= (A[13,1] - 7000)/10183.08;
TDB[9,1]:= (A[14,1] + 691)/10210.56;
TWB[9,1]:= (A[15,1] - 478)/10201.15;

TDB[1,2]:= -0.2+ (A[0,2] - 6949)/10226.99;
TWB[1,2]:= -0.3+ (A[1,2] - 1843)/10178.87;
TDB[2,2]:= -0.2+ (A[2,2] - 5457)/10206.61;
TDB[3,2]:= -0.2+ (A[3,2] - 6736)/10177.00;
TWB[3,2]:= -0.3+ (A[4,2] - 7732)/10203.59;
TDB[4,2]:= -0.2+ (A[5,2] - 6351)/10211.31;
TWB[4,2]:= -0.3+ (A[6,2] - 2577)/10185.98;
TDB[5,2]:= -0.2+ (A[7,2] - 6868)/10180.03;
```

```
TWB[5,2]:= -0.3+ (A[8,2] + 121)/10    5.73;
TDB[6,2]:= -0.2+ (A[9,2] + 6628)/10201.81;
TWB[6,2]:= -0.3+ (A[10,2] - 6756)/10198.54;
TDB[7,2]:= -0.2+ (A[11,2] - 7120)/10199.93;
TWB[7,2]:= -0.3+ (A[12,2] - 3183)/10172.12;
TDB[8,2]:= -0.2+ (A[13,2] - 7000)/10183.08;
TDB[9,2]:= -0.2+ (A[14,2] + 691)/10210.56;
TWB[9,2]:= -0.3+ (A[15,2] - 478)/10201.15;

TDB[1,3]:= 0.2+ (A[0,3] - 6949)/10226.99;
TWB[1,3]:= 0.3+ (A[1,3] - 1843)/10178.87;
TDB[2,3]:= 0.2+ (A[2,3] - 5457)/10206.61;
TDB[3,3]:= 0.2+ (A[3,3] - 6736)/10177.00;
TWB[3,3]:= 0.3+ (A[4,3] - 7732)/10203.59;
TDB[4,3]:= 0.2+ (A[5,3] - 6351)/10211.31;
TWB[4,3]:= 0.3+ (A[6,3] - 2577)/10185.98;
TDB[5,3]:= 0.2+ (A[7,3] - 6868)/10180.03;
TWB[5,3]:= 0.3+ (A[8,3] + 121)/10155.73;
TDB[6,3]:= 0.2+ (A[9,3] + 6628)/10201.81;
TWB[6,3]:= 0.3+ (A[10,3] - 6756)/10198.54;
TDB[7,3]:= 0.2+ (A[11,3] - 7120)/10199.93;
TWB[7,3]:= 0.3+ (A[12,3] - 3183)/10172.12;
TDB[8,3]:= 0.2+ (A[13,3] - 7000)/10183.08;
TDB[9,3]:= 0.2+ (A[14,3] + 691)/10210.56;
TWB[9,3]:= 0.3+ (A[15,3] - 478)/10201.15;
writeln;  writeln('ENTER 1=REPEAT ,2=CONT/EXIT');  readln(zz);  until zz=2
end;

(*MAIN PROGRAM*)
BEGIN
clrscr;  repeat
tempconv; (* get temperatures fron. binary input*)
writeln;  writeln('ENTER 1=exit, 2=cont');  readln(yy);  if yy=2 then
begin   repeat
addinfo;(* input operating parameters*)
```

```
moistairprop;(* calculate moist air properties*)
process;(* calculate changes in each step of process*)
simulation; (* simulated process *)
result; (* displays results and psychrometric chart*)
presult; (* prints results, if requested*)
writeln('ENTER 1=REPEAT (NEW MASS FLOW), 2=cont'); readln(yy); until yy=2;
end
else yy:=1; writeln; writeln('ENTER 1=REPEAT, 2=EXIT'); readln(zz); until zz=2;
END.
```

APPENDIX C

COMPUTER PROGRAM TO CALCULATE AIR FLOW RATE

This appendix is a printout of the computer program that was used to calculated the air flow rates from pitot tube and micromanometer pressure measurements (see section 5.3.2).

```
PROGRAM FLOW;

var P:ARRAY[1..5,1..6,1..3] OF REAL;  {pressure kPa}
   V:ARRAY[1..5,1..6,1..3] OF REAL; {velocity m/s}
SV:ARRAY[1..3] OF REAL; {specific volume m3/kg}
   Q:ARRAY[1..3] OF REAL; {volumetric flow rate m3/s}
   A:ARRAY[1..3] OF REAL; {area m2}
  VA:ARRAY[1..3] OF REAL;    Z, I, J, K : INTEGER;

BEGIN   repeat
writeln;  write('enter spec. vol.: '); readln(SV[1]);  write('enter area    : '); readln(A[1]);
SV[2]:=SV[1] - 0.001;  SV[3]:=SV[1] + 0.001;
A[2]:=A[1]*0.98; A[3]:=A[1]*1.02;  writeln;

FOR J:=1 TO 6 DO  begin
FOR I:=1 TO 5 DO  begin
write('enter row', J,' pt', I,'  '); readln(P[I,J,1]);
P[I,J,2]:=0.99*P[I,J,1]-0.05;  P[I,J,3]:=1.01*P[I,J,1]+0.05;
IF P[I,J,2] <= 0 THEN P[I,J,2]:=0.0   ELSE P[I,J,2]:=P[I,J,2];
end;  end;

FOR K:=1 TO 3 DO   begin  VA[K]:=0;
FOR J:=1 TO 6 DO   begin
FOR I:=1 TO 5 DO   begin
 V[I,J,K]:=sqrt(2*P[I,J,K]*SV[K]);    VA[K]:=VA[K]+V[I,J,K];
end; end;
 VA[K]:=VA[K]/30;   Q[K]:=VA[K]*A[K];
end;
writeln('q nom. (m3/s) = ',Q[1]:4:3);  writeln('q min. (m3/s) = ',0.987*Q[2]:4:3);
writeln('q max. (m3/s) = ',1.013*Q[3]:4:3);  writeln;
write('enter 1=end, 2=repeat'); readln(z);  until z=1;
END.
```

APPENDIX D

DEC SIMULATION COMPUTER PROGRAM

This appendix is a printout of the computer program that was used to simulate a desiccant-evaporative cooling (DEC) system (see section 5.3.3).

```
PROGRAM SIMUL;
(* This program simulates the performance of a DEC system and displays performance parameters, based
on entered operating parameters *)
uses crt,graph,dos;
var   t, I, J, zz, yy, xx: integer;   (* dummy variables *)
 MAS: REAL;  (* supply air flow rate in kg/s *)
 MAR: REAL;  (* return air flow rate in kg/s *)
 NOR: REAL;  (* heat input *)
 NOE: REAL;  (* total electrical energy input *)
 PAT:REAL;  (*atmospheric pressure*)
 W2: REAL;  (* minimum. possible humidity ratio for pt 2 *)
 CC: REAL;  (* cooling capacity in kW (basic vent. mode)*)
 TCC: REAL;  (* cooling capacity in kW (vent. credit mode)*)
 Q: REAL;  (* regen. heat supplied in kW *)
 COP: REAL;  (* COP for basic vent. mode  *)
 TCOP: REAL;  (* COP for ventilation credit mode *)
 EER: REAL;  (* electrical efficiency ratio for basic vent. mode *)
 TEER: REAL;  (* electrical efficiency ratio for vent. credit mode*)
 EDH1: REAL; (*efficiency  of dehumidifier (moisture removal*)
 EDH2: REAL; (*efficiency  of dehumidifier (heat transfer)*)
 ERG: REAL;  (* efficiency of regeneration *)
 EHXS: REAL; (*efficiency of heat exchanger (supply air)*)
 EHXR: REAL; (* efficiency of heat exchanger (return air)*)
 EVS: REAL;  (*efficiency of supply air spray chambers *)
 EVR: REAL;  (*efficiency of return air spray chambers *)
 TDB:ARRAY[1..9] OF REAL; (* dry bulb temp. oC *)
 TWB:ARRAY[1..9] OF REAL; (* wet bulb temp. oC *)
 RH:ARRAY[1..9] OF REAL; (* relative humidity (frac) *)
 PSDB:ARRAY[1..9] OF REAL; (* saturation pressure at TDB kPa *)
 PSWB:ARRAY[1..9] OF REAL; (* saturation pressure at TWB kPa *)
 PA:ARRAY[1..9] OF REAL; (* air pressure kPa *)
  W:ARRAY[1..9] OF REAL; (* humidity ratio kg/kg *)
 SV:ARRAY[1..9] OF REAL; (* specific volume m3/kg *)
  U:ARRAY[1..9] OF REAL; (* percentage saturation % *)
```

```
  HT:ARRAY[1..9] OF REAL; (* total specific enthalpy air kJ/kg *)
 TDP:ARRAY[1..9] OF REAL; (* dew point temperature oC *)
  PW:ARRAY[1..9] OF REAL; (* vapour pressure kPa *)
CHTOT:ARRAY[1..8] OF REAL; (* change of total sp. enthalpy kJ/kg *)
  CW:ARRAY[1..8] OF REAL; (* change of humidity ratio kg/kg *)

FUNCTION psat(T:real):real; (* calculate          ition pressure for given T *)
var  Z: real;
begin
  T:=T+273.16;
  Z:=(2*..9051+0.0024804*T-3142.31/T)*ln(10)-8.2*ln(T);
  PSAT:=100*exp(Z);
end;

FUNCTION tsat(P:real):real; (* calculates dew point temp. oC *)
var z:real;
begin
   if P<0.001 then P:=0.001; z:=ln(P);
   if P>0.6112 then  (* ie. TDP>0 oC *)
    tsat:= 6.54+(14.526*z)+(0.7389*z*z)+(0.09486*z*z*z)+(0.4569*(exp(0.1984*z)))
   else  tsat:= 6.09+(12.608*z)+(0.4959*z*z);
end;

PROCEDURE psychart;  (* displays psychromatric chart showing process *)
var grdriver, grmode, grerror: integer;    x,y:integer;        P,GG,T:real;
begin
grdriver:=detect;  initgraph(grdriver,grmode,'');    grerror:=graphresult;
if grerror<>grok  then  writeln('graphics error:',grapherrormsg(grerror))
else      begin
     setcolor(green);      moveto(0,380);      lineto(600,380);  (* draws axes *)
     lineto(600,110);      moveto(250,420);      setcolor(5);      outtext('DBT (oC)');
     moveto(595,40);      outtext('W');      moveto(592,60);      outtext('g/kg');
end;
setcolor(5);
for I:=0 to 8 do  (* displays TDB increments on horizontal axis *)
begin
```

```
    T:=10*I;
    putpixel(I*75,385,5);
    moveto(I*75,390);
    case I of
    0:outtext('0');     1:outtext('10');     2:outtext('20');     3:outtext('30');     4:outtext('40');
    5:outtext('50');     6:outtext('60');     7:outtext('70');     8:outtext('80');     end;
   end;

   for I:=0 to 6 do  (* prints humidity ratio increments on vertical axis *)
   begin
    GG:=5*I;     putpixel(602,380-I*45,5);     moveto(605,380-I*45);
    case I of
    0:outtext('0');     1:outtext('5');     2:outtext('10');     3:outtext('15');     4:outtext('20');
    5:outtext('25');     6:outtext('30');     end;
   end;

setcolor(6);     moveto(0,340);

for I:=0 to 14 do   (* draws saturation curve *)

begin

T:=2*I;   P:=psat(T);   GG:=0.622*P/(PA1-P);   X:=I*15;   Y:=round(380-GG*9000);   lineto(X,Y);
end;
setcolor(7); line(0,100,30,100); outtextxy(33,100,'inlet');
setcolor(5); line(0,110,30,110); outtextxy(33,110,'room');
setcolor(9); line(0,120,30,120); outtextxy(33,120,'outlet');
setcolor(7);          (* plots measured point on chart *)
X:=round(7.5*TDB[1]);     Y:=round(380-W[1]*9000);     moveto(X,Y);outtext('1');
for I:=2 to 9 do     begin
case I of     2,3,4:setcolor(7);     5:setcolor(5);     6,7,8,9:setcolor(9);     end;
X:=round(TDB[I]*15/2);     Y:=round(380 -W[I]*9000);     lineto(X,Y);
case I of  2:outtextxy(x,y,'2');  3:outtextxy(x,y,'3');   4:outtextxy(x,y,'4');  5:outtextxy(x,y,'5');
          6:outtextxy(x,y,'6');  7:outtextxy(x,y,'7');   8:outtextxy(x,y,'8');  9:outtextxy(x,y,'9'); end;     end;
readln;   closegraph
end;
```

```
PROCEDURE tableD; (* displays results in tabular form *)
begin   clrscr;
writeln('MOIST AIR PROPERTIES ');
writeln('-------------------------------------------------------');
writeln('PT TDB  TWB  TDP  PW    W    RH   U   SV    H');
writeln('  (oC) (oC) (oC) (kPa) (g/kg) (%)  (%) (m3/kg) (kJ/kg)');
  for I:= 1 to 9 do  writeln(I,TDB[I]:7:1,TWB[I]:6:1,TDP[I]:6:1,PW[I]:7:2,
W[I]*1000:8:2,RH[I]*100:5:0,U[I]*100:6:0,SV[I]:8:3,HT[I]:8:2);   readln;   clrscr;
writeln('PERFORMANCE PARAMETERS (CALCULATED) ');
writeln('-------------------------------------------------------');

writeln('Dehumidifier eff.(W)  (%) EDH1=',100*EDH1:5:0);

writeln('Dehumidifier eff.(Q)  (%) EDH2=',100*EDH2:5:0);
writeln('Regeneration eff.    (%)  ERG=',100*ERG:5:0);
writeln('Regen. heat input    (kW)  Q=',Q:5:2);
writeln('Heat Exch. eff. (SUP) (%) EHXS=',100*EHXS:5:0);
writeln('Heat Exch. eff. (RET) (%) EHXR=',100*EHXR:5:0);
writeln('Sup. air spr. ch. eff.(%)  EVS=',100*EVS:5:0);
writeln('Ret. air spr. ch. eff.(%)  EVR=',100*EVR:5:0);
writeln('FOR VENTILATION MODE: ');
writeln('Cooling capacity    (kW)  CC =',CC:5:2);
writeln('Coeff. of performance     COP=',COP:5:2);
writeln('Electricity eff. ratio    EER=',EER:5:2);
writeln('FOR VENTILATION CREDIT MODE: ');
writeln('Cooling capacity    (kW) TCC =',TCC:5:2);
writeln('Total Coeff. of perf.    TCOP=',TCOP:5:2);
writeln('Electricity eff. ratio   TEER=',TEER:5:2);   readln;
end;

PROCEDURE result;
var xx: integer;
begin   clrscr;
repeat   psychart;   tableD;   writeln('ENTER 1=SEE PSYCH. CHART AGAIN, 2=CONT.');
readln(xx);   until xx=2;
```

```
end;

PROCEDURE map2;
var WS:REAL;
begin
   PSDB[I]:= PSAT(TDB[I]);
   PSWB[I]:=PSAT(TWB[I]);
   WS:=0.622*PSWB[I]/(PAT-PSWB[I]);
   W[I]:=((2501-2.381*TWB[I])*WS-(TDB[I]-TWB[I]))/(2501+1.805*TDB[I]-4.186*TWB[I]);
end;

PROCEDURE map1;
var T, P, Z, WS, WT: real;
begin
   PSDB[I]:= PSAT(TDB[I]);
   W[8]:=W[7];
   PW[I]:=(W[I]*PAT)/(W[I]+0.622);
   TDP[I]:=tsat(PW[I]);
   T:=TDP[I]-1;
   repeat
      T:=T+2;
      TWB[I]:=T;
      PSWB[I]:=psat(T);
      WS:=0.622*PSWB[I]/(PAT-PSWB[I]);
      WT:=((2501-2.381*TWB[I])*WS-(TDB[I]-TWB[I]))/(2501+1.805*TDB[I]-4.186*TWB[I]);
      Z:=W[I]-WT;
   until Z<0.0 ;

   repeat
      T:=T-0.1;
      TWB[I]:=T;
      PSWB[I]:=psat(T);
      WS:=0.622*PSWB[I]/(PAT-PSWB[I]);
      WT:=((2501-2.381*TWB[I])*WS-(TDB[I]-TWB[I]))/(2501+1.805*TDB[I]-4.186*TWB[I]);
      Z:=W[I]-WT;
      until Z>0.0 ;
```

```
end;

PROCEDURE maxw; (* calculates max. possible humidity ratio of pt 2 *)
var T,P,Ps,WS,WT,RH2,PSDB2,PSWB2,Z:real;
begin
  T:=TWB[1];
  PSWB[1]:=psat(TWB[1]);
  WS:=0.622*PSWB[1]/(PAT-PSWB[1]);
repeat
  T:=T+2;
  WT:=((2501-2.381*TWB[1])*WS-(T-TWB[1]))/(2501+1.805*T-4.186*TWB[1]);
  P:=(WT*PAT)/(WT+0.622);
  Ps:=PSAT(T);
  RH2:=P/Ps;
  Z:=RH[8]-RH2;
until Z>0.0 ;

repeat
  T:=T-0.1;
  WT:=((2501-2.381*TWB[1])*WS-(T-TWB[1]))/(2501+1.805*T-4.186*TWB[1]);
  P:=(WT*PAT)/(WT+0.622);
  Ps:=PSAT(T);
  RH2:=P/Ps;
  Z:=RH[8]-RH2;
until Z<0.0 ;

W2:=WT;
end;

PROCEDURE moisteqns; (* equations for moist air properties *)
begin
    PW[I]:=(W[I]*PAT)/(W[I]+0.622);
    RH[I]:=PW[I]/PSDB[I];
    SV[i]:=287*(TDB[I]+273.16)/((PAT-PW[I])*1000);
    U[I]:=RH[I]*(PAT-PSDB[I])/(PAT-PW[I]);
    TDP[I]:=tsat(PW[I]);
```

```
    HT[I]:=(1.005*TDB[I])+W[I]*(2501+1.805*TDB[I]);
end;

PROCEDURE simulation;
var M3,M7,M9,TDB2:real;
begin    writeln;
writeLN('enter EHXS (FRAC.) ');readln(EHXS); writeLN('enter EHXR (FRAC.) ');readln(EHXR);
writeLN('enter EVS  (FRAC.) ');readln(EVS); writeLN('enter EVR  (FRAC.) ');readln(EVR);
writeLN('enter MAS  (KG/S) ');readln(MAS); writeLN('enter MAR  (KG/S)  ');readln(MAR);
writeLN('enter TDB1 (oC) ');readln(TDB[1]);   writeLN('enter W1   (G/KG)');readln(W[1]);
W[1]:=W[1]/1000;    writeLN('enter TDB5 (oC) ');readln(TDB[5]);writeLN('enter W5
(G/KG)');readln(W[5]);   W[5]:=W[5]/1000;    writeLN('enter TDB8 (oC)');readln(TDB[8]);
writeLN('enter TDB2 (oC) ');readln(TDB[2]); writeLN('enter W2   (G/KG)');readln(W[2]);
W[2]:=W[2]/1000;
{PAT:= 82.5;  NOE:=1;   EHXS:=0.84;   EHXR:=0.84;  EVS:=1;   EVR:=0.95;  MAS:=1;
MAR:=1;   TDB[8]:=70;   TDB[1]:=23;   W[1]:=0.010;  TDB[2]:=38.2;  W[2]:=0.0048;}
I:=1;map1;moisteqns;
TDB[5]:=23;      W[5]:=0.010;      I:=5;map1;moisteqns;
TDB[6]:=TDB[5]-EVR*(TDB[5]-TWB[5]);      TWB[6]:=TWB[5];    I:=6;map2;moisteqns;
(* calculates point 2 for constant wbt process*)
TWB[2]:=TWB[1];  PSWB[2]:=psat(TWB[2]);   PW[2]:=W[2]*PAT/(W[2]+0.622);
TDB2:=((PSWB[2]-PW[2])/(PAT*0.000666))+TWB[2];    I:=2;map1;moisteqns;
TDB[7]:=TDB[6]+EHXR*(TDB[2]-TDB[6]);   W[7]:=W[6]; I:=7;map1;moisteqns;
TDB[3]:=TDB[2]-EHXS*(TDB[2]-TDB[6]);  W[3]:=W[2]; I:=3;map1;moisteqns;
M3:=0.01384/SV[6];  (*air carryover*)   M7:=0.01384/SV[2];
W[3]:=(W[3]*(MAS-M3)+W[6]*M3)/MAS;      W[7]:=(W[7]*(MAR-M7)+W[2]*M7)/MAR;
HT[3]:=(HT[3]*(MAS-M3)+((HT[6]+HT[7])/2)*M3)/MAS;
HT[7]:=(HT[7]*(MAR-M7)+((HT[2]+HT[3])/2)*M7)/MAR;
TDB[3]:=(HT[3]-2501*W[3])/(1.005+1.84*W[3]);
TDB[7]:=(HT[7]-2501*W[7])/(1.005+1.84*W[7]);
I:=3;map1;moisteqns;   I:=7;map1;moisteqns;   I:=8;map1;moisteqns;
W[9]:=W[8]+(W[1]-W[2])*(MAS/MAR);   TWB[9]:=TWB[8];  PW[9]:=W[9]*PAT/(W[9]+0.622);
PSWB[9]:=psat(TWB[9]);
TDB[9]:=((PSWB[9]-PW[9])/(PAT*0.000666))+TWB[9]-((MAS/MAR)*(TDB[2]-TDB2));
```

```
I:=9;map1;moisteqns;

TDB[4]:=TDB[3]-EVS*(TDB[3]-TWB[3]);   TWB[4]:=TWB[3];   I:=4;map2;moisteqns;  maxw;

  for I:=1 to 8 do   begin   CHTOT[I]:=HT[I+1]-HT[I];   CW[I]:=W[I+1]-W[I];   end;
  CC:=(HT[5]-HT[4])*MAS;   TCC:=(HT[1]-HT[4])*MAS;   Q:=(HT[8]-HT[7])*MAR;
  COP:=CC/Q;   TCOP:=TCC/Q;   EER:=CC/NOE;   TEER:=TCC/NOE;
  EDH1:=(W[1]-W[2])/(W[1]-W2);
  EDH2:=CHTOT[1]/(CHTOT[1]+(TDB[8]-TDB[2])*(1.005+W[2]*1.84));
  ERG:=(2501*CW[8]*MAR)/Q;
end;

(*MAIN PROGRAM*)
BEGIN
repeat
clrscr;
  simulation;   (* simulated process *)
  result;
  writeln;   writeln('ENTER 1=REPEAT, 2=EXIT');   readln(zz)
until zz=2;
END.
```

APPENDIX E

SPECIFICATIONS FOR INSTRUMENTATION

This appendix contains specifications for the following instrumentation and equipment:

(1) MEDM 500 microprocessor manometer (micromanometer).
(2) Humidity sensor HD 8907TC/150 (hygrotransmitter).
(3) PC 30 analog to digital card.
(4) LM 35D temperature sensors.
(5) Calibration certificate for Fluke thermometer.

Specifications of MEDM 500 Microprocessor Manometer

Pressure range	0 – 500 Pa
Velocity range	0 – 28.8 m/s
Volume range	0 – 999.9 m^3/s
Max overload	5000 Pa
K factor range	1 – 2.99
Duct temperaure temperature	0 – 699 °C
Duct absolute pressure range	70 – 140 Pa
Area input range	0.00001 to 99.9999 m^2
Memory size	80 Pressure, velocity or volume readings
Accuracy of displayed reading	± 1 % of reading
Output facility	0 – 1 mA on each range
Temperature operating range	0 – 40 °C

Specifications of the Humidity Sensor HD 8907TC/150 (hygrotransmitter)

HYGROTRANSMITTER HD 8907TO, HD 8907TV, HD 8907TC/150, HD 8907TC/350

CHARACTERISTICS SHARED BY THE VARIOUS MODELS:
- "H3000" capacitive humidity sensor.
- Output 0 ÷ 20 mA, 4 ÷ 20 mA, 0 ÷ 10 V with selection by means of a jumper.
- Two-wire connection.
- Transmitter power supply 220 Vac (on request 24 Vac)
- The transmitters (that is sensor and electronics) are interchangeable with other transmitters
- Model HD 8907TO, HD 8907TV is an enbloc relative humidity transmitter
- Models HD 8907TC/150, HD 8907TC/350 are relative humidity transmitters the sensor of which is separate from the electronic part and is connected to it by means of a cable L = 1.5 m.
- The sensors are fitted at the end of a stainless steel tube and are protected against dust and dirt by a stainless steel filter.

SENSOR
The humidity sensor is a condenser the dielectric of which is a hygroscopic polymer. As the dielectric constant for water is around 80, a strong variation of capacity is obtained with the variation of the humidity content of this polymer. The particular advantage of this type of sensor are good linearity, insensitivity to temperature variations, brief response time and long life. **When using, check the compatibility of the sensor with the atmosphere in which it is inserted.** The sensor has a temporary lack of precision if condensation forms on its surface (the value transmitted is higher than the actual value due to an increase of its real capacity).

SIGNAL TRANSMISSION
The electronic circuit is designed in such a way that there is a linear increase of the absorbed current as humidity increases. For this series of transmitters the connection uses only 2 wires. The absorbed current is proportional to the relative humidity. The line resistance does not influence precision of measurement. If the voltage ou (0 ... 10 V) is selected, you must remember that the transmitter's put impedance is 500 ohm ± 0.2% so the receiver must have a l impedance.
In the presence of cables transmitting strong currents or machi that provoke electromagnetic disturbances, the transmitter connec cables must be laid in a separate channel or at a certain distanc that the disturbances are screened.

INSTALLATION
Precision of measurement does not depend on the position of transmitter. However it is advisable to fit the transmitter in such a that the sensor is facing downwards so as to minimize the accum tion of dust on the filter. The transmitter must not be installed in immediate vicinity of a source of heat, as the heating of the air lo to a decrease of the relative humidity (with the same amount of w vapour present) close to doors or draughts.

ASSEMBLY
The electronics are housed in a sturdy plastic container (degre protection IP 65). When the lid is opened four holes are access which allow the base of the transmitter to be fixed directly to the The position of the holes is 50 x 108 mm. For the electric connec there are a cable clamp and two terminals that can take leads wi diameter of up to 3 mm. Versions HD 8907TC/150 and 8907TC/350 may be fixed to the wall by means of a 1/2" sliding nector. **Attention: the sensor and the electronics have the s serial number, they cannot be interchanged with other trans tors.**

TECHNICAL DATA
Relative humidity
Measuring range: 5% R.H.... 95% R.H.
Precision: ± 2% R.H. in the temperature range from 10 to 50°C
Temperature influence: zero, between -20°C ... 40°C, negligi between 40°C ... 80°C
Working temperature: -20°C ...+80°C (temporarily for brief period to 90°C).
Absorption: 0 mA, 4 mA, 0V ≙ 0% R.H., 20 mA, 10V ≙ 100% R.H.
Response time at 63% variation:
without filter: 6 seconds
with filter: 4 minutes

Working temperature:
Probe: -20 ... +80°C
Electronics: 0°C ... +50°C
Supply voltage:
220 Vac, on request 24 Vac
Absorption: 1VA

The HD 8907T... series of transmitters may be connected to the lowing DELTA OHM instruments:
HD 4046, HD 046: Relative humidity Indicator 4 ÷ 20 in the measuring range 0% R.H....100% R.H.
HD 4049, HD 049: Relative humidity ON/OFF regul 4 ÷ 20 mA, in the regulation range 0% R.H....100% R.H
HD 5002/2: Dual regulator; input temperature signal f Pt100 sensor; adjustment range -50 to +200°C, rela humidity 4 ÷ 20 mA in the adjustment ra 0% R.H....100% R.H. ON/OFF regulation and neutral zo

Specifications of the PC 30 Analog to Digital Card

Supplier	Eagle Technology
Input channels	16 single ended
Input voltage range	Monopolar: 0 -- 10 V
	Bipolar: ± 5 V or ± 10 V
Conversion type	Successive approx A/D converter
Resolution	12 bits
Max A/D throughput	20 kHz
Input impedance	22 kΩ
Linearity	0.025 % (11 bits)
Offset	Adjustable to zero
Power requirements	800mA @ +5 V DC

Analog inputs:

Total system accuracy	± 1 LSB
Differential non-linearity	+ or – ¾ LSB
Input ranges	-5 V to +5 V
	0 to 10 V
	-10 V to +10 V

Specifications for LM 35D Temperature Sensors

National Semiconductor

LM35/LM35A/LM35C/LM35CA/LM35D
Precision Centigrade Temperature Sensors

General Description

The LM35 series are precision integrated-circuit temperature sensors, whose output voltage is linearly proportional to the Celsius (Centigrade) temperature. The LM35 thus has an advantage over linear temperature sensors calibrated in ° Kelvin, as the user is not required to subtract a large constant voltage from its output to obtain convenient Centigrade scaling. The LM35 does not require any external calibration or trimming to provide typical accuracies of ±¼°C at room temperature and ±¾°C over a full −55 to +150°C temperature range. Low cost is assured by trimming and calibration at the wafer level. The LM35's low output impedance, linear output, and precise inherent calibration make interfacing to readout or control circuitry especially easy. It can be used with single power supplies, or with plus and minus supplies. As it draws only 60 µA from its supply, it has very low self-heating, less than 0.1°C in still air. The LM35 is rated to operate over a −55° to +150°C temperature range, while the LM35C is rated for a −40° to +110°C range (−10° with improved accuracy). The LM35 series is available packaged in hermetic TO-46 transistor packages, while the LM35C is also available in the plastic TO-92 transistor package.

Features

- Calibrated directly in ° Celsius (Centigrade)
- Linear + 10.0 mV/°C scale factor
- 0.5°C accuracy guaranteeable (at +25°C)
- Rated for full −55° to +150°C range
- Suitable for remote applications
- Low cost due to wafer-level trimming
- Operates from 4 to 30 volts
- Less than 60 µA current drain
- Low self-heating, 0.08°C in still air
- Nonlinearity only ±¼°C typical
- Low impedance output, 0.1 Ω for 1 mA load

Connection Diagrams

TO-46
Metal Can Package*



TL/H/5516–1

*Case is connected to negative pin

Order Number LM35H, LM35AH, LM35CH, LM35CAH or LM35DH
See NS Package Number H03H

TO-92
Plastic Package



TL/H/5516–2

Order Number LM35CZ or LM35DZ
See NS Package Number Z03A

Typical Applications

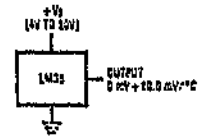

TL/H/5516–3

FIGURE 1. Basic Centigrade Temperature Sensor (+2°C to +150°C)

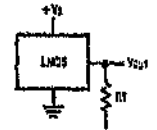

Choose $R_1 = -V_S/50\ \mu A$

V_{OUT} = +1,500 mV at +150°C
= +250 mV at +25°C
= −550 mV at −55°C

TL/H/5516–4

FIGURE 2. Full-Range Centigrade Temperature Sensor

Electrical Characteristics (Note 1) (Note 8) (Continued)

Parameter	Conditions	LM35			LM35C, LM35D			Units (Max)
		Typical	Tested Limit (Note 4)	Design Limit (Note 5)	Typical	Tested Limit (Note 4)	Design Limit (Note 6)	
Accuracy, LM35, LM35C (Note 7)	T_A = +25°C	±0.4	±1.0		±0.4	±1.0		°C
	T_A = −10°C	±0.5			±0.5		±1.5	°C
	T_A = T_{MAX}	±0.8	±1.5		±0.8		±1.5	°C
	T_A = T_{MIN}	±0.8		±1.5	±0.8		±2.0	°C
Accuracy, LM35D (Note 7)	T_A = +25°C				±0.6	±1.5		°C
	T_A = T_{MAX}				±0.9		±2.0	°C
	T_A = T_{MIN}				±0.9		±2.0	°C
Nonlinearity (Note 8)	$T_{MIN} \le T_A \le T_{MAX}$	±0.3		±0.5	±0.2		±0.5	°C
Sensor Gain (Average Slope)	$T_{MIN} \le T_A \le T_{MAX}$	+10.0	+9.8, +10.2		+10.0		+9.8, +10.2	mV/°C
Load Regulation (Note 3) $0 \le I_L \le 1$ mA	T_A = +25°C	±0.4	±2.0		±0.4	±2.0		mV/mA
	$T_{MIN} \le T_A \le T_{MAX}$	±0.5		±5.0	±0.5		±5.0	mV/mA
Line Regulation (Note 3)	T_A = +25°C	±0.01	±0.1		±0.01	±0.1		mV/V
	$4V \le V_S \le 30V$	±0.02		±0.2	±0.02		±0.2	mV/V
Quiescent Current (Note 9)	V_S = +5V, +25°C	56	80		56	80		µA
	V_S = +5V	105		158	91		138	µA
	V_S = +30V, +25°C	56.2	82		56.2	82		µA
	V_S = +30V	105.5		161	91.5		141	µA
Change of Quiescent Current (Note 3)	$4V \le V_S \le 30V$, +25°C	0.2	2.0		0.2	2.0		µA
	$4V \le V_S \le 30V$	0.5		3.0	0.5		3.0	µA
Temperature Coefficient of Quiescent Current		+0.39		+0.7	+0.39		+0.7	µA/°C
Minimum Temperature for Rated Accuracy	In circuit of *Figure 1*, I_L = 0	+1.5		+2.0	+1.5		+2.0	°C
Long Term Stability	T_J = T_{MAX}, for 1000 hours	±0.08			±0.08			°C

Note 3: Regulation is measured at constant junction temperature, using pulse testing with a low duty cycle. Changes in output due to heating effects can be computed by multiplying the internal dissipation by the thermal resistance.

Note 4: Tested Limits are guaranteed and 100% tested in production.

Note 5: Design Limits are guaranteed (but not 100% production tested) over the indicated temperature and supply voltage ranges. These limits are not used to calculate outgoing quality levels.

Note 6: Specifications in boldface apply over the full rated temperature range.

Note 7: Accuracy is defined as the error between the output voltage and 10mV/°C times the device's case temperature, at specified conditions of voltage, current and temperature (expressed in °C).

Note 8: Nonlinearity is defined as the deviation of the output-voltage-versus-temperature curve from the best-fit straight line, over the device's rated temperature range.

Note 9: Quiescent current is defined in the circuit of *Figure 1*.

Note 10: Absolute Maximum Ratings indicate limits beyond which damage to the device may occur. DC and AC electrical specifications do not apply when operating the device beyond its rated operating conditions. See Note 1.

Calibration Certificate for Fluke Thermometer

ESKOM

CERTIFICATE OF CALIBRATION

NATIONAL CALIBRATION SERVICE
APPROVED LABORATORY
No 306

This certificate is issued in accordance with the conditions of the approval granted by the National Calibration Service. It is a correct record of the measurements made. This certificate may not be reproduced other than in full except with prior written approval of the issuing laboratory.

TECHNOLOGY RESEARCH AND INVESTIGATIONS
TEMPERATURE METROLOGY LABORATORY

Date of issue 5-5-97

Certificate number 970577264

Head of Laboratory

M Mathews

The values in this certificate are correct at the time of calibration. Subsequently the accuracy will depend on such factors as the care executed in handling and use of the device, and the frequency of use. Recalibration should be performed after a period so chosen to ensure that the instrument's accuracy remains within the desired limits.

NLA

ESKOM - TECHNOLOGY RESEARCH AND INVESTIGATIONS

CERTIFICATE OF CALIBRATION

ESKOM

Calibration of a : Digital Thermometer
Calibrated for : Eskom TRI
Certificate number : 9705T264
Date of calibration : 5/5/97

Serial number : 5695242
Instrument range : 0 to 80°C
Type : Fluke 52 K/J digital thermometer with S/N 5095242
: coupled to a type K thermocouple.

Procedure number : 306-1003
Laboratory temp : 22.5°C
Humidity : 34%
Reference standards : Fluke 2180A digital thermometer S/N 2620007
:

The accuracies of the reference standards are traceable to the National Measuring Standards.

Reference Temperature °C	Indicated Reading °C	Correction °C
0.0	-0.2	0.2
19.3	19.5	-0.2
29.4	29.4	0.0
39.6	39.6	0.0
49.6	49.6	0.0
59.4	59.5	-0.1
69.6	69.7	-0.2
79.5	79.8	-0.3

The uncertainty of measurement is +/-0.6°C, estimated for a 95% confidence level.

Recommended re-calibration date: 5/5/98

Comments : The correction should be added to the indicated temperature in order
: to obtain the true temperature.
:
:

Calibrated by : D D Bhimma

Checked by : M Mathieson

Head of laboratory

Private Bag X40176, Cleveland, 2022. Tel (011) 629-5111 or (011) 629-5335

APPENDIX F

EQUIPMENT PERFORMANCE DATA

This appendix contains the manufacturer's performance data for the desiccant wheel and sensible heat exchanger.

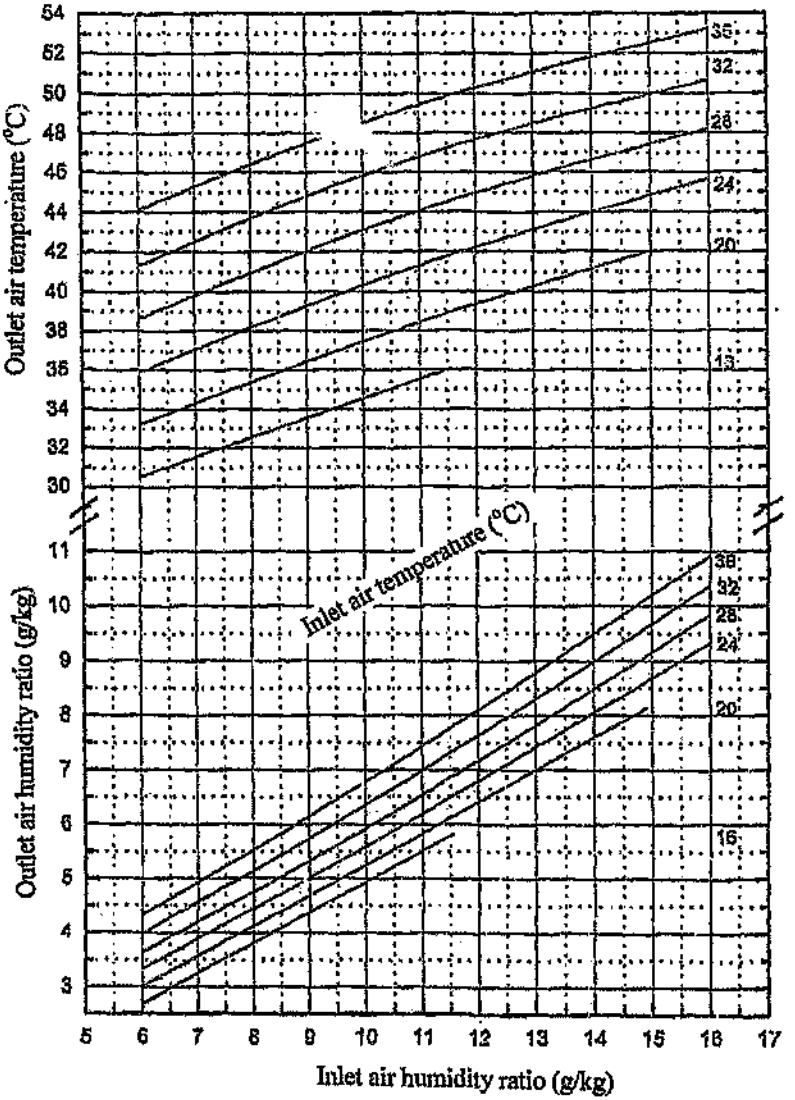

Air velocity = 2.5 m/s

rotational speed = 21.9 rev per hour

Regenerating temperature = 70 °C

$X_{ReE} = X_{TrE}$

where X_{ReE}= humidity ratio of regen. air

X_{TrE}=humidity ratio of inlet air

If X_{ReE} not equal to X_{TrE} then subtract $0.05(X_{ReE} - X_{TrE})$ from the outlet air humidity ratio

FIGURE F.1: Desiccant wheel outlet air conditions for specific inlet air conditions (Klingenburg, 1997a).

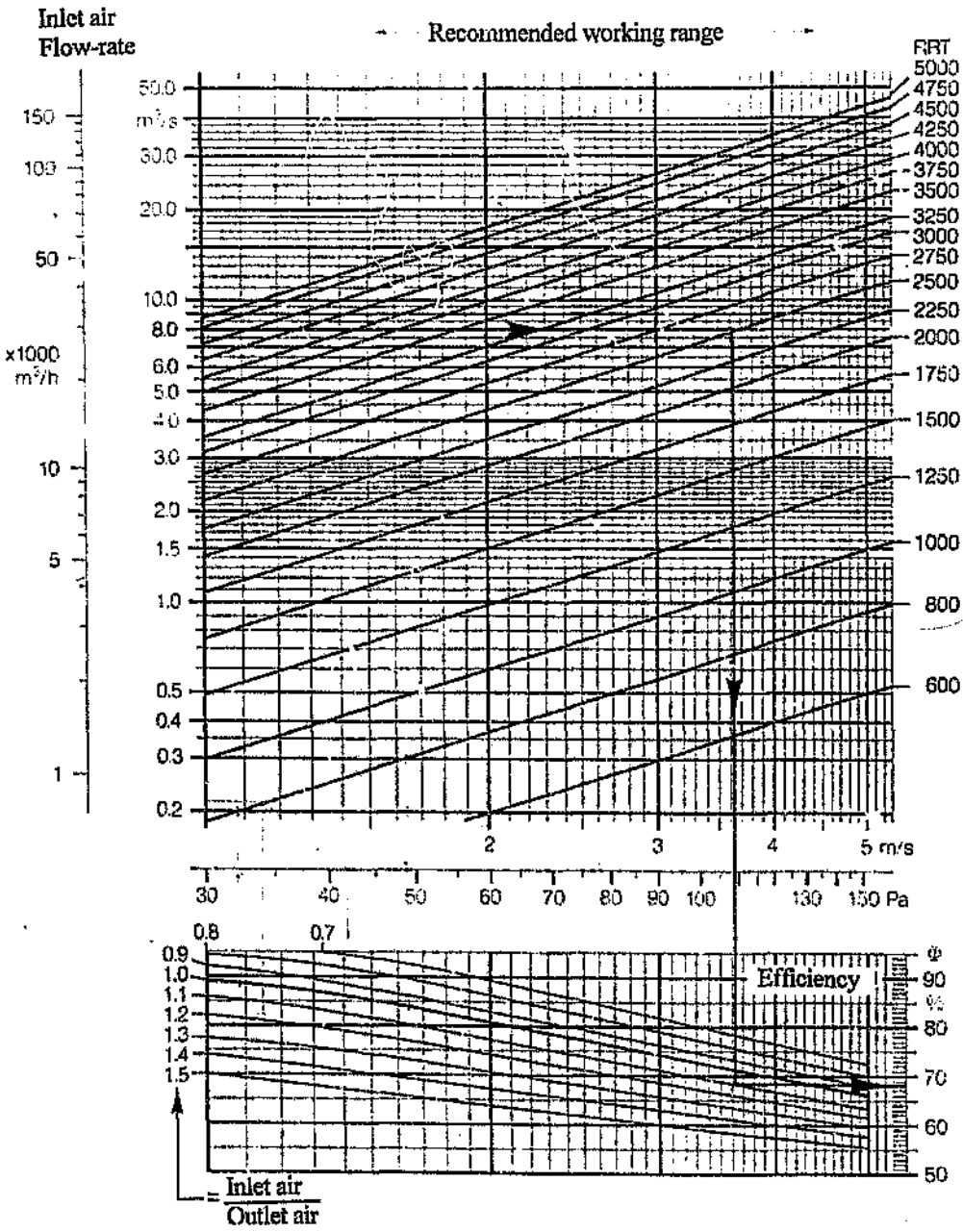

FIGURE F.2: Performance chart for the sensible heat exchanger (RRT 300) (Klingenburg, 1997b).

APPENDIX G
OPERABILITY OF DEC SYSTEMS IN SOUTH AFRICA

G1 Overview

Part of the scope of this project was to do an assessment of the feasibility of DEC systems in South Africa. This appendix G gives the following results:

(a) A general survey was done concerning the climatic variations in South Africa throughout the year. These results are given in section G2. The results give a general indication of the air conditioning requirements in South Africa concerning dehumidification and cooling.

(b) Simulations of DEC systems operating in various modes in all 12 climatic regions of South Africa at different times of the day throughout the year, were done based on average weather data. The simulations used the manufacturer's information (see appendix F) for the desiccant wheel. The purpose of these simulations was to determine the operability, performance and practical implications of operating DEC systems (balanced flow, non-optimized) in South Africa. The weather data, simulation results and a brief discussion of the results, for each of the different climatic regions is covered in sections G3 to G14 (see table G2.1 for a list of the regions and the relevant sections).

TABLE G2.1: Climatic zones of South Africa and representative cities.

ZONE		CLIMATE	CITY	
W	Namaqualand and North-western Cape	Desert	Upington	G3
M	South-western Cape	Winter rain	Cape Town	G4
A	Southern Coastal Belt	Rain all seasons	Port Elizabeth	G5
SE	South-eastern Coastal Belt	Warm. Summer rain	East London	G6
E	Eastern Coastal Belt and Zululand	Subtropical. Summer rain	Durban	G7
D	Drakensberg Escarpment	Warm. Summer rain	Ladysmith	G8
L	Lowveld	Hot steppe. Summer rain	Phalaborwa	G9
NT	Northern Transvaal	Hot steppe. Summer rain	Pietersburg	G10
H	Highveld	Warm. Summer rain	Johannesburg	G11
SN	Northern Steppe	Steppe. Summer rain	Bloemfontein	G12
SS	Southern Steppe	Cold steppe. Autumn rain	Queenstown	G13
K	Karoo	Desert	Beaufort West	G14

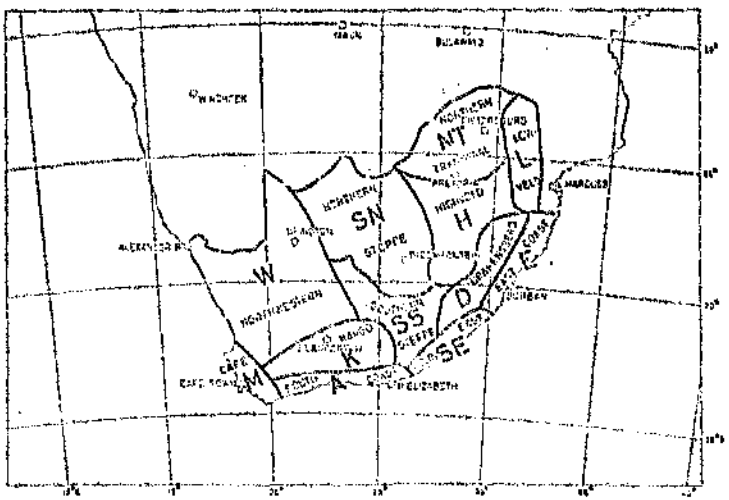

FIGURE G2.1: Climatic zones of South Africa (Weather Bureau, 1960).

TABLE G7 : Months when average dry-bulb temperature or humidity ratio exceeds room conditions

MONTH	Upington			Cape Town			Port Elizabeth			East London			Durban			Ladysmith		
	08	14	20	08	14	20	08	14	20	08	14	20	08	14	20	08	14	20
JAN	T	T	T	W	TW	W	W	TW	W	W	TW	W	TW	TW	TW	W	TW	W
FEB	W	TW	TW	W	TW	W	W	TW	W	W	TW	W	TW	TW	TW	W	TW	W
MAR	W	TW	TW	W	TW	W	W	TW	W	W	TW	W	TW	TW	TW	W	TW	W
APR		T		W	W	W	W	W	W	W	W	W	W	TW	W		T	
MAY		T						W	W		W	W	W	TW	W			
JUN														W	W			
JUL														W	W			
AUG													W	W	W			
SEP		T						W	W		W	W	W	W	W		T	
OCT		T	T				W	W	W	W	W	W	W	W	W		T	
NOV		T	T	W	W	W	W	W	W	W	W	W	W	TW	W	W	TW	W
DEC		T	T	W	TW	W	W	TW	W	W	W	W	TW	TW	V	W	TW	W

T= Ambient dry-bulb temperature exceeds that in room of 23 °C.

W= Ambient humidity ratio exceeds that in room at 50 % relative humidity.

The calculations were based on average monthly climatic data at the specified times of the day (08h00, 14h00 and 20h00).

TABLE G2.2b: Months when average dry-bulb temperature or humidity ratio exceeds room conditions

MONTH	Phalaborwa			Pietersburg			Johannesburg			Bloemfontein			Queenstown			Beaufort West		
	08	14	20	08	14	20	08	14	20	08	14	20	08	14	20	08	14	20
JAN	TW	TW	TW	W	TW	W	W	TW	W	W	TW	TW	W	TW	W	W	T	T
FEB	TW	TW	TW	W	TW	W	W	TW	W	W	TW	W	W	TW	W	W	T	T
MAR	W	TW	TW	W	TW	W	W	W	W	W	TW	W	W	TW	W		T	T
APR	W	TW	W	W	T	W											T	
MAY	W	TW	W															
JUN		T																
JUL		T																
AUG		T																
SEP	W	TW	W		T						T							
OCT	W	TW	TW		T						T						T	
NOV	W	TW	TW	W	TW	W	W				T			T	W		T	
DEC	TW	TW	TW	W	TW	W	W	TW	W	W	T	T	W	TW	W		T	T

T= Ambient dry-bulb temperature exceeds that in room of 23 °C.

W= Ambient humidity ratio exceeds that in room at 50 % relative humidity.

The calculations were based on average monthly climatic data at the specified times of the day (08h00, 14h00 and 20h00).

G3 Upington (Namaqualand and North-western Cape)

This region has a desert climate and is generally hot and dry except in February and March when the average humidity ratio is slightly higher than that in the room (see table G3.1). All of the air conditioning requirements could probably be met with only evaporative cooling, although dehumidification could be required if room latent loads are high. The ventilation mode generally performs slightly better than the recirculation mode throughout the year but the ventilation credit mode performs the best during the middle of the day in the summer months (see table G3.2). The best strategy would be to operate year round in the ventilation mode, which would give relatively high COPs throughout the year (minimum of 0.34 in ventilation mode).

TABLE G3.1: UPINGTON average monthly weather conditions (Weather Bureau, 1997).

MONTH	08H00			14H00			20H00		
	TDB	RH	W	TDB	RH	W	TDB	RH	W
JAN	23.3	46	9.1	33.6	21	8.7	31.2	22	8.4
FEB	22.5	54	10.2	32.5	26	9.6	29.7	29	9.7
MAR	20.2	61	10.0	30.6	28	9.6	26.7	34	9.7
APR	15.4	69	8.2	26.6	29	8.2	21.3	40	8.4
MAY	10.0	68	5.8	23.1	27	6.4	16.3	39	6.3
JUN	6.3	68	4.6	19.6	29	5.4	12.5	40	5.1
JUL	5.6	65	4.2	19.7	27	5.0	12.6	34	4.7
AUG	7.6	58	4.3	21.6	23	5.0	15.3	27	4.6
SEP	12.9	52	5.4	25.4	20	5.5	20.1	23	5.4
OCT	17.3	47	6.5	28.1	19	6.3	23.8	21	6.3
NOV	21.0	43	7.5	31.0	18	7.1	27.3	20	7.0
DEC	22.9	43	8.4	32.9	18	7.8	30.0	19	7.6

Note: (1) Elevation: 836 m (2) Weather office no.: 03174741

(3) Zone: W (Namaqualand and Northwestern Cape)

(4) Climate: Desert

(5) Room conditions: TDB= 23 °C, RH= 50 %, W= 9.6 g/kg

TABLE G3.2: DEC simulated performance parameters for UPINGTON

Month	Ventilation mode						Ventilation credit mode						Recirculation mode					
	CC (kW/kg)			COP			CC (kW/kg)			COP			CC (kW/kg)			COP		
	08	14	20	08	14	20	08	14	20	08	14	20	08	14	20	08	14	20
JAN	14.3	11.2	12.8	0.40	0.37	0.40	13.4	19.7	18.1	0.37	0.65	0.56	13.8	10.7	11.9	0.39	0.30	0.33
FEB	12.6	10.2	10.9	0.35	0.34	0.34	13.6	19.9	18.0	0.38	0.66	0.57	13.3	10.4	11.3	0.37	0.29	0.32
MAR	13.8	10.8	11.9	0.37	0.34	0.35	12.0	18.6	16.0	0.32	0.59	0.47	14.1	11.0	12.2	0.39	0.31	0.34
APR		14.7	16.0		0.42	0.42		14.8	11.2		0.42	0.30		13.3	15.0		0.37	0.42
MAY		18.7	21.0		0.49	0.49		10.7	5.8		0.28	0.14		15.8	18.4		0.44	0.50
JUN																		
JUL																		
AUG																		
SEP																		
OCT	20.4	17.3	18.7	0.49	0.48	0.49	6.8	14.1	11.1	0.16	0.39	0.29	17.9	14.2	15.3	0.49	0.39	0.44
NOV	17.7	15.0	16.4	0.46	0.45	0.46	10.3	16.8	14.1	0.27	0.50	0.40	15.8	12.8	13.9	0.44	0.36	0.39
DEC	15.5	13.3	14.4	0.42	0.42	0.43	12.3	18.8	16.4	0.33	0.59	0.49	14.4	11.6	12.8	0.40	0.33	0.36

NOTE: (1) The performance parameters are for a balanced flow DEC system operating with T_{REG}= 70 °C, EV_R= 95 % and EHX= 84 %.

(2) The calculations were based on average monthly climatic data at the specified times of the day (08h00, 14h00 and 20h00).

(3) Blank spaces are where ambient TDB < 16 °C or W < 6 g/kg (unlikely that cooling or dehumidification would be required).

G4 Cape Town (South-W[illegible])

This region has a winter rainfall climate that is very cold in w[illegible] but can become hot and humid in summer (see table G4.1). Cooling and dehumidification is required in the summer months. The recirculation mode (minimum COP=0.28) performs better than the ventilation mode throughout the year although the ventilation credit mode performs better during the middle of the day in summer (see table G4.2). The best strategy would be to operate continuously in the recirculation mode.

TABLE G4.1: CAPE TOWN average monthly weather conditions (Weather Bureau, 1997).

MONTH	08H00			14H00			20H00		
	TDB	RH	W	TDB	RH	W	TDB	RH	W
JAN	19.6	74	10.7	24.7	51	10.7	20.1	73	10.8
FEB	18.7	79	10.8	25.2	51	11.0	19.9	75	11.2
MAR	16.8	85	10.3	24.2	52	10.5	18.6	79	10.7
APR	14.1	89	9.0	22.1	55	9.5	16.5	82	9.7
MAY	11.2	89	7.5	19.2	60	8.7	14.1	84	8.6
JUN	9.6	87	6.5	17.3	61	7.9	12.2	84	7.7
JUL	8.7	89	6.3	16.5	62	7.6	11.8	85	7.4
AUG	9.3	88	6.5	16.9	59	7.5	12.4	82	7.5
SEP	11.6	87	7.5	18.0	58	7.9	13.6	81	8.0
OCT	14.7	79	8.3	20.2	53	8.3	15.2	78	8.5
NOV	17.6	72	9.1	22.2	52	9.2	17.2	76	9.3
DEC	19.1	72	10.1	23.5	52	10.1	18.9	74	10.3

Note: (1) Elevation: 42 m (2) Weather office no.: 00211790

(3) Zone: M (Southwestern Cape)

(4) Climate: Winter rain

(5) Room conditions: TDB= 23 °C, RH= 50 %, W= 8.8 g/kg

TABLE G4.2: DEC simulated performance parameters for CAPE TOWN

Month	Ventilation mode						Ventilation credit mode						Recirculation mode					
	CC (kW/kg)			COP			CC (kW/kg)			COP			CC (kW/kg)			COP		
	08	14	20	08	14	20	08	14	20	08	14	20	08	14	20	08	14	20
JAN	10.5	8.7	10.4	0.29	0.26	0.29	11.9	15.3	12.5	0.32	0.45	0.34	12.3	10.7	12.0	0.34	0.30	0.33
FEB	10.7	8.1	9.6	0.29	0.24	0.27	11.4	16.0	12.5	0.31	0.48	0.35	12.6	10.1	11.8	0.35	0.28	0.32
MAR	12.3	9.2	10.9	0.32	0.27	0.29	9.7	14.7	11.2	0.25	0.43	0.30	13.6	10.9	12.6	0.37	0.30	0.35
APR		11.6	13.3		0.32	0.34		12.5	8.9		0.34	0.23		12.3	14.2		0.34	0.39
MAY		14.0			0.36			9.9			0.26			13.9			0.38	
JUN		16.0			0.40			7.9			0.19			15.2			0.41	
JUL		16.5			0.40			6.9			0.17			15.7			0.43	
AUG		16.6			0.41			7.1			0.17			15.7			0.43	
SEP		15.7			0.39			8.3			0.21			15.0			0.41	
OCT		14.3			0.37			10.2			0.27			13.9			0.38	
NOV	13.9	12.0	13.6	0.36	0.33	0.35	9.2	12.2	9.0	0.23	0.33	0.23	14.2	12.6	14.2	0.39	0.35	0.39
DEC	11.8	10.3	11.4	0.31	0.29	0.30	11.1	14.1	11.0	0.30	0.40	0.29	12.9	11.5	12.8	0.35	0.32	0.35

NOTE: (1) The performance parameters are for a balanced flow DEC system operating with T_{REG}= 70 °C, EV_R= 95 % and EHX= 84 %.

(2) The calculations were based on average monthly climatic data at the specified times of the day (08h00, 14h00 and 20h00).

(3) Blank spaces are where ambient TDB < 16 °C or W < 6 g/kg (unlikely that cooling or dehumidification would be required).

G5 Port Elizabeth (Southern Coastal Belt)

This region has rainfall in all seasons with a moderate climate throughout the year although the summers can become humid (see table G5.1). The recirculation mode generally performs the best (minimum COP=0.26) with the ventilation credit mode performing better in summer (see table G5.2). The best strategy would be to operate in the recirculation mode.

TABLE G5.1: PORT ELIZABETH average monthly weather conditions (Weather Bureau, 1997).

MONTH	08H00			14H00			20H00		
	TDB	RH	W	TDB	RH	W	TDB	RH	W
JAN	21.1	76	12.5	24.2	61	12.6	20.9	80	12.8
FEB	20.7	82	12.6	24.2	64	12.8	20.7	85	13.0
MAR	19.3	85	12.1	23.4	64	12.4	19.8	85	12.5
APR	16.6	85	10.1	21.9	62	10.8	17.8	85	10.9
MAY	13.6	83	8.1	20.6	56	9.1	15.6	82	9.2
JUN	11.2	81	6.8	19.4	52	8.0	13.9	79	8.1
JUL	10.5	81	6.6	18.8	53	7.8	13.6	79	7.9
AUG	12.0	82	7.2	18.5	57	8.1	13.9	82	8.3
SEP	14.3	80	8.3	18.7	61	8.9	15.0	82	9.0
OCT	16.4	77	9.3	19.6	63	9.7	16.2	82	9.6
NOV	18.4	75	10.3	21.1	62	10.6	17.6	82	10.6
DEC	20.2	73	11.4	23.0	61	11.6	19.6	80	11.8

Note: (1) Elevation: 60m (2) Weather office no.: 00351795

(3) Zone: A (Southern coastal belt)

(4) Climate: Rain all seasons

(5) Room conditions: TDB= 23 °C, RH= 50 %, W= 8.8 g/kg

TABLE G5.2: DEC simulated performance parameters for PORT ELIZABETH

Month	Ventilation mode						Ventilation credit mode						Recirculation mode					
	CC (kW/kg)			COP			CC (kW/kg)			COP			CC (kW/kg)			COP		
	08	14	20	08	14	20	08	14	20	08	14	20	08	14	20	08	14	20
JAN	7.3	5.9	6.7	0.21	0.18	0.20	14.7	16.8	14.7	0.43	0.52	0.43	10.5	9.6	10.5	0.29	0.27	0.29
FEB	7.2	5.6	6.5	0.21	0.17	0.19	14.5	17.0	14.8	0.42	0.53	0.43	10.7	9.4	10.5	0.30	0.26	0.29
MAR	8.6	6.5	7.8	0.24	0.20	0.22	13.2	16.1	13.9	0.37	0.49	0.40	11.6	9.9	11.0	0.32	0.27	0.30
APR	12.8	9.6	11.1	0.33	0.27	0.29	9.5	13.6	11.1	0.24	0.38	0.29	13.8	11.6	12.7	0.38	0.32	0.35
MAY		13.0			0.35			11.3			0.30			13.2			0.36	
JUN		15.1			0.39			9.4			0.24			14.5			0.40	
JUL		15.7			0.40			8.9			0.22			14.8			0.40	
AUG		15.3			0.39			8.9			0.22			14.6			0.40	
SEP		13.9			0.36			9.7			0.25			14.0			0.38	
OCT	14.0	12.3	13.7	0.35	0.33	0.35	8.6	11.1	8.8	0.22	0.30	0.22	14.5	13.2	14.3	0.40	0.36	0.39
NOV	11.3	10.3	11.5	0.31	0.29	0.30	10.9	12.9	10.5	0.29	0.36	0.28	13.0	11.9	13.2	0.36	0.33	0.36
DEC	9.4	8.0	8.9	0.26	0.24	0.25	13.1	15.2	13.0	0.37	0.45	0.36	11.6	10.8	11.6	0.32	0.30	0.32

NOTE: (1) The performance parameters are for a balanced flow DEC system operating with T_{REG}= 70 °C, EV_R= 95 % and EHX= 84 %.

(2) The calculations were based on average monthly climatic data at the specified times of the day (08h00, 14h00 and 20h00).

(3) Blank spaces are where ambient TDB < 16 °C or W < 6 g/kg (unlikely that cooling or dehumidification would be required).

36 East London (South-Eastern Coastal Belt)

This region has a warm climate with summer rainfall (see table G6.1). The recirculation mode generally performs the best (minimum COP=0.25) with the ventilation credit mode performing better in summer (see table G6.2). The best strategy would be to operate in the recirculation mode.

TABLE G6.1: EAST LONDON average monthly weather conditions (Weather Bureau, 1997).

MONTH	08H00			14H00			20H00		
	TDB	RH	W	TDB	RH	W	TDB	RH	W
JAN	21.7	78	13.0	24.0	71	13.6	21.2	85	13.4
FEB	21.4	81	13.2	24.2	72	13.8	21.3	87	13.8
MAR	20.2	83	12.4	23.5	72	13.3	20.4	87	13.1
APR	17.7	81	10.3	22.3	66	11.5	18.4	85	11.2
MAY	15.1	76	8.1	21.2	58	9.5	16.3	80	9.2
JUN	12.8	70	6.5	19.8	52	8.0	14.5	75	7.7
JUL	12.4	70	6.3	19.6	52	7.7	14.2	77	7.7
AUG	13.5	73	7.0	19.4	58	8.3	14.6	80	8.3
SEP	15.4	76	8.4	9.4	65	9.5	15.8	83	9.3
OCT	3	75	9.6	19.8	69	10.4	16.8	83	10.1
NOV	19.2	75	10.8	21.0	72	11.5	18.2	85	11.3
DEC	20.9	75	11.9	22.8	70	12.6	20.0	84	12.4

Note: (1) Elevation: 125m (2) Weather office no.: 00595729

(3) Zone: SE (South-eastern Coastal belt)

(4) Climate: Warm Summer rain

(5) Room conditions: TDB= 23 °C, RH= 50 %, W= 8.9 g/kg

TABLE G6.2: DEC simulated performance parameters for EAST LONDON

Month	Venulation mode						Ventilation credit mode						Recirculation mode					
	CC (kW/kg)			COP			CC (kW/kg)			COP			CC (kW/kg)			COP		
	08	14	20	08	14	20	08	14	20	08	14	20	08	14	20	08	14	20
JAN	6.5	4.4	5.8	0.19	0.14	0.17	15.6	17.4	15.4	0.46	0.55	0.46	10.4	9.2	10.1	0.29	0.26	0.28
FEB	6.1	4.0	5.4	0.18	0.13	0.16	15.4	17.7	16.1	0.46	0.56	0.49	10.1	9.0	9.8	0.28	0.25	0.27
MAR	8.0	5.0	6.7	0.23	0.16	0.20	14.0	16.8	14.7	0.40	0.52	0.43	11.2	9.5	10.7	0.31	0.27	0.30
APR	12.1	8.6	10.5	0.32	0.25	0.28	10.3	14.5	11.6	0.27	0.42	0.31	13.4	11.0	12.6	0.37	0.30	0.35
MAY		12.2	14.4		0.33	0.36		11.9	8.3		0.32	0.21		12.9	14.8		0.35	0.40
JUN		15.2			0.39			9.6			0.25			14.5			0.40	
JUL		15.7			0.40			9.2			0.23			14.8			0.40	
AUG		14.8			0.38			9.6			0.25			14.3			0.39	
SEP		12.8			0.34			10.7			0.28			13.5			0.37	
OCT	13.6	11.4	13.0	0.35	0.31	0.33	9.5	12.0	9.7	0.24	0.32	0.25	14.2	12.6	14.0	0.39	0.35	0.38
NOV	10.9	9.1	10.5	0.30	0.26	0.28	11.8	13.7	11.7	0.32	0.39	0.32	12.6	11.5	12.6	0.35	0.32	0.35
DEC	8.4	6.6	8.1	0.24	0.20	0.23	13.9	15.8	13.9	0.40	0.47	0.40	11.3	10.1	11.2	0.31	0.28	0.31

NOTE: (1) The performance parameters are for a balanced flow DEC system operating with T_{REG}= 70 °C, EV_R= 95 % and EHX= 84 %.

(2) The calculations were based on average monthly climatic data at the specified times of the day (08h00, 14h00 and 20h00).

(3) Blank spaces are where ambient TDB < 16 °C or W < 6 g/kg (unlikely that cooling or dehumidification would be required).

G7 Durban (Eastern Coastal Belt and Zululand)

This region has a sub-tropical climate with summer rainfall. Dehumidification is required year round with cooling required during most of the year (see table G7.1). The recirculation mode performs significantly better than the ventilation mode (see table G7.2). The recirculation mode has a relatively low minimum COP of 0.20 and the ventilation mode provides little or no cooling in summer. The best strategy would be to operate in the recirculation mode, although a second DEC unit could be used to cool the ventilation air since the COP in the ventilation credit mode is generally high (maximum COP of 0.78).

TABLE G7.1: DURBAN average monthly weather conditions (Weather Bureau, 1997).

MONTH	08H00			14H00			20H00		
	TDB	RH	W	TDB	RH	W	TDB	RH	W
JAN	24.3	77	14.9	26.6	69	15.9	24.0	83	15.7
FEB	24.3	78	15.1	26.8	69	15.9	24.4	82	15.8
MAR	23.3	79	14.4	26.5	67	15.3	23.7	83	15.3
APR	20.6	79	12.2	25.1	64	13.3	21.7	82	13.4
MAY	17.3	79	9.7	23.5	59	11.3	19.0	83	11.3
JUN	13.9	77	7.6	22.1	52	9.3	16.4	80	9.3
JUL	13.7	78	7.6	21.7	53	9.4	16.5	80	9.3
AUG	16.0	78	8.8	21.9	59	10.1	18.1	80	10.4
SEP	18.8	77	10.4	22.1	65	11.3	19.3	82	11.4
OCT	20.4	74	11.3	22.6	68	12.0	20.0	82	12.1
NOV	21.9	74	12.5	23.8	69	13.3	21.3	83	13.2
DEC	23.6	74	14.0	25.6	68	14.7	22.9	82	14.7

Note: (1) Elevation: 8 m (2) Weather office no.: 02408088

(3) Zone: E (Eastern Coastal belt and Zululand)

(4) Climate: Subtropical Summer rain

(5) Room conditions: TDB= 23 °C, RH= 50 %, W= 8.8 g/kg

TABLE G7.2: DEC simulated performance parameters for DURBAN

Month	Ventilation mode						Ventilation credit mode						Recirculation mode					
	CC (kW/kg)			COP			CC (kW/kg)			COP			CC (kW/kg)			COP		
	08	14	20	08	14	20	08	14	20	08	14	20	08	14	20	08	14	20
JAN	1.7	-1.0	0.8	0.06	-0.03	0.03	18.6	20.8	19.3	0.61	0.73	0.64	8.2	7.0	7.9	0.23	0.20	0.22
FEB	1.7	-1.0	-0.7	0.06	-0.03	-0.02	18.6	20.8	18.6	0.61	0.73	0.63	8.2	7.0	7.9	0.23	0.20	0.22
MAR	3.3	0.5	1.4	0.10	0.02	0.05	17.8	20.6	18.6	0.57	0.72	0.61	8.8	7.6	8.2	0.25	0.21	0.23
APR	7.9	4.4	5.3	0.23	0.14	0.16	14.3	18.0	15.7	0.41	0.58	0.47	11.1	9.1	10.0	0.31	0.25	0.28
MAY	12.9	8.6	9.8	0.33	0.25	0.27	9.3	15.4	12.1	0.24	0.46	0.33	14.1	10.8	12.5	0.39	0.30	0.34
JUN		12.0	13.9		0.33	0.35		12.3	8.5		0.34	0.21		12.8	14.8		0.35	0.41
JUL		12.0	13.9		0.33	0.35		12.3	8.5		0.34	0.21		12.8	14.8		0.35	0.41
AUG	14.9	10.9	11.6	0.37	0.31	0.31	7.8	13.0	10.6	0.19	0.37	0.28	15.4	12.2	13.3	0.42	0.34	0.37
SEP	11.4	8.9	9.5	0.31	0.26	0.26	11.2	14.3	12.4	0.30	0.42	0.34	13.0	11.4	12.2	0.36	0.32	0.34
OCT	9.5	7.6	8.3	0.27	0.23	0.24	13.2	15.4	13.6	0.37	0.46	0.39	11.9	10.8	11.4	0.33	0.30	0.32
NOV	7.0	4.9	5.9	0.21	0.15	0.18	15.3	17.2	15.4	0.45	0.54	0.46	10.5	9.7	10.3	0.29	0.27	0.29
DEC	4.0	2.0	2.7	0.13	0.07	0.09	17.8	19.6	17.6	0.56	0.66	0.56	9.1	8.2	8.8	0.25	0.23	0.25

NOTE: (1) The performance parameters are for a balanced flow DEC system operating with T_{REG}=70 °C, EV_R= 95 % and EHX= 84 %.

(2) The calculations were based on average monthly climatic data at the specified times of the day (08h00, 14h00 and 20h00).

(3) Blank spaces are where ambient TDB < 16 °C or W < 6 g/kg (unlikely that cooling or dehumidification would be required).

G8 Ladysmith (Drakensberg Escarpment)

This region has a warm climate with summer rainfall (see table G8.1). The recirculation mode generally performs the best (minimum COP=0.30) with the ventilation credit mode performing better in summer (see table G8.2). The best strategy would be to operate in the recirculation mode.

TABLE G8.1: LADYSMITH average monthly weather conditions (Weather Bureau, 1997).

MONTH	08H00			14H00			20H00		
	TDB	RH	W	TDB	RH	W	TDB	RH	W
JAN	20.6	81	13.4	28.1	48	13.1	22.0	71	13.2
FEB	19.6	84	13.3	27.4	46	13.1	22.0	67	13.2
MAR	18.0	86	12.4	26.4	44	12.1	20.7	65	11.9
APR	14.2	88	9.9	24.3	37	9.7	18.0	55	9.1
MAY	9.7	83	7.0	21.9	30	7.3	14.5	50	6.8
JUN	5.0	84	5.0	19.4	29	6.0	11.3	47	5.4
JUL	5.5	78	4.9	19.7	28	6.3	12.4	44	5.4
AUG	9.5	75	6.0	21.6	31	6.2	14.5	47	6.2
SEP	13.9	74	8.1	24.1	35	7.5	17.3	52	7.7
OCT	16.6	76	9.7	25.0	41	9.1	18.5	61	9.5
NOV	18.6	76	11.2	26.0	46	10.8	19.7	66	10.9
DEC	20.2	76	12.5	27.9	44	12.2	21.4	66	12.2

Note: (1) Elevation: 1078 m (2) Weather office no.: 0300454B2

(3) Zone: D (Drakensberg Escarpment)

(4) Climate: Warm. Summer rain.

(5) Room conditions: TDB= 23 °C, RH= 50 %, W = 9.0 g/kg

TABLE G8.2: DEC simulated performance parameters for LADYSMITH

Month	Ventilation mode						Ventilation credit mode						Recirculation mode					
	CC (kW/kg)			COP			CC (kW/kg)			COP			CC (kW/kg)			COP		
	08	14	20	08	14	20	08	14	20	08	14	20	08	14	20	08	14	20
JAN	9.2	6.9	9.0	0.27	0.23	0.27	15.4	20.0	16.1	0.45	0.67	0.48	12.5	10.4	12.2	0.35	0.30	0.35
FEB	9.8	7.0	9.0	0.28	0.23	0.27	14.7	19.4	16.1	0.43	0.64	0.48	12.8	10.4	12.2	0.36	0.30	0.35
MAR	11.8	9.1	11.5	0.33	0.29	0.33	12.8	17.9	14.0	0.35	0.56	0.40	13.9	11.3	13.4	0.39	0.32	0.38
APR		14.0	17.2		0.40	0.44		14.6	9.8		0.42	0.25		13.7	16.2		0.39	0.45
MAY		18.7			0.49			10.7			0.28			16.2			0.45	
JUN		21.7			0.53			7.9			0.19			18.1			0.50	
JUL		21.0			0.52			8.2			0.20			17.8			0.49	
AUG		20.7			0.52			9.6			0.24			17.0			0.47	
SEP		17.5	19.7		0.47	0.48		12.3	8.0		0.33	0.20		15.4	17.5		0.43	0.49
OCT	16.7	14.6	16.2	0.42	0.42	0.42	9.4	14.4	10.4	0.24	0.41	0.27	16.2	14.0	15.6	0.45	0.39	0.44
NOV	13.4	11.6	13.5	0.36	0.35	0.37	11.9	16.7	12.4	0.32	0.50	0.34	14.5	12.5	14.2	0.41	0.35	0.40
DEC	10.9	8.4	10.9	0.31	0.27	0.32	14.4	19.1	14.9	0.41	0.62	0.43	13.0	11.0	12.8	0.37	0.31	0.36

NOTE: (1) The performance parameters are for a balanced flow DEC system operating with T_{REG}=70 °C, EV_R= 95 % and EHX= 84 %.

(2) The calculations were based on average monthly climatic data at the specified times of the day (08h00, 14h00 and 20h00).

(3) Blank spaces are where ambient TDB < 16 °C or W < 5 g/kg (unlikely that cooling or dehumidification would be required).

G9 Phalaborwa (Lowveld)

This region has a hot climate with summer rainfall (see table G9.1). Cooling is required year round and dehumidification is required for most of the year. The observations and recommendations are the same as for Durban. The ventilation mode provides little cooling in summer and very high regenerating temperatures would be required to increase the cooling capacity. The recirculation mode performs best with a minimum COP of 0.20, which is also relatively low. The ventilation credit mode has a maximum COP of 0.86 (see table G9.2). Evaporative cooling could be used alone during the winter months, since it is relatively dry but still hot during these months.

TABLE G9.1: PHALABORWA average monthly weather conditions (Weather Bureau, 1997).

MONTH	08H00			14H00			20H00		
	TDB	RH	W	TDB	RH	W	TDB	RH	W
JAN	23.7	82	15.5	30.5	51	15.1	26.7	63	15.1
FEB	23.1	85	15.4	29.8	52	14.9	26.0	65	14.8
MAR	22.2	86	14.8	29.3	50	14.4	25.1	64	14.3
APR	19.8	87	12.7	27.6	49	12.5	22.4	66	12.3
MAY	16.5	85	10.0	26.3	42	10.3	19.5	62	9.8
JUN	13.2	82	7.9	24.0	39	8.4	17.0	58	7.9
JUL	13.1	82	7.8	23.9	39	8.2	17.1	56	7.8
AUG	15.6	79	8.8	25.5	41	9.0	19.5	53	8.5
SEP	18.7	77	10.5	27.5	42	10.6	22.2	52	9.9
OCT	20.7	76	11.8	28.1	46	11.7	23.7	55	11.3
NOV	22.1	77	13.3	28.9	50	13.4	24.8	61	13.1
DEC	23.3	79	14.5	29.8	51	14.5	25.9	63	14.2

Note: (1) Elevation: 427 m (2) Weather office no.: 0681266C7

(3) Zone: L (Lowveld) (4) Climate: Hot Steppe. Summer rain.

(5) Room conditions: TDB= 23 °C, RH= 50 %, W= 9.2 g/kg

TABLE G9.2: DEC simulated performance parameters for PHALABORWA

Month	Ventilation mode						Ventilation credit mode						Recirculation mode					
	CC (kW/kg)			COP			CC (kW/kg)			COP			CC (kW/kg)			COP		
	08	14	20	08	14	20	08	14	20	08	14	20	08	14	20	08	14	20
JAN	2.3	0.2	1.7	0.08	0.01	0.06	19.0	22.9	20.5	0.63	0.86	0.71	8.9	7.1	8.0	0.25	0.20	0.23
FEB	2.3	0.8	2.7	0.09	0.03	0.09	18.8	22.4	20.0	0.61	0.82	0.68	8.9	7.4	8.6	0.25	0.21	0.24
MAR	4.0	2.0	3.8	0.13	0.07	0.12	17.4	21.7	18.9	0.55	0.77	0.62	9.5	7.7	8.9	0.27	0.22	0.25
APR	8.5	5.9	8.2	0.24	0.19	0.24	14.1	19.1	15.5	0.40	0.62	0.46	11.8	9.5	11.2	0.33	0.27	0.31
MAY	14.1	10.1	13.4	0.36	0.30	0.36	9.4	16.3	11.3	0.24	0.49	0.30	14.8	11.3	13.7	0.41	0.31	0.38
JUN		14.1	17.2		0.39	0.42		13.1	7.7		0.36	0.19		13.2	16.1		0.37	0.44
JUL		14.5	17.4		0.40	0.43		12.9	7.9		0.35	0.19		13.5	16.1		0.37	0.44
AUG		12.4	15.4		0.36	0.40		14.5	10.0		0.42	0.26		12.4	14.8		0.34	0.41
SEP	12.5	9.1	12.3	0.33	0.28	0.34	11.4	17.3	13.2	0.30	0.53	0.37	13.5	10.7	12.9	0.37	0.30	0.36
OCT	9.6	6.9	9.2	0.27	0.22	0.27	13.8	18.5	15.3	0.39	0.59	0.45	12.1	9.8	11.3	0.34	0.27	0.31
NOV	6.6	3.8	5.9	0.20	0.13	0.19	16.1	20.5	17.7	0.49	0.70	0.56	10.6	8.6	9.8	0.30	0.24	0.27
DEC	4.2	1.4	3.6	0.14	0.05	0.12	18.0	21.9	19.3	0.57	0.79	0.64	9.5	7.7	8.9	0.27	0.22	0.25

NOTE: (1) The performance parameters are for a balanced flow DEC system operating with T_{REG}= 70 °C, EV_R= 95 % and EHX= 84 %.

(2) The calculations were based on average monthly climatic data at the specified times of the day (08h00, 14h00 and 20h00).

(3) Blank spaces are where ambient TDB < 16°C or W < 6 g/kg (unlikely that cooling or dehumidification would be required).

G10 Pietersburg (Northern Transvaal)

This region has a hot climate with summer rainfall. Cooling and dehumidification are required during the six months around summer (see table G10.1). The recirculation mode (minimum COP=0.32) performs better than the ventilation mode (minimum COP=0.26) although the difference in performance is small (see table G10.2). The ventilation credit mode performs better in the summer months with a maximum COP of 0.61. The best strategy would be to operate in the recirculation mode although the ventilation mode is acceptable if more ventilation air is required.

TABLE G10.1: PIETERSBURG average monthly weather conditions (Weather Bureau, 1997).

MONTH	08H00			14H00			20H00		
	TDB	RH	W	TDB	RH	W	TDB	RH	W
JAN	20.2	77	13.4	26.5	48	12.9	22.7	64	13.4
FEB	19.5	80	13.2	26.1	49	12.8	22.1	67	13.3
MAR	18.2	82	12.5	25.3	47	11.9	20.7	68	12.4
APR	15.1	85	10.5	23.4	45	9.9	18.0	67	10.5
MAY	11.1	82	7.8	21.6	38	7.8	14.9	60	7.9
JUN	7.5	80	5.9	18.9	35	6.2	11.9	54	6.2
JUL	7.3	79	5.7	19.1	33	6.0	12.3	51	5.9
AUG	10.2	75	6.7	21.2	33	6.8	15.0	48	6.6
SEP	14.7	69	8.3	24.1	34	7.9	18.3	48	7.9
OCT	17.6	69	9.9	24.8	41	9.6	19.9	55	9.8
NOV	19.0	72	11.4	25.1	46	11.2	20.8	62	11.5
DEC	20.0	74	12.5	25.9	48	12.2	21.9	64	12.7

Note: (1) Elevation: 1230 m (2) Weather office no.: 0677802A5

(3) Zone: NT (Northern Transvaal) (4) Climate: Hot steppe. Summer rain.

(5) Room conditions: TDB= 23 °C, RH= 50 %, W= 10.1 g/kg

TABLE G10.2: DEC simulated performance parameters for PIETERSBURG

Month	Ventilation mode						Ventilation credit mode						Recirculation mode					
	CC (kW/kg)			COP			CC (kW/kg)			COP			CC (kW/kg)			COP		
	08	14	20	08	14	20	08	14	20	08	14	20	08	14	20	08	14	20
JAN	9.7	8.1	8.7	0.28	0.26	0.27	15.2	18.8	16.8	0.44	0.61	0.51	12.9	11.1	12.0	0.36	0.32	0.34
FEB	10.4	8.3	9.1	0.30	0.27	0.27	14.7	18.4	16.3	0.42	0.59	0.49	13.2	11.4	12.3	0.37	0.33	0.35
MAR	11.9	10.4	11.2	0.33	0.32	0.32	13.0	17.3	14.7	0.36	0.53	0.42	14.0	12.0	13.2	0.40	0.34	0.37
APR		14.3	15.3		0.40	0.40		14.2	11.2		0.40	0.29		14.1	15.5		0.40	0.43
MAY		18.2			0.48			11.0			0.29			16.1			0.45	
JUN		21.7			0.53			7.6			0.19			18.2			0.51	
JUL		22.1			0.54			7.7			0.19			18.5			0.51	
AUG		20.0			0.51			9.8			0.25			16.9			0.47	
SEP		17.2	19.4		0.47	0.48		12.7	9.0		0.35	0.22		15.2	17.1		0.43	0.48
OCT	16.3	14.3	15.6	0.42	0.41	0.42	10.2	14.9	11.7	0.26	0.43	0.31	16.0	13.8	15.2	0.45	0.39	0.43
NOV	13.5	11.5	12.5	0.37	0.34	0.35	12.7	16.4	13.8	0.35	0.49	0.39	14.4	12.6	13.8	0.40	0.36	0.39
DEC	11.3	9.6	10.3	0.32	0.30	0.30	14.3	17.9	15.8	0.41	0.56	0.47	13.5	11.7	12.6	0.38	0.33	0.36

NOTE: (1) The performance parameters are for a balanced flow DEC system operating with T_{REG}= 70 °C, EV_R= 95 % and EHX= 84 %.

(2) The calculations were based on average monthly climatic data at the specified times of the day (08h00, 14h00 and 20h00).

(3) Blank spaces are where ambient TDB < 16 °C or W < 6 g/kg (unlikely that cooling or dehumidification would be required).

G11 Johannesburg (Highveld)

This region has a warm climate with summer rain. Cooling and dehumidification are only required in summer (see table 11.1). The recirculation mode (minimum COP=0.40) performs better than the ventilation mode (minimum COP=0.35) although the difference in performance is small (see table 11.2). The ventilation credit mode performs only marginally better in the summer months with a maximum COP of 0.50. The best strategy would be to operate in the recirculation mode although the ventilation mode is acceptable if more ventilation air is required.

TABLE G11.1: JOHANNESBURG average monthly weather conditions (Weather Bureau, 1997).

MONTH	08H00			14H00			20H00		
	TDB	RH	W	TDB	RH	W	TDB	RH	W
JAN	17.9	78	12.4	24.1	50	12.3	19.9	65	12.0
FEB	17.1	80	12.1	23.6	50	11.9	19.4	65	11.7
MAR	16.0	80	11.3	22.8	48	10.9	18.3	63	10.8
APR	13.3	79	9.2	20.1	46	9.0	15.3	61	8.8
MAY	10.3	71	6.8	18.1	37	6.6	12.4	51	6.4
JUN	6.7	70	5.3	15.3	34	5.2	9.4	47	5.1
JUL	6.8	68	5.2	15.9	31	5.0	9.9	42	4.8
AUG	9.5	64	5.7	18.5	28	5.5	12.7	38	5.2
SEP	13.3	62	7.1	21.9	29	6.6	16.4	38	6.5
OCT	15.4	67	8.7	22.6	38	8.5	17.6	50	8.1
NOV	16.7	73	10.4	22.8	46	10.3	18.3	62	10.1
DEC	17.7	74	11.4	23.8	47	11.5	19.2	61	11.0

Note: (1) Elevation: 1694 m (2) Weather office no.: 04763990

(3) Zone: H (Highveld) (4) Climate: Warm. Summer rain.

(5) Room conditions: TDB= 23 °C, RH= 50 %, W= 10.8 g/kg

TABLE G11.2: DEC simulated performance parameters for JOHANNESBURG

Month	Ventilation mode						Ventilation credit mode						Recirculation mode					
	CC (kW/kg)			COP			CC (kW/kg)			COP			CC (kW/kg)			COP		
	08	14	20	08	14	20	08	14	20	08	14	20	08	14	20	08	14	20
JAN	14.1	11.7	13.9	0.39	0.35	0.39	12.9	16.6	13.8	0.35	0.50	0.39	15.6	13.8	15.0	0.45	0.40	0.43
FEB	14.8	12.8	14.7	0.40	0.38	0.41	12.0	16.2	13.3	0.32	0.48	0.37	15.9	14.1	15.6	0.46	0.41	0.45
MAR	16.4	14.6	16.5	0.43	0.42	0.44	10.5	14.6	11.6	0.27	0.42	0.31	16.7	15.0	16.4	0.48	0.43	0.47
APR		18.7			0.49			11.1			0.29			17.0			0.43	
MAY		23.3			0.56			7.6			0.18			19.5			0.55	
JUN																		
JUL																		
AUG																		
SEP		21.9	24.0		0.56	0.57		10.2	6.4		0.26	0.15		18.2	20.3		0.52	0.58
OCT		18.6	21.0		0.50	0.52		12.3	8.6		0.33	0.21		16.7	18.7		0.48	0.53
NOV	17.7	15.7	17.7	0.46	0.44	0.46	10.2	14.2	10.8	0.26	0.40	0.28	17.3	15.3	17.0	0.50	0.44	0.49
DEC	15.8	13.6	15.7	0.42	0.40	0.42	11.8	15.7	12.3	0.32	0.46	0.33	16.2	14.4	15.9	0.46	0.42	0.46

NOTE: (1) The performance parameters are for a balanced flow DEC system operating with T_{REG}= 70 °C, EV_R= 95 % and EHX= 84 %.

(2) The calculations were based on average monthly climatic data at the specified times of the day (08h00, 14h00 and 20h00).

(3) Blank spaces are where ambient TDB < 16 °C or W < 6 g/kg (unlikely that cooling or dehumidification would be required).

G12 Bloemfontein (Northern Steppe)

This region has a moderate climate that can become very cold in winter. Cooling and dehumidification are only required in summer although cooling is also required during the middle of the day in spring (see table 12.1). The ventilation mode (minimum COP=0.34) generally has marginally better performance than the recirculation mode (minimum COP=0.34). The ventilation credit mode has the best performance in summer with maximum COP of 0.59 (see table 12.1). The best strategy would be to use the ventilation mode. Alternatively the recirculation mode would also be acceptable.

TABLE G12.1: BLOEMFONTEIN average monthly weather conditions (Weather Bureau, 1997).

MONTH	08H00			14H00			20H00		
	TDB	RH	W	TDB	RH	W	TDB	RH	W
JAN	20.7	69	11.8	29.1	35	10.5	24.0	46	10.4
FEB	18.9	77	12.0	27.3	41	11.3	22.3	55	11.2
MAR	16.3	82	10.8	25.7	41	10.4	19.8	58	10.4
APR	11.3	88	8.3	22.2	40	8.4	15.2	62	8.4
MAY	5.4	88	5.6	19.3	34	6.3	10.7	56	5.9
JUN	0.9	88	4.4	16.1	33	5.2	7.0	54	4.7
JUL	0.6	85	4.4	16.7	29	4.9	7.5	45	4.3
AUG	4.0	77	4.5	19.1	27	5.0	10.8	38	4.6
SEP	10.8	66	6.0	23.0	26	6.0	15.6	35	5.7
OCT	15.4	64	8.0	24.8	29	7.3	18.3	41	7.1
NOV	18.5	64	9.6	26.7	31	8.3	20.7	43	8.3
DEC	20.3	64	10.8	28.5	30	9.2	23.0	41	9.1

Note: (1) Elevation: 1351 m (2) Weather office no.: 02615161

(3) Zone: SN (Northern Steppe) (4) Climate: Steppe. Summer rain.

(5) Room conditions: TDB= 23 °C, RH= 50 %, W= 10.2 g/kg

TABLE G12.2: DEC simulated performance parameters for BLOEMFONTEIN

Month	Ventilation mode						Ventilation credi. mode						Recirculation mode					
	CC (kW/kg)			COP			CC (kW/kg)			COP			CC (kW/kg)			COP		
	08	14	20	08	14	20	08	14	20	08	14	20	08	14	20	08	14	20
JAN	12.6	11.5	13.6	0.36	0.36	0.39	14.3	18.5	15.1	0.40	0.59	0.44	13.8	12.1	13.9	0.39	0.35	0.39
FEB	12.7	10.8	12.8	0.35	0.34	0.37	13.1	18.0	14.7	0.36	0.56	0.42	14.4	12.1	13.8	0.41	0.34	0.39
MAR	15.7	12.8	15.2	0.41	0.38	0.41	10.4	16.1	12.4	0.27	0.48	0.33	16.1	13.3	15.0	0.45	0.38	0.42
APR		17.5			0.47			12.1			0.32			15.8			0.45	
MAY		21.8			0.53			8.1			0.20			18.3			0.51	
JUN																		
JUL																		
AUG																		
SEP		21.2			0.54			10.6			0.27			17.2			0.48	
OCT		18.5	20.9		0.50	0.51		12.9	8.3		35	0.20		15.6	18.0		0.44	0.50
NOV	15.8	16.0	18.2	0.44	0.46	0.47	10.7	14.9	11.0	0.28	0.43	0.29	16.1	14.2	16.4	0.45	0.40	0.46
DEC	14.2	14.1	16.1	0.39	0.43	0.44	12.9	17.1	13.3	0.36	0.52	0.37	14.7	13.3	15.0	0.41	0.38	0.42

NOTE: (1) The performance parameters are for a balanced flow DEC system operating with T_{RLG}= 70 °C, EV_R= 95 % and EHX= 84 %.

(2) The calculations were based on average monthly climatic data at the specified times of the day (08h00, 14h00 and 20h00).

(3) Blank spaces are where ambient TDB < 16 °C or W < 6 g/kg (unlikely that cooling or dehumidification would be required).

G13 Queenstown (Southern Steppe)

This region has a moderate climate with autumn rainfall (see table 13.1). The recirculation mode (minimum COP=0.33) is marginally better in summer but the ventilation mode (minimum COP=0.30) is better in winter, when air conditioning is not required (see table 13.2). The performance of the ventilation credit mode is high in summer (maximum COP=0.56). The best strategy would be to use either the recirculation or ventilation modes, depending on ventilation requirements.

TABLE G13.1: QUEENSTOWN average monthly weather conditions (Weather Bureau, 1997).

MONTH	08H00			14H00			20H00		
	TDB	RH	W	TDB	RH	W	TDB	RH	W
JAN	18.4	80	11.7	27.5	44	11.3	20.5	72	12.1
FEB	17.3	85	11.8	26.6	47	11.8	20.6	72	12.5
MAR	15.6	86	11.1	25.0	48	11.0	19.2	71	11.4
APR	11.5	87	8.3	22.2	44	9.0	16.1	66	9.0
MAY	7.7	83	5.9	19.5	42	6.9	13.3	59	6.8
JUN	5.1	79	4.7	17.0	40	5.9	10.8	55	5.7
JUL	5.0	74	4.4	17.3	36	5.6	11.5	48	5.3
AUG	7.1	74	5.0	18.9	35	5.7	13.3	48	5.7
SEP	10.5	79	6.7	21.3	38	6.8	15.4	57	7.1
OCT	13.3	80	8.2	22.6	43	8.1	16.1	66	8.6
NOV	15.5	80	9.6	24.5	43	9.2	17.6	72	10.2
DEC	17.6	78	10.7	26.8	42	10.3	19.6	71	11.3

Note: (1) Elevation: 1094 m (2) Weather office no.: 0123654AO

(3) Zone: SS (Southern Steppe) (4) Climate: Cold steppe. Autumn rain.

(5) Room conditions: TDB= 23 °C, RH= 50 %, W= 10.0 g/kg

TABLE G13.2: DEC simulated performance parameters for QUEENSTOWN

Month	Ventilation mode						Ventilation credit mode						Recirculation mode					
	CC (kW/kg)			COP			CC (kW/kg)			COP			CC (kW/kg)			COP		
	08	14	20	08	14	20	08	14	20	08	14	20	08	14	20	08	14	20
JAN	12.9	10.1	11.3	0.35	0.32	0.32	12.5	18.0	14.0	0.34	0.56	0.40	14.2	11.7	13.4	0.40	0.33	0.38
FEB	13.0	9.4	10.7	0.35	0.30	0.31	11.7	17.7	14.6	0.31	0.55	0.42	14.5	11.7	13.1	0.41	0.33	0.37
MAR		11.5	13.1		0.34	0.36		16.1	12.8		0.48	0.35		12.6	14.2		0.36	0.40
APR		15.8	18.0		0.43	0.45		12.5	8.4		0.34	0.21		14.8	17.0		0.42	0.47
MAY		20.3			0.50			8.8			0.22			17.3			0.48	
JUN																		
JUL																		
AUG																		
SEP		19.8			0.50			9.9			0.25			16.8			0.47	
OCT		17.1	18.6		0.46	0.46		11.9	8.0		0.32	0.20		15.4	17.3		0.43	0.48
NOV		14.6	15.4		0.41	0.40		14.1	10.4		0.40	0.27		14.0	15.6		0.39	0.44
DEC	14.8	12.1	13.0	0.39	0.37	0.36	11.1	16.8	12.8	0.29	0.51	0.35	15.1	12.6	14.0	0.42	0.36	0.39

NOTE: (1) The performance parameters are for a balanced flow DEC system operating with T_{REG}=70 °C, EV_R= 95 % and EHX= 84 %.

(2) The calculations were based on average monthly climatic data at the specified times of the day (08h00, 14h00 and 20h00).

(3) Blank spaces are where ambient TDB < 16°C or W < 6 g/kg (unlikely that cooling or dehumidification would be required).

G14 Beaufort West (Karoo)

This region has a desert climate and is generally dry and hot (see table 14.1). The ventilation mode (minimum COP=0.36) performs better than the recirculation mode (minimum COP=0.33). The ventilation credit mode (maximum COP=0.53) performs only slightly better than the ventilation mode during the middle of the day in summer (see table 14.2). The best strategy would be to use only evaporative cooling, since the average humidity ratio is almost always below that in the room and evaporative cooling can supply all sensible cooling needs. Alternatively, if the room latent loads are high then the ventilation mode can be used.

TABLE G14.1: BEAUFORT WEST average monthly weather conditions (Weather Bureau, 1997).

MONTH	08H00			14H00			20H00		
	TDB	RH	W	TDB	RH	W	TDB	RH	W
JAN	9.3	67	10.0	29.8	26	8.6	27.4	27	8.0
FEB	18.7	69	10.1	29.2	29	9.3	26.2	34	9.1
MAR	16.5	74	9.3	26.9	33	8.9	23.5	38	8.6
APR	13.0	70	7.1	23.6	32	7.3	18.8	42	7.1
MAY	10.1	65	5.2	20.8	29	5.9	14.6	42	5.5
JUN	7.8	65	4.6	17.6	33	5.1	12.2	46	5.0
JUL	6.5	65	4.0	17.1	32	4.8	11.6	44	4.5
AUG	8.0	65	4.4	18.7	31	4.8	13.0	40	4.6
SEP	11.2	68	5.8	21.6	29	5.6	16.1	41	5.8
OCT	14.5	68	7.2	23.9	31	6.7	19.2	39	6.4
NOV	16.8	66	8.2	26.2	29	7.3	21.9	35	6.9
DEC	18.7	64	9.2	28.7	26	7.8	25.5	31	7.4

Note: (1) Elevation: 842 m (2) Weather office no.: 00921716

(3) Zone: K (Karoo) (4) Climate: Desert

(5) Room conditions: TDB= 23 °C, RH= 50 %, W= 9.6 g/kg

TABLE G14.2: DEC simulated performance parameters for BEAUFORT WEST

Month	Ventilation mode						Ventilation credit mode						Recirculation mode					
	CC (kW/kg)			COP			CC (kW/kg)			COP			CC (kW/kg)			COP		
	08	14	20	08	14	20	08	14	20	08	14	20	08	14	20	08	14	20
JAN	14.1	12.8	14.8	0.38	0.39	0.43	11.4	17.2	15.2	0.30	0.52	0.44	14.4	12.2	13.3	0.40	0.34	0.37
FEB	14.2	11.7	13.3	0.37	0.36	0.39	11.0	17.3	15.3	0.29	0.53	0.44	14.7	11.9	12.8	0.41	0.33	0.36
MAR	16.3	13.4	15.0	0.41	0.39	0.41	8.9	15.6	12.9	0.22	0.46	0.36	16.0	12.8	14.1	0.44	0.36	0.39
APR		17.2	19.1		0.46	0.47		12.0	8.4		0.32	0.21		15.0	16.8		0.42	0.46
MAY																		
JUN																		
JUL																		
AUG																		
SEP																		
OCT		18.1	20.1		0.48	0.49		11.6	8.1		0.31	0.20		15.3	17.1		0.42	0.47
NOV	17.9	16.2	18.4	0.44	0.45	0.48	8.1	13.6	10.4	0.20	0.38	0.27	16.8	14.2	15.8	0.46	0.39	0.44
DEC	15.7	14.6	16.2	0.41	0.43	0.45	10.3	15.8	13.1	0.27	0.46	0.36	15.2	12.8	14.2	0.42	0.36	0.39

NOTE: (1) The performance parameters are for a balanced flow DEC system operating with T_{REG}= 70 °C, EV_R= 95 % and εHX= 84 %.

(2) The calculations were based on average monthly climatic data at the specified times of the day (08h00, 14h00 and 20h00).

(3) Blank spaces are where ambient TDB < 16 °C or W < 6 g/kg (unlikely that cooling or dehumidification would be required).

APPENDIX H1
AIR LEAKAGE RESULTS

The results given in this appendix are from air leakage tests with both inspection doors open. These results are similar to those with both inspection doors closed which are given in section 6.1 (since that specific case is relevant to normal operating conditions and the experimental tests in appendices H3 to H6).

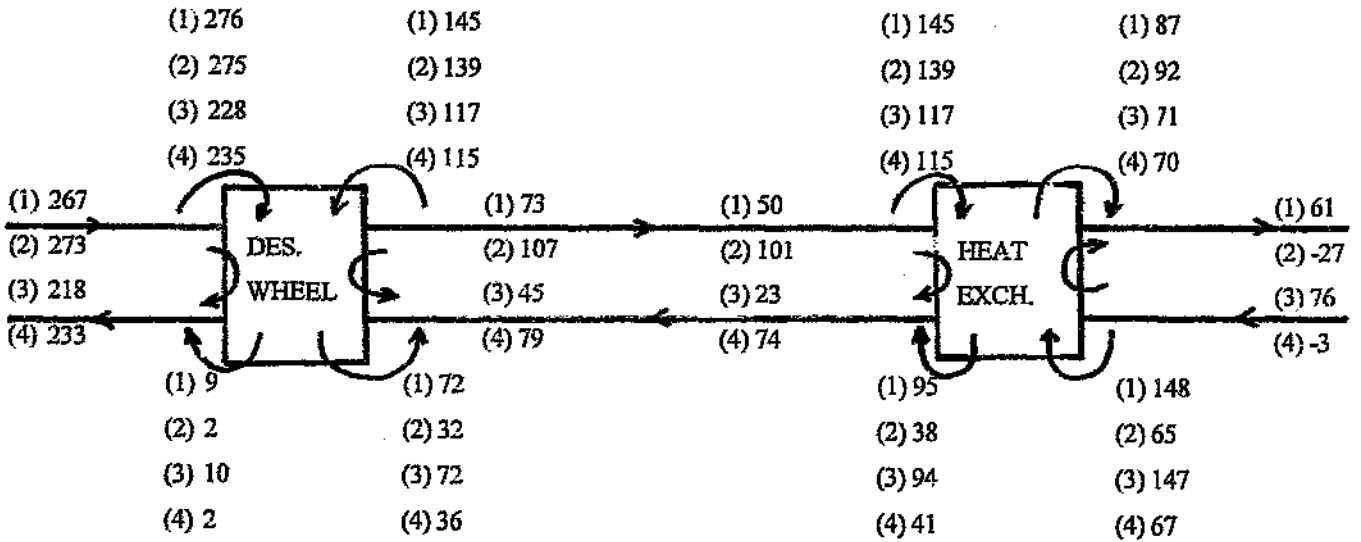

(1)= MAX SF & MAX RF
(2)= MAX SF & MIN RF
(3.= MIN SF & MAX RF
(4)= MIN SF & MIN RF

SF = supply air flow rate
RF = return air flow rate

Note: 1) values are shown for both inspection doors open. See figure 6.1.3 for values with both doors closed.

2) Positive differential pressure is in direction of arrows shown.

FIGURE H1.1: Differential pressure at various air flow rate combinations (calculated from fig. 6.1.2).

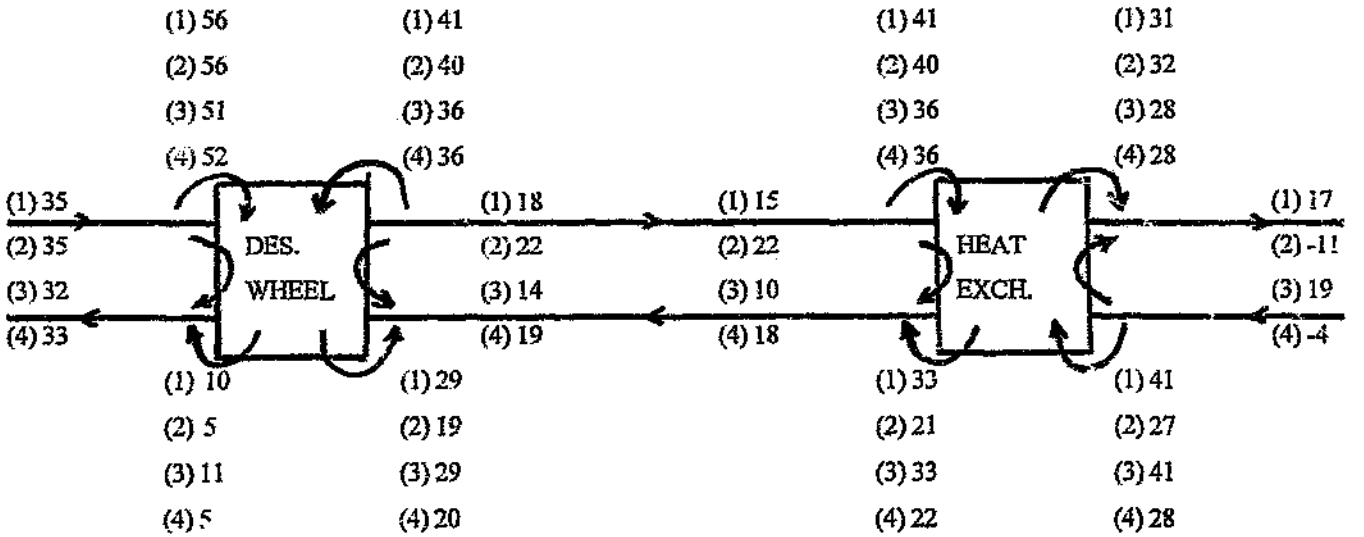

(1)= MAX SF & MAX RF
(2)= MAX SF & MIN RF
(3)= MIN SF & MAX RF
(4)= MIN SF & MIN RF

SF = supply air flow rate
RF = return air flow rate

Note: 1) values are shown for both inspection doors open. See figure 6.1.4 for values with both doors closed.

2) Positive leakage airflow is in direction of arrows.

FIGURE H1.2: Leakage air flow rate at various air flow rate combinations (calculated from fig. H1.1).

TABLE H1.1: Estimated supply and return air flow rates at desiccant wheel (with both inspection doors open).

FLOW COMBINATION		SF (litres/s)				RF (litres/s)			
		in-let	leak out	leak in	Out-let	in-let	leak out	Leak in	out-let
1	MAX SF & MAX RF	450	150	0	300	150	39	53	164
2	MAX SF & MIN RF	480	153	0	327	53	24	57	86
3	MIN SF & MAX RF	428	133	0	295	140	40	46	146
4	MIN SF & MIN RF	448	140	0	308	34	25	52	61

SF = supply air flow rate
RF = return air flow rate

TABLE H1.2: Estimated supply and return air flow rates at heat exchanger (with both inspection doors open).

FLOW COMBINATION		SF (litres/s)				RF (litres/s)			
		in-let	leak out	leak in	out-let	in-let	leak out	leak in	out-let
1	MAX SF & MAX RF	300	104	17	213	226	91	15	150
2	MAX SF & MIN RF	327	105	0	222	68	48	33	53
3	MIN SF & MAX RF	295	74	19	221	223	93	10	140
4	MIN SF & MIN RF	308	86	0	222	52	40	22	34

SF = supply air flow rate
RF = return air flow rate

APPENDIX H2

REGENERATION AND DEHUMIDIFICATION SINGLE BLOW TESTS

The results given in this appendix are the computer printouts from the regeneration and dehumidification single blow tests. These results are presented in graphical form in section 6.2.

TEST NUMBER: H2/1

RESULTS OF REGENERATION SINGLE BLOW TEST
****
DATE (d,m,y): 16- 5-1997
TIME (h,m) : 16-42

supply air flow rate (kg/s): 0.158

TIME (s)	W9-W8 (g/kg)	MW (g/s)	TDB[9] (oC)	W[9] (g/kg)	RH[9] (%)	TDB[8] (oC)	W[8] (g/kg)	RH[8] (%)
9	2.44	0.39	39.1	8.75	16.3	56.1	6.31	5.0
21	2.52	0.40	38.8	8.82	16.7	57.1	6.31	4.8
32	2.63	0.42	38.7	8.90	16.9	57.5	6.26	4.6
43	2.80	0.44	38.7	8.99	17.1	57.6	6.19	4.6
54	2.85	0.45	38.9	9.03	17.0	57.6	6.18	4.6
65	2.79	0.44	39.1	8.97	16.7	57.5	6.18	4.6
77	2.71	0.43	39.3	8.89	16.3	57.3	6.18	4.6
89	2.67	0.42	39.5	8.84	16.1	57.0	6.17	4.7
101	2.64	0.42	39.7	8.75	15.7	56.9	6.10	4.7
112	2.60	0.41	39.8	8.73	15.6	56.8	6.13	4.7
123	2.58	0.41	39.9	8.69	15.5	56.7	6.11	4.7
134	2.55	0.40	40.0	8.64	15.3	56.6	6.09	4.7
145	2.54	0.40	40.1	8.64	15.3	56.5	6.09	4.7
157	2.53	0.40	40.1	8.64	15.3	56.4	6.10	4.8
168	2.48	0.39	40.1	8.57	15.1	56.3	6.08	4.8

TEST NUMBER: H2/2

RESULTS OF REGENERATION SINGLE BLOW TEST
****
DATE (d,m,y): 16- 5-1997
TIME (h,m) : 16-19

supply air flow rate (kg/s): 0.158

TIME (s)	W9-W8 (g/kg)	MW (g/s)	TDB[9] (oC)	W[9] (g/kg)	RH[9] (%)	TDB[8] (oC)	W[8] (g/kg)	RH[8] (%)
9	4.42	0.70	48.5	10.64	12.1	77.8	6.22	1.9
20	4.98	0.79	47.5	11.21	13.4	81.5	6.23	1.6
30	5.53	0.87	46.8	11.75	14.6	83.6	6.22	1.5
40	5.93	0.94	46.4	12.12	15.3	85.0	6.19	1.4
51	6.09	0.96	46.3	12.26	15.6	85.6	6.17	1.4
62	6.14	0.97	46.5	12.31	15.5	86.4	6.18	1.3
73	6.00	0.95	46.8	12.17	15.1	86.7	6.17	1.3
83	5.77	0.91	47.4	11.93	14.4	87.0	6.16	1.3
94	5.53	0.87	47.9	11.69	13.7	87.3	6.15	1.3
105	5.36	0.85	48.5	11.51	13.1	87.5	6.16	1.3
116	5.25	0.83	49.1	11.44	12.6	87.6	6.18	1.3
128	5.12	0.81	49.7	11.30	12.1	87.6	6.17	1.3
139	4.96	0.78	50.2	11.12	11.6	87.7	6.16	1.3
150	4.97	0.79	50.6	11.13	11.4	87.6	6.16	1.3
210	4.62	0.73	52.3	10.79	10.2	87.1	6.17	1.3
241	4.65	0.73	52.7	10.79	10.0	86.7	6.14	1.3

TEST NUMBER: H2/3

RESULTS OF DEHUMIDIFIER SINGLE BLOW TEST
****
DATE (d,m,y): 19- 5-1997
TIME (h,m,s): 13-29-20

regen TDB (oC): 75.4
W (g/kg): 5.86
RH (%): 2.0

supply TDB (oC): 19.1
W (g/kg): 5.15
RH (%): 31.0

supply air flow rate (kg/s): 0.244

TIME (s)	W1-W2 (g/kg)	MW (g/s)	TDB[2] (oC)	W[2] (g/kg)	RH[2] (%)
10	-0.65	-0.16	31.9	5.80	16.1
20	-0.47	-0.12	32.8	5.62	14.9
30	-0.25	-0.06	33.2	5.40	14.0
41	0.15	0.04	33.0	5.00	13.1
51	0.48	0.12	32.4	4.67	12.7
62	0.70	0.17	31.7	4.45	12.6
71	0.80	0.19	30.9	4.35	12.8
82	0.88	0.21	30.1	4.27	13.2
92	0.86	0.21	29.4	4.29	.8
102	0.84	0.21	28.7	4.31	14.4
112	0.92	0.22	28.1	4.23	14.6
122	0.88	0.21	27.5	4.27	15.3
132	0.86	0.21	27.1	4.29	15.8
142	0.80	0.19	26.7	4.35	16.4
152	0.76	0.19	26.2	4.39	17.0
162	0.69	0.17	25.8	4.46	17.7
172	0.68	0.17	25.5	4.47	18 0
182	0.66	0.16	25.2	4.49	18.4
192	0.63	0.15	24.9	4.52	18.8
202	0.63	0.15	24.7	4.52	19.1
214	0.61	0.15	24.5	4.54	19.4
224	0.58	0.14	24.3	4.57	19.8
235	0.57	0.14	24.1	4.58	20.1
246	0.55	0.13	23.9	4.60	20.4
258	0.55	0.14	23.7	4.60	20.6
357	0.36	0.09	22.8	4.79	22.7
459	0.41	0.10	22.1	4.74	23.4

TEST NUMBER: H2/4

RESULTS OF DEHUMIDIFIER SINGLE BLOW TEST
****
DATE (d,m,y): 16- 5-1997 TIME (h,m,s): 11-17-19

regen TDB (oC): 73.6
W (g/kg): 8.50
RH (%): 3.0

supply TDB (oC): 17.0
W (g/kg): 8.00
RH (%): 53.0

supply air flow rate (kg/s): 0.240

TIME (s)	W1-W2 (g/kg)	MW (g/s)	TDB[2] (oC)	W[2] (g/kg)	RH[2] (%)
30	-0.24	-0.06	40.8	8.24	14.0
44	0.23	0.05	40.4	7.77	13.5
59	0.93	0.22	39.9	7.07	13.3
71	1.23	0.29	37.6	6.77	13.7
83	1.39	0.33	36.4	6.61	14.3
99	1.41	0.34	35.0	6.59	15.4
112	1.43	0.34	34.1	6.57	16.1
125	1.47	0.35	33.1	6.53	16.9
138	1.46	0.35	32.3	6.54	17.7
149	1.42	0.34	31.6	6.58	18.6
160	1.43	0.34	31.0	6.57	19.2
172	1.49	0.36	30.4	6.51	19.7
214	1.45	0.35	28.4	6.55	22.2
254	1.34	0.32	27.1	6.66	24.3
319	1.33	0.32	25.6	6.67	26.6
386	1.16	0.28	24.5	6.84	29.2
484	1.29	0.31	23.3	6.71	30.9
632	1.08	0.26	22.0	6.92	34.4
753	0.91	0.22	21.3	7.09	36.4
880	0.74	0.18	21.1	7.26	38.1
1136	0.88	0.21	20.0	7.12	39.9

APPENDIX H3

EFFICIENCY OF RETURN AIR SPRAY CHAMBER

The results in this appendix are the computer printouts of two sets of tests to investigate the effect that the efficiency of the return air spray chamber had on overall DEC performance. Both sets of tests varied the water flow rate to the return air spray chamber to change the efficiency of the spray chamber. One set of tests was done with a return air flow rate of approximately 0.10 kg/s (tests H3/1 to H3/10) and the other set was with a return air flow rate of approximately 0.15 kg/s (tests H3/11 to H3/20). In both sets of tests all other operating parameters were kept constant, including the supply air flow rate (0.15 kg/s).

The more important results of these tests are given in tabular and graphical form in section 6.3 (unbalanced flow) and section 6.4 (balanced flow).

RESULTS OF DEC TEST (sheet 1 of 2) DATE: 5-6-1997
********** TIME: 18H42

TEST NUMBER: H3/1

OPERATING PARAMETERS (MEASURED AND ENTERED AS INPUT)

		NOM.	MIN.	MAX.
Supply air flow rate	(g/s)=	147	137	156
Return air flow rate	(g/s)=	99	90	108
Regen. heat input	(kW)=	3.670	3.523	3.817
Elec. energy (exc. reg.)	(kW)=	2.380	2.285	2.475
Spray chambers: water T	(oC)=	19.2	19.0	19.4
Water flow rate (S S/CH)	(g/s)=	1.47	1.40	1.54
at pressure	(bar)=	57	55	59
Water flow rate (R S/CH)	(g/s)=	0.00	0.00	0.00
at pressure	(bar)=	0	0	2

PROCESS CHANGES OF ENTHALPY AND HUMIDITY RATIO

ST PT	END PT	H (kJ/KG) NOM.	MIN.	MAX.	SIM.	W (g/kg) NOM.	MIN.	MAX.	SIM.
1	2	4.8	3.4	6.3	4.8	-3.01	-3.46	-2.56	-3.01
2	3	-7.4	-8.8	-6.0	-7.2	0.33	-0.10	0.75	0.34
3	4	0.0	-1.4	1.4	-0.1	4.24	3.80	4.67	4.26
4	5	4.7	3.2	6.1	4.5	-1.90	-2.35	-1.45	-1.93
5	6	-0.7	-2.2	0.8	0.1	0.86	0.40	1.31	1.13
6	7	9.0	7.5	10.6	9.3	-0.76	-1.25	-0.27	-0.49
7	8	37.1	35.4	38.8	37.1	0.00	-0.53	0.53	0.00
8	9	-28.2	-29.9	-26.5	-8.9	1.99	1.45	2.54	4.47

PERFORMANCE PARAMETERS (CALCULATED)

			NOM.	MIN.	MAX.	SIM.
Dehumidifier eff.(W)	(%)	EDH1=	38	32	44	39
Dehumidifier eff.(Q)	(%)	EDH2=	12	9	15	12
Regeneration eff.	(%)	ERG=	13	10	17	30
Regen. heat input	(kW)	Q =	3.67	3.29	4.04	3.67
Heat Exch. eff. (SUP)	(%)	EHXS=	66	63	70	66
Heat Exch. eff. (RET)	(%)	EHXR=	88	85	91	88
Sup. air spr. ch. eff.	(%)	EVS=	99	94	103	99
Ret. air spr. ch. eff.	(%)	EVR=	35	31	39	35
FOR VENTILATION MODE:						
Cooling capacity	(kW)	CC =	0.69	0.47	0.90	0.67
Coeff. of performance		COP=	0.19	0.13	0.25	0.18
Electricity eff. ratio		EER=	0.29	0.20	0.38	0.28
FOR VENTILATION CREDIT MODE:						
Cooling capacity	(kW)	TCC =	0.37	0.15	0.59	0.35
Total Coeff. of perf.		TCOP=	0.10	0.04	0.16	0.10
Electricity eff. ratio		TEER=	0.16	0.06	0.25	0.15

RESULTS OF DEC TEST (sheet 2 of 2) DATE: 5-6-1997
********** TIME: 18H42

MOIST AIR PROPERTIES AT MEASURED POINTS IN PROCESS

NOMINAL MEASURED VALUES:

PT	TDB (oC)	TWB (oC)	TDP (oC)	PW (kPa)	W (g/kg)	RH (%)	U (%)	SV (m3/kg)	H (kJ/kg)
1	20.3	14.7	11.8	1.38	10.59	58	57	1.038	47.32
2	32.6	16.3	6.9	0.99	7.58	20	19	1.077	52.15
3	24.5	14.0	7.5	1.04	7.91	34	33	1.049	44.78
4	14.0	13.9	13.9	1.58	12.15	99	99	1.019	44.80
5	23.3	15.4	11.3	1.34	10.25	47	46	1.048	49.47
6	20.5	15.2	12.5	1.45	11.11	60	60	1.040	48.74
7	31.1	17.9	11.5	1.35	10.35	30	29	1.076	57.75
8	67.4	26.6	11.5	1.35	10.35	5	3	1.204	94.84
9	34.8	20.2	14.1	1.61	12.34	29	27	1.093	66.64

VALUES FOR TDB & W FROM ERROR ANALYSIS & SIMULATION :
(UNITS AS ABOVE)

PT	1	2	3	4	5	6	7	8	9
TDB(MIN)	20.1	32.3	24.3	13.8	23.1	20.2	30.9	67.1	34.6
TDB(MAX)	20.6	32.8	24.7	14.3	23.5	20.7	31.3	67.6	35.0
W (MIN)	10.3	7.3	7.6	11.8	9.9	10.8	10.0	10.0	12.0
W (MAX)	10.9	7.9	8.2	12.5	10.6	11.4	10.7	10.7	12.7
TDB(SIM)	20.3	32.6	24.7	14.1	23.3	20.5	30.9	67.1	47.2
W (SIM)	10.6	7.6	7.9	12.2	10.3	11.4	10.9	10.9	15.4

POSITION OF SAMPLING POINTS



PSYCHROMETRIC CHART: ALTITUDE 1700m BAROMETRIC PRESSURE 82.5 kPa

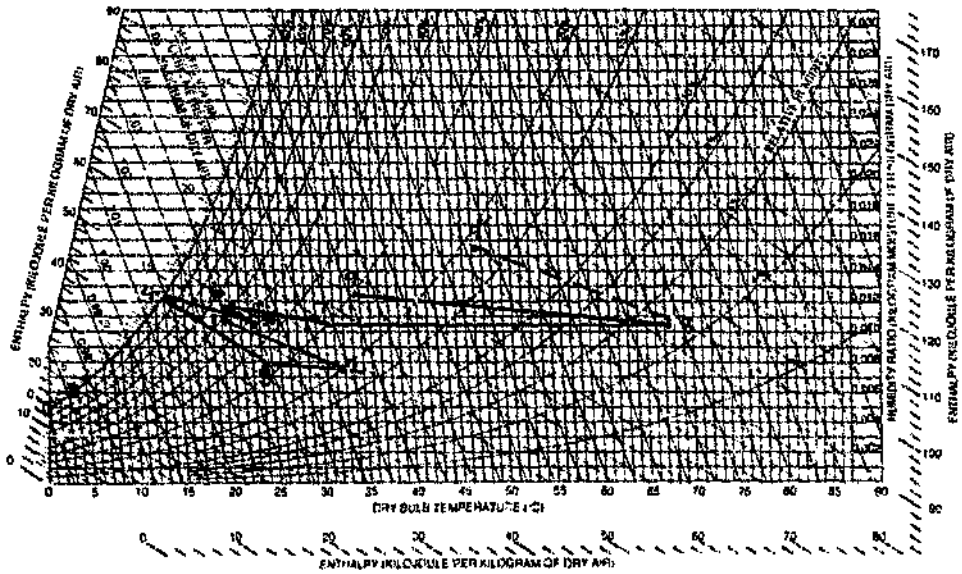

RESULTS OF DEC TEST (sheet 1 of 2) DATE: 5-6-1997
********** TIME: 18H30

TEST NUMBER: H3/2

OPERATING PARAMETERS (MEASURED AND ENTERED AS INPUT)

		NOM.	MIN.	MAX.
Supply air flow rate	(g/s)=	147	138	155
Return air flow rate	(g/s)=	99	90	108
Regen. heat input	(kW)=	3.670	3.523	3.817
Elec. energy (excl. reg.)	(kW)=	2.412	2.316	2.508
Spray chambers: water T	(oC)=	19.2	19.0	19.4
Water flow rate (S S/CH)	(g/s)=	1.47	1.40	1.54
at pressure	(bar)=	57	55	59
Water flow rate (R S/CH)	(g/s)=	0.62	0.59	0.65
at pressure	(bar)=	2	0	4

PROCESS CHANGES OF ENTHALPY AND HUMIDITY RATIO

ST PT	END PT	H (kJ/KG) NOM.	MIN.	MAX.	SIM.	W (g/kg) NOM.	MIN.	MAX.	SIM.
1	2	4.2	2.8	5.6	4.2	-2.92	-3.36	-2.48	-2.92
2	3	-7.5	-8.9	-6.0	-7.8	0.65	0.22	1.08	0.42
3	4	-0.1	-1.5	1.3	0.0	4.01	3.58	4.44	4.17
4	5	5.7	4.3	7.1	5.9	-1.64	-2.07	-1.21	-1.57
5	6	-0.4	-1.9	1.0	0.1	1.46	1.00	1.91	1.63
6	7	9.9	8.3	11.4	10.2	-0.89	-1.38	-0.40	-0.61
7	8	37.9	36.3	39.6	37.1	0.00	-0.51	0.51	0.00
8	9	-30.5	-32.3	-28.7	-7.8	1.51	0.96	2.07	4.33

PERFORMANCE PARAMETERS (CALCULATED)

			NOM.	MIN.	MAX.	SIM.
Dehumidifier eff.(W)	(%)	EDH1=	39	33	46	40
Dehumidifier eff.(Q)	(%)	EDH2=	10	7	14	11
Regeneration eff.	(%)	ERG=	10	6	14	29
Regen. heat input	(kW)	Q =	3.75	3.37	4.14	3.67
Heat Exch. eff. (SUP)	(%)	EHXS=	67	64	70	67
Heat Exch. eff. (RET)	(%)	EHXR=	88	85	91	88
Sup. air spr. ch. eff.	(%)	EVS=	99	94	104	99
Ret. air spr. ch. eff.	(%)	EVR=	50	46	55	50
FOR VENTILATION MODE:						
Cooling capacity	(kW)	CC =	0.83	0.62	1.05	0.87
Coeff. of performance		COP=	0.23	0.17	0.29	0.24
Electricity eff. ratio		EER=	0.35	0.26	0.44	0.36
FOR VENTILATION CREDIT MODE:						
Cooling capacity	(kW)	TCC =	0.49	0.28	0.71	0.53
Total Coeff. of perf.		TCOP=	0.13	0.08	0.19	0.14
Electricity eff. ratio		TEER=	0.20	0.12	0.29	0.22

RESULTS OF DEC TEST (sheet 2 of 3) DATE: 5-6-1997
********** TIME: 18H30

MOIST AIR PROPERTIES AT MEASURED POINTS IN PROCESS

NOMINAL MEASURED VALUES :

PT	TDB (oC)	TWB (oC)	TDP (oC)	PW (kPa)	W (g/kg)	RH (%)	U (%)	SV (m3/kg)	H (kJ/kg)
1	21.3	14.7	11.1	1.32	10.[illegible]	52	51	1.041	47.01
2	32.7	16.0	6.1	0.94	7.18	19	18	1.076	51.21
3	23.7	13.6	7.4	[illegible]03	[illegible].83	35	34	1.046	43.76
4	13.7	13.5	13.[illegible]	[illegible]	11.85	99	99	1.017	43.66
5	23.3	15.4	11.[illegible]	[illegible]	[illegible].21	47	46	1.048	49.34
6	19.2	15.2	13.[illegible]	[illegible]	[illegible]	68	68	1.036	48.89
7	31.1	18.2	12.[illegible]	[illegible]	[illegible]	31	30	1.077	58.77
8	68.1	26.9	12.1	[illegible]	[illegible]	5	3	1.208	96.71
9	34.5	20.1	14.0	[illegible]	[illegible]	29	28	1.092	66.19

VALUES FOR TDB & W FROM ERROR ANALYSIS & SIMULATION :
(UNITS AS ABOVE)

PT	1	2	3	4	5	6	7	8	9
TDB(MIN)	21.0	32.4	23.5	13.4	23.1	19.0	30.8	67.9	34.3
TDB(MAX)	21.5	32.9	23.9	13.9	23.5	19.5	31.3	68.3	34.7
W (MIN)	9.8	6.9	7.5	11.6	9.9	11.3	10.4	10.4	11.9
W (MAX)	10.4	7.5	8.1	12.1	10.5	12.0	11.1	11.1	12.7
TDB(SIM)	21.3	32.7	23.9	13.6	23.3	19.3	30.8	66.9	48.4
W (SIM)	10.1	7.2	7.6	11.8	10.2	11.8	11.2	11.2	15.6

POSITION OF SAMPLING POINTS



PSYCHROMETRIC CHART: ALTITUDE 1700m BAROMETRIC PRESSURE 82.5 kPa

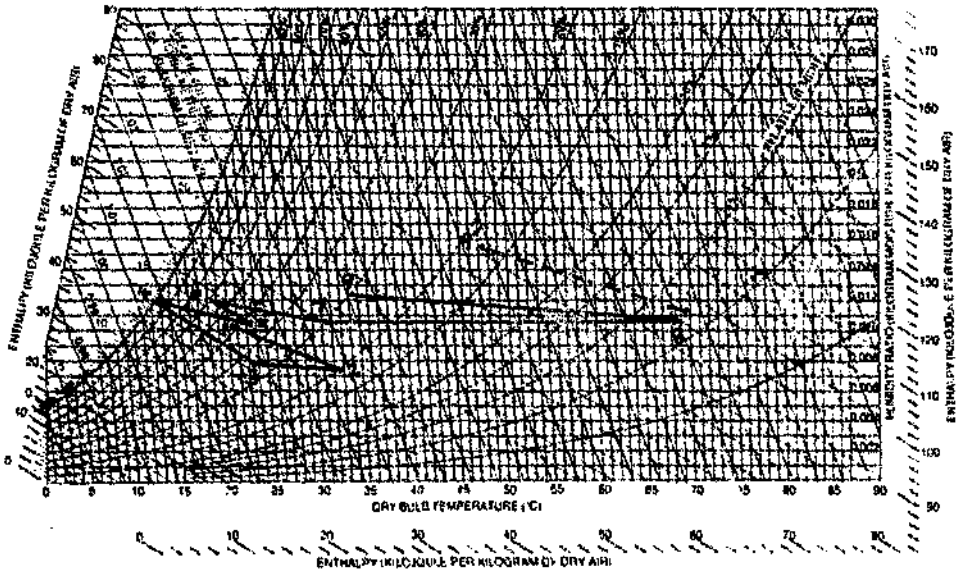

RESULTS OF DEC TEST (sheet 1 of 2) DATE: 5-6-1997
********** TIME: 18H13

TEST NUMBER: H3/3

OPERATING PARAMETERS (MEASURED AND ENTERED AS INPUT)

		NOM.	MIN.	MAX.
Supply air flow rate	(g/s)=	147	138	156
Return air flow rate	(g/s)=	99	90	108
Regen. heat input	(kW)=	3.670	3.523	3.817
Elec. energy (excl. reg.)	(kW)=	2.457	2.359	2.555
Spray chambers: water T	(oC)=	19.2	19.0	19.4
Water flow r (S S/CH)	(g/s)=	1.47	1.40	1.54
at essure	(bar)=	57	55	59
Water flow rate (R S/CH)	(g/s)=	0.87	0.83	0.91
at pressure	(bar)=	10	8	12

PROCESS CHANGES OF ENTHALPY AND HUMIDITY RATIO

ST PT	END PT	H (kJ/KG) NOM.	MIN.	MAX.	SIM.	W (g/kg) NOM.	MIN.	MAX.	SIM.
1	2	3.7	2.3	5.1	3.7	-2.68	-3.11	-2.26	-2.68
2	3	-8.1	-9.5	6.7	-9.0	0.89	0.48	1.30	0.47
3	4	-0.6	-2.0	0.7	0.2	3.57	3.17	3.98	3.96
4	5	6.4	5.0	7.8	6.5	-1.55	-1.98	-1.11	-1.52
5	6	-0.0	-1.5	1.5	0.1	2.21	1.75	2.66	2.25
6	7	10.9	9.3	12.5	11.5	-1.05	-1.55	-0.56	-0.67
7	8	37.4	35.7	39.1	37.2	0.00	-0.54	0.54	0.00
8	9	-29.7	-31.5	-28.0	-6.9	1.14	0.60	1.69	3.99

PERFORMANCE PARAMETERS (CALCULATED)

			NOM.	MIN.	MAX.	SIM.
Dehumidifier eff.(W)	(%)	EDH1=	40	33	46	40
Dehumidifier eff.(Q)	(%)	EDH2=	10	6	13	10
Regeneration eff.	(%)	ERG=	8	4	11	27
Regen. heat input	(kW)	Q =	3.69	3.31	4.07	3.67
Heat Exch. eff. (SUP)	(%)	EHXS=	67	65	70	68
Heat Exch. eff. (RET)	(%)	EHXR=	88	85	90	88
Sup. air spr. ch. eff.	(%)	EVS=	98	93	103	98
Ret. air spr. ch. eff.	(%)	EVR=	67	62	72	67
FOR VENTILATION MODE:						
Cooling capacity	(kW)	CC =	0.94	0.72	1.15	0.95
Coeff. of performance		COP=	0.26	0.20	0.32	0.26
Electricity eff. ratio		EER=	0.38	0.29	0.47	0.39
FOR VENTILATION CREDIT MODE:						
Cooling capacity	(kW)	TCC =	0.74	0.53	0.95	0.75
Total Coeff. of perf.		TCOP=	0.20	0.14	0.26	0.20
Electricity eff. ratio		TEER=	0.30	0.21	0.39	0.31

RESULTS OF DEC TEST (sheet 2 of 2) DATE: 5-6-1997
********** TIME: 18H13

MOIST AIR PROPERTIES AT MEASURED POINTS IN PROCESS

NOMINAL MEASURED VALUES:

PT	TDB (oC)	TWB (oC)	TDP (oC)	PW (kPa)	W (g/kg)	RH (%)	U (%)	SV (m3/kg)	H (kJ/kg)
1	22.4	14.6	10.3	1.25	9.57	46	45	1.044	46.79
2	32.7	15.8	5.5	0.90	6.88	18	17	1.076	50.51
3	22.5	13.2	7.3	1.02	7.77	37	36	1.042	42.41
4	13.1	12.9	12.8	1.48	11.34	98	98	1.014	41.78
5	23.1	15.0	10.6	1.28	9.80	45	44	1.047	48.16
6	17.6	15.0	13.7	1.56	12.00	77	77	1.031	48.14
7	30.9	18.2	12.3	1.43	10.95	32	31	1.076	59.02
8	67.3	26.8	12.3	1.43	10.95	5	3	1.205	96.39
9	35.4	20.2	13.8	1.57	12.09	27	26	1.094	66.64

VALUES FOR TDB & W FROM ERROR ANALYSIS & SIMULATION :
(UNITS AS ABOVE)

PT	1	2	3	4	5	6	7	8	9
TDB(MIN)	22.1	32.5	22.3	12.9	22.9	17.4	30.7	67.1	35.2
TDB(MAX)	22.6	33.0	22.8	13.3	23.4	17.9	31.1	67.6	35.7
W (MIN)	9.3	6.6	7.5	11.1	9.5	11.7	10.6	10.6	11.7
W (MAX)	9.9	7.2	8.1	11.6	10.1	12.3	11.3	11.3	12.5
TDB(SIM)	22.4	32.7	22.7	13.0	23.1	17.7	30.5	66.8	50.0
W (SIM)	9.6	6.9	7.4	11.3	9.8	12.0	11.4	11.4	15.4

POSITION OF SAMPLING POINTS

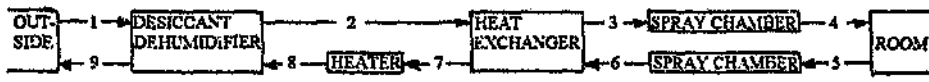

PSYCHROMETRIC CHART: ALTITUDE 1700m BAROMETRIC PRESSURE 82.5 kPa

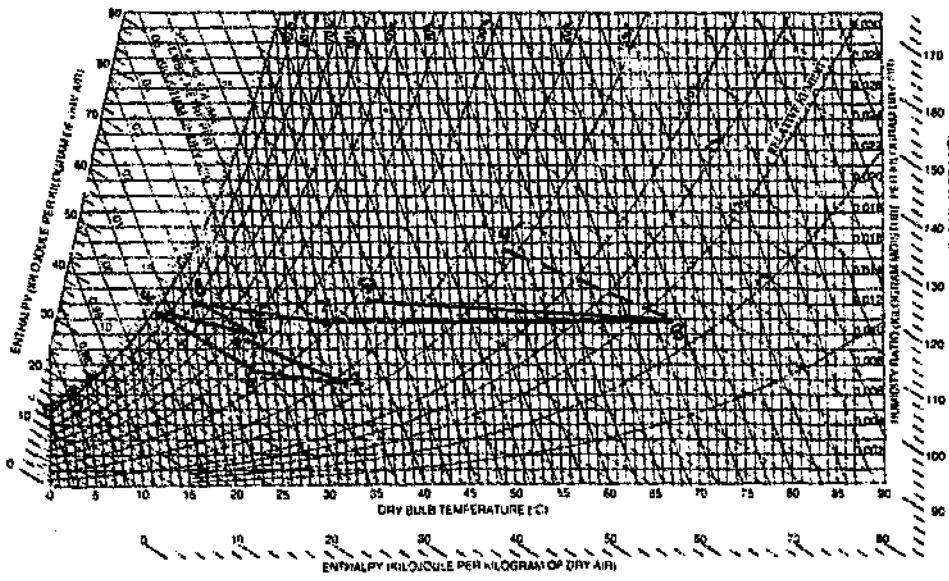

RESULTS OF DEC TEST (sheet 1 of 2) DATE: 5-6-1997
********** TIME: 17h57

TEST NUMBER: H3/4

OPERATING PARAMETERS (MEASURED AND ENTERED AS INPUT)

		NOM.	MIN.	MAX.
Supply air flow rate	(g/s)=	146	137	155
Return air flow rate	(g/s)=	99	89	108
Regen. heat input	(kW)=	3.670	3.523	3.817
Elec. energy (excl. reg.)	(kW)=	2.486	2.387	2.585
Spray chambers: water T	(oC)=	19.2	19.0	19.4
Water flow rate (S S/CH)	(g/s)=	1.47	1.40	1.54
at pressure	(bar)=	57	55	59
Water flow rate (R S/CH)	(g/s)=	1.15	1.09	1.21
at pressure	(bar)=	20	18	22

PROCESS CHANGES OF ENTHALPY AND HUMIDITY RATIO

ST PT	END PT	H (kJ/KG) NOM.	MIN.	MAX.	SIM.	W (g/kg) NOM.	MIN.	MAX.	SIM.
1	2	4.7	3.2	6.1	4.7	-2.79	-3.24	-2.35	-2.79
2	3	-9.8	-11.2	-8.4	-11.4	1.28	0.87	1.69	0.55
3	4	-0.0	-1.3	1.3	-0.0	3.30	2.90	3.69	3.60
4	5	6.2	4.7	7.6	7.8	-1.55	-1.99	-1.12	-1.12
5	6	-0.1	-1.6	1.4	0.2	2.84	2.39	3.29	2.91
6	7	12.3	10.7	13.9	13.2	-1.28	-1.78	-0.78	-0.77
7	8	37.1	35.4	38.9	37.2	0.00	-0.55	0.55	0.00
8	9	-28.7	-30.6	-26.9	-8.7	1.60	1.02	2.18	4.14

PERFORMANCE PARAMETERS (CALCULATED)

			NOM.	MIN.	MAX.	SIM.
Dehumidifier eff.(W)	(%)	EDH1=	41	34	48	42
Dehumidifier eff.(Q)	(%)	EDH2=	12	9	16	12
Regeneration eff.	(%)	ERG=	11	7	15	28
Regen. heat input	(kW)	Q =	3.66	3.28	4.04	3.67
Heat Exch. eff. (SUP)	(%)	EHXS=	70	68	72	70
Heat Exch. eff. (RET)	(%)	EHXR=	83	81	85	83
Sup. air spr. ch. eff.	(%)	EVS=	99	93	106	99
Ret. air spr. ch. eff.	(%)	EVR=	90	84	96	90
FOR VENTILATION MODE:						
Cooling capacity	(kW)	CC =	0.90	0.68	1.11	1.14
Coeff. of performance		COP=	0.24	0.19	0.30	0.31
Electricity eff. ratio		EER=	0.36	0.27	0.45	0.46
FOR VENTILATION CREDIT MODE:						
Cooling capacity	(kW)	TCC =	0.75	0.54	0.96	0.99
Total Coeff. of perf.		TCOP=	0.20	0.15	0.26	0.27
Electricity eff. ratio		TEER=	0.30	0.22	0.39	0.40

RESULTS OF DEC TEST (sheet 2 of 2) DATE: 5-6-1997
********** TIME: 17H57

MOIST AIR PROPERTIES AT MEASURED POINTS IN PROCESS

NOMINAL MEASURED VALUES:

PT	TDB (oC)	TWB (oC)	TDP (oC)	PW (kPa)	W (g/kg)	RH (%)	U (%)	SV (m3/kg)	H (kJ/kg)
1	22.7	14.9	10.7	1.29	9.85	47	46	1.045	47.84
2	34.3	16.4	5.9	0.93	7.06	17	16	1.082	52.52
3	21.4	13.3	8.3	1.09	8.34	43	42	1.039	42.72
4	13.3	13.2	13.2	1.52	11.64	100	100	1.015	42.71
5	23.1	15.2	11.1	1.32	10.09	47	46	1.047	48.86
6	16.0	15.2	14.8	1.68	12.93	93	92	1.027	48.76
7	31.1	18.8	13.2	1.52	11.65	34	32	1.078	61.06
8	67.3	27.1	13.2	1.52	11.65	5	4	1.207	98.17
9	35.3	20.9	15.2	1.72	13.25	30	29	1.096	69.44

VALUES FOR TDB & W FROM ERROR ANALYSIS & SIMULATION :
(UNITS AS ABOVE)

PT	1	2	3	4	5	6	7	8	9
TDB(MIN)	22.5	34.0	21.2	13.0	22.9	15.8	30.9	67.1	35.1
TDB(MAX)	22.9	34.5	21.7	13.5	23.3	16.2	31.3	67.5	35.5
W (MIN)	9.5	6.8	8.1	11.4	9.8	12.6	11.3	11.3	12.8
W (MAX)	10.2	7.4	8.6	11.9	10.4	13.2	12.0	12.0	13.7
TDB(SIM)	22.7	34.3	21.7	12.7	23.1	16.0	30.8	67.0	48.2
W (SIM)	9.9	7.1	7.6	11.2	10.1	13.0	12.2	12.2	16.4

POSITION OF SAMPLING POINTS



PSYCHROMETRIC CHART: ALTITUDE 1700m BAROMETRIC PRESSURE 82.5 kPa

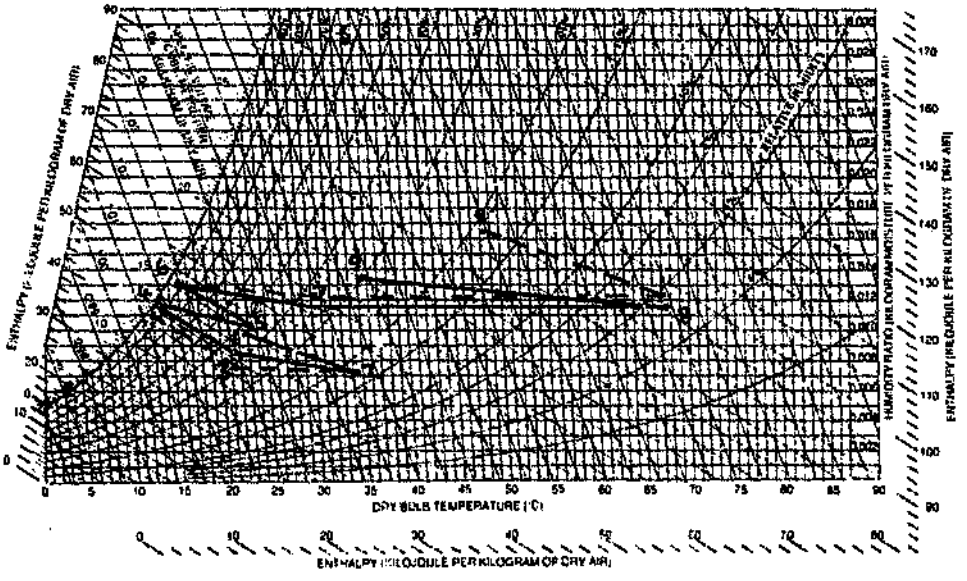

RESULTS OF DEC TEST (sheet 1 of 2) DATE: 5-6-1997
********** TIME: 17:41

TEST NUMBER: H3/5

OPERATING PARAMETERS (MEASURED AND ENTERED AS INPUT)

		NOM.	MIN.	MAX.
Supply air flow rate	(g/s)=	146	137	156
Return air flow rate	(g/s)=	98	89	107
Regen. heat input	(kW)=	3.670	3.523	3.817
Elec. energy (excl. reg.)	(kW)=	2.509	2.409	2.609
Spray chambers: water T	(oC)=	19.2	19.0	19.4
Water flow rate (S S/CH)	(g/s)=	1.47	1.40	1.54
at pressure	(bar)=	57	55	59
Water flow rate (R S/CH)	(g/s)=	1.30	1.23	1.36
at pressure	(bar)=	30	28	32

PROCESS CHANGES OF ENTHALPY AND HUMIDITY RATIO

ST PT	END PT	H (kJ/KG) NOM.	MIN.	MAX.	SIM.	W (g/kg) NOM.	MIN.	MAX.	SIM.
1	2	4.5	3.0	5.9	4.5	-2.62	-3.06	-2.18	-2.62
2	3	-10.0	-11.4	-8.6	-11.2	1.11	0.69	1.53	0.53
3	4	-0.2	-1.6	1.2	-0.1	2.98	2.57	3.39	3.26
4	5	6.4	5.0	7.8	7.6	-1.48	-1.92	-1.03	-1.18
5	6	0.0	-1.5	1.5	0.2	3.12	2.65	3.59	3.16
6	7	12.9	11.3	14.5	13.5	-1.17	-1.69	-0.65	-0.75
7	8	37.8	36.0	39.5	37.3	0.00	-0.56	0.56	0.00
8	9	-30.8	-32.6	-28.9	-8.4	0.57	-0.01	1.15	3.89

PERFORMANCE PARAMETERS (CALCULATED)

			NOM.	MIN.	MAX.	SIM.
Dehumidifier eff.(W)	(%)	EDH1=	37	31	44	38
Dehumidifier eff.(Q)	(%)	EDH2=	11	8	15	12
Regeneration eff.	(%)	ERG=	4	-0	8	26
Regen. heat input	(kW)	Q =	3.71	3.33	4.10	3.67
Heat Exch. eff. (SUP)	(%)	EHXS=	70	68	72	70
Heat Exch. eff. (RET)	(%)	EHXR=	86	84	88	86
Sup. air spr. ch. eff.	(%)	EVS=	100	93	106	100
Ret. air spr. ch. eff.	(%)	EVR=	98	91	104	98
FOR VENTILATION MODE:						
Cooling capacity	(kW)	CC =	0.94	0.72	1.16	1.11
Coeff. of performance		COP=	0.26	0.20	0.32	0.30
Electricity eff. ratio		EER=	0.37	0.29	0.46	0.44
FOR VENTILATION CREDIT MODE:						
Cooling capacity	(kW)	TCC =	0.85	0.63	1.06	1.01
Total Coeff. of perf.		TCOP=	0.23	0.17	0.29	0.28
Electricity eff. ratio		TEER=	0.34	0.25	0.42	0.40

RESULTS OF DEC TEST (sheet 2 of 2) DATE: 5-6-1997
********** TIME: 17H41

MOIST AIR PROPERTIES AT MEASURED POINTS IN PROCESS

NOMINAL MEASURED VALUES:

PT	TDB (oC)	TWB (oC)	TDP (oC)	PW (kPa)	W (g/kg)	RH (%)	U (%)	SV (m3/kg)	H (kJ/kg)
1	22.5	15.1	11.2	1.33	10.15	49	48	1.045	48.43
2	33.4	16.5	6.8	0.99	7.54	19	18	1.079	52.88
3	20.8	13.3	8.8	1.13	8.65	46	45	1.037	42.86
4	13.2	13.2	13.2	1.51	11.63	100	100	1.015	42.65
5	23.1	15.3	11.2	1.33	10.15	47	46	1.048	49.06
6	15.4	15.3	15.2	1.72	13.27	98	98	1.025	49.08
7	30.9	19.0	13.8	1.57	12.10	35	34	1.078	61.99
8	67.7	27.5	13.8	1.57	12.10	6	4	1.209	99.75
9	36.3	20.8	14.5	1.65	12.67	27	26	1.098	68.97

VALUES FOR TDB & W FROM ERROR ANALYSIS & SIMULATION :
(UNITS AS ABOVE)

PT	1	2	3	4	5	6	7	8	9
TDB(MIN)	22.3	33.2	20.6	13.0	22.9	15.2	30.7	67.4	36.0
TDB(MAX)	22.7	33.6	21.0	13.4	23.4	15.6	31.1	67.9	36.5
W (MIN)	9.8	7.2	8.4	11.3	9.8	12.9	11.7	11.7	12.2
W (MAX)	10.5	7.8	8.9	11.9	10.5	13.6	12.5	12.5	13.1
TDB(SIM)	22.5	33.4	21.1	12.8	23.1	15.5	30.5	66.8	48.8
W (SIM)	10.2	7.5	8.1	11.3	10.2	13.3	12.6	12.6	16.5

POSITION OF SAMPLING POINTS



PSYCHROMETRIC CHART: ALTITUDE 1700m BAROMETRIC PRESSURE 82.5 kPa

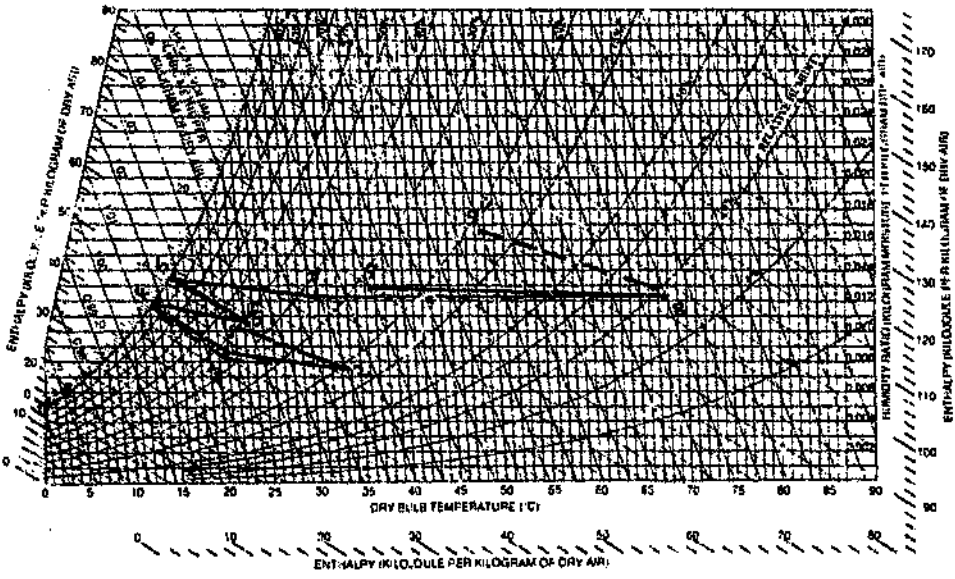

RESULTS OF DEC TEST (sheet 1 of 2) DATE: 5-6-1997
********** TIME: 17H22

TEST NUMBER: H3/6

OPERATING PARAMETERS (MEASURED AND ENTERED AS INPUT)

		NOM.	MIN.	MAX.
Supply air flow rate	(g/s)=	146	137	156
Return air flow rate	(g/s)=	98	89	108
Regen. heat input	(kW)=	3.670	3.523	3.817
Elec. energy (excl. reg.)	(kW)=	2.534	2.433	2.635
Spray chambers: water T	(oC)=	19.2	19.0	19.4
Water flow rate (S S/CH)	(g/s)=	1.47	1.40	1.54
at pressure	(bar)=	57	55	59
Water flow rate (R S/CH)	(g/s)=	1.58	1.50	1.66
at pressure	(bar)=	40	38	42

PROCESS CHANGES OF ENTHALPY AND HUMIDITY RATIO

ST PT	END PT	H (kJ/KG) NOM.	MIN.	MAX.	SIM.	W (g/kg) NOM.	MIN.	MAX.	SIM.
1	2	3.6	2.2	5.0	3.6	-2.83	-3.26	-2.40	-2.83
2	3	-10.0	-11.5	-8.6	-11.9	1.39	0.97	1.81	0.54
3	4	-0.5	-1.9	0.8	-0.1	2.61	2.20	3.02	3.09
4	5	6.8	5.4	8.3	8.3	-1.30	-1.74	-0.86	-0.93
5	6	0.0	-1.4	1.5	0.2	3.14	2.68	3.60	3.18
6	7	12.5	10.8	14.1	13.2	-1.23	-1.73	-0.73	-0.77
7	8	37.1	35.4	38.9	37.3	0.00	-0.54	0.54	0.00
8	9	-29.5	-31.3	-27.7	-6.9	0.82	0.24	1.40	4.21

PERFORMANCE PARAMETERS (CALCULATED)

			NOM.	MIN.	MAX.	SIM.
Dehumidifier eff.(W)	(%)	EDH1=	40	34	47	41
Dehumidifier eff.(Q)	(%)	EDH2=	10	6	13	10
Regeneration eff.	(%)	ER=	6	2	9	28
Regen. heat input	(kW)	Q =	3.65	3.27	4.03	3.67
Heat Exch. eff. (SUP)	(%)	EHXS=	73	71	76	73
Heat Exch. eff. (RET)	(%)	EHXR=	83	81	86	84
Sup. air spr. ch. eff.	(%)	EVS=	99	92	106	99
Ret. air spr. ch. eff.	(%)	EVR=	99	93	106	99
FOR VENTILATION MODE:						
Cooling capacity	(kW)	CC =	1.00	0.78	1.22	1.21
Coeff. of performance		COP=	0.27	0.21	0.33	0.33
Electricity eff. ratio		EER=	0.39	0.31	0.48	0.48
FOR VENTILATION CREDIT MODE:						
Cooling capacity	(kW)	TCC =	1.02	0.81	1.24	1.23
Total Coeff. of perf.		TCOP=	0.28	0.22	0.34	0.34
Electricity eff. ratio		TEER=	0.40	0.32	0.49	0.49

RESULTS OF DEC TEST (sheet 2 of 2) DATE: 5-6-1997
********** TIME: 17H22

MOIST AIR PROPERTIES AT MEASURED POINTS IN PROCESS

NOMINAL MEASURED VALUES:

PT	TDB (oC)	TWB (oC)	TDP (oC)	PW (kPa)	W (g/kg)	RH (%)	U (%)	SV (m3/kg)	H (kJ/kg)
1	22.9	15.4	11.5	1.35	10.37	48	48	1.047	49.42
2	33.5	16.6	6.8	0.99	7.54	19	18	1.080	53.02
3	20.2	13.3	9.3	1.17	8.93	49	49	1.035	42.97
4	13.2	13.1	13.1	1.50	11.54	99	99	1.015	42.42
5	23.1	15.4	11.3	1.34	10.24	47	46	1.048	49.25
6	15.4	15.3	15.3	1.74	13.38	100	100	1.025	49.29
7	30.5	19.0	13.9	1.58	12.15	36	35	1.077	61.74
8	66.7	27.3	13.9	1.58	12.15	6	4	1.205	98.87
9	35.9	20.9	14.8	1.69	12.98	29	27	1.098	69.36

VALUES FOR TDB & W FROM ERROR ANALYSIS & SIMULATION :
(UNITS AS ABOVE)

PT	1	2	3	4	5	6	7	8	9
TDB(MIN)	22.7	33.3	20.0	13.0	22.9	15.1	30.3	66.5	35.7
TDB(MAX)	23.2	33.8	20.4	13.4	23.3	15.6	30.8	66.9	36.1
W (MIN)	10.1	7.2	8.6	11.3	9.9	13.1	11.8	11.8	12.5
W (MAX)	10.7	7.8	9.2	11.8	10.6	13.7	12.5	12.5	13.4
TDB(SIM)	22.9	33.5	20.5	12.7	23.1	15.4	30.2	66.4	49.1
W (SIM)	10.4	7.5	8.1	11.2	10.2	13.4	12.7	12.7	16.9

POSITION OF SAMPLING POINTS



PSYCHROMETRIC CHART: ALTITUDE 1700m BAROMETRIC PRESSURE 82.5 kPa

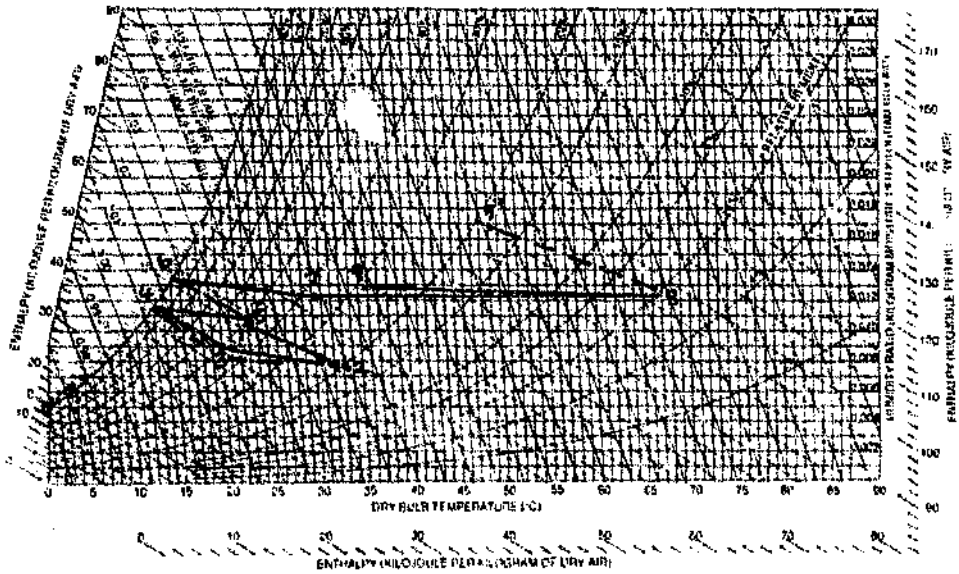

RESULTS OF DEC TEST (sheet 1 of 2) DATE: 5-6-1997
********** TIME: 17H10

TEST NUMBER: H3/"

OPERATING PARAMETERS (MEASURED AND ENTERED AS INPUT)

		NOM.	MIN.	MAX.
Supply air flow rate	(g/s)=	146	137	155
Return air flow rate	(g/s)=	98	89	107
Regen. heat input	(kW)=	3.670	3.523	3.817
Elec. energy (excl. reg.)	(kW)=	2.563	2.460	2.666
Spray chambers: water T	(oC)=	19.2	19.0	19.4
Water flow rate (S S/CH)	(g/s)=	1.47	1.40	1.54
at pressure	(bar)=	57	55	59
Water flow rate (R S/CH)	(g/s)=	1.74	1.65	1.83
at pressure	(bar)=	50	48	52

PROCESS CHANGES OF ENTHALPY AND HUMIDITY RATIO

ST PT	END PT	H (kJ/KG) NOM.	MIN.	MAX.	SIM.	W (g/kg) NOM.	MIN.	MAX.	SIM.
1	2	4.4	3.9	5.8	4.4	-2.83	-3.28	-2.37	-2.83
2	3	-10.7	-12.1	-9.3	-13.2	1.71	1.28	2.13	0.56
3	4	-0.0	-1.4	1.3	0.1	2.65	2.25	3.06	3.17
4	5	6.4	5.0	7.8	8.8	-1.47	-1.89	-1.04	-0.84
5	6	-0.0	-1.5	1.5	0.2	3.18	2.72	3.63	3.21
6	7	13.7	12.0	15.3	13.7	-1.00	-1.50	-0.50	-0.80
7	8	36.7	34.9	38.4	37.4	0.00	-0.55	0.55	0.00
8	9	-28.0	-29.9	-26.1	-7.9	1.08	0.48	1.68	4.21

PERFORMANCE PARAMETERS (CALCULATED)

			NOM.	MIN.	MAX.	SIM.
Dehumidifier eff.(W)	(%)	EDH1=	41	34	48	41
Dehumidifier eff.(Q)	(%)	EDH2=	12	8	15	12
Regeneration eff.	(%)	ERG=	7	3	11	28
Regen. heat input	(kW)	Q =	3.59	3.22	3.97	3.67
Heat Exch. eff. (SUP)	(%)	EHXS=	76	74	78	76
Heat Exch. eff. (RET)	(%)	EHXR=	81	79	84	81
Sup. air spr. ch. eff.	(%)	EVS=	100	92	108	100
Ret. air spr. ch. eff.	(%)	EVR=	101	94	107	100
FOR VENTILATION MODE:						
Cooling capacity	(kW)	CC =	0.93	0.72	1.15	1.28
Coeff. of performance		COP=	0.25	0.19	0.31	0.35
Electricity eff. ratio		EER=	0.36	0.28	0.45	0.50
FOR VENTILATION CREDIT MODE:						
Cooling capacity	(kW)	TCC =	0.93	0.71	1.14	1.28
Total Coeff. of perf.		TCOP=	0.25	0.19	0.31	0.35
Electricity eff. ratio		TEER=	0.36	0.28	0.45	0.50

RESULTS OF DEC TEST (sheet 2 of 2) DATE: 5-5-1997
********** TIME: 17H10

MOIST AIR PROPERTIES AT MEASURED POINTS IN PROCESS

NOMINAL MEASURED VALUES:

PT	TDB (oC)	TWB (oC)	TDP (oC)	PW (kPa)	W (g/kg)	RH (%)	U (%)	SV (m3/kg)	H (kJ/kg)
1	23.4	15.5	11.3	1.34	10.26	47	46	1.049	49.60
2	34.7	16.8	6.5	0.97	7.43	18	17	1.084	53.95
3	20.0	13.4	9.6	1.19	9.14	51	51	1.035	43.25
4	13.4	13.4	13.4	1.53	11.79	100	100	1.016	43.23
5	23.2	15.5	11.4	1.35	10.33	47	46	1.048	49.61
6	15.4	15.4	15.5	1.75	13.50	100	100	1.026	49.60
7	31.1	19.4	14.3	1.63	12.50	36	35	1.080	63.25
8	66.8	27.5	14.3	1.63	12.50	6	4	1.207	99.93
9	36.9	21.5	15.5	1.76	13.58	28	27	1.102	71.94

VALUES FOR TDB & W FROM ERROR ANALYSIS & SIMULATION :
(UNITS AS ABOVE)

PT	1	2	3	4	5	6	7	8	9
TDB(MIN)	23.2	34.5	19.7	13.1	23.0	15.1	30.9	66.6	36.7
TDB(MAX)	23.6	34.9	20.2	13.6	23.5	15.6	31.4	67.1	37.1
W (MIN)	9.9	7.1	8.9	11.5	10.0	13.2	12.1	12.1	13.1
W (MAX)	10.6	7.7	9.4	12.1	10.7	13.8	12.9	12.9	14.0
TDB(SIM)	23.4	34.7	20.3	12.6	23.2	15.5	30.8	67.2	48.9
W (SIM)	10.3	7.4	8.0	11.2	10.3	13.5	12.7	12.7	16.9

POSITION OF SAMPLING POINTS



PSYCHROMETRIC CHART ALTITUDE 1700m BAROMETRIC PRESSURE 82.5 kPa

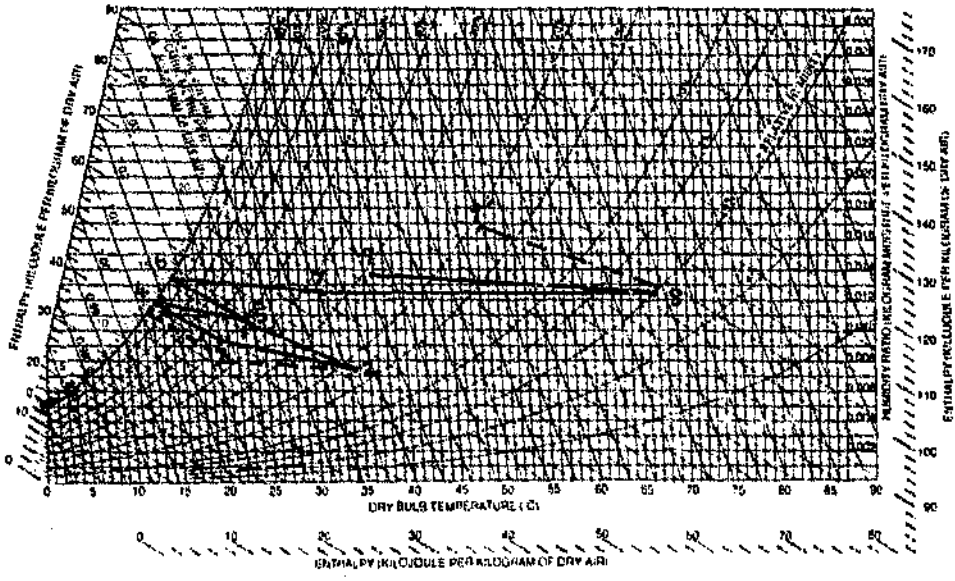

RESULTS OF DEC TEST (sheet 1 of 2) DATE: 5-6-1997
********** TIME: 16H52

TEST NUMBER: H3/8

OPERATING PARAMETERS (MEASURED AND ENTERED AS INPUT)

		NOM.	MIN.	MAX.
Supply air flow rate	(g/s)=	146	137	156
Return air flow rate	(g/s)=	98	89	107
Regen. heat input	(kW)=	3.670	3.523	3.817
Elec. energy (excl. reg.)	(kW)=	2.599	2.495	2.703
Spray chambers: water T	(oC)=	19.2	19.0	19.4
Water flow rate (S S/CH)	(g/s)=	1.47	1.40	1.54
at pressure	(bar)=	57	55	59
Water flow rate (R S/CH)	(g/s)=	2.10	1.99	2.20
at pressure	(bar)=	60	58	62

PROCESS CHANGES OF ENTHALPY AND HUMIDITY RATIO

ST PT	END PT	H (kJ/KG) NOM.	MIN.	MAX.	SIM.	W (g/kg) NOM.	MIN.	MAX.	SIM.
1	2	3.8	2.3	5.3	3.8	-2.58	-3.02	-2.13	-2.58
2	3	-9.9	-11.3	-8.5	-12.2	1.60	1.18	2.01	0.56
3	4	-0.3	-1.7	1.0	-0.0	2.56	2.16	2.96	3.08
4	5	7.0	5.6	8.4	9.0	-1.31	-1.75	-0.88	-0.79
5	6	0.0	-1.5	1.5	0.2	3.19	2.71	3.66	3.23
6	7	13.2	11.6	14.9	13.4	-1.06	-1.58	-0.53	-0.80
7	8	38.0	36.2	39.8	37.5	0.00	-0.57	0.57	0.00
8	9	-29.9	-31.8	-28.1	-7.0	0.51	-0.09	1.11	3.85

PERFORMANCE PARAMETERS (CALCULATED)

			NOM.	MIN.	MAX.	SIM.
Dehumidifier eff.(W)	(%)	EDH1=	38	31	45	39
Dehumidifier eff.(Q)	(%)	EDH2=	10	6	13	10
Regeneration eff.	(%)	ER3=	3	-1	7	26
Regen. heat input	(kW)	Q =	3.72	3.33	4.11	3.67
Heat Exch. eff. (SUP)	(%)	EHXS=	76	73	78	76
Heat Exch. eff. (RET)	(%)	EHXR=	85	83	87	85
Sup. air spr. ch. eff.	(%)	EVS=	99	92	107	99
Ret. air spr. ch. eff.	(%)	EVR=	100	94	106	100
FOR VENTILATION MODE:						
Cooling capacity	(kW)	CC =	1.02	0.80	1.24	1.32
Coeff. of performance		COP=	0.28	0.22	0.34	0.36
Electricity eff. ratio		EER=	0.39	0.31	0.48	0.51
FOR VENTILATION CREDIT MODE:						
Cooling capacity	(kW)	TCC =	0.94	0.73	1.16	1.24
Total Coeff. of perf.		TCOP=	0.26	0.20	0.32	0.34
Electricity eff. ratio		TEER=	0.36	0.28	0.45	0.48

RESULTS OF DEC TEST (sheet 2 of 2) DATE: 5-6-1997
********** TIME: 16H52

MOIST AIR PROPERTIES AT MEASURED POINTS IN PROCESS

NOMINAL MEASURED VALUES:

PT	TDB (oC)	TWB (oC)	TDP (oC)	PW (kPa)	W (g/kg)	RH (%)	U (%)	SV (m3/kg)	H (kJ/kg)
1	23.4	15.3	11.0	1.31	10.01	45	45	1.048	48.99
2	33.6	16.5	6.6	0.97	7.43	19	18	1.080	52.78
3	19.8	13.3	9.4	1.18	9.03	51	50	1.034	42.85
4	13.2	13.2	13.1	1.51	11.59	100	100	1.015	42.54
5	23.3	15.4	11.4	1.34	10.28	47	46	1.048	49.52
6	15.4	15.4	15.4	1.75	13.47	100	100	1.026	49.54
7	30.9	19.2	14.2	1.61	12.41	36	35	1.079	62.76
8	67.9	27.7	14.2	1.61	12.41	6	4	1.210	100.76
9	37.5	21.3	14.8	1.68	12.92	26	25	1.103	70.83

VALUES FOR TDB & W FROM ERROR ANALYSIS & SIMULATION :
(UNITS AS ABOVE)

PT	1	2	3	4	5	6	7	8	9
TDB(MIN)	23.2	33.3	19.6	13.0	23.0	15.2	30.7	67.6	37.2
TDB(MAX)	23.6	33.8	20.1	13.4	23.5	15.6	31.1	68.1	37.7
W (MIN)	9.7	7.1	8.7	11.3	10.0	13.1	12.0	12.0	12.5
W (MAX)	10.3	7.7	9.3	11.9	10.6	13.8	12.8	12.8	13.4
TDB(SIM)	23.4	33.6	20.2	12.5	23.3	15.5	30.4	66.9	50.4
W (SIM)	10.0	7.4	8.0	11.1	10.3	13.5	12.7	12.7	16.6

POSITION OF SAMPLING POINTS



PSYCHROMETRIC CHART: ALTITUDE 1700m BAROMETRIC PRESSURE 82.5 kPa

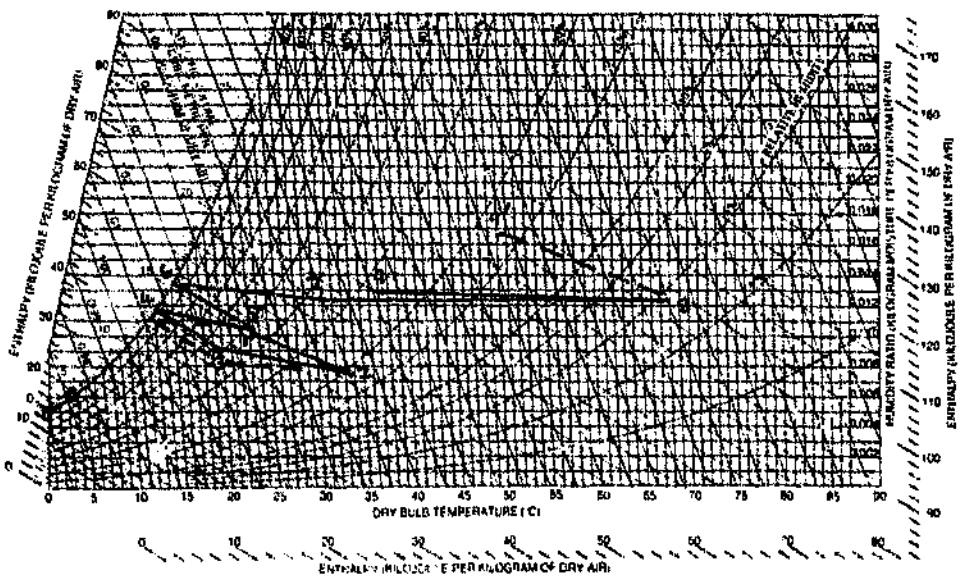

RESULTS OF DEC TEST (sheet 1 of 2) DATE: 5-6-1997
********** TIME: 16H29

TEST NUMBER: H3/9

OPERATING PARAMETERS (MEASURED AND ENTERED AS INPUT)

		NOM.	MIN.	MAX.
Supply air flow rate	(g/s)=	147	137	156
Return air flow rate	(g/s)=	98	89	107
Regen. heat input	(kW)=	3.670	3.523	3.817
Elec. energy (excl. reg.)	(kW)=	2.607	2.503	2.711
Spray chambers: water T	(oC)=	19.2	19.0	19.4
Water flow rate (S S/CH)	(g/s)=	1.47	1.40	1.54
at pressure	(bar)=	57	55	59
Water flow rate (R S/CH)	(g/s)=	2.30	2.18	2.41
at pressure	(bar)=	70	68	72

PROCESS CHANGES OF ENTHALPY AND HUMIDITY RATIO

ST PT	END PT	H (kJ/KG) NOM.	MIN.	MAX.	SIM.	W (g/kg) NOM.	MIN.	MAX.	SIM.
1	2	3.9	2.4	5.3	3.9	-2.50	-2.94	-2.05	-2.50
2	3	-9.4	-10.8	-8.1	-12.0	1.66	1.24	2.08	0.57
3	4	-0.6	-1.9	0.8	-0.1	2.47	2.06	2.87	3.04
4	5	7.3	5.9	8.7	9.3	-1.32	-1.75	-0.88	-0.80
5	6	0.6	-0.9	2.1	0.2	3.48	3.02	3.93	3.33
6	7	12.9	11.3	14.5	13.1	-1.05	-1.56	-0.54	-0.80
7	8	38.2	36.4	40.0	37.4	0.00	-0.56	0.56	0.00
8	9	-30.7	-32.5	-28.9	-7.4	0.39	-0.19	0.96	3.73

PERFORMANCE PARAMETERS (CALCULATED)

			NOM.	MIN.	MAX.	SIM.
Dehumidifier eff.(W)	(%)	EDH1=	37	30	44	38
Dehumidifier eff.(Q)	(%)	EDH2=	10	6	13	10
Regeneration eff.	(%)	ERG=	3	-1	6	25
Regen. heat input	(kW)	Q =	3.75	3.36	4.14	3.67
Heat Exch. eff. (SUP)	(%)	EHXS=	76	74	78	76
Heat Exch. eff. (RET)	(%)	EHXR=	86	83	88	86
Sup. air spr. ch. eff.	(%)	EVS=	99	92	106	99
Ret. air spr. ch. eff.	(%)	EVR=	101	94	107	100
FOR VENTILATION MODE:						
Cooling capacity	(kW)	CC =	1.07	0.85	1.29	1.36
Coeff. of performance		COP=	0.29	0.23	0.35	0.37
Electricity eff. ratio		EER=	0.41	0.33	0.50	0.52
FOR VENTILATION CREDIT MODE:						
Cooling capacity	(kW)	TCC =	0.90	0.69	1.12	1.20
Total Coeff. of perf.		TCOP=	0.25	0.19	0.31	0.33
Electricity eff. ratio		TEER=	0.35	0.26	0.43	0.46

RESULTS OF DEC TEST (sheet 2 of 2) DATE: 5-6-1997
********** TIME: 16H29

MOIST AIR PROPERTIES AT MEASURED POINTS IN PROCESS

NOMINAL MEASURED VALUES:

PT	TDB (oC)	TWB (oC)	TDP (oC)	PW (kPa)	W (g/kg)	RH (%)	U (%)	SV (m3/kg)	H (kJ/kg)
1	23.1	15.1	10.7	1.29	9.86	45	45	1.047	48.34
2	33.2	16.3	6.5	0.97	7.36	19	18	1.078	52.21
3	19.8	13.3	9.4	1.18	9.02	51	50	1.034	42.76
4	13.1	13.0	13.0	1.50	11.49	99	99	1.014	42.17
5	23.5	15.4	11.2	1.33	10.17	46	45	1.049	49.48
6	15.5	15.6	15.6	1.77	13.65	101	101	1.026	50.10
7	30.7	19.3	14.4	1.64	12.60	37	36	1.078	63.03
8	67.9	27.7	14.4	1.64	12.60	6	4	1.210	101.25
9	37.0	21.2	14.9	1.69	12.99	27	25	1.101	70.52

VALUES FOR TDB & W FROM ERROR ANALYSIS & SIMULATION :
(UNITS AS ABOVE)

PT	1	2	3	4	5	6	7	8	9
TDB(MIN)	22.9	33.0	19.6	12.9	23.3	15.3	30.4	67.6	36.8
TDB(MAX)	23.4	33.4	20.0	13.3	23.7	15.7	30.9	68.1	37.2
W (MIN)	9.5	7.1	8.7	11.2	9.9	13.3	12.2	12.2	12.6
W (MAX)	10.2	7.7	9.3	11.8	10.5	14.0	13.0	13.0	13.4
TDB(SIM)	23.1	33.2	20.0	12.4	23.5	15.4	30.2	66.6	50.0
W (SIM)	9.9	7.4	7.9	11.0	10.2	13.5	12.7	12.7	16.4

POSITION OF SAMPLING POINTS



PSYCHROMETRIC CHART: ALTITUDE 1700m BAROMETRIC PRESSURE 82.5 kPa

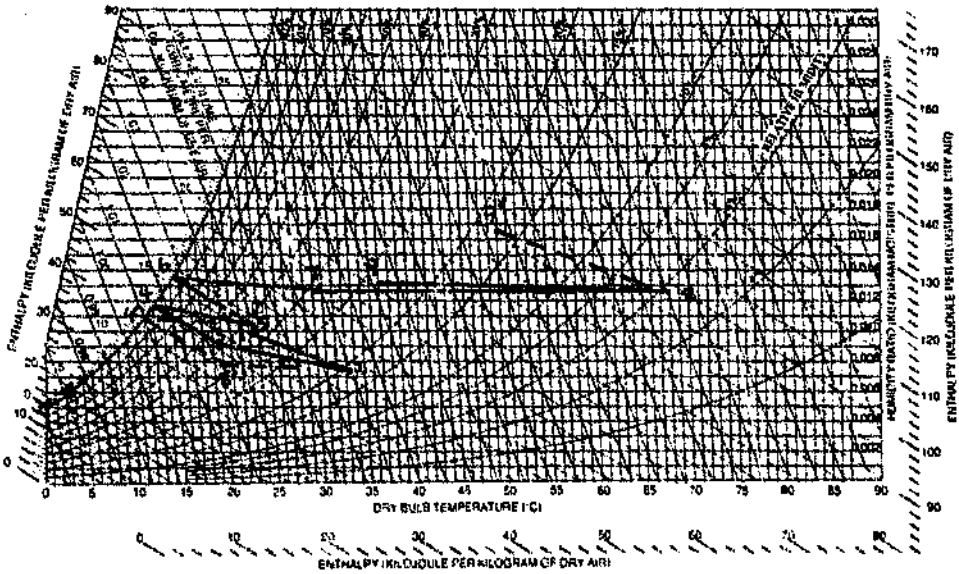

RESULTS OF DEC TEST (sheet 1 of 2) DATE: 5-6-1997
********** TIME: 16H12

TEST NUMBER: H3/10

OPERATING PARAMETERS (MEASURED AND ENTERED AS INPUT)

		NOM.	MIN.	MAX.
Supply air flow rate	(g/s)=	147	138	156
Return air flow rate	(g/s)=	98	89	107
Regen. heat input	(kW)=	3.670	3.523	3.817
Elec. energy (excl. reg.)	(kW)=	2.674	2.567	2.781
Spray chambers: water T	(oC)=	19.2	19.0	19.4
Water flow rate (S S/CH)	(g/s)=	1.47	1.40	1.54
at pressure	(bar)=	57	55	59
Water flow rate (R S/CH)	(g/s)=	2.47	2.35	2.59
at pressure	(bar)=	80	78	82

PROCESS CHANGES OF ENTHALPY AND HUMIDITY RATIO

ST PT	END PT	H (kJ/KG) NOM.	MIN.	MAX.	SIM.	W (g/kg) NOM.	MIN.	MAX.	SIM.
1	2	4.1	2.7	5.5	4.1	-2.40	-2.82	-1.98	-2.40
2	3	-6.9	-8.3	-5.5	-11.0	2.39	1.97	2.80	0.70
3	4	-1.1	-2.4	0.3	-0.1	2.69	2.28	3.10	3.57
4	5	9.3	7.8	10.7	12.4	-0.90	-1.34	-0.47	-0.09
5	6	0.9	-0.6	2.4	0.2	3.65	3.18	4.11	3.45
6	7	13.3	11.6	14.9	13.0	-1.02	-1.54	-0.50	-1.00
7	8	40.8	39.0	42.6	37.3	0.00	-0.57	0.57	0.00
8	9	-37.2	-39.1	-35.3	-7.7	-0.65	-1.24	-0.07	3.59

PERFORMANCE PARAMETERS (CALCULATED)

			NOM.	MIN.	MAX.	SIM.
Dehumidifier eff.(W)	(%)	EDH1=	41	33	48	43
Dehumidifier eff.(Q)	(%)	EDH2=	10	7	13	11
Regeneration eff.	(%)	ERG=	-4	-0	-8	24
Regen. heat input	(kW)	Q =	4.01	3.60	4.42	3.67
Heat Exch. eff. (SUP)	(%)	EHXS=	74	72	76	74
Heat Exch. eff. (RET)	(%)	EHXR=	89	87	91	89
Sup. air spr. ch. eff.	(%)	EVS=	99	92	105	99
Ret. air spr. ch. eff.	(%)	EVR=	100	94	106	100
FOR VENTILATION MODE:						
Cooling capacity	(kW)	CC =	1.36	1.13	1.59	1.82
Coeff. of performance		COP=	0.37	0.31	0.43	0.50
Electricity eff. ratio		EER=	0.51	0.42	0.60	0.68
FOR VENTILATION CREDIT MODE:						
Cooling capacity	(kW)	TCC =	0.56	0.36	0.76	1.02
Total Coeff. of perf.		TCOP=	0.15	0.10	0.21	0.28
Electricity eff. ratio		TEER=	0.21	0.13	0.29	0.38

RESULTS OF DEC TEST (sheet 2 of 2) DATE: 5-6-1997
********** TIME: 16H12

MOIST AIR PROPERTIES AT MEASURED POINTS IN PROCESS

NOMINAL MEASURED VALUES:

PT	TDB (oC)	TWB (oC)	TDP (oC)	PW (kPa)	W (g/kg)	RH (%)	U (%)	SV (m3/kg)	H (kJ/kg)
1	23.1	14.0	8.6	1.11	8.50	39	39	1.045	44.83
2	33.2	15.3	3.8	0.80	6.10	16	15	1.076	48.96
3	20.4	13.0	8.5	1.11	8.48	46	46	1.035	42.07
4	12.7	12.6	12.6	1.46	11.17	99	99	1.012	41.01
5	24.0	15.7	11.3	1.34	10.27	45	44	1.051	50.27
6	15.9	15.9	15.9	1.81	13.92	100	100	1.028	51.16
7	31.3	19.7	14.8	1.68	12.90	37	35	1.081	64.43
8	70.9	28.5	14.8	1.68	12.90	5	3	1.222	105.20
9	36.4	20.6	14.0	1.59	12.24	26	25	1.098	68.01

VALUES FOR TDB & W FROM ERROR ANALYSIS & SIMULATION :
(UNITS AS ABOVE)

PT	1	2	3	4	5	6	7	8	9
TDB(MIN)	22.9	33.0	20.2	12.5	23.8	15.7	31.1	70.7	36.2
TDB(MAX)	23.3	33.4	20.7	13.0	24.2	16.1	31.5	71.2	36.6
W (MIN)	8.2	5.8	8.2	10.9	9.9	13.6	12.5	12.5	11.8
W (MAX)	8.8	6.4	8.8	11.5	10.6	14.3	13.3	13.3	12.7
TDB(SIM)	23.1	33.2	20.6	11.7	24.0	15.7	30.8	67.1	50.6
W (SIM)	8.5	6.1	6.8	10.4	10.3	13.7	12.7	12.7	16.3

POSITION OF SAMPLING POINTS



PSYCHROMETRIC CHART: ALTITUDE 1700m BAROMETRIC PRESSURE 82.5 kPa

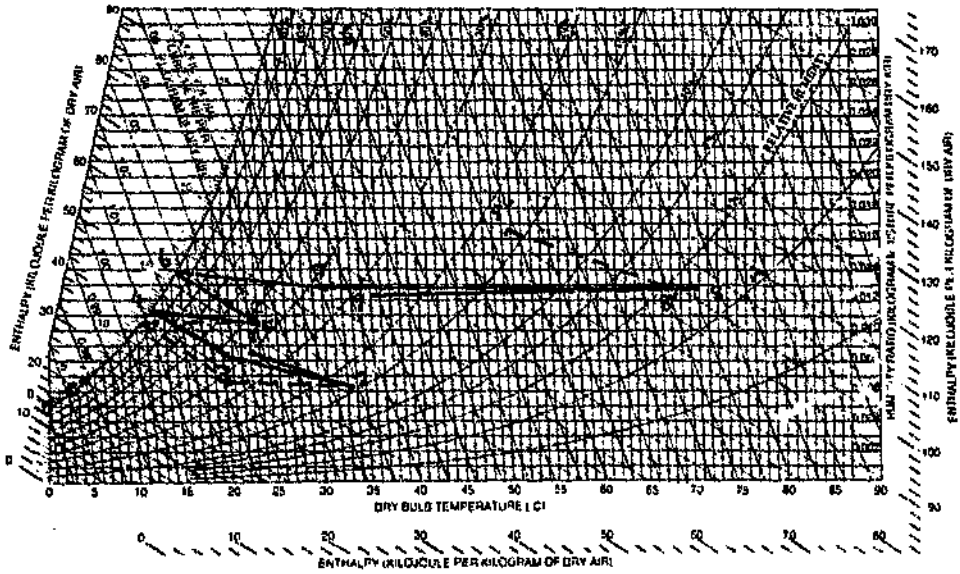

RESULTS OF DEC TEST (sheet 1 of 2) DATE: 4-6-1997
********** TIME: 18H10

TEST NUMBER: H3/11

OPERATING PARAMETERS (MEASURED AND ENTERED AS INPUT)

		NOM.	MIN.	MAX.
Supply air flow rate	(g/s)=	146	137	155
Return air flow rate	(g/s)=	147	138	156
Regen. heat input	(kW)=	5.317	5.104	5.530
Elec. energy (excl. reg.)	(kW)=	1.768	1.697	1.839
Spray chambers: water T	(oC)=	19.2	19.0	19.4
Water flow rate (S S/CH)	(g/s)=	1.69	1.61	1.77
at pressure	(bar)=	59	57	61
Water flow rate (R S/CH)	(g/s)=	0.00	0.00	0.00
at pressure	(bar)=	0	0	2

PROCESS CHANGES OF ENTHALPY AND HUMIDITY RATIO

ST PT	END PT	H (kJ/KG) NOM.	MIN.	MAX.	SIM.	W (g/kg) NOM.	MIN.	MAX.	SIM.
1	2	4.3	2.9	5.8	4.3	-3.38	-3.82	-2.93	-3.38
2	3	-8.8	-10.2	-7.4	-10.6	1.18	0.75	1.60	0.34
3	4	-0.5	-1.8	0.9	0.0	3.91	3.50	4.33	4.40
4	5	4.9	3.5	6.3	6.2	-1.60	-2.03	-1.17	-1.25
5	6	-0.2	-1.6	1.3	0.0	0.15	-0.29	0.59	0.22
6	7	11.2	9.7	12.8	10.2	-0.04	-0.52	0.45	-0.32
7	8	38.0	36.4	39.7	36.2	0.00	-0.51	0.51	0.00
8	9	-21.1	-23.0	-19.2	-5.9	2.29	1.69	2.90	3.35

PERFORMANCE PARAMETERS (CALCULATED)

			NOM.	MIN.	MAX.	SIM.
Dehumidifier eff.(W)	(%)	EDH1=	46	39	52	46
Dehumidifier eff.(Q)	(%)	EDH2=	11	7	14	12
Regeneration eff.	(%)	ERG=	16	12	20	23
Regen. heat input	(kW)	Q =	5.58	5.17	6.00	5.32
Heat Exch. eff. (SUP)	(%)	EHXS=	85	82	88	86
Heat Exch. eff. (RET)	(%)	EHXR=	82	79	85	82
Sup. air spr. ch. eff.	(%)	EVS=	99	94	103	99
Ret. air spr. ch. eff.	(%)	EVR=	7	3	12	7
FOR VENTILATION MODE:						
Cooling capacity	(kW)	CC =	0.71	0.50	0.92	0.90
Coeff. of performance		COP=	0.13	0.09	0.17	0.17
Electricity eff. ratio		EER=	0.40	0.28	0.52	0.51
FOR VENTILATION CREDIT MODE:						
Cooling capacity	(kW)	TCC =	0.71	0.50	0.93	0.91
Total Coeff. of perf.		TCOP=	0.13	0.09	0.17	0.17
Electricity eff. ratio		TEER=	0.40	0.28	0.53	0.51

RESULTS OF DEC TEST (sheet 2 of 2) DATE: 4-6-1997
********** TIME: 15H10

MOIST AIR PROPERTIES AT MEASURED POINTS IN PROCESS

NOMINAL MEASURED VALUES:

PT	TDB (oC)	TWB (oC)	TDP (oC)	PW (kPa)	W (g/kg)	RH (%)	U (%)	SV (m3/kg)	H (kJ/kg)
1	22.4	14.9	10.8	1.30	9.92	48	47	1.045	47.75
2	35.1	16.3	4.8	0.86	6.55	15	14	1.084	52.10
3	23.5	13.5	7.2	1.01	7.72	35	34	1.045	43.31
4	13.4	13.3	13.2	1.51	11.64	99	99	1.016	42.85
5	22.1	15.9	11.0	1.31	10.04	49	48	1.044	47.73
6	21.6	14.8	11.2	1.33	10.19	52	51	1.042	47.56
7	32.6	18.2	11.2	1.32	10.15	27	26	1.081	58.78
8	69.8	27.0	11.2	1.32	10.15	4	3	1.212	96.79
9	43.4	22.5	14.2	1.62	12.45	18	17	1.123	75.73

VALUES FOR TDB & W FROM ERROR ANALYSIS & SIMULATION :
(UNITS AS ABOVE)

PT	1	2	3	4	5	6	7	8	9
TDB(MIN)	22.2	34.9	23.3	13.2	21.9	21.4	32.4	69.6	43.2
TDB(MAX)	22.6	35.4	23.8	13.6	22.4	21.8	32.9	70.0	43.6
W (MIN)	9.6	6.2	7.4	11.3	9.7	9.9	9.8	9.8	12.0
W (MAX)	10.3	6.9	8.0	11.9	10.4	10.5	10.5	10.5	12.9
TDB(SIM)	22.4	35.1	23.9	13.0	22.1	21.6	32.4	67.8	53.5
W (SIM)	9.9	6.5	6.9	11.3	10.0	10.3	9.9	9.9	13.3

POSITION OF SAMPLING POINTS



PSYCHROMETRIC CHART: ALTITUDE 1700m BAROMETRIC PRESSURE 82.5 kPa

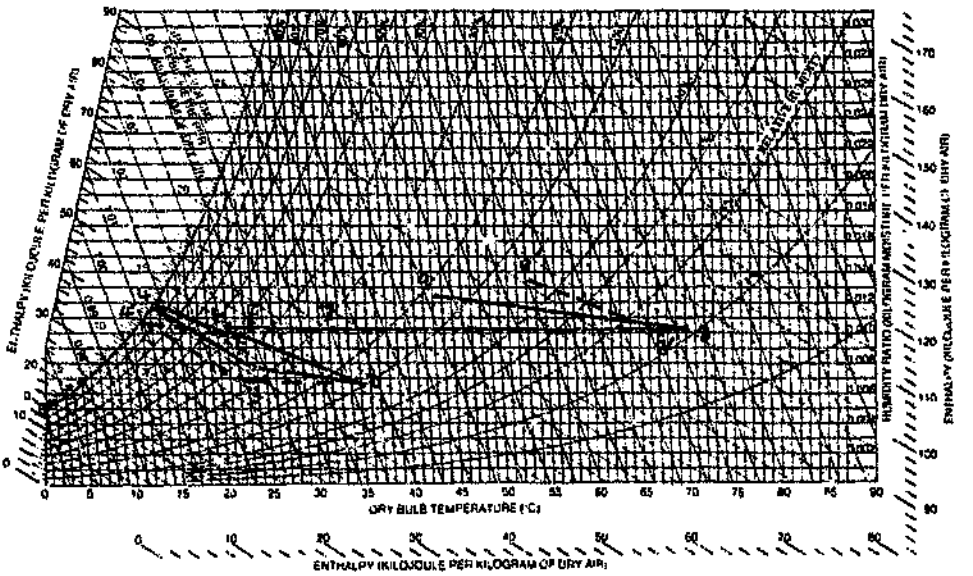

RESULTS OF DEC TEST (sheet 1 of 2) DATE: 4-6-1997
********** TIME: 17H43

TEST NUMBER: H3/12

OPERATING PARAMETERS (MEASURED AND ENTERED AS INPUT)

		NOM.	MIN.	MAX.
Supply air flow rate	(g/s)=	146	136	155
Return air flow rate	(g/s)=	147	138	155
Regen. heat input	(kW)=	5.317	5.104	5.530
Elec. energy (excl. reg.)	(kW)=	1.800	1.728	1.872
Spray chambers: water T	(oC)=	19.3	19.1	19.5
Water flow rate (S S/CH)	(g/s)=	1.69	1.61	1.77
at pressure	(bar)=	59	57	61
Water flow rate (K S/CH)	(g/s)=	0.64	0.61	0.67
at pressure	(bar)=	2	0	4

PROCESS CHANGES OF ENTHALPY AND HUMIDITY RATIO

ST	END	H (kJ/KG)				W (g/kg)			
PT	PT	NOM.	MIN.	MAX.	SIM.	NOM.	MIN.	MAX.	SIM.
1	2	4.5	3.1	6.0	4.5	-3.30	-3.76	-2.85	-3.30
2	3	-10.7	-12.1	-9.3	-12.0	1.00	0.57	1.43	0.32
3	4	-0.1	-1.5	1.2	0.0	3.52	3.10	3.93	3.89
4	5	4.3	2.9	5.7	5.5	-1.79	-2.21	-1.38	-1.48
5	6	-0.0	-1.4	1.4	0.0	0.78	0.35	1.21	0.80
6	7	11.7	10.2	13.2	11.4	-0.31	-0.77	0.16	-0.31
7	8	38.2	36.6	39.8	36.3	0.00	-0.50	0.50	0.00
8	9	-19.7	-21.5	-17.8	-6.2	2.55	1.96	3.14	3.28

PERFORMANCE PARAMETERS (CALCULATED)

			NOM.	MIN.	MAX.	SIM.
Dehumidifier eff.(W)	(%)	EDH1=	43	37	49	44
Dehumidifier eff.(Q)	(%)	EDH2=	11	8	15	12
Regeneration eff.	(%)	ERG=	18	13	22	23
Regen. heat input	(kW)	Q =	5.60	5.19	6.02	5.32
Heat Exch. eff. (SUP)	(%)	EHXS=	86	83	88	86
Heat Exch. eff. (RET)	(%)	EHXR=	80	78	83	80
Sup. air spr. ch. eff.	(%)	EVS=	99	94	105	99
Ret. air spr. ch. eff.	(%)	EVR=	27	22	31	27
FOR VENTILATION MODE:						
Cooling capacity	(kW)	CC =	0.63	0.42	0.83	0.60
Coeff. of performance		COP=	0.12	0.08	0.16	0.15
Electricity eff. ratio		EER=	0.35	0.23	0.46	0.44
FOR VENTILATION CREDIT MODE:						
Cooling capacity	(kW)	TCC =	0.92	0.70	1.13	1.09
Total Coeff. of perf.		TCOP=	0.17	0.13	0.21	0.21
Electricity eff. ratio		TEER=	0.51	0.39	0.63	0.61

RESULTS OF DEC TEST (sheet 1 of 2) DATE: 4-6-1997
********** TIME: 17H43

MOIST AIR PROPERTIES AT MEASURED POINTS IN PROCESS

NOMINAL MEASURED VALUES:

PT	TDB (oC)	TWB (oC)	TDP (oC)	PW (kPa)	W (g/kg)	RH (%)	U (%)	SV (m3/kg)	H (kJ/kg)
1	22.5	15.3	11.6	1.36	10.42	50	49	1.046	49.07
2	35.2	16.7	6.0	0.93	7.12	16	15	1.085	53.59
3	22.2	13.3	7.9	1.06	8.12	40	39	1.041	42.91
4	13.3	13.2	13.2	1.52	11.64	99	99	1.015	42.77
5	21.9	14.7	10.7	1.29	9.84	49	48	1.043	47.06
6	20.0	14.7	11.8	1.39	10.62	59	59	1.037	47.05
7	32.2	18.2	11.4	1.35	10.31	28	27	1.080	58.76
8	69.6	27.0	11.4	1.35	10.31	4	3	1.212	96.99
9	43.9	22.8	14.7	1.67	12.87	18	17	1.126	77.33

VALUES FOR TDB & W FROM ERROR ANALYSIS & SIMULATION :
(UNITS AS ABOVE)

PT	1	2	3	4	5	6	7	8	9
TDB(MIN)	22.3	34.9	21.9	13.1	21.7	19.8	32.0	69.3	43.7
TDB(MAX)	22.7	35.4	22.4	13.5	22.2	20.2	32.4	69.8	44.1
W (MIN)	10.1	6.8	7.8	11.4	9.5	10.3	10.0	10.0	12.4
W (MAX)	10.8	7.4	8.4	11.9	10.2	10.9	10.7	10.7	13.3
TDB(SIM)	22.5	35.2	22.5	12.9	21.9	20.0	31.9	67.4	53.0
W (SIM)	10.4	7.1	7.4	11.3	9.8	10.6	10.3	10.3	13.6

POSITION OF SAMPLING POINTS



PSYCHROMETRIC CHART: ALTITUDE 1700m BAROMETRIC PRESSURE 82.5 kPa

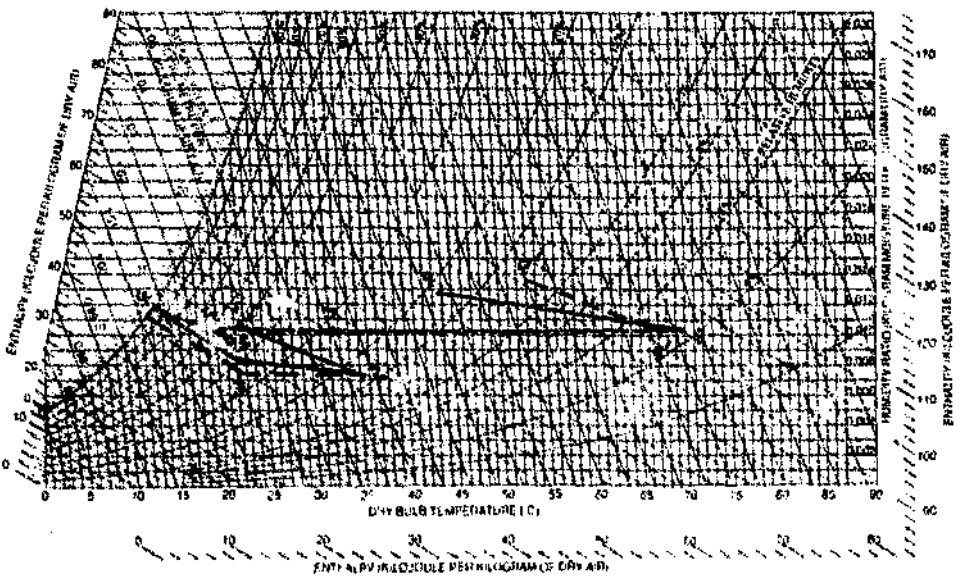

RESULTS OF DEC TEST (sheet 1 of 2) DATE: 4-6-1997
********** TIME: 17H21

TEST NUMBER: H3/13

OPERATING PARAMETERS (MEASURED AND ENTERED AS INPUT)

		NOM.	MIN.	MAX.
Supply air flow rate	(g/s)=	145	136	155
Return air flow rate	(g/s)=	146	137	155
Regen. heat input	(kW)=	5.317	5.104	5.530
Elec. energy (excl. reg.)	(kW)=	1.845	1.771	1.919
Spray chambers: water T	(oC)=	19.0	18.8	19.2
Water flow rate (S S/CH)	(g/s)=	1.69	1.61	1.77
at pressure	(bar)=	59	57	61
Water flow rate (R S/CH)	(g/s)=	0.89	0.85	0.93
at pressure	(bar)=	10	8	12

PROCESS CHANGES OF ENTHALPY AND HUMIDITY RATIO

ST PT	END PT	H (kJ/KG) NOM	MIN.	MAX.	SIM.	W (g/kg) NOM.	MIN.	MAX.	SIM.
1	2	5.0	3.5	6.5	5.0	-2.81	-3.28	-2.35	-2.81
2	3	-13.2	-14.6	-11.8	-13.3	0.48	0.04	0.92	0.30
3	4	-0.2	-1.6	1.2	-0.1	3.13	2.72	3.54	3.32
4	5	4.7	3.3	6.1	4.7	-1.63	-2.06	-1.21	-1.64
5	6	-0.1	-1.6	1.3	-.1	1.18	0.74	1.62	1.25
6	7	12.6	11.0	14.2	12.6	-0.42	-0.92	0.08	-0.28
7	8	38.4	36.7	40.2	36.3	0.00	-0.55	0.55	0.00
8	9	-19.5	-21.4	-17.6	-7.0	2.58	1.97	3.19	2.79

PERFORMANCE PARAMETERS (CALCULATED)

			NOM.	MIN.	MAX.	SIM.
Dehumidifier eff.(W)	(%)	EDH1=	36	30	42	37
Dehumidifier eff.(Q)	(%)	EDH2=	12	9	16	13
Regeneration eff.	(%)	ERG=	18	13	22	19
Regen. heat input	(kW)	Q =	5.63	5.20	6.05	5.32
Heat Exch. eff. (S.)	(%)	EHXS=	86	83	88	86
Heat Exch. eff. (ET)	(%)	EHXR=	81	78	83	81
Sup. air spr. ch. eff.	(%)	EVS=	99	93	105	99
Ret. air spr. ch. eff.	(%)	EVR=	43	38	48	43
FOR VENTILATION MODE:						
Cooling capacity	(kW)	CC =	0.68	0.48	0.89	0.68
Coeff. of performance		COP=	0.13	0.09	0.17	0.13
Electricity eff. ratio		EER=	0.37	0.26	0.48	0.37
FOR VENTILATION CREDIT MODE:						
Cooling capacity	(kW)	TCC =	1.23	1.00	1.45	1.22
Total Coeff. of perf.		TCOP=	0.23	0.19	0.27	0.23
Electricity eff. ratio		TEER=	0.66	0.54	0.79	0.66

RESULTS OF DEC TEST (sheet 2 of 2) DATE: 4-6-1997
********** TIME: 17H21

MOIST AIR PROPERTIES AT MEASURED POINTS IN PROCESS

NOMINAL MEASURED VALUES:

PT	TDB (oC)	TWB (oC)	TDP (oC)	PW (kPa)	W (g/kg)	RH (%)	U (%)	SV (m3/kg)	H (kJ/kg)
1	23.4	15.9	12.1	1.41	10.80	49	48	1.050	51.03
2	35.3	17.4	7.7	1.05	7.98	18	17	1.087	56.00
3	21.2	13.3	8.5	1.11	8.47	44	43	1.038	42.79
4	13.2	13.2	13.2	1.51	11.60	99	99	1.015	42.59
5	21.9	14.7	10.9	1.30	9.96	50	49	1.043	47.29
6	18.8	14.7	12.6	1.45	11.14	67	66	1.034	47.15
7	32.1	18.4	12.0	1.40	10.72	29	28	1.080	59.75
8	69.7	27.2	12.0	1.40	10.72	5	3	1.213	98.20
9	44.1	23.1	15.2	1.73	13.30	19	17	1.127	78.69

VALUES FOR TDB & W FROM ERROR ANALYSIS & SIMULATION :
(UNITS AS ABOVE)

PT	1	2	3	4	5	6	7	8	9
TDB(MIN)	23.2	35.1	21.0	13.0	21.6	18.6	31.9	69.5	43.9
TDB(MAX)	23.7	35.6	21.4	13.5	22.1	19.0	32.4	69.9	44.4
W (MIN)	10.5	7.7	8.2	11.3	9.7	10.8	10.3	10.3	12.8
W (MAX)	11.1	8.3	8.8	11.9	10.3	11.5	11.1	11.1	13.8
TDB(SIM)	23.4	35.3	21.6	13.3	21.9	18.8	31.9	67.3	53.4
W (SIM)	10.8	8.0	8.3	11.6	10.0	11.2	10.9	10.9	13.7

POSITION OF SAMPLING POINTS



PSYCHROMETRIC CHART: ALTITUDE 1700m BAROMETRIC PRESSURE 82.5 kPa

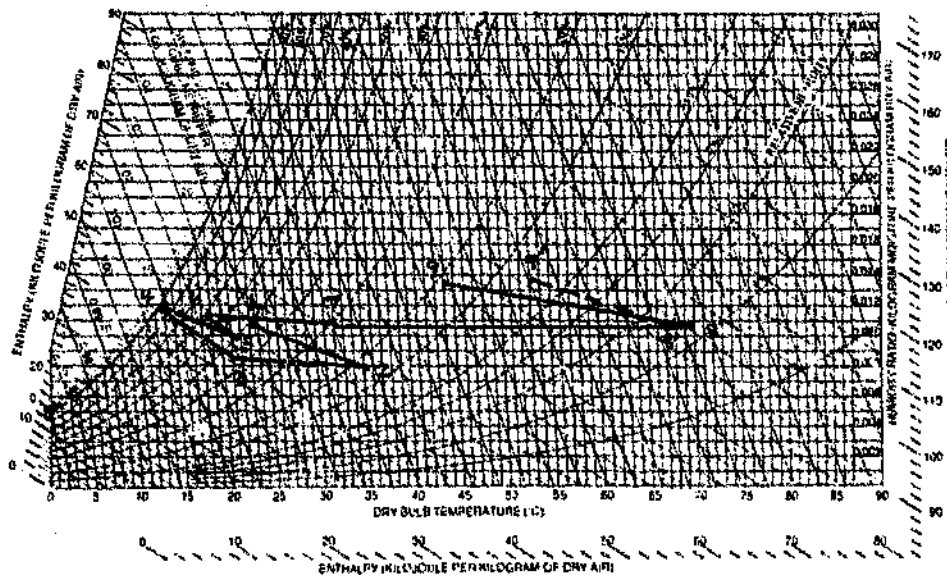

RESULTS OF DEC TEST (sheet 1 of 2) DATE: 4-6-1997
********** TIME: 16H58

TEST NUMBER: H3/14

OPERATING PARAMETERS (MEASURED AND ENTERED AS INPUT)

		NOM.	MIN.	MAX.
Supply air flow rate	(g/s)=	146	137	155
Return air flow rate	(g/s)=	147	138	156
Regen. heat input	(kW)=	5.317	5.104	5.530
Elec. energy (excl. reg.)	(kW)=	1.874	1.799	1.949
Spray chambers: water T	(oC)=	19.0	18.8	19.2
Water flow rate (S S/CH)	(g/s)=	1.69	1.61	1.77
at pressure	(bar)=	59	57	61
Water flow rate (R S/CH)	(g/s)=	1.17	1.11	1.23
at pressure	(bar)=	20	18	22

PROCESS CHANGES OF ENTHALPY AND HUMIDITY RATIO

ST PT	END PT	H (kJ/KG) NOM.	MIN.	MAX.	SIM.	W (g/kg) NOM.	MIN.	MAX.	SIM.
1	2	3.7	2.3	5.2	3.7	-3.15	-3.59	-2.71	-3.15
2	3	-11.6	-13.0	-10.2	-13.5	1.38	0.98	1.79	0.44
3	4	-0.3	-1.6	1.0	-0.0	2.89	2.50	3.28	3.40
4	5	6.1	4.7	7.5	7.8	-1.34	-1.76	-0.92	-0.91
5	6	-0.1	-1.5	1.4	0.1	1.75	1.30	2.19	1.80
6	7	13.4	11.8	15.0	13.4	-0.51	-1.02	-0.01	-0.41
7	8	38.5	36.7	40.3	36.2	0.00	-0.56	0.56	0.00
8	9	-21.4	-23.4	-19.5	-5.4	2.15	1.53	2.77	3.13

PERFORMANCE PARAMETERS (CALCULATED)

			NOM.	MIN.	MAX.	SIM.
Dehumidifier eff.(W)	(%)	EDH1=	44	38	51	46
Dehumidifier eff.(Q)	(%)	EDH2=	10	6	13	10
Regeneration eff.	(%)	ERG=	15	10	19	22
Regen. heat input	(kW)	Q =	5.66	5.23	6.09	5.31
Heat Exch. eff. (SUP)	(%)	EHXS=	85	83	87	85
Heat Exch. eff. (RET)	(%)	EHXR=	82	80	85	82
Sup. air spr. ch. eff.	(%)	EVS=	99	92	105	99
Ret. air spr. ch. eff.	(%)	EVR=	60	55	65	60
FOR VENTILATION MODE:						
Cooling capacity	(kW)	CC =	0.89	0.68	1.10	1.13
Coeff. of performance		COP=	0.17	0.13	0.21	0.21
Electricity eff. ratio		EER=	0.47	0.36	0.59	0.60
FOR VENTILATION CREDIT MODE:						
Cooling capacity	(kW)	TCC =	1.19	0.97	1.41	1.44
Total Coeff. of perf.		TCOP=	0.22	0.18	0.27	0.27
Electricity eff. ratio		TEER=	0.64	0.52	0.75	0.77

RESULTS OF DEC TEST (sheet 2 of 2) DATE: 4-6-1997
********** TIME: 16H58

MOIST AIR PROPERTIES AT MEASURED POINTS IN PROCESS

NOMINAL MEASURED VALUES:

PT	TDB (oC)	TWB (oC)	TDP (oC)	PW (kPa)	W (g/kg)	RH (%)	U (%)	SV (m3/kg)	H (kJ/kg)
1	23.3	15.2	10.8	1.29	9.92	45	44	1.048	48.65
2	34.8	16.4	5.3	0.89	6.77	16	15	1.083	52.37
3	20.0	12.6	8.0	1.07	8.15	46	45	1.033	40.78
4	12.6	12.5	12.4	1.44	11.04	99	99	1.012	40.48
5	21.8	14.5	10.5	1.27	9.70	49	48	1.042	46.56
6	17.4	14.5	13.0	1.49	11.45	75	75	1.029	46.48
7	31.8	18.5	12.3	1.43	10.93	30	29	1.080	59.92
8	69.4	27.2	12.3	1.43	10.93	5	3	1.213	98.42
9	43.1	22.7	15.0	1.70	13.08	20	18	1.123	77.00

VALUES FOR TDB & W FROM ERROR ANALYSIS & SIMULATION :
(UNITS AS ABOVE)

PT	1	2	3	4	5	6	7	8	9
TDB(MIN)	23.1	34.6	19.8	12.3	21.6	17.2	31.6	69.1	42.8
TDB(MAX)	23.5	35.1	20.2	12.8	22.0	17.6	32.0	69.6	43.3
W (MIN)	9.6	6.5	7.9	10.8	9.4	11.1	10.5	10.5	12.6
W (MAX)	10.2	7.1	8.4	11.3	10.0	11.8	11.3	11.3	13.6
TDB(SIM)	23.3	34.8	20.5	12.0	21.8	17.4	31.5	66.8	53.6
W (SIM)	9.9	6.8	7.2	10.6	9.7	11.5	11.1	11.1	14.2

POSITION OF SAMPLING POINTS



PSYCHROMETRIC CHART: ALTITUDE 1700m BAROMETRIC PRESSURE 82.5 kPa

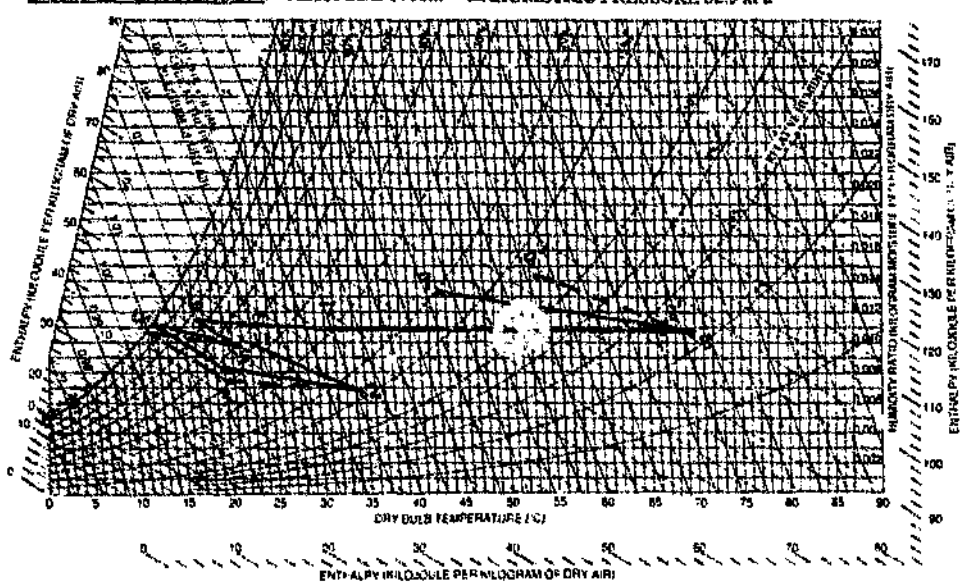

RESULTS OF DEC TEST (sheet 1 of 2) DATE: 4-6-1997
********** TIME: 1[illegible]

TEST NUMBER: H3/15

OPERATING PARAMETERS (MEASURED AND ENTERED AS INPUT)

		NOM.	MIN.	MAX.
Supply air flow rate	(g/s)=	145	136	155
Return air flow rate	(g/s)=	147	138	155
Regen. heat input	(kW)=	5.317	5.104	5.530
Elec. energy (excl. reg.)	(kW)=	1.897	1.821	1.973
Spray chambers: water T	(oC)=	19.2	19.0	19.4
Water flow rate (S S/CH)	(g/s)=	1.69	1.61	1.77
at pressure	(bar)=	59	57	61
Water flow rate (R S/CH)	(g/s)=	1.26	1.20	1.32
at pressure	(bar)=	30	28	32

PROCESS CHANGES OF ENTHALPY AND HUMIDITY RATIO

ST PT	END PT	H (kJ/KG) NOM.	MIN.	MAX.	SIM.	W (g/kg) NOM.	MIN.	MAX.	SIM.
1	2	4.2	2.7	5.7	4.2	-3.02	-3.48	-2.57	-3.02
2	3	-13.4	-14.8	-12.0	-14.9	1.19	0.76	1.61	0.41
3	4	-0.0	-1.4	1.3	-0.1	2.60	2.20	3.00	2.98
4	5	5.3	3.9	6.7	6.8	-1.59	-2.02	-1.16	-1.20
5	6	-0.1	-1.6	1.3	0.1	2.18	1.74	2.63	2.25
6	7	15.0	13.4	16.6	14.7	-0.43	-0.93	0.07	-0.39
7	8	38.6	36.9	40.3	36.3	0.00	-0.55	0.55	0.00
8	9	-21.2	-23.1	-19.3	-5.7	2.12	1.52	2.72	3.00

PERFORMANCE PARAMETERS (CALCULATED)

			NOM.	MIN.	MAX.	SIM.
Dehumidifier eff.(W)	(%)	EDH1=	41	34	47	42
Dehumidifier eff.(Q)	(%)	EDH2=	11	7	14	11
Regeneration eff.	(%)	ERG=	15	10	19	21
Regen. heat input	(kW)	Q =	5.66	5.23	6.08	5.31
Heat Exch. eff. (SUP)	(%)	EHXS=	85	83	87	85
Heat Exch. eff. (RET)	(%)	EHXR=	83	81	85	83
Sup. air spr. ch. eff.	(%)	EVS=	98	91	106	98
Ret. air spr. ch. eff.	(%)	EVR=	73	68	79	73
FOR VENTILATION MODE:						
Cooling capacity	(kW)	CC =	0.77	0.56	0.98	0.99
Coeff. of performance		COP=	0.15	0.11	0.19	0.19
Electricity eff. ratio		EER=	0.41	0.30	0.52	0.52
FOR VENTILATION CREDIT MODE:						
Cooling capacity	(kW)	TCC =	1.35	1.12	1.57	1.57
Total Coeff. of perf.		TCOP=	0.25	0.21	0.30	0.29
Electricity eff. ratio		TEER=	0.71	0.59	0.83	0.83

RESULTS OF DEC TEST (sheet 2 of 2) DATE: 4-6-1997
********** TIME: 16H43

MOIST AIR PROPERTIES AT MEASURED POINTS IN PROCESS

NOMINAL MEASURED VALUES:

PT	TDB (oC)	TWB (oC)	TDP (oC)	PW (kPa)	W (g/kg)	RH (%)	U (%)	SV (m3/kg)	H (kJ/kg)
1	23.7	15.7	11.6	1.36	10.43	46	46	1.050	50.35
2	35.4	17.0	6.6	0.97	7.41	17	16	1.086	54.52
3	19.2	12.7	8.7	1.12	8.59	50	50	1.031	41.11
4	12.8	12.7	12.6	1.46	11.19	99	99	1.013	41.08
5	21.9	14.5	10.3	1.25	9.60	48	47	1.042	46.39
6	16.4	14.4	13.4	1.53	11.78	82	82	1.026	46.29
7	32.1	18.9	12.8	1.48	11.35	31	30	1.081	61.30
8	69.7	27.5	12.8	1.48	11.35	5	3	1.215	99.90
9	43.7	23.1	15.4	1.75	13.47	20	18	1.126	78.68

VALUES FOR TDB & W FROM ERROR ANALYSIS & SIMULATION :
(UNITS AS ABOVE)

PT	1	2	3	4	5	6	7	8	9
TDB(MIN)	23.5	35.1	19.0	12.6	21.7	16.2	31.9	69.5	43.5
TDB(MAX)	23.9	35.6	19.4	13.0	22.1	16.6	32.3	70.0	43.9
W (MIN)	10.1	7.1	8.3	10.9	9.3	11.5	11.0	11.0	13.0
W (MAX)	10.8	7.7	8.9	11.5	9.9	12.1	11.7	11.7	13.9
TDB(SIM)	23.7	35.4	19.7	12.3	21.9	16.4	31.7	67.1	54.0
W (SIM)	10.4	7.4	7.8	10.8	9.6	11.8	11.5	11.5	14.5

POSITION OF SAMPLING POINTS



PSYCHROMETRIC CHART: ALTITUDE 1700m BAROMETRIC PRESSURE 82.5 kPa

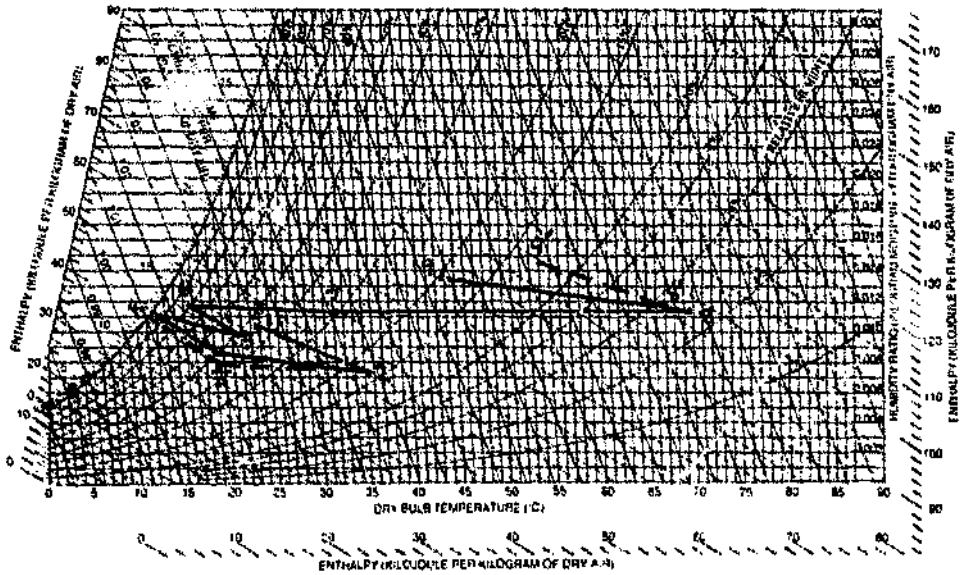

RESULTS OF DEC TEST (sheet 1 of 2) DATE: 4-6-1997
********** TIME: 16H23

TEST NUMBER: H3/16

OPERATING PARAMETERS (MEASURED AND ENTERED AS INPUT)

		NOM.	MIN.	MAX.
Supply air flow rate	(g/s)=	146	137	155
Return air flow rate	(g/s)=	147	138	155
Regen. heat input	(kW)=	5.317	5.104	5.530
Elec. energy (excl. reg.)	(kW)=	1.922	1.845	1.999
Spray chambers: water T	(oC)=	19.4	19.2	19.6
Water flow rate (S S/CH)	(g/s)=	1.69	1.61	1.77
at pressure	(bar)=	59	57	61
Water flow rate (R S/CH)	(g/s)=	1.59	1.51	1.67
at pressure	(bar)=	40	38	42

PROCESS CHANGES OF ENTHALPY AND HUMIDITY RATIO

ST PT	END PT	H (kJ/KG) NOM.	MIN.	MAX.	SIM.	W (g/kg) NOM.	MIN.	MAX.	SIM.
1	2	4.4	3.0	5.8	4.4	-2.78	-3.20	-2.37	-2.78
2	3	-10.1	-11.4	-8.8	-14.4	2.57	2.18	2.97	0.66
3	4	0.1	-1.2	1.4	-0.1	2.86	2.46	3.25	3.68
4	5	8.5	7.1	9.8	12.9	-0.77	-1.17	-0.36	0.32
5	6	-0.3	-1.7	1.1	0.1	2.38	1.95	2.81	2.50
6	7	14.9	13.3	16.5	14.5	-0.65	-1.14	-0.15	-0.62
7	8	38.5	36.8	40.2	36.3	0.00	-0.55	0.55	0.00
8	9	-22.5	-24.4	-20.6	-6.2	1.50	0.91	2.10	2.78

PERFORMANCE PARAMETERS (CALCULATED)

			NOM.	MIN.	MAX.	SIM.
Dehumidifier eff.(W)	(%)	EDH1=	51	42	59	53
Dehumidifier eff.(Q)	(%)	EDH2=	11	8	14	12
Regeneration eff.	(%)	ERG=	10	6	15	19
Regen. heat input	(kW)	Q =	5.65	5.22	6.07	5.31
Heat Exch. eff. (SUP)	(%)	EHXS=	85	82	87	85
Heat Exch. eff. (RET)	(%)	EHXR=	83	81	85	83
Sup. air spr. ch. eff.	(%)	EVS=	100	93	107	100
Ret. air spr. ch. eff.	(%)	EVR=	83	77	90	83
FOR VENTILATION MODE:						
Cooling capacity	(kW)	CC =	1.24	1.02	1.45	1.88
Coeff. of performance		COP=	0.23	0.19	0.27	0.35
Electricity eff. ratio		EER=	0.64	0.53	0.76	0.98
FOR VENTILATION CREDIT MODE:						
Cooling capacity	(kW)	TCC =	0.83	0.62	1.03	1.47
Total Coeff. of perf.		TCOP=	0.16	0.12	0.19	0.25
Electricity eff. ratio		TEER=	0.43	0.32	0.54	0.77

RESULTS OF DEC TEST (sheet 2 of 2) DATE: 4-6-1997
********** TIME: 16H23

MOIST AIR PROPERTIES AT MEASURED POINTS IN PROCESS

NOMINAL MEASURED VALUES:

PT	TDB (oC)	TWB (oC)	TDP (oC)	PW (kPa)	W (g/kg)	RH (%)	U (%)	SV (m3/kg)	H (kJ/kg)
1	23.9	13.8	7.6	1.04	7.96	35	34	1.047	44.26
2	35.2	15.2	1.5	0.68	5.18	12	11	1.082	48.63
3	18.8	11.8	7.2	1.02	7.75	47	46	1.028	38.52
4	11.8	11.8	11.8	1.38	10.61	100	100	1.008	38.59
5	22.0	14.7	10.7	1.28	9.84	49	48	1.043	47.06
6	15.8	14.5	13.9	1.59	12.22	89	88	1.025	46.77
7	31.9	18.9	13.1	1.51	11.57	32	31	1.081	61.65
8	69.4	27.5	13.1	1.51	11.57	5	3	1.214	100.16
9	43.7	22.9	15.0	1.70	13.07	19	17	1.126	77.66

VALUES FOR TDB & W FROM ERROR ANALYSIS & SIMULATION :
(UNITS AS ABOVE)

PT	1	2	3	4	5	6	7	8	9
TDB(MIN)	23.7	34.9	18.6	11.6	21.7	15.6	31.7	69.2	43.5
TDB(MAX)	24.1	35.4	19.0	12.0	22.2	16.0	32.1	69.6	43.9
W (MIN)	7.7	4.9	7.5	10.3	9.5	11.9	11.2	11.2	12.6
W (MAX)	8.3	5.5	8.0	10.9	10.1	12.5	12.0	12.0	13.5
TDB(SIM)	23.9	35.2	19.3	10.2	22.0	15.9	31.6	66.9	53.9
W (SIM)	8.0	5.2	5.8	9.5	9.8	12.3	11.7	11.7	14.5

POSITION OF SAMPLING POINTS



PSYCHROMETRIC CHART: ALTITUDE 1700m BAROMETRIC PRESSURE 82.5 kPa

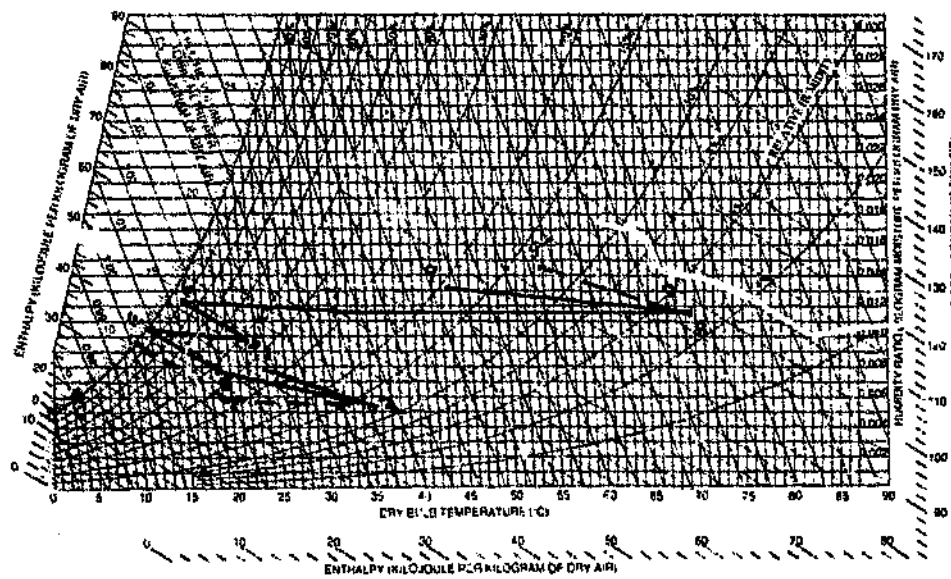

RESULTS OF DEC TEST (sheet 1 of 2) DATE: 4-6-1997
********** TIME: 15H59

TEST NUMBER: H3/17

OPERATING PAR ..IERS (MEASURED AND ENTERED AS INPUT)

		NOM.	MIN.	MAX.
Supply air flow rate	(g/s)=	145	136	154
Return air flow rate	(g/s)=	147	138	156
Regen. heat input	(kW)=	5.317	5.104	5.530
Elec. energy (excl. reg.)	(kW)=	1.951	1.873	2.029
Spray chambers: water T	(oC)=	18.9	18.7	19.1
Water flow rate (S S/CH)	(g/s)=	1.69	1.61	1.77
at pressure	(bar)=	59	57	61
Water flow rate (R S/CH)	(g/s)=	1.76	1.67	1.85
at pressure	(bar)=	50	48	52

PROCESS CHANGES OF ENTHALPY AND HUMIDITY RATIO

ST PT	END PT	H (kJ/KG) NOM.	MIN.	MAX.	SIM.	W (g/kg) NOM.	MIN.	MAX.	SIM.
1	2	3.9	2.4	5.4	3.9	-3.43	-3.88	-2.97	-3.43
2	3	-13.0	-14.4	-11.6	-16.1	1.94	1.51	2.37	0.50
3	4	-0.2	-1.5	1.2	-0.1	2.28	1.87	2.68	2.96
4	5	5.7	4.3	7.1	8.7	-1.54	-1.96	-1.12	-0.79
5	6	-0.1	-1.5	1.3	0.1	2.69	2.25	3.12	2.75
6	7	15.1	13.7	16.6	15.6	-0.82	-1.31	-0.33	-0.47
7	8	38.5	36.7	40.2	36.2	0.00	-0.54	0.54	0.00
8	9	-21.3	-23.2	-19.5	-5.4	2.27	1.66	2.87	3.39

PERFORMANCE PARAMETERS (CALCULATED)

			NOM.	MIN.	MAX.	SIM.
Dehumidifier eff.(W)	(%)	EDH1=	47	40	53	49
Dehumidifier eff.(Q)	(%)	EDH2=	10	6	14	11
Regeneration eff.	(%)	ERG=	16	11	20	23
Regen. heat input	(kW)	Q =	5.64	5.22	6.07	5.31
Heat Exch. eff. (SUP)	(%)	EHXS=	85	83	87	85
Heat Exch. eff. (RET)	(%)	EHXR=	80	79	82	80
Sup. air spr. ch. eff.	(%)	EVS=	99	90	108	99
Ret. air spr. ch. eff.	(%)	EVR=	89	82	95	89
FOR VENTILATION MODE:						
Cooling capacity	(kW)	CC =	0.83	0.62	1.04	1.26
Coeff. of performance		COP=	0.16	0.12	0.20	0.24
Electricity eff. ratio		EER=	0.43	0.32	0.53	0.65
FOR VENTILATION CREDIT MODE:						
Cooling capacity	(kW)	TCC =	1.35	1.13	1.58	1.78
Total Coeff. of perf.		TCOP=	0.25	0.21	0.30	0.34
Electricity eff. ratio		TEER=	0.69	0.58	0.81	0.91

RESULTS OF DEC TEST (sheet 2 of 2) DATE: 4-6-1997
**** ************** TIME: 15H59

MOIST AIR PROPERTIES AT MEASURED POINTS IN PROCESS

NOMINAL MEASURED VALUES:

PT	TDB (oC)	TWB (oC)	TDP (oC)	PW (kPa)	W (g/kg)	RH (%)	U (%)	SV (m3/kg)	H (kJ/kg)
1	23.7	15.7	11.5	1.35	10.39	46	45	1.050	50.26
2	36.1	16.9	5.7	0.91	6.96	15	14	1.088	54.13
3	18.5	12.7	9.2	1.16	8.90	55	54	1.029	41.12
4	12.7	12.6	12.6	1.46	11.17	99	99	1.012	40.93
5	22.1	14.5	10.4	1.26	9.63	47	47	1.043	46.65
6	15.3	14.5	14.1	1.60	12.32	92	92	1.023	46.56
7	32.0	18.9	13.0	1.50	11.50	31	30	1.081	61.63
8	69.5	27.5	13.0	1.50	11.50	5	3	1.214	100.09
9	43.0	23.1	15.7	1.79	13.77	21	19	1.124	78.75

VALUES FOR TDB & W FROM ERROR ANALYSIS & SIMULATION :
(UNITS AS ABOVE)

PT	1	2	3	4	5	6	7	8	9
TDB(MIN)	23.5	35.9	18.3	12.4	21.8	15.1	31.8	69.3	42.8
TDB(MAX)	24.0	36.3	18.7	12.9	22.3	15.6	32.3	69.8	43.3
W (MIN)	10.1	6.6	8.6	10.9	9.3	12.0	11.1	11.1	13.3
W (MAX)	10.7	7.3	9.2	11.5	9.9	12.6	11.9	11.9	14.2
TDB(SIM)	23.7	36.1	19.0	11.6	22.1	15.4	31.7	67.0	53.2
W (SIM)	10.4	7.0	7.5	10.4	9.6	12.4	11.9	11.9	15.3

POSITION OF SAMPLING POINTS



PSYCHROMETRIC CHART: ALTITUDE 1700m BAROMETRIC PRESSURE 82.5 kPa

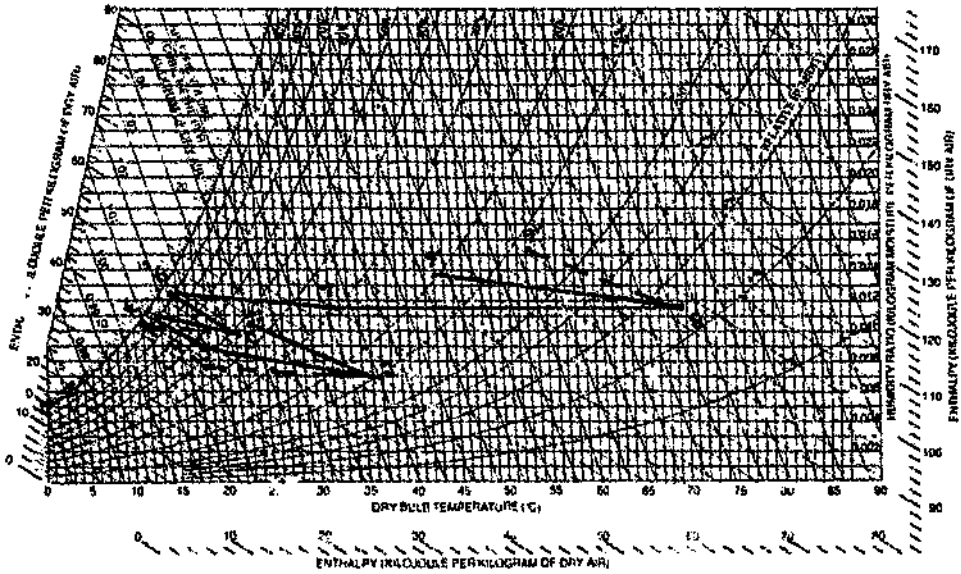

RESULTS OF DEC TEST (sheet 1 of 2) DATE: 4-6-1997
********** TIME: 15H30

TEST NUMBER: H3/18

OPERATING PARAMETERS (MEASURED AND ENTERED AS INPUT)

		NOM.	MIN.	MAX.
Supply air flow rate	(g/s)=	146	137	155
Return air flow rate	(g/s)=	146	138	155
Regen. heat input	(kW)=	5.317	5.104	5.530
Elec. energy (excl. reg.)	(kW)=	1.987	1.908	2.066
Spray chambers: water T	(oC)=	18.9	18.7	19.1
Water flow rate (S S/CH)	(g/s)=	1.69	1.61	1.77
at pressure	(bar)=	59	57	61
Water flow rate (R S/CH)	(g/s)=	2.13	2.02	2.24
at pressure	(bar)=	60	58	62

PROCESS CHANGES OF ENTHALPY AND HUMIDITY RATIO

ST PT	END PT	H (kJ/KG) NOM.	MIN.	MAX.	SIM.	W (g/kg) NOM.	MIN.	MAX.	SIM.
1	2	3.5	2.1	5.0	3.5	-3.00	-3.44	-2.56	-3.00
2	3	-12.5	-13.9	-11.1	-15..	1.82	1.40	2.23	0.51
3	4	0.0	-1.3	1.3	0.1	2.32	1.94	2.71	2.94
4	5	6.0	4.6	7.4	8.7	-1.52	-1.93	-1.11	-0.83
5	6	0.1	-1.3	1.6	0.1	2.90	2.46	3.34	2.91
6	7	14.9	13.4	16.5	15.5	-0.84	-1.33	-0.35	-0.48
7	8	38.1	36.4	39.8	36.3	0.00	-0.53	0.53	0.00
8	9	-20.7	-22.6	-18.8	-5.4	1.83	1.22	2.44	2.99

PERFORMANCE PARAMETERS (CALCULATED)

			NOM.	MIN.	MAX.	SIM.
Dehumidifier eff.(W)	(%)	EDH1=	44	37	50	45
Dehumidifier eff.(Q)	(%)	EDH2=	9	6	13	10
Regeneration eff.	(%)	ERG=	13	8	17	21
Regen. heat input	(kW)	Q =	5.58	5.16	6.00	5.31
Heat Exch. eff. (SUP)	(%)	EHXS=	84	82	86	84
Heat Exch. eff. (RET)	(%)	EHXR=	83	81	85	83
Sup. air spr. ch. eff.	(%)	EVS=	101	92	110	101
Ret. air spr. ch. eff.	(%)	EVR=	94	87	100	94
FOR VENTILATION MODE:						
Cooling capacity	(kW)	CC =	0.88	0.67	1.08	1.28
Coeff. of performance		COP=	0.16	0.13	0.20	0.24
Electricity eff. ratio		EER=	0.44	0.33	0.55	0.64
FOR VENTILATION CREDIT MODE:						
Cooling capacity	(kW)	TCC =	1.30	1.08	1.52	1.70
Total Coeff. of perf.		TCOP=	0.24	0.20	0.29	0.32
Electricity eff. ratio		TEER=	0.65	0.54	0.77	0.86

RESULTS OF DEC TEST (sheet 2 of 2) DATE: 4-6-1997
******************* TIME: 15H30

MOIST AIR PROPERTIES AT MEASURED POINTS IN PROCESS

NOMINAL MEASURED VALUES:

PT	TDB (oC)	TWB (oC)	TDP (oC)	PW (kPa)	W (g/kg)	RH (%)	U (%)	SV (m3/kg)	H (kJ/kg)
1	23.9	15.4	10.9	1.30	9.95	44	43	1.050	49.34
2	34.9	16.5	5.6	0.91	6.94	16	15	1.084	52.88
3	18.1	12.5	9.0	1.15	8.76	55	55	1.028	40.40
4	12.4	12.4	12.5	1.44	11.09	101	101	1.011	40.42
5	22.0	14.5	10.3	1.25	9.57	47	46	1.043	46.42
6	15.0	14.5	14.2	1.62	12.47	95	95	1.022	46.54
7	31.6	18.9	13.2	1.51	11.63	33	31	1.080	61.48
8	68.7	27.4	13.2	1.51	11.63	5	3	1.212	99.61
9	44.0	23.2	15.4	1.75	13.46	19	17	1.127	78.89

VALUES FOR TDB & W FROM ERROR ANALYSIS & SIMULATION :
(UNITS AS ABOVE)

PT	1	2	3	4	5	6	7	8	9
TDB(MIN)	23.7	34.7	17.9	12.2	21.8	14.7	31.4	68.5	43.7
TDB(MAX)	24.1	35.1	18.3	12.6	22.2	15.2	31.8	69.0	44.2
W (MIN)	9.6	6.6	8.5	10.8	9.3	12.2	11.3	11.3	13.0
W (MAX)	10.3	7.3	9.0	11.4	9.9	12.8	12.0	12.0	13.9
TDB(SIM)	23.9	34.9	18.6	11.4	22.0	15.0	31.2	66.6	53.7
W (SIM)	9.9	6.9	7.5	10.4	9.6	12.5	12.0	12.0	15.0

POSITION OF SAMPLING POINTS



PSYCHROMETRIC CHART: ALTITUDE 1700m BAROMETRIC PRESSURE 82.5 kPa

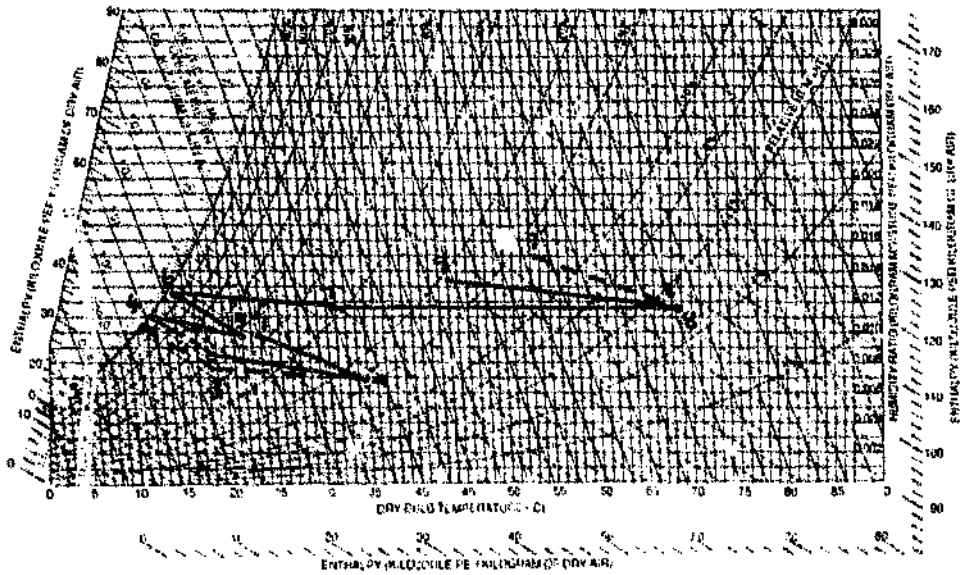

RESULTS OF DEC TEST (sheet 1 of 2) DATE: 4- 1997
********** TIME: 15H12

TEST NUMBER: H3/19

OPERATING PARAMETERS (MEASURED AND ENTERED AS INPUT)

		NOM.	MIN.	MAX.
Supply air flow rate	(g/s)=	146	136	155
Return air flow rate	(g/s)=	147	138	156
Regen. heat input	(kW)=	5.317	5.104	5.530
Elec. energy (excl. reg.)	(kW)=	1.995	1.915	2.075
Spray chambers' water T	(oC)=	18.9	18.7	19.1
Water flow rate (S S/CH)	(g/s)=	1.69	1.61	1.77
at pressure	(bar)=	59	57	61
Water flow rate (R S/CH)	(g/s)=	2.33	2.21	2.45
at pressure	(bar)=	70	68	72

PROCESS CHANGES OF ENTHALPY AND HUMIDITY RATIO

ST PT	END PT	H (kJ/KG) NOM.	MIN.	MAX.	SIM.	W (g/kg) NOM.	MIN.	MAX.	SIM.
1	2	3.2	1.8	4.7	3.2	-3.11	-3.55	-2.66	-3.11
2	3	-12.6	-13.9	-11.2	-15.8	2.05	1.64	2.46	0.57
3	4	-0.4	-1.7	0.9	0.0	2.20	1.81	2.59	2.97
4	5	7.5	6.2	8.9	10.3	-1.03	-1.45	-0.62	-0.33
5	6	0.1	-1.4	1.5	0.1	2.94	2.49	3.38	2.96
6	7	14.7	13.1	16.3	15.4	-0.94	-1.44	-0.44	-0.54
7	8	38.2	36.4	39.9	36.2	0.00	-0.54	0.54	0.00
8	9	-21.3	-23.2	-19.4	-4.7	1.91	1.30	2.52	3.08

PERFORMANCE PARAMETERS (CALCULATED)

			NOM.	MIN.	MAX.	SIM.
Dehumidifier eff.(W)	(%)	EDH1=	47	40	55	49
Dehumidifier eff.(Q)	(%)	EDH2=	9	5	13	9
Regeneration eff.	(%)	ERG=	13	9	18	21
Regen. heat input	(kW)	Q =	5.60	5.18	6.03	5.31
Heat Exch. eff. (SUP)	(%)	EHXS=	85	83	87	85
Heat Exch. eff. (RET)	(%)	EHXR=	81	79	83	81
Sup. air spr. ch. eff.(%)		EVS=	100	91	108	100
Ret. air spr. ch. eff.(%)		EVR=	97	90	104	97
FOR VENTILATION MODE:						
Cooling capacity	(kW)	CC =	1.10	0.88	1.31	1.50
Coeff. of performance		COP=	0.21	0.17	0.25	0.28
Electricity eff. ratio		EER=	0.55	0.44	0.66	0.75
FOR VENTILATION CREDIT MODE:						
Cooling capacity	(kW)	TCC =	1.42	1.20	1.64	1.83
Total Coeff. of perf.		TCOP=	0.27	0.22	0.31	0.34
Electricity eff. ratio		TEER=	0.71	0.60	0.83	0.92

RESULTS OF DEC TEST (sheet 2 of 2) DATE: 4-6-1997
********** TIME: 15H12

MOIST AIR PROPERTIES AT MEASURED POINTS IN PROCESS

NOMINAL MEASURED VALUES:

PT	TDB (oC)	TWB (oC)	TDP (oC)	PW (kPa)	W (g/kg)	RH (%)	U (%)	SV (m3/kg)	H (kJ/kg)
1	24.4	15.3	10.4	1.26	9.61	41	40	1.951	48.98
2	35.4	16.3	4.7	0.85	6.51	15	14	1.084	52.23
3	17.9	12.2	8.7	1.12	8.56	55	54	1.026	39.66
4	12.0	12.0	12.0	1.40	10.75	100	101	1.009	39.23
5	22.0	14.6	10.5	1.27	9.72	48	47	1.043	46.76
6	14.8	14.6	14.5	1.65	12.66	98	98	1.022	46.83
7	31.4	18.9	13.3	1.53	11.72	33	32	1.079	61.52
8	68.6	27.4	13.3	1.53	11.72	5	3	1.211	99.69
9	43.0	23.1	15.6	1.77	13.63	20	19	1.124	78.38

VALUES FOR TDB & W FROM ERROR ANALYSIS & SIMULATION :
(UNITS AS ABOVE)

PT	1	2	3	4	5	6	7	8	9
TDB(MIN)	24.2	35.1	17.7	11.8	21.7	14.5	31.2	68.4	42.8
TDB(MAX)	24.6	35.6	18.1	12.3	22.2	15.0	31.6	68.8	43.2
W (MIN)	9.3	6.2	8.3	10.5	9.4	12.3	11.3	11.3	13.2
W (MAX)	9.9	6.8	8.8	11.0	10.0	13.0	12.1	12.1	14.1
TDB(SIM)	24.4	35.4	18.4	11.1	22.0	14.8	31.1	66.3	53.9
W (SIM)	9.6	6.5	7.1	10.1	9.7	12.7	12.1	12.1	15.2

POSITION OF SAMPLING POINTS



PSYCHROMETRIC CHART: ALTITUDE 1700m BAROMETRIC PRESSURE 82.5 kPa

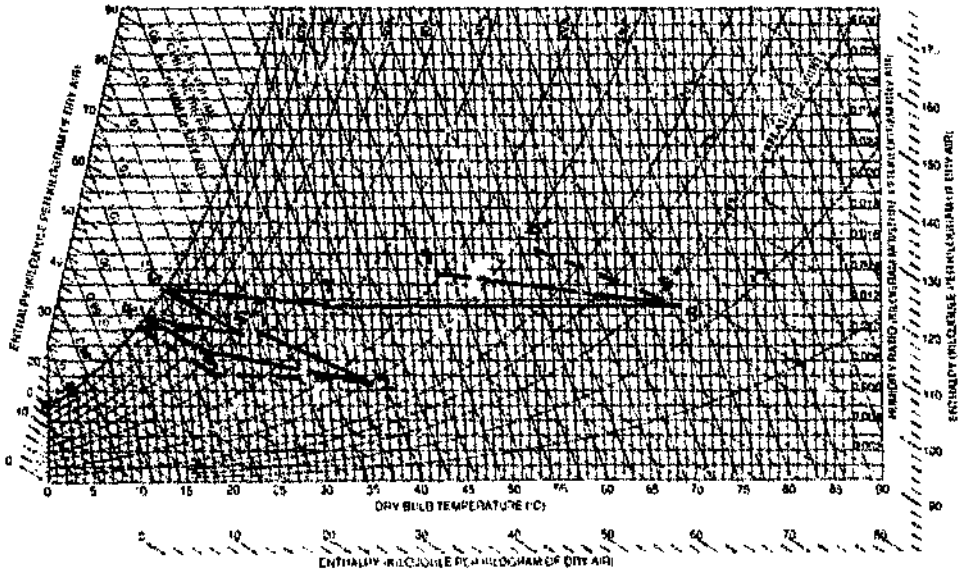

RESULTS OF DEC TEST (sheet 1 of 2) DATE: 4-6-1997
********** TIME: 14H58

TEST NUMBER: H3/20

OPERATING PARAMETERS (MEASURED AND ENTERED AS INPUT)

		NOM.	MIN.	MAX.
Supply air flow rate	(g/s)=	147	137	156
Return air flow rate	(g/s)=	147	138	156
Regen. heat input	(kW)=	5.317	5.104	5.530
Elec. energy (excl. reg.)	(kW)=	2.062	1.980	2.144
Spray chambers: water T	(oC)=	18.9	18.7	19.1
Water flow rate (S S/CH)	(g/s)=	1.69	1.61	1.77
at pressure	(bar)=	59	57	61
Water flow rate (R S/CH)	(g/s)=	2.56	2.43	2.69
at pressure	(bar)=	80	78	82

PROCESS CHANGES OF ENTHALPY AND HUMIDITY RATIO

ST PT	END PT	H (kJ/KG) NOM.	MIN.	MAX.	SIM.	W (g/kg) NOM.	MIN.	MAX.	SIM.
1	2	3.4	1.9	4.8	3.4	-2.50	-2.94	-2.06	-2.50
2	3	-13.2	-14.6	-11.9	-14.9	1.32	0.92	1.72	0.46
3	4	-1.0	-2.3	0.3	-0.1	1.78	1.41	2.16	2.43
4	5	7.3	6.0	8.7	8.2	-1.20	-1.59	-0.81	-0.99
5	6	0.1	-1.3	1.5	0.1	3.09	2.67	3.50	3.10
6	7	13.3	11.8	14.8	14.0	-0.84	-1.32	-0.37	-0.44
7	8	38.2	36.5	39.8	36.1	0.00	-0.52	0.52	0.00
8	9	-20.2	-22.0	-18.3	-4.8	1.38	0.80	1.97	2.50

PERFORMANCE PARAMETERS (CALCULATED)

			NOM.	MIN.	MAX.	SIM.
Dehumidifier eff.(W)	(%)	EDH1=	39	31	46	41
Dehumidifier eff.(Q)	(%)	EDH2=	9	5	13	10
Regeneration eff.	(%)	ERG=	10	5	14	17
Regen. heat input	(kW)	Q =	5.61	5.19	6.03	5.31
Heat Exch. eff. (SUP)	(%)	EHXS=	85	83	88	85
Heat Exch. eff. (RET)	(%)	EHXR=	79	77	81	79
Sup. air spr. ch. eff.	(%)	EVS=	98	89	107	98
Ret. air spr. ch. eff.	(%)	EVR=	96	91	104	98
FOR VENTILATION MODE:						
Cooling capacity	(kW)	CC =	1.08	0.88	1.28	1.20
Coeff. of performance		COP=	0.20	0.16	0.24	0.23
Electricity eff. ratio		EER=	0.52	0.42	0.62	0.58
FOR VENTILATION CREDIT MODE:						
Cooling capacity	(kW)	TCC =	1.59	1.37	1.82	1.71
Total Coeff. of perf.		TCOP=	0.30	0.26	0.34	0.32
Electricity eff. ratio		TEER=	0.77	0.66	0.89	0.83

RESULTS OF DEC TEST (sheet 1 of 2) DATE: 4-6-1997
********** TIME: 14H58

MOIST AIR PROPERTIES AT MEASURED POINTS IN PROCESS

NOMINAL MEASURED VALUES:

PT	TDB (oC)	TWB (oC)	TDP (oC)	PW (kPa)	W (g/kg)	RH (%)	U (%)	SV (m3/kg)	H (kJ/kg)
1	23.3	14.8	10.1	1.24	9.46	43	42	1.047	47.50
2	32.9	15.9	5.7	0.91	6.96	18	17	1.077	50.87
3	16.6	11.5	8.2	1.08	8.28	57	57	1.021	37.64
4	11.2	11.1	11.0	1.31	10.06	99	99	1.005	36.64
5	21.4	13.7	9.2	1.16	8.86	46	45	1.039	43.99
6	13.8	13.7	13.6	1.55	11.94	98	98	1.018	44.08
7	28.9	17.8	12.5	1.45	11.10	36	35	1.070	57.38
8	66.1	26.7	12.5	1.45	11.10	6	4	1.201	95.54
9	43.0	22.4	14.3	1.62	12.49	19	17	1.122	75.36

VALUES FOR TDB & W FROM ERROR ANALYSIS & SIMULATION :
(UNITS AS ABOVE)

PT	1	2	3	4	5	6	7	8	9
TDB(MIN)	23.1	32.7	16.4	11.0	21.2	13.6	28.7	65.9	42.7
TDB(MAX)	23.6	33.1	16.8	11.5	21.6	14.1	29.1	66.3	43.2
W (MIN)	9.1	6.7	8.0	9.8	8.6	11.6	10.7	10.7	12.0
W (MAX)	9.8	7.3	8.6	10.3	9.1	12.2	11.5	11.5	12.9
TDB(SIM)	23.3	32.9	17.1	10.9	21.4	13.9	28.6	63.8	52.8
W (SIM)	9.5	7.0	7.4	9.8	8.9	12.0	11.5	11.5	14.0

POSITION OF SAMPLING POINTS



PSYCHROMETRIC CHART ALTITUDE 1700m BAROMETRIC PRESSURE 82.5 kPa

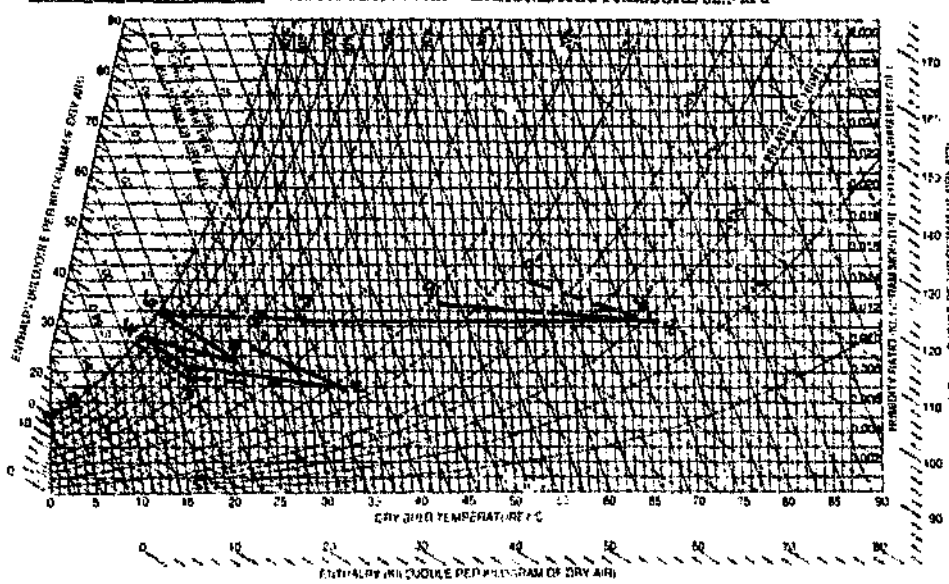

APPENDIX H4

EFFICIENCY OF SUPPLY AIR SPRAY CHAMBER

The results in this appendix are the computer printouts of seven tests (H4/1 to H4/7) that were done to investigate the effect that the efficiency of the supply air spray chamber had on overall DEC performance. The airflow was balanced and was approximately 0.15 kg/s for both the supply and return air and all operating parameters were kept constant. Only the flow rate of the water to the nozzles of the spray chamber was varied to change the efficiency of the spray chamber.

The more important results of these tests are given in tabular and graphical form in section 6.5.

RESULTS OF DEC TEST (sheet 1 of 2) DATE: 6-6-1997
********** TIME: 13H14

TEST NUMBER: H4/1

OPERATING PARAMETERS (MEASURED AND ENTERED AS INPUT)

		NOM.	MIN.	MAX.
Supply air flow rate	(g/s)=	146	137	155
Return air flow rate	(g/s)=	146	137	154
Regen. heat input	(kW)=	5.608	5.384	5.832
Elec. energy (excl. reg.)	(kW)=	1.233	1.181	1.282
Spray chambers: water T	(oC)=	18.8	18.6	19.0
Water flow rate (S S/CH)	(g/s)=	0.49	0.47	0.51
at pressure	(bar)=	2	0	4
Water flow rate (R S/CH)	(g/s)=	1.58	1.50	1.66
at pressure	(bar)=	40	38	42

PROCESS CHANGES OF ENTHALPY AND HUMIDITY RATIO

ST		H (kJ/KG)				W (g/kg)			
PT		NOM.	MIN.	MAX.	SIM.	NOM.	MIN.	MAX.	SIM.
1	2	3.8	2.4	5.3	3.8	-2.41	-2.56	-1.97	-2.41
2	3	-13.4	-14.8	-12.1	-13.6	0.83	0.42	1.23	0.47
3	4	-0.0	-1.3	1.3	-0.1	0.49	0.11	0.88	0.52
4	5	6.9	5.6	8.3	7.2	0.42	-0.00	0.84	0.75
5	6	-1.1	-2.5	0.3	0.2	2.97	2.54	3.41	3.33
6	7	16.4	14.8	18.0	15.6	-0.44	-0.93	0.05	-0.44
7	8	40.0	38.2	41.8	38.5	0.00	-0.55	0.55	0.00
8	9	-21.4	-23.4	-19.4	-5.7	1.98	1.34	2.62	2.42

PERFORMANCE PARAMETERS (CALCULATED)

			NOM.	MIN.	MAX.	SIM.
Dehumidifier eff.(W)	(%)	EDH1=	35	29	42	37
Dehumidifier eff.(Q)	(%)	EDH2=	9	6	13	10
Regeneration eff.	(%)	ERG=	13	9	17	16
Regen. heat input	(kW)	Q =	5.83	5.39	6.26	5.61
Heat Exch. eff. (SUP)	(%)	EHXS=	80	78	82	80
Heat Exch. eff. (RET)	(%)	EHXR=	89	87	91	89
Sup. air spr. ch. eff.	(%)	EVS=	17	13	22	17
Ret. air spr. ch. eff.	(%)	EVR=	87	82	92	87
FOR VENTILATION MODE:						
Cooling capacity	(kW)	CC =	1.01	0.80	1.22	1.05
Coeff. of performance		COP=	0.18	0.14	0.22	0.19
Electricity eff. ratio		EER=	0.82	0.65	1.00	0.85
FOR VENTILATION CREDIT MODE:						
Cooling capacity	(kW)	TCC =	1.40	1.18	1.63	1.44
Total Coeff. of perf.		TCOP=	0.25	0.21	0.29	0.26
Electricity eff. ratio		TEER=	1.14	0.95	1.32	1.17

RESULTS OF DEC TEST (sheet 2 of 2) DATE: 6-6-1997
********** TIME: 13H14

MOIST AIR PROPERTIES AT MEASURED POINTS IN PROCESS

NOMINAL MEASURED VALUES:

PT	TDB (oC)	TWB (oC)	TDP (oC)	PW (kPa)	W (g/kg)	RH (%)	U (%)	SV (m3/kg)	H (kJ/kg)
1	24.7	15.4	10.3	1.25	9.57	40	39	1.052	49.22
2	34.5	16.6	6.1	0.94	7.16	17	16	1.083	53.06
3	19.3	12.2	7.7	1.05	7.99	47	46	1.030	39.62
4	18.0	12.2	8.5	1.11	8.48	54	53	1.027	39.62
5	23.8	14.5	9.2	1.16	8.90	39	39	1.048	46.55
6	15.4	14.1	13.5	1.55	11.87	89	88	1.023	45.47
7	32.4	19.0	12.9	1.49	11.43	31	29	1.083	61.86
8	71.4	27.8	12.9	1.49	11.43	4	3	1.221	101.85
9	45.6	23.5	15.4	1.74	13.41	18	16	1.133	80.46

VALUES FOR TDB & W FROM ERROR ANALYSIS & SIMULATION :
(UNITS AS ABOVE)

PT	1	2	3	4	5	6	7	8	9
TDB(MIN)	24.5	34.3	19.1	17.8	23.6	15.1	32.2	71.2	45.4
TDB(MAX)	25.0	34.8	19.5	18.3	24.0	15.6	32.7	71.6	45.8
W (MIN)	9.3	6.9	7.7	8.2	8.6	11.6	11.0	11.0	12.9
W (MAX)	9.9	7.5	8.3	8.8	9.2	12.2	11.8	11.8	13.9
TDB(SIM)	24.7	34.5	20.0	18.6	23.8	15.7	32.1	69.6	57.9
W (SIM)	9.6	7.2	7.6	8.1	8.9	12.2	11.8	11.8	14.2

POSITION OF SAMPLING POINTS



PSYCHROMETRIC CHART: ALTITUDE 1700m BAROMETRIC PRESSURE 82.5 kPa

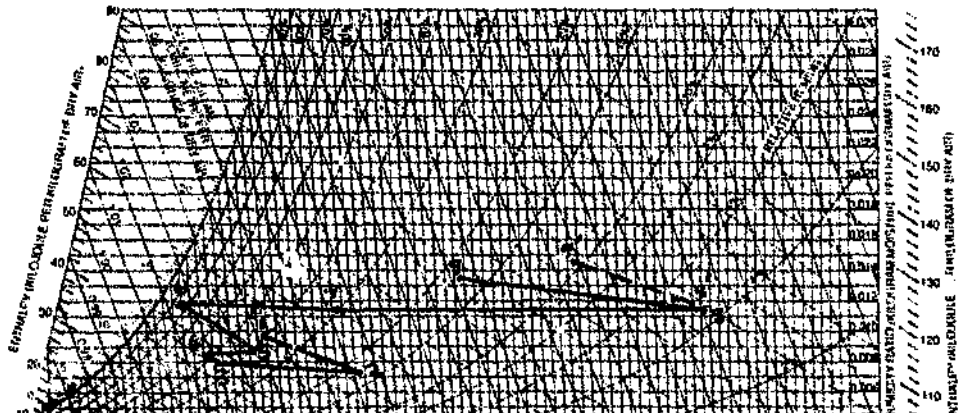

RESULTS OF DEC TEST (sheet 1 of 2) DATE: 6-6-1997
********** TIME: 13H10

TEST NUMBER: H4/2

OPERATING PARAMETERS (MEASURED AND ENTERED AS INPUT)

		NOM.	MIN.	MAX.
Supply air flow rate	(g/s)=	146	137	155
Return air flow rate	(g/s)=	146	137	155
Regen. heat input	(kW)=	5.608	5.384	5.832
Elec. energy (excl. reg.)	(kW)=	1.288	1.236	1.340
Spray chambers: water T	(oC)=	18.8	18.6	19.0
Water flow rate (S S/CH)	(g/s)=	0.58	0.55	0.61
at pressure	(bar)=	10	8	12
Water flow rate (R S/CH)	(g/s)=	1.58	1.50	1.66
at pressure	(bar)=	40	38	42

PROCESS CHANGES OF ENTHALPY AND HUMIDITY RATIO

ST PT	END PT	H (kJ/KG) NOM.	MIN.	MAX.	SIM.	W (g/kg) NOM.	MIN.	MAX.	SIM.
1	2	3.6	2.1	5.1	3.6	-2.37	-2.82	-1.92	-2.37
2	3	-13.0	-14.4	-11.6	-13.3	0.83	0.41	1.24	0.46
3	4	0.1	-1.2	1.4	0.0	0.88	0.50	1.27	0.93
4	5	6.6	5.2	7.9	7.0	-0.05	-0.46	0.35	0.27
5	6	-0.7	-2.2	0.7	0.2	3.04	2.60	3.48	3.39
6	7	16.0	14.5	17.6	15.4	-0.43	-0.93	0.07	-0.43
7	8	39.8	38 1	41.5	38.4	0.00	-0.55	0.55	0.00
8	9	-21.4	-23.4	-19.5	-5.5	2.25	1.62	2.88	2.37

PERFORMANCE PARAMETERS (CALCULATED)

			NOM.	MIN.	MAX.	SIM.
Dehumidifier eff.(W)	(%)	EDH1=	35	28	41	36
Dehumidifier eff.(Q)	(%)	EDH2=	9	5	12	9
Regeneration eff.	(%)	ERG=	15	10	19	15
Regen. heat input	(kW)	Q =	5.81	5.38	6.25	5.61
Heat Exch. eff. (SUP)	(%)	EHXS=	80	78	82	80
Heat Exch. eff. (RET)	(%)	EHXR=	90	87	92	90
Sup. air spr. ch. eff.	(%)	EVS=	30	25	34	30
Ret. air spr. ch. eff.	(%)	EVR=	87	82	91	87
FOR VENTILATION MODE:						
Cooling capacity	(kW)	CC =	0.96	0.75	1.17	1.02
Coeff. of performance		COP=	0.17	0.13	0.21	0.18
Electricity eff. ratio		EER=	0.74	0.58	0.91	0.79
FOR VENTILATION CREDIT MODE:						
Cooling capacity	(kW)	TCC =	1.35	1.13	1.58	1.42
Total Coeff. of perf.		TCOP=	0.24	0.20	0.28	0.25
Electricity eff. ratio		TEER=	1.05	0.87	1.23	1.10

RESULTS OF DEC TEST (sheet 2 of 2) DATE: 6-6-1997
********** TIME: 13H10

MOIST AIR PROPERTIES AT MEASURED POINTS IN PROCESS

NOMINAL MEASURED VALUES:

PT	TDB (oC)	TWB (oC)	TDP (oC)	PW (kPa)	W (g/kg)	RH (%)	U (%)	SV (m3/kg)	H (kJ/kg)
1	24.8	15.5	10.5	1.27	9.69	41	40	1.053	49.55
2	34.2	16.6	6.4	0.96	7.32	18	17	1.082	53.17
3	19.4	12.4	7.9	1.07	8.14	47	47	1.031	40.14
4	17.3	12.4	9.4	1.18	9.03	60	59	1.025	40.28
5	23.9	14.6	9.4	1.17	8.97	40	39	1.043	46.84
6	15.6	14.3	13.7	1.56	12.02	88	88	1.024	46.0[illegible]
7	32.3	19.1	13.1	1.51	11.59	31	30	1.082	62.13
8	71.1	27.8	13.1	1.51	11.59	5	3	1.220	101.94
9	44.6	23.5	15.8	1.80	13.84	19	17	1.130	80.52

VALUES FOR TDB & W FROM ERROR ANALYSIS & SIMULATION :
(UNITS AS ABOVE)

PT	1	2	3	4	5	6	7	8	9
TDB(MIN)	24.5	34.0	19.2	17.1	23.7	15.4	32.1	70.9	44.3
TDB(MAX)	25.0	34.5	19.6	17.6	24.1	15.8	32.5	71.3	44.8
W (MIN)	9.4	7.0	7.9	8.8	8.7	11.7	11.2	11.2	13.3
W (MAX)	10.0	7.6	8.4	9.3	9.3	12.3	12.0	12.0	14.3
TDB(SIM)	24.8	34.2	20.0	17.7	23.9	15.9	31.9	69.3	58.0
W (SIM)	9.7	7.3	7.8	8.7	9.0	12.3	11.8	11.8	14.2

POSITION OF SAMPLING POINTS



PSYCHROMETRIC CHART: ALTITUDE 1700m BAROMETRIC PRESSURE 82.5 kPa

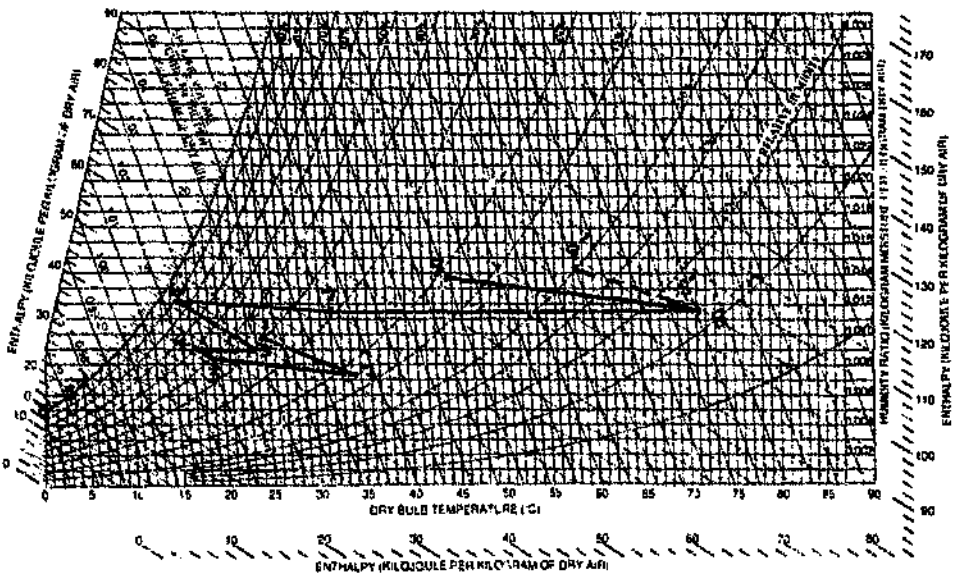

RESULTS OF DEC TEST (sheet 1 of 2) DATE: 5-6-1997
********** TIME: 13H33

TEST NUMBER: H4/3

OPERATING PARAMETERS (MEASURED AND ENTERED AS INPUT)

		NOM.	MIN.	MAX.
Supply air flow rate	(g/s)=	146	137	156
Return air flow rate	(g/s)=	146	138	155
Regen. heat input	(kW)=	5.608	5.384	5.832
Elec. energy (excl. reg.)	(kW)=	1.324	1.271	1.377
Spray chambers: water T	(oC)=	18.8	18.6	19.0
Water flow rate (S S/CH)	(g/s)=	0.82	0.78	0.86
at pressure	(bar)=	20	18	22
Water flow rate (R S/CH)	(g/s)=	1.58	1.50	1.66
at pressure	(bar)=	40	38	42

PROCESS CHANGES OF ENTHALPY AND HUMIDITY RATIO

ST PT	END PT	H (kJ/KG) NOM.	MIN.	MAX.	SIM.	W (g/kg) NOM.	MIN.	MAX.	SIM.
1	2	3.1	1.6	4.5	3.1	-2.40	-2.85	-1.96	-2.40
2	3	-12.6	-14.0	-11.3	-13.0	0.88	0.47	1.29	0.49
3	4	-0.6	-1	0.7	-0.0	1.42	1.04	1.81	1.75
4	5	7.9	6.5	9.2	7.7	-0.22	-0.64	0.20	-0.16
5	6	-0.5	-1.9	0.9	0.2	3.03	2.58	3.47	3.21
6	7	13.9	12.3	15.5	15.4	-1.28	-1.78	-0.78	-0.46
7	8	39.9	38.2	41.6	38.3	0.00	-0.54	0.54	0.00
8	9	-21.5	-23.4	-19.6	-4.8	2.47	1.85	3.08	2.40

PERFORMANCE PARAMETERS (CALCULATED)

			NOM.	MIN.	MAX.	SIM.
Dehumidifier eff.(W)	(%)	EDH1=	35	28	42	37
Dehumidifier eff.(Q)	(%)	EDH2=	8	4	11	8
Regeneration eff.	(%)	ERG=	16	12	20	16
Regen. heat input	(kW)	Q =	5.84	5.41	6.28	5.61
Heat Exch. eff. (SUP)	(%)	EHXS=	79	77	81	79
Heat Exch. eff. (RET)	(%)	EHXR=	91	89	93	91
Sup. air spr. ch. eff.	(%)	EVS=	56	51	61	56
Ret. air spr. ch. eff.	(%)	EVR=	89	83	94	89
FOR VENTILATION MODE:						
Cooling capacity	(kW)	CC =	1.15	0.93	1.36	1.13
Coeff. of performance		COP=	0.21	0.17	0.24	0.20
Electricity eff. ratio		EER=	0.87	0.70	1.03	0.85
FOR VENTILATION CREDIT MODE:						
Cooling capacity	(kW)	TCC =	1.48	1.25	1.70	1.46
Total Coeff. of perf.		TCOP=	0.26	0.22	0.31	0.26
Electricity eff. ratio		TEER=	1.13	0.94	1.29	1.10

RESULTS OF DEC TEST (sheet 2 of 3) DATE: 6-6-1997
****************** TIME: 13H33

MOIST AIR PROPERTIES AT MEASURED POINTS IN PROCESS

NOMINAL MEASURED VALUES:

PT	TDB (oC)	TWB (oC)	TDP (oC	PW (kPa)	W (g/kg)	RH (%)	U (%)	SV (m3/kg)	H (kJ/kg)
1	24.8	15.3	10.2	1.24	9.50	40	39	1.052	49.11
2	33.8	16.3	5.9	0.93	7.09	18	17	1.080	52.19
3	19.3	12.2	7.6	1.04	7.97	47	46	1.030	39.58
4	15.2	12.0	10.0	1.23	9.39	71	71	1.018	39.00
5	23.4	14.6	9.7	1.20	9.17	42	41	1.047	46.86
6	15.4	14.4	13.9	1.59	12.20	91	90	1.024	46.36
7	32.1	18.6	12.3	1.42	10.92	30	28	1.084	60.23
8	71.1	27.6	12.3	1.42	10.92	4	3	1.219	100.15
9	43.9	23.1	15.3	1.74	13.39	19	17	1.127	78.67

VALUES FOR TDB & W FROM ERR\ ANALYSIS & SIMULATION :
(UNITS AS ABOVE)

PT	1	2	3	4	5	6	7	8	9
TDB(MIN)	24.6	33.6	19.0	15.0	23.2	15.2	31.9	70.9	43.7
TDB(MAX)	25.0	34.1	19.5	15.4	23.6	15.6	32.4	71.3	44.1
W (MIN)	9.2	6.8	7.7	9.1	8.9	11.9	10.5	10.5	12.9
W (MAX)	9.8	7.4	8.2	9.7	9.5	12.5	11.3	11.3	13.9
TDB(SIM)	24.8	33.8	19.8	15.4	23.4	15.6	31.7	69.0	58.2
W (SIM)	9.5	7.1	7.6	9.3	9.2	12.4	11.9	11.9	14.3

POSITION OF SAMPLING POINTS



PSYCHROMETRIC CHART: ALTITUDE 1700m BAROMETRIC PRESSURE 82.5 kPa

